Background: *Daphnia pulex* is challenged by severe food and temperature changes in its habitat. Food shortage arises as a consequence of herbivore grazing and *Daphnia* populations will frequently meet severe food shortages of quantitative as well as qualitative nature resulting in a reduction of growth and reproduction. Temperature changes occur diurnally, seasonally and interannually and are a key factor for the performance of ectothermic animals, affecting cellular, systemic, or behavioral functions. To identify cellular adjustments of the model organism *Daphnia pulex* on the protein level at a temperature near to its thermal limit under food-rich and starvation conditions as well as cellular adjustments under starvation conditions under moderate temperature, the proteomes of two *D. pulex* clones, which differed in thermal tolerance, were studied upon acute heat stress, acute starvation stress as well as both stress conditions simultaneously in a time-resolved manner. Major aims of this study were to assess clone-specific differences in protein expression and the temporal sequence of protein expressions under severe stress conditions. In the first set of experiments the animals were well supplied with food to exclude other stressors than heat. During the second experiments animals were starved at moderate temperatures. Finally in the third set of experiment starvation and heat stress were applied at the same time. Differentially expressed proteins were identified by 2D gel electrophoresis and mass spectrometry.

Conclusions: For *Daphnia pulex*, 2D electrophoresis gels and mass spectrometry revealed specific protein spot patterns and a large number of identified proteins. These specific temporal patterns in protein expression likely reflect the demand for more or less important (time-critical) proteins for pro-survival mechanisms under severe heat stress. The physiological assays as well as the proteomic data of this study showed stress and stress effects to be higher in the less thermotolerant clone, not surviving heat-and-starvation stress for more than 24 hours. This clone was more susceptible to heat, showed a breakdown of protein stores during starvation, and exhibited a rather limited cell response spectrum to stress at the level of protein expressions. Availability of food resources and the nutrional status of an animal seem to be of fundamental importance to the survival during acute stress situations.

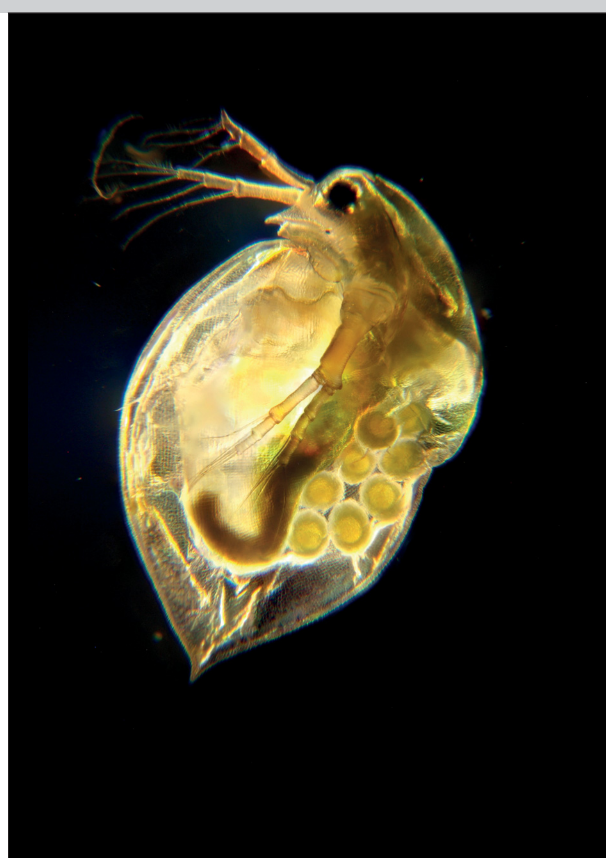

REYDELET – 2015 – Clone-specific differences and dynamics of abiotic stress effects on the *Daphnia pulex* proteome

Westfälische
Wilhelms-Universität
Münster

Yann Reydelet

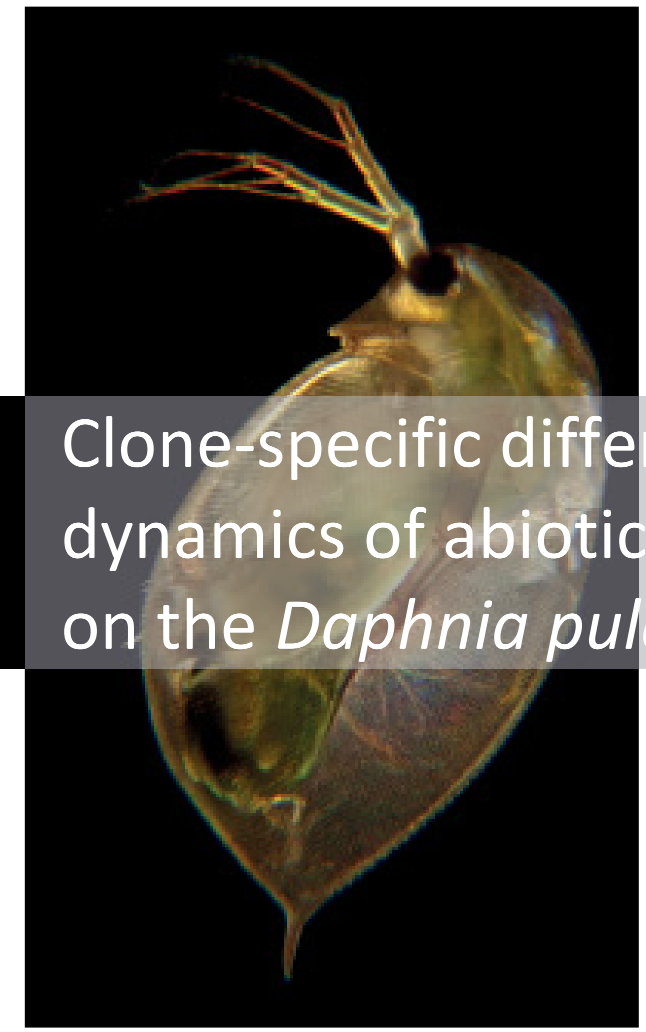

Clone-specific differences and dynamics of abiotic stress effects on the *Daphnia pulex* proteome

- 2015 -

Westfälische
Wilhelms-Universität
Münster

Biologie

Dissertationsthema

Clone-specific differences and dynamics of abiotic stress effects on the Daphnia pulex proteome

Inaugural-Dissertation

zur Erlangung des Doktorgrades

der Naturwissenschaften im Fachbereich Biologie

der Mathematisch-Naturwissenschaftlichen Fakultät

der Westfälischen Wilhelms-Universität Münster

vorgelegt von

Yann Didier Reydelet

aus Juvisy-sur-Orge (Frankreich)

- 2015 -

Dekanin/Dekan:	Prof. Dr. Michael Weber
Erster Gutachter:	Prof. Dr. R. J. Paul
Zweite Gutachterin:	Prof. Dr. E. Liebau

Tag der mündlichen Prüfung(en): 10.08.2015
Tag der Promotion: 10.08.2015

Acknowledgement

At this point I would like to express my deep appreciation and gratitude to my advisor, Prof. Dr. Rüdiger J. Paul that I could conduct my dissertation at the Institute of Animal Physiology in recent years and for the patient guidance and mentorship he provided to me, all the way from when I was first considering applying to the PhD program. I am very grateful towards Prof. Dr. Eva Liebau for the acquisition of the second opinion of this work. I also would like to thank Prof. Dr. Michael Hippler that he agreed at short notice to serve as third examiner in my committee. I want to express my heartfelt thanks to Dr. Bettina Zeis for her constant support and advice not only in experimental questions but also in private concerns.

I am also very grateful to Ina Buchen, Ulrike Gigengack, Marita Koch, and Franziska Erbe for technical assistance and supporting measurements.

My special thanks go to my PhD colleagues Dörthe, Peter and Ansgar for the good time together; all the technical support and for the many constructive and uplifting conversations. Especially I thank you Dörthe for the support until the end of this work, even after our paths had separated.

Additionally I would like to thank Markus Kolbe, Georg Wrettos, Christin Lebing (DECODON GmbH, Bio-Technikum Greifswald) for their support and technical advice, Till Bald and Michael Specht (IPBB, University of Münster) for their help in the adaptation of proteomic software and Dr. Kathleen Clauß (NH DyeAGNOSTICS), Dr. Frank Scholz, Dr. Reiner Westermeier and Günter Theßeling (Serva Electrophoresis GmbH) for their amazing and very much appreciated support, ideas as well as technical advise during my research.

Finally, I would like to thank my friends who have supported me all the time in every respect and for their understanding. Special thanks certainly will be given to my parents and Nur Gül for the constant support and confidence in me.

Parts of this work have been published:

Presentations / Poster Presentation:

Reydelet, Y., Erbe, F., Hawat, S., Hippler, M., Zeis, B. & Paul, R. J. (2012): Proteomische Studien zur Auswirkung zur abiotischer Stressoren auf *Daphnia*. Proteomics 2.0 Initiative (Neue Entwicklungen und methodische Möglichkeiten in der Proteom Analyse) Institut für Rechtsmedizin, Münster (Germany) (Presentation)

Reydelet, Y., Becker, D., Colbourne, J. K., Jackson, C., Hawat, S., Hippler, M., Lopez, J. A., Zeis, B. & Paul, R. J. (2011): Proteomic and transcriptomic analysis of short-term heat stress response in two Daphnia pulex clones. 9th International Symposium on Cladocera, Verbania (Italy) (Poster Presentation)

Reydelet, Y., Zeis, B. & Paul, R. J. (2010): Proteomic analysis of short-term heat stress response in two *Daphnia pulex* clones. Münster Meeting on Stress and Evolution, Münster (Germany) (Poster Presentation)

Reydelet, Y., Zeis, B. & Paul, R. J. (2010): Proteomic analysis of short-term heat stress response in two *Daphnia pulex* clones. Daphnia Genomics Consortium (DGC) Meeting, Leuven (Belgium) (Poster Presentation)

Content

List of Figures

List of Tables

List of Abbreviations

%	percent
®	registered trademark
°C	Degree Celsius
µg	Microgram
µl	Microliter
µm	Micro meter
µmol	Micromol
2D	Two Dimension
Å	ångström
ACT	Actin
ANOVA	analysis of variance
AO	Aldehyde Oxidase
BRE*d*	*down*stream TFII*B* *R*ecognition *E*lement
BRE*u*	*up*stream TFII*B* *R*ecognition *E*lement
BSA	*bovine serum albumin*
BTC	Basal Transcriptional Complex
BTF	Basal Transcription Factor
C	Control Conditions
CGI	*CG* Islands
CHR	Cellular Homeostasis Response
CpG	*C*ytosin-*p*hosphatidyl-*G*uanin
CR	coding regions
CRE	Carbohydrate Response Element
CRT	Calreticulin
CSR	Cellular Stress Response
D. galeata-hyalina	*Daphnia galeata-hyalina*
D. magna	*Daphnia magna*
D. pulex	*Daphnia pulex*
Da	Dalton
DCE	*D*ownstream *C*ore *E*lement
DEPs	Differentially Expressed Proteins
DNA	Desoxyribonucleinacid
DPE	Downstream Promoter Element
DTT	Dithiotreitol
e.g.	*Exempli gratia*, "for example"
EBS	Ets binding site
ECPR	estimated core promoter region
EDTA	Ethylenediaminetetraacetic acid
et al.	et (“and”) alii (“others”)

FCP	Focused Core Promoters
Fig.	Figure
FWHM	Full width at half maximum
g	gramm
g	gravity = 9.80665 m/s^2
GOT	Glutamat-Oxalacetat-Transaminase
GPI	Glucose-6-Phosphate Isomerase
h	hour
HeLa cell	Henrietta Lacks immortal cell line
HPLC	High-performance liquid chromatography
HRE	HIF Response Element
HSE	Heat Shock Response element
HSP60	Heat Shock Protein 60
HS-stress	Heat and Starvation Stress
i.d.	inner diameter
i.e.	id est (this is)
IAA	Iodacetamid
IEF	Isoelectric focusing
IN	intron
Inr	Initiator
IPCC	Intergovernmental Panel on Climate Change
IPG	Immobilized pH gradient
Kbp	kilo base pairs
kDa	Kilodalton
l	Liter
LC-MS/MS	Liquid chromatography– tandem mass spectrometry
LDH	Lactate Dehydrogenase
m	meter
m/z	mass-to-charge
m^2	square meter
mA	Milliampere
MDH	Malate Dehydrogenase
mg	milligramm
min	minute
ml	milliliter
mm	millimeter
mmol	millimole
mol	mole
MPI	Mannose-6-Phosphate Isomerase
$M_r e$	experimental Molecular Weight
$M_r p$	predicted Molecular Weight

MTE	*M*otif *T*en *E*lement
MTT	Dimethylthiazoldiphenyltetrazoliumbromid
MW	Molecular Weight
n	Number of Biological Sampels
N	Number of Individuals
Na	Natrium
NAD	Nicotinamide adenine dinukleotide
NIH	National Institutes of Health
nm	nanometer
NP	Peptide Count
OD	Optic Density
P	probability
p.m.	post meridiem, "after noon"
PAGE	Polyacrylamidgel-Electrophoresis
PCD	Programmed Cell Death
PEP	Peptidase
PGM	Phosphoglucomutase
pH	power of hydrogen
pI	Isoelectric Point
PIC	Pre-Initiation Complex
pI*e*	experimental Isoelectric Point
pI*p*	predicted Isoelectric Point
PMS	Phenanzinmetasulfat
ppm	Parts per million
rel. %V	relative Prozentvolume
RNA	Ribonucleic acid
RNA pol II	RNA polymerase II
ROS	Reactive Oxygen Species
rpm	rotations per minute
RT	Room Temperature
RuBPs	ruthenium II tris (bathophenanthroline disulfonate)
S	Starvation Stress
SC	Sequence Coverage
SCP	Super Core Promoter
SDS	Sodium Dodecyl Sulfat
sec	seconds
SI	Subelement I
SII	Subelement II
SIII	Subelement III
sINR	Strict Initiator
SNK	Student-Newman-Keuls method

SOD	Superoxide Dismutase
T	Temperature
TATA box	Goldberg-Hogness box
TBP	TATA binding protein
TCA	trichloroacetic acid
TEMED	Tetramethylethylendiamin
TF	Transcription Factor
TFII	Transcription Factor for Polymerase II
™	Trademark
TOP	5' Terminal Oligopyrimidine Sequence
TRIS	Tris(hydroxymethyl)-aminomethan
TSS	Transcription Start Site
UTR	untranslated region
V	Volt
v/v	volume per volume
V-ATPase	Vacuolar H^+-ATPase
Vh	Volthours
VTG	Vitellogenin
w/v	weight per volume
XPCE	*X* Core *P*romoter *E*lement

Abstract

Background: *Daphnia pulex* is challenged by severe food and temperature changes in its habitat. Food shortage arises as a consequence of herbivore grazing and *Daphnia* populations will frequently meet severe food shortages of quantitative as well as qualitative nature resulting in a reduction of growth and reproduction. Temperature changes occur diurnally, seasonally and interannually and are a key factor for the performance of ectothermic animals, affecting cellular, systemic, or behavioral functions. To identify cellular adjustments of the model organism *Daphnia pulex* on the protein level at a temperature near to its thermal limit under food-rich and starvation conditions as well as cellular adjustments under starvation conditions under moderate temperature, the proteomes of two *D. pulex* clones (clones G and M), which differed in thermal tolerance (lower thermal tolerance of clone G), were studied upon acute heat stress (transfer from 20°C to 30°C with *ad libitum* food supply or starvation) and acute starvation stress (20 °C), in a time-resolved manner (0, 24, and 48 hours of stress). Major aims of this study were to assess clone-specific differences in protein expression and the temporal sequence of protein expressions under severe stress conditions. In the first set of experiments the animals were well supplied with food to exclude other stressors than heat. During the second experiments animals were starved at moderate temperatures. Finally in the third set of experiment starvation and heat stress were applied at the same time. Differentially expressed proteins were identified by 2D gel electrophoresis and mass spectrometry.

Results: Characterization of both *D. pulex* clones via allozyme analysis, revealed a difference in three of the eight analyzed enzyme loci, aldehyde oxidase, lactate dehydrogenase and malate dehydrogenase. All analyzed enzymes showed homozygous patterns. Both clones were tested on their heat and starvation stress tolerance window by long term swimming activity assays as a test parameter. While the clones showed no significant difference under starvation stress (half-maximal values (MT_{50}) for clone G and M at 167 h) under heat stress and combined heat and starvation stress significant differences in stress tolerance were observed, with clone M (heat stress MT_{50} 98 h and heat and starvation stress MT_{50} 49 h) showing a higher stress tolerance than clone G (heat stress MT_{50} 48 h and heat and starvation stress MT_{50} 17 h).

Of the 674 protein spots detected on the fusion (averaged) images of 2D gels 95 dominant protein spots were excised and analyzed. A total of 34 proteins were identified by mass spectrometry within 78 spots. Under heat stress, significant up-regulations were found for 18 proteins, with seven of them specific for clone G, and six for clone M. Significant down-regulations were detected for eleven proteins, with five of them specific for clone G and four for clone M. Under starvation stress, protein expression was significantly up-regulated for 16 proteins, with five of them specific for clone G and six for clone M. Down-regulation was significant for 13 proteins, with four of them specific for clone G and six for clone M. With both stressors combined a total of 18 proteins were significantly upregulated with two of them specific to clone G and 11 specific to clone M.

Frequently, different protein isoforms were up-/down-regulated in the two clones, and expression intensities or regulatory patterns often differed between clone G and M. In both clones, there were significant up-regulations of glutathion transferases, V-ATPase subunits and proteins of the cytoskeleton and down-regulations of proteins for proteolytic processes and carbohydrate binding or metabolism. Chaperones showed clone and stress-specific up-regulation (clone G, CRT only under heat stress and heat shock protein 60, HSP60 only under combined (heat and starvation) stress; clone M, PDI under heat stress and heat shock protein 60, HSP60 under all stress conditions).

Cytoskeleton/muscle proteins (actins, alpha and beta tubulins) were more intensely up-regulated in clone G under heat stress; under all other stress conditions cytoskeleton/muscle proteins were more intensely upregulated in clone M. Arginine kinases were only significantly upregulated in clone G during all three types of acute stress applied. In contrast clone G showed reduced amounts of proteins for the ubiquitin/proteasome system upon all stress situations. Conversely, clone M exhibited a strong up-regulation of a specific vitellogenin (VTG) with a superoxide dismutase (SOD) domain under all stress conditions. Most proteins related to proteolysis and carbohydrate binding/metabolism showed either reduced or unchanged expression in both clones under all stress conditions. The expression of all proteins followed specific temporal patterns.

Conclusions: For *Daphnia pulex*, 2D electrophoresis gels and mass spectrometry revealed specific protein spot patterns and a large number of identified proteins, which can also be used for future proteome studies. The specific temporal patterns in protein expression likely reflect the demand for more or less important (time-critical) proteins for pro-survival mechanisms under severe heat stress. The physiological assays as well as the proteomic data of this study showed stress and stress effects to be higher in the less thermotolerant clone G, not surviving heat-and-starvation stress for more than 24 hours; it was more susceptible to heat, showed a breakdown of protein stores during starvation, and exhibited a rather limited cell response spectrum to stress at the level of protein expressions. The up-regulated calreticulin expression in clone G indicates endoplasmic reticulum stress, the up-regulated expression of cytoskeleton/muscle proteins likely served for cytoskeleton reconstruction, and the reduced amounts of proteins for the ubiquitin/proteasome system was possibly due to autophagic processes. Conversely, the strong up-regulation of HSP60 in clone M probably supports the refolding of denatured proteins and counteracts apoptotic processes, and the up-regulated expression of the VTG-SOD fusion protein possibly indicates the formation of resting stages (ephippia) as a still feasible emergency measure. Higher stress tolerances in clone M therefore might be attained by differences in the use of autophagic resources and mechanisms and/or to accessing different sources of food (e. g. bacterial food). Availability of food resources and the nutrional status of an animal seem to be of fundamental importance to the survival during acute stress situations.

1 Background

1.1 Stress – Response and Adaptation

Throughout lifetime, organisms are subject to periodic and sudden changes in environmental conditions. Stress can be defined as a specific internal state of an organism resulting from the confrontation with a situation outside of normal or ideal operating conditions (Steinberg, 2011), with the stress response being independent of the nature of stress (Selye, 1973; Van Straalen, 2003). In case stress cannot be avoided but must be tolerated, the stress response can be separated into three different phases (Fig. 1.1). In the alarm phase, modifications of molecular and systemic parameters occur, which aim at the maintainance and restoration of cellular integrity but do not affect any vital or growth activities. If the impact of stress is too fast and/or strong, it will result in acute cell damage or death. The activation of defense mechanisms such as antioxidant defense, protein repair and biotransformation is triggered during the resistance phase and is accompanied by first signs of reduced vital activity and growth. If adjustment to stress cannot be achieved, the exhaustion phase follows, characterized by the collapse of vital cellular functions that leads to chronic damage and, in the most severe case, to death (Steinberg, 2011).

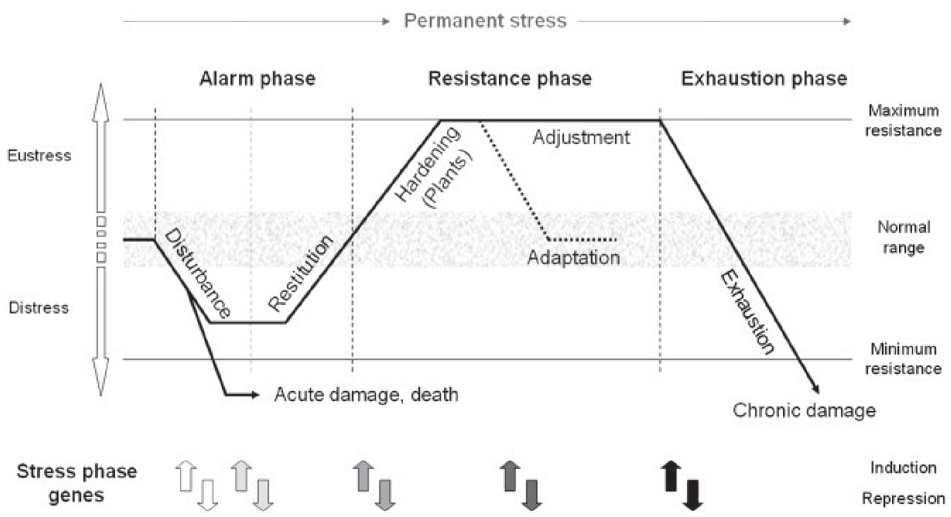

Fig. 1.1 Classical stress phase model

Different grey arrows represent different genes specifically expressed in the individual stress phases (Steinberg *et al.*, 2008)

Cellular stress responses

Cells are particularly sensitive to external or internal stress stimuli, and the survival of a cell depends on its ability to mount an appropriate stress response. The latter fact explains why cellular stress responses and associated signaling pathways were highly conserved during evolution. During the alarm phase and the resistance phase, two cellular responses to stress may occur. The cellular stress response (CSR) is an acute stressor-unspecific response serving as primary protective reaction against stress to ensure macromolecular integrity (Fig. 1.2). Antioxidant defense mechanisms against oxidative damage or heat shock proteins against protein denaturations are major components of the CSR. It is triggered by sensing mechanisms, which activate the first steps of stress-sensitive signaling pathways that regulate the expression of highly conserved genes for the protection and repair of macromolecules (Hochachka, 2000; Kültz, 2003; Roelofs *et al.*, 2008). In addition to CSR, a second stress response, the slower and stressor-specific cellular homeostasis response (CHR; Fig. 1.2), can be induced, which aims at the restoration of cellular homeostasis (Kültz, 2005).

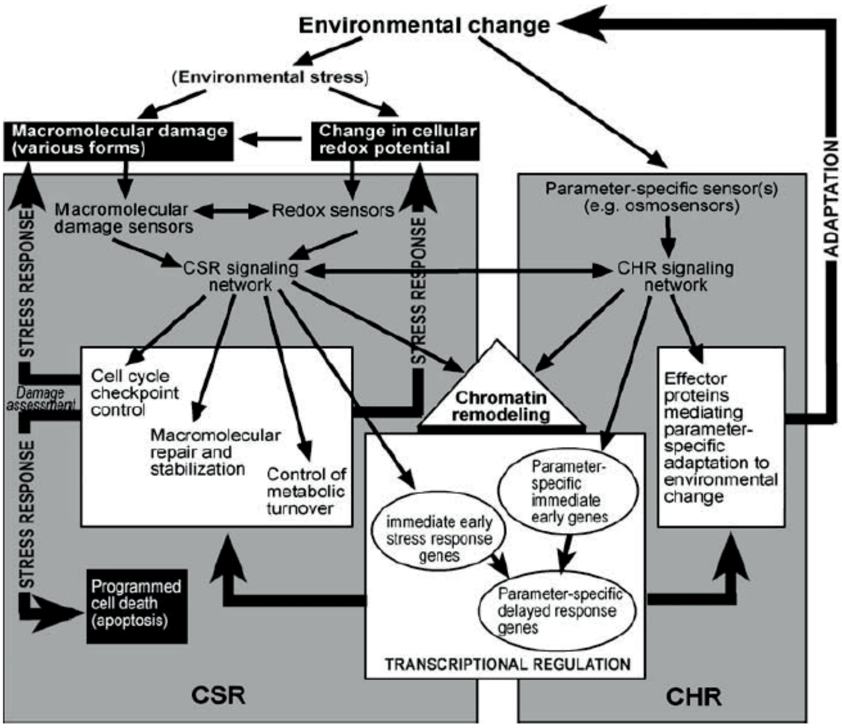

Fig. 1.2 Schematic representation of the cellular stress response (CSR) and its interaction with the cellular homeostasis response (CHR)

The aim of the CSR is to restore macromolecular integrity and redox potential disturbed by stress. The CHR serves to restore cellular homeostasis upon environmental changes. Both types of cellular responses are interconnected and mostly initiated in parallel (Kültz, 2005).

The heat shock response

Exposure of cells and organisms to stress such as heat, oxidative and osmatic stress, heavy metals and proteasome inhibitors will induce the heat shock response that is directed by a set of heat shock transcription factors (HSFs) (Lindquist and Craig, 1988; Steinberg, 2011). During initiation of the heat shock response, general protein transcription and translation is halted, presumably to alleviate the burden of misfolded proteins in the cell. However, HSF that enhance expression of a specific subset of protective genes are selectively activated under these conditions (Fulda *et al.*, 2010). While vertebrates and plants have at least four members of the HSF gene family (HSF1 - 4), *Drosophila*, *Caenorhabditis elegans* and yeast only express one them (HSF1) (Jolly and Morimoto, 2000; Kourtis and Tavernarakis, 2011). Heat stress will trigger two main sensing mechanisms specific to this type of stress that will lead to the activation of HSF and the subsequent activation of heat shock proteins (HSP). The first main trigger is the evolutionary conserved response to the heat-induced accumulation of denatured proteins and the second trigger is the direct sensing of temperature changes through thermosensitive macromolecules like DNA, RNA, proteins and lipids. Such thermosensitive macromolecules can be found from bacteria to mammals. They activate signal transduction pathways through alterations of their macromolecule structure, such as melting of RNA hairpins, changes in DNA topology or conformational changes of HSP26 (De Nadal *et al.*, 2011). Until stressful conditions occur, inactive HSF1 is maintained in a monomeric form in the cytoplasm through interaction with Hsp90 and co-chaperones. Under stressful conditions, the accumulation of unfolded proteins will compete with HSF1 for Hsp90 binding. Thus, HSF1 is released from the complex, stimulating its transition from a monomer to a homotrimer that can translocate to the nucleus, where it will bind to heat shock elements (HSE) upstream of the transcription start site (TSS) within the promoters of heat shock genes (Fig. 1.3), which result in the expression of heat shock proteins (HSPs).

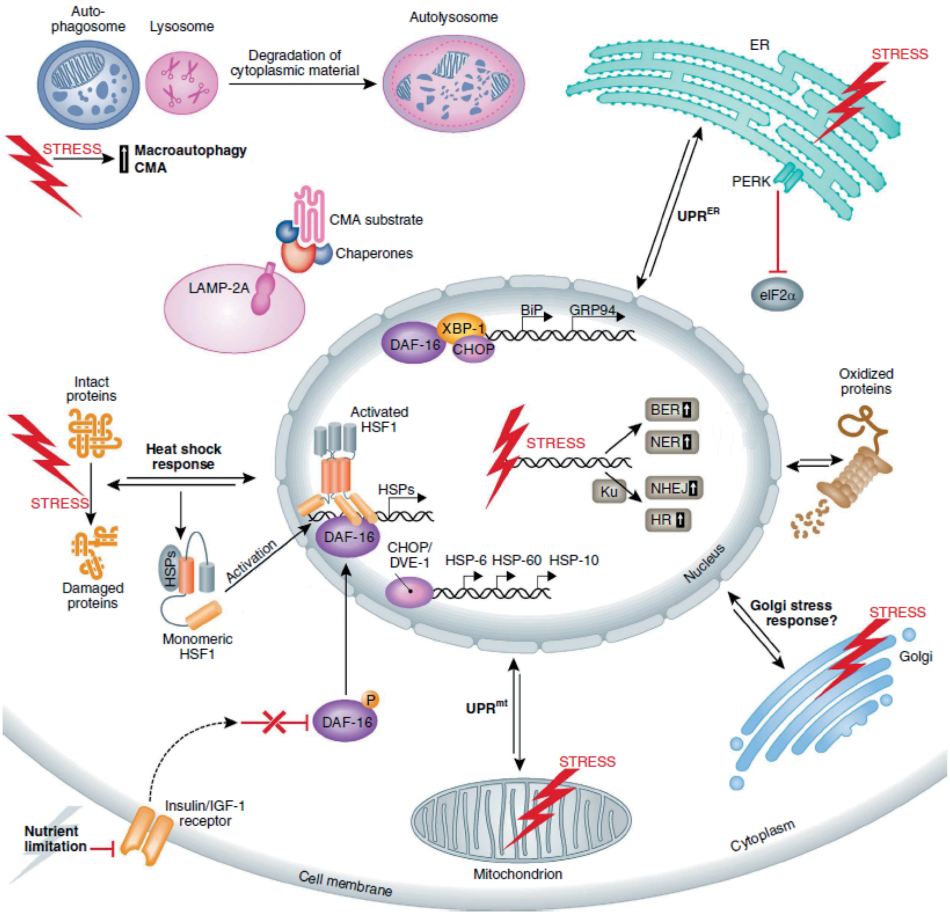

Fig. 1.3 Examples of general and organelle-specific stress response pathways

Depending on the type of macromolecule and the site of damage, distinct stress response pathways, such as autophagy, heat shock response, unfolded protein response in the endoplasmic reticulum (UPR^{ER}) and in the mitochondrion (UPR^{mt}), remodelled proteasome and the DNA damage response are initiated. Double arrows denote bi-directional communication with the nucleus, which involves generation of stress signals in the stressed organelle or the cytoplasm, transduction of the signals to the nucleus and up-regulation of stress-relieving proteins, which in turn function to ameliorate damage. Question marks denote lack of information about specific molecules mediating the effects. Although a typical Golgi stress response pathway has not been described yet, several types of stress may influence gene expression in the nucleus and cell homeostasis by impinging on Golgi function. BER, base-excision repair; BiP, Ig-binding protein; CHOP, C/EBP homologous protein; CMA, chaperone-mediated autophagy; DAF-16, abnormal dauer formation 16; DVE-1, defective proventriculus 1; GRP94, glucose-regulated protein 94; HSF1, heat shock factor 1; HSP, heat shock protein; HR, homologous recombination; IGF-1, insulin growth factor 1; LAMP-2A, lysosome-associated membrane protein 2A; NER, nucleotide-excision repair; NHEJ, non-homologous end joining; PERK, PKR-like ER kinase; UPR$^{ER/mt}$, unfolded protein response endoplasmic reticulum/mitochondrion; XBP-1, X-box-binding protein 1 (Kourtis and Tavernarakis, 2011).

Organelle-specific stress response pathways

The endoplasmic reticulum (ER) is the organelle of secretory protein biogenesis. Since the ER is especially sensitive to alterations in homeostasis, it provides a stringent quality control system. This quality control system ensures the correct folding of the proteins and comprises chaperones, processing enzymes and client proteins (Zhang and Kaufman, 2006; Kourtis and Tavernarakis, 2011; Snapp, 2012). Conditions such as glucose starvation, inhibition of protein glycosylation, disturbance of Ca^{2+} homeostasis and oxygen deprivation cause accumulation of unfolded and misfolded proteins in the ER lumen and trigger a highly specific signaling pathway called the unfolded protein response (UPR^{ER}). During homeostasis, the ER resident UPR^{ER} sensors, notably in metazoans inositol-requiring protein-1 (IRE1), protein kinase RNA (PKR)-like ER kinase (PERK), and activating transcription factor 6 (ATF6) are bound to luminal ER chaperone BiP/GRP78. As ER stress rises, BiP is released and the sensors activated launch the UPR^{ER} (Zhang and Kaufman, 2006; Kourtis and Tavernarakis, 2011, Snapp, 2012).

IRE1 and PERK are both type I transmembrane protein kinases. In higher species activated IRE1 cleaves mRNA in the nucleous that encodes a transcription factor named X-box binding protein-1 (XBP1). XBP1 in turn activates the transcription of target genes involved in the ER homeostasis as well as in export and degradation of misfolded proteins. In contrast, activated PERK initiates the PERK-eIF2α signaling pathway by phosphorylating the α-subunit of eukaryotic translation initiation factor-2 (eIF2α). Activation of the PERK-eIF2α signaling pathway leads, firstly, to lower levels of eIF2 and therefore results in a translational suppression, and secondly, to an activation of the transcription of the UPR target genes through CAP-independent upregulation of the translation of a transcription factor 4 (ATF4). PERK can also directly phosphorylate and activate the transcription factor, NF-E2-related factor-2 (Nrf2), which contributes to cellular redox homeostatis by inducing the expression of anti-oxidant genes. ATF6 is a type II transmembrane protein, which under activation translocates to the Golgi apparatus and is cleaved to a 50 kDa transcription factor. The cleaved N-terminal fragment will translocate to the nucleus and increase the transcription of the UPR target genes such as BiP, PDI and GRP94. UPR signaling generally promotes cell survival by improving the balance between the protein load and the folding capacity in the ER and/or by improving the secretion of trophic factors/growth factors (Fig. 1.4) (Zhang and Kaufman, 2006; Fulda *et al.*, 2010; Kourtis and Tavernarakis, 2011; Snapp, 2012). However, if the protein load in the ER exceeds its folding capacity, or some defects in the UPR exist, cells tend to die, typically, with apoptotic features (ER stress-induced cell death). Although the exact molecular mechanisms that regulate this type of cell death remain to be elucidated, at least three pathways have been identified to be involved: the caspase- 12/caspase-4 pathway and CHOP and IRE1-JNK pathways (Puthalakath *et al.*, 2007; Fulda *et al.*, 2010).

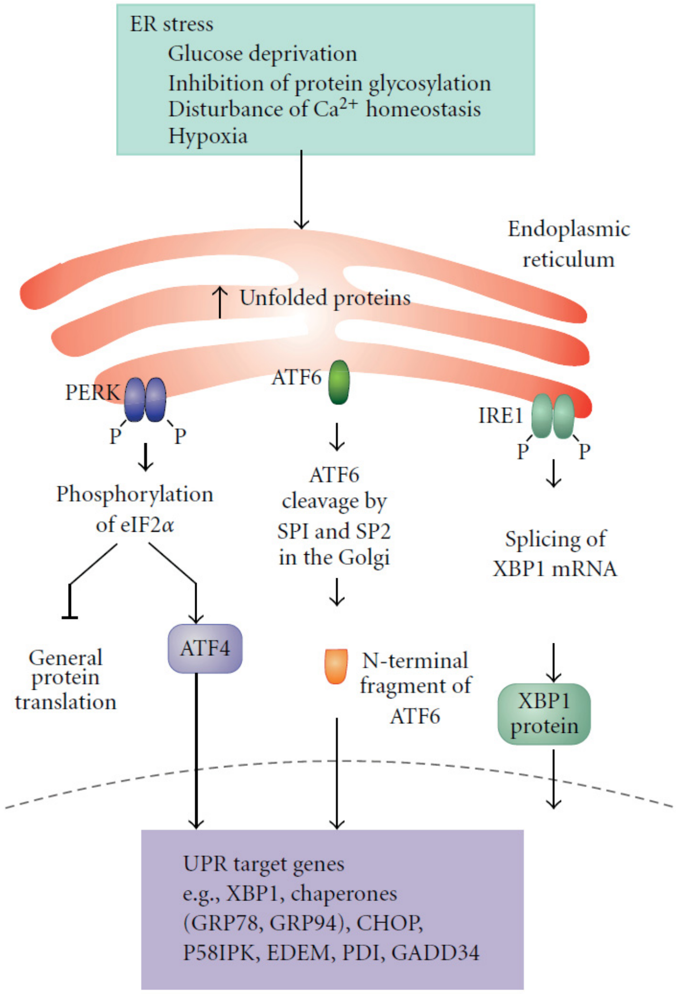

Fig. 1.4 ER stress and the unfolded protein response

"Stress to the ER stimulates the activation of the three endoplasmic reticulum (ER) stress receptors, PKR-like ER kinase (PERK), activating transcription factor 6 (ATF6) and inositol-requiring enzyme 1 (Ire1) that are involved in the unfolded protein response (UPR). PERK phosphorylates eukaryotic initiation factor 2 (eIF2α) which inhibits general protein translation, allowing eIF2α-independent translation of ATF4, which activates transcription of chaperones such as GRP78. ATF6 undergoes specific proteolysis in the Golgi apparatus which leads to activation. One of the ATF6 target genes is XBP1. IRE1 catalyzes the alternative splicing of XBP1 mRNA leading to expression of the active XBP1 transcription factor. Together the three arms of the UPR block protein translation, increase chaperone expression and enhance ER-associated protein degradative pathways" (Fulda et al., 2010).

The mitochondrial matrix contains its own set of chaperones involved in importing, refolding and preventing aggregation of proteins encoded by the nuclear genome as well as the mtDNA. The main mitochondrial chaperones are chaperonin 60 (Cpn60/HSP60), chaperonin 10 (Cpn10/HSP10), mtHSP70, mtGrpE and mtDnaJ. Pertubation of the mitochondrial homeostasis by stresses results in accumulation of unfolded proteins within the mitochondrial matrix and the activation of the mitochondrial unfolded protein responses

(UPR^{mt}). UPR^{mt} is initiated by the activation of transcription of the chop and the c/ebpß gene. CHOP and C/EBPß then hetero-dimerise and induce the expression of nuclear genes that encode mitochondrial chaperones such as Cpn60/HSP60 and Cpn10/HSP10 (Zhao *et al.*, 2002; Aldridge *et al.*, 2007; Kourtis and Tavernarakis, 2011).

1.2 *Daphnia*: a model organism

Members of the genus *Daphnia* (Fig. 1.5) commonly known as "water-fleas", belong to the order Cladocera, and are among the best-studied invertebrates. With over 200 different species of *Daphnia* (Colbourne *et al.*, 1997) they are found in almost all limnic ecosystems over the world, ranging from acidic swamps to deep permanent lakes, shallow temporary ponds, side arms of streams and rivers and even in areas with brackish water (Lampert and Rothhaupt, 1991; Hairston *et al.*, 2005).

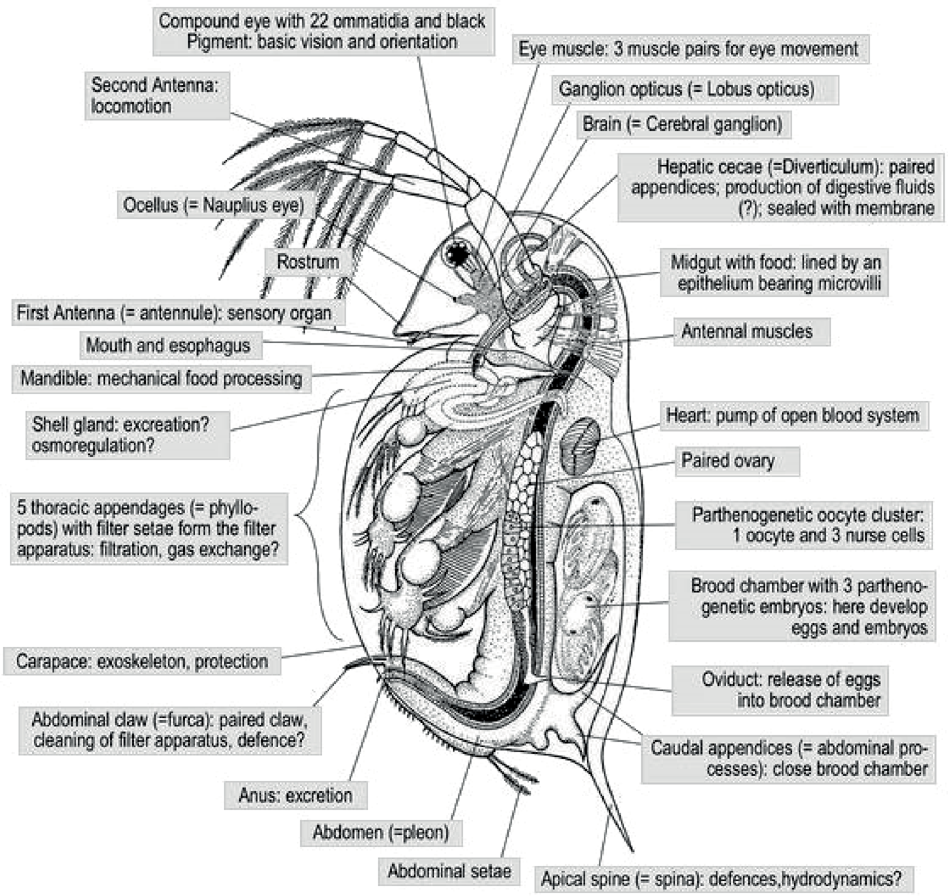

Fig. 1.5 The functional anatomy of *Daphnia*.

Adult female with parthenogenetic embryos in the brood chamber. For better illustration, the carapace is shown as transparent. The animal measures about 2 mm from the top of its head to the base of its tail spine (Ebert, 2005).

As the most important group of zooplankton, *Daphnia* form the major prey of planktivorous fresh water fish and of invertebrate predators (Flössner, 2000) and thus provide an important link in the transfer of carbon and energy from primary producers (phytoplankton) to higher trophic levels. Their small body sizes range from 0.2 mm to 5 mm in length, the short generation time, the relatively simple conditions required for mass culture, but especially their specific life cycle of cyclical parthenogenesis (Fig. 1.6) makes *Daphnia* an ideal model organism, which is subject to biological studies for a very long time.

Daphnia serves as a model organism in ecology, evolutionary biology as well as in applied research, such as physiology, ecotoxicology (Peters and Bernardi, 1987; Benzie, 2005) and laboratory controlled experiments on environmental stressors (Barata *et al.*, 2005). In 1908, Elie Metchnikoff was rewarded with the Nobel Prize in Physiology/Medicine for his research with *Daphnia* on the immunity in infectious diseases (Kaufmann, 2008; Ebert, 2011). With the recent public release of the complete genome of *D. pulex* (Colbourne *et al.*, 2011), *Daphnia* became the 13th model system for biomedical research of the National Institutes of Health (NIH) (Ebert, 2011) and new possibilities to investigate the molecular principles of acclimation an adaptation to environmental stress arise.

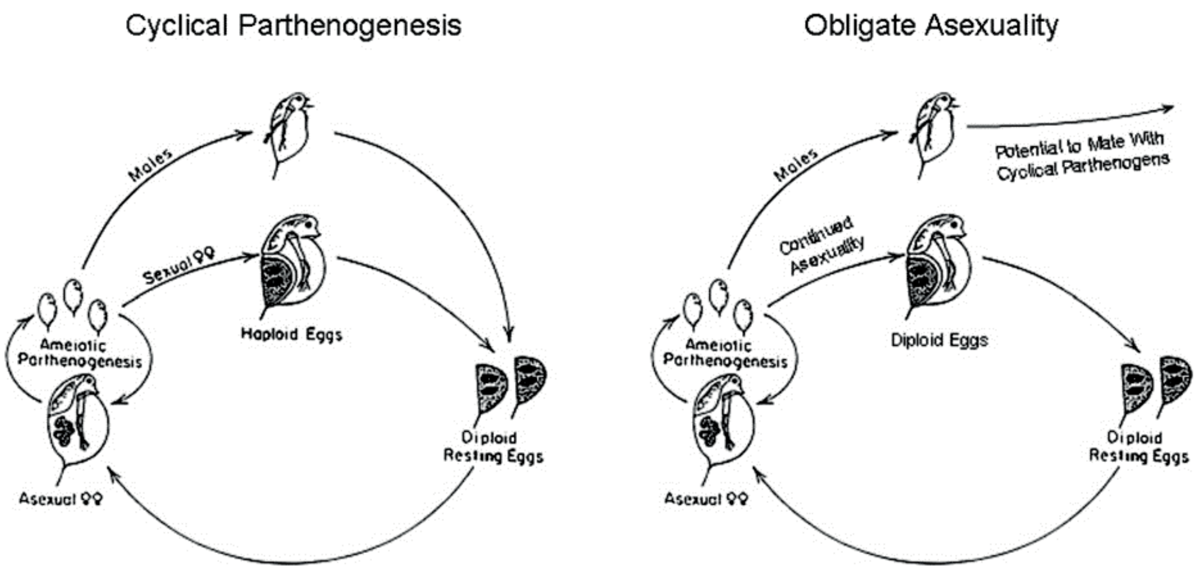

Fig. 1.6 Scheme of the breeding systems of *Daphnia*.

Nearly all members of the Cladocera are capable of cyclical parthenogenesis (1). Cyclical parthenogens are not truly ‘‘cyclical,’’ as they are capable of switching to sexual reproduction at any time. However, the *D. pulex* complex is unique in harboring lineages that are obligate asexual (2) in which females have lost the ability to engage in meiosis and instead produce diploid resting eggs by a mechanism that is genetically equivalent to mitosis. Not all cyclical or obligate parthenogens produce males, although males are essential for resting-egg production by cyclical parthenogens and nonessential in obligate asexuals (Lynch *et al.*, 2008).

1.3 Clonal variation and local adaptation

The absence of sexual reproduction in asexual populations leads to the assumption that these lack genetic variation. There is general acceptance that this lack of recombinatorial variability leads to a decrease of the adaptive evolution, the specification level and to an increase in the extinction rate. However, coexistence among different asexual clones and with the sexual ancestors depends in part upon specializations characteristic of individual clones. Clonal reproduction is an effective way to maintain part of niche-width variation within the gene pool. Significantly higher densities are achieved relatively to sexual forms by multiclonal populations than by monoclonal populations. This relationship is a function of clonal variability on which natural selection can act and upon the capacity of a multiclonal population to make better use of the heterogeneous environment by niche diversification (Vrijenhoek, 1979).

Studies of the factors that determine the clonal diversity and coexistence of fish of the genus *Poeciliopsis* have revealed that the clonal composition of a population at a particular location is mainly determined by hybridization, migration and mutation. The success of individual clones that compete for limiting resources with other clones and sexually reproducing individuals is due to the absence of recombination. The rate of evolution to obtain recombinational variability in sexual populations can significantly delay adaptation (Vrijenhoek, 1979). Responses of populations to stressful environments are determined by the phenotypic reaction norm of individuals as well as the genetic reaction norms of populations. The amount of heritable variation in a trait will therefore determine adaptation and the evolutionary change in response to selection. Genetic variability will change in response to stressful environments, yet the debate is still open if they will in- or decrease (Mitchell *et al.*, 2004).

Daphnia was for long periods a leading research system, and population genetic studies on *Daphnia* have been performed for more than 30 years (Hebert and Ward, 1972; De Meester, 1996). The concept of reaction norms was developed in 1909 by Richard Woltereck on the basis of research on *Daphnia* and is still part of many experiments to distinguish genetic effects from environmental effects (Sarkar, 1999; Ebert, 2011). The completed sequencing of the genome of *D. pulex* in 2005 (Colbourne *et al.*, 2011) as well as numerous accompanying studies working on the *D. pulex* genome have accomplished decisive steps and opened the door for further exploration in the field of environmental genomics, which investigates how a population adapts to new environments and studies the link between gene function and environmental conditions (Ebert, 2011). For this purpose, clonal reproduction is an important aspect to help to explore the molecular basis of phenotypic plasticity. Clones are useful in order to investigate differences in gene expression in response to environmental influences by performing replicate measurements on genetically identical individuals with the same conditions. Also direct control systems can be produced to determine background noise and thus to identify the specific responses to changing environmental conditions (Miner *et al.*, 2012). By observing the different phenotypes that a single genotype can express over different environmental conditions it is possibile to quantify the genetic variation of phenotypic plasticity (Ebert *et al.*, 1993). *Daphnia* populations might range from a few to several thousand clonal lines (Carvalho and Crisp, 1987) and have an enormous phenotypic plasticity within each species. Phenotypic plasticity is defined as a set of phenotypes displayed by a given genotype in response to environmental variation (i.e. norm of reaction) (Walsh and Post, 2012). By physiological changes, individuals of a single species will adapt to changing environmental conditions caused by e.g. predators, changes in pH, toxins, different oxygen concentrations, changing temperature and food availability (Laforsch *et al.*, 2004; Moenickes *et al.*, 2010). Seasonal or long-term fluctuation of abiotic factors in the environment will favor specialists adapted to the prevailing condition, whereas heterogeneous or unpredictable variations favor phenotypic plasticity (Lynch and Gabriel, 1987; Mitchell *et al.*, 2004). Short-lived species such as zooplankton may exhibit seasonal species successions or successive dominance of specialist genotypes. The ability of *Daphnia* populations to undergo fast evolutionary changes has aroused the attention to investigate genetic differences. *Daphnia* populations showed alterations in phototactic behavior in presence of predators (Cousyn *et al.*, 2001). Specifically, the fact that within populations of *Daphnia* along with seasonal and interanual environmental changes, definite seasonal clonal lines can be observed, which differ significantly in their phenotypic and physiological properties, emphasizes the fast reaction of *Daphnia* populations to environmental changes (Pinkhaus *et al.*, 2007; Paul *et al.*, 2012).

The answer of this phenotypic plasticity of *Daphnia* can be found in its genome. *D. pulex* possesses a genome that is comparatively modest in size, 200 megabases. However, it contains more than 30000 coding genes and exceeds so the number found in other genomes. Moreover, 36% of the genes have no detectable homologs. 13000 *Daphnia* genes are paralogs that were gained through an accumulative process by tandem duplication. Gene duplications give rise to novel expression patterns by integrating the copied gene into new genomic locations or dissociating the gene from its previous regulatory framework and therefore allowing expression of novel gene combinations under different environmental conditions (Colbourne *et al.*, 2011; Ebert, 2011).

Because *Daphnia's* ecology is profoundly influenced by both, genetic polymorphism and phenotypic plasticity, *Daphnia* represents an excellent model system with tremendous potential for developing a mechanistic understanding of the relationship between traits at the genetic, organismal and population levels, and consequences for community and ecosystem dynamics. It is known that phenotypic intra-type variations within a single species in critical traits may lead to a cascade triggering changes in the composition of biological communities and have a profound impact on the functioning of the ecosystem. This chain of causation goes in both ways and is referred to as "eco-evolutionary dynamics" where evolutionary and ecological processes influence each other. *D. pulex* as a keystone species and its sequenced genome has an exceptional potential to get a detailed insight on the genomics of cellular responses to changing environmental factors and to improve our understanding of ecology and evolution (Ebert, 2011). With the function as the primary phytoplankton consumers, its role in the nutrient cycle and function as a key prey, *Daphnia* occupies a central and significant position in the pelagic ecosystem (Fig. 1.7). For each of these ecological interactions, *Daphnia* has a range of morphological, physiological and behavioral adjustments that are known to be genetically variable and which will influence the strength of interactions (Miner *et al.*, 2012).

There are examples of among-population genetic variations for antipredator traits in *Daphnia*, typically fitting a pattern of local adaptation (De Meester, 1996). Due to the high vulnerability to predators, *Daphnia* species have considerable phylogenetic variability in antipredator traits. For many of these traits, extensive phenotypic plasticity and genetic variability has been shown (Fig. 1.8) (Boersma *et al.*, 1998; Cousyn *et al.*, 2001; Ebert, 2011; Walsh and Post, 2012).

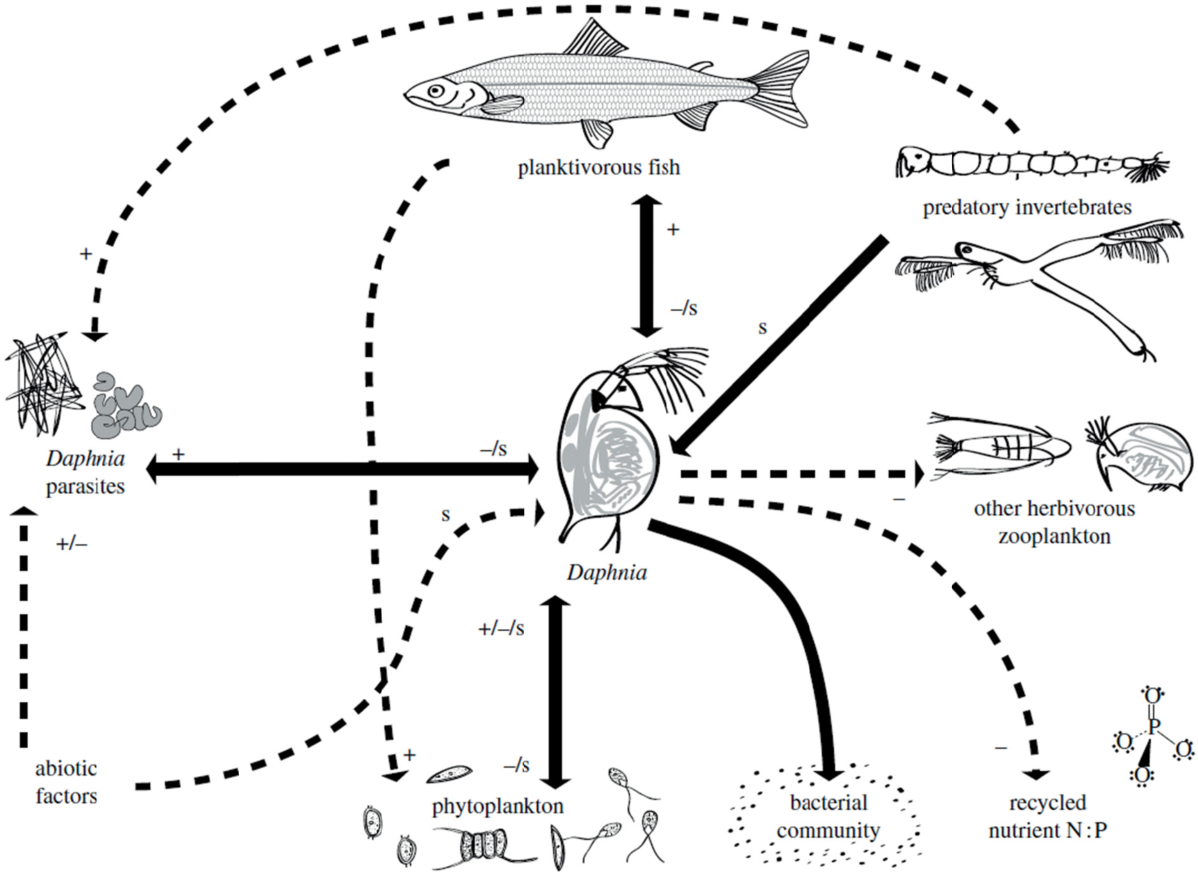

Fig. 1.7 Central position of *Daphnia* in the interaction web of a lake ecosystem.

Solid lines represent direct interactions and dashed lines represent indirect interactions. Plus (+) and minus (-) signs indicate positive or negative demographic interactions, while s represents natural selection acting on *Daphnia* populations (Miner *et al.*, 2012).

For example *Daphnia ambigua* under seasonal predation pressure grew faster, matured earlier and larger, produced more offspring and invested more in sex than *Daphnia* that are under constant predation pressure (Walsh and Post, 2012). Also *Daphnia* in presence of predators will be driven to smaller body size and earlier reproduction compared to *Daphnia* without predation pressure (Boersma *et al.*, 1999; Fisk *et al.*, 2007). Seven known and three novel genes out of 31 candidates were reported to be upregulated when *Daphnia* is exposed to predatory insects (Miyakawa *et al.*, 2010).

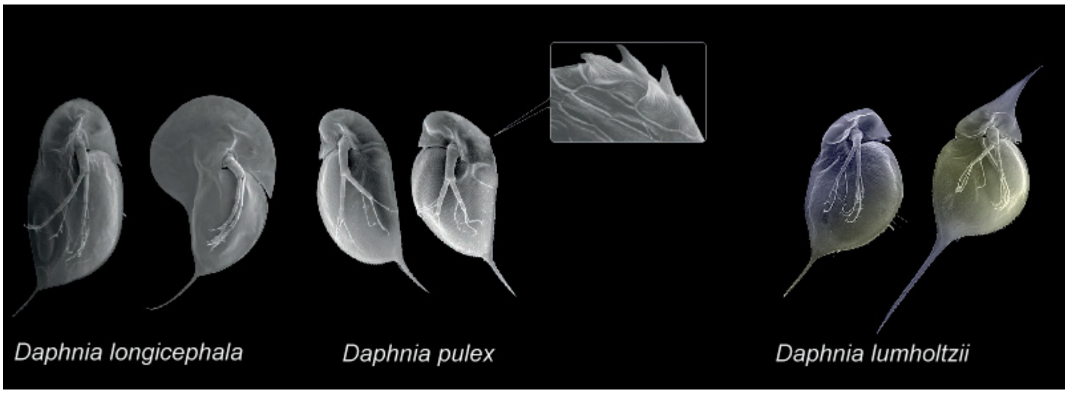

Fig. 1.8 Phenotypic plasticity in species of the genus *Daphnia*.

Kairomones from predators induce the formation of morphological defense structures such as helmets, lengthened spine or neck teeth (Ebert, 2011).

But not only under predation pressure will *Daphnia* show phenotypic intra-type variations within a single species. *Daphnia* is known to have a genetically based dietary tolerance against toxic cyanobacteria allowing it to persist cyanobacteria blooms (Hairston *et al.*, 2001; Schwarzenberger *et al.*, 2009). In *D. magna* three out of a total of seven investigated genes were identified to be significantly up regulated in the presence of toxic *Microcystis* strains (Schwarzenberger *et al.*, 2009). Under changing food conditions, regardless to body size, changes in filter sizes through phenotypic plasticity within single clones can be observed (Bednarska and Dawidowicz, 2007). Also clonal competition in *Daphnia* metapopulations is altered through parasites, with different parasite species causing different *Daphnia* clones to dominate as well as promoting host gene flow through immigrating hosts (Haag and Ebert, 2004; Altermatt and Ebert, 2007).

Further investigations will improve our understanding of the molecular mechanisms involved in phenotypic changes of characteristics and properties and their genomic structure and regulation. This knowledge will help to identify key characteristics and connect them to target genes that influence phenotypes, populations dynamics, biotic communities and in the end whole ecosystems (Miner *et al.*, 2012).

1.4 Effects of changes in temperature on organisms and their coping mechanisms

Temperature is a key factor for the performance and geographical distribution of aquatic and terrestrial animals, affecting particularly ectotherms in their cellular, systemic, and behavioral functions (Hochachka and Somero, 2002). Therefore, changes in the global climate and local temperature affect individual organisms, the size and structure of their populations, the species composition of communities, and the structure and functioning of ecosystems (Pörtner and Knust, 2007). The temperature tolerance of an animal is defined as the temperature range, in which the animal can actively maintain its life and its reproduction. Optimal reproduction and growth are only possible within the thermal optimum, outside that range, survival is possible only for limited time periods. . In aquatic ectotherms such as *Daphnia*, the rising metabolic rate with increasing temperature in combination with the decreasing oxygen content of water may cause tissue hypoxia and a formation of reactive oxygen species. At temperatures near to the thermal limit of the animal, cell stress due to macromolecular damage may arise. (Pörtner, 2002; Pörtner and Knust, 2007). Thus, cellular responses to heat include measures for improved oxygen transport or elevated heat tolerance, for instance, by an up-regulated expression of hemoglobin, antioxidant enzymes, or chaperones. Also characteristic is the switch from mechanisms and processes related to growth and reproduction to others related to cell maintenance and repair, including the programmed cell death (PCD) on the cellular level or the formation of resting stages on the organismic level.

In the natural habitat of *D. pulex* (ponds and small lakes), rapid and intense variations in temperature and oxygen content occur that require various short- and long-term adjustment mechanisms (Sell, 1998; Paul *et al.*, 2004; Paul *et al.*, 2012). The high number of gene duplications in *D. pulex* resulting in tandem gene clusters can strongly contribute to the great ability of *Daphnia* to withstand and adjust to environmental changes (Colbourne *et al.*, 2011). Thus, metabolic adjustments in *Daphnia* include, aside from changes in substrate or cofactor concentration, the induction and/or activation of isozymes and variations in the subunit composition of macromolecules based on the differential expression of isoforms (Lamkemeyer *et al.*, 2003; Schwerin *et al.*, 2009; Gerke *et al.*, 2011).

Even though numerous studies have been carried out on *Daphnia* (Ebert, 2011), only few studies focused on the *Daphnia* proteome so far (Fröhlich *et al.*, 2009; Schwerin *et al.*, 2009; Zeis *et al.*, 2009). In an overall qualitative approach, 531 proteins were identified in *D. pulex* (Fröhlich *et al.*, 2009). Quantitative analyses of environment-specific adjustments in long-term-acclimated *D. pulex* revealed specific sets of differentially expressed proteins (DEPs) for the comparisons hypoxia- versus normoxia-acclimation (Zeis *et al.*, 2009) and 10°C versus 20°C acclimation (Schwerin *et al.*, 2009). Hypoxia-acclimation mainly promoted the expression of hemoglobin subunits and enzymes involved in carbohydrate metabolism. 10°C acclimation particularly caused a down-regulation of proteolytic enzymes and an up-regulation of several vitellogenin and actin isoforms, indicating adjustments of the protein metabolism and reproductive processes.

1.5 Adaptation to the change of food availability

Natural populations are shaped by mutual action of top-down and bottom-up control. Top-down influences through predation on zooplankton populations such as *Daphnia* populations can be easily explained with the size-efficiency hypothesis. The size-efficiency hypothesis predicts that whenever predation by planktivores is intense, the standing crop of small algae will be high because of relatively inefficient utilization by small planktonic herbivores, and that of large algae will also be high because these cannot be eaten by the small herbivores (Brooks and Dodson, 1965). Factors in bottom-up control and their influences are more indistinct. A key factor of bottom-up control is food. Several studies have revealed that freshwater zooplankton frequently meet severe food shortages of quantitative as well as qualitative nature in natural environments (Lampert, 1985; Sommer *et al.*, 1986; Lampert, 1989; Müller-Navarra and Lampert, 1996; Bukovinszky *et al.*, 2012; Sommer *et al.*, 2012). In temperate lakes, seasonal food shortage arises as a consequence of herbivore grazing, since the phytoplankton biomass decreases rapidly to very low levels. During this 'clear-water' equilibrium phase, nutrients are recycled by the grazing process and may accumulate. These nutrients will be consumed during the period of growth of inedible algae species, which will develop in significant numbers. Competition for phosphate, for instance, leads to a replacement of green algae by large diatoms, which are only partly available to zooplankton as food (Sommer *et al.*, 1986). Herbivorous zooplanktonic species become food-limited during this time, which results in a decrease in their population densities and biomasses (Fig. 1.9) (Sommer *et al.*, 1986).

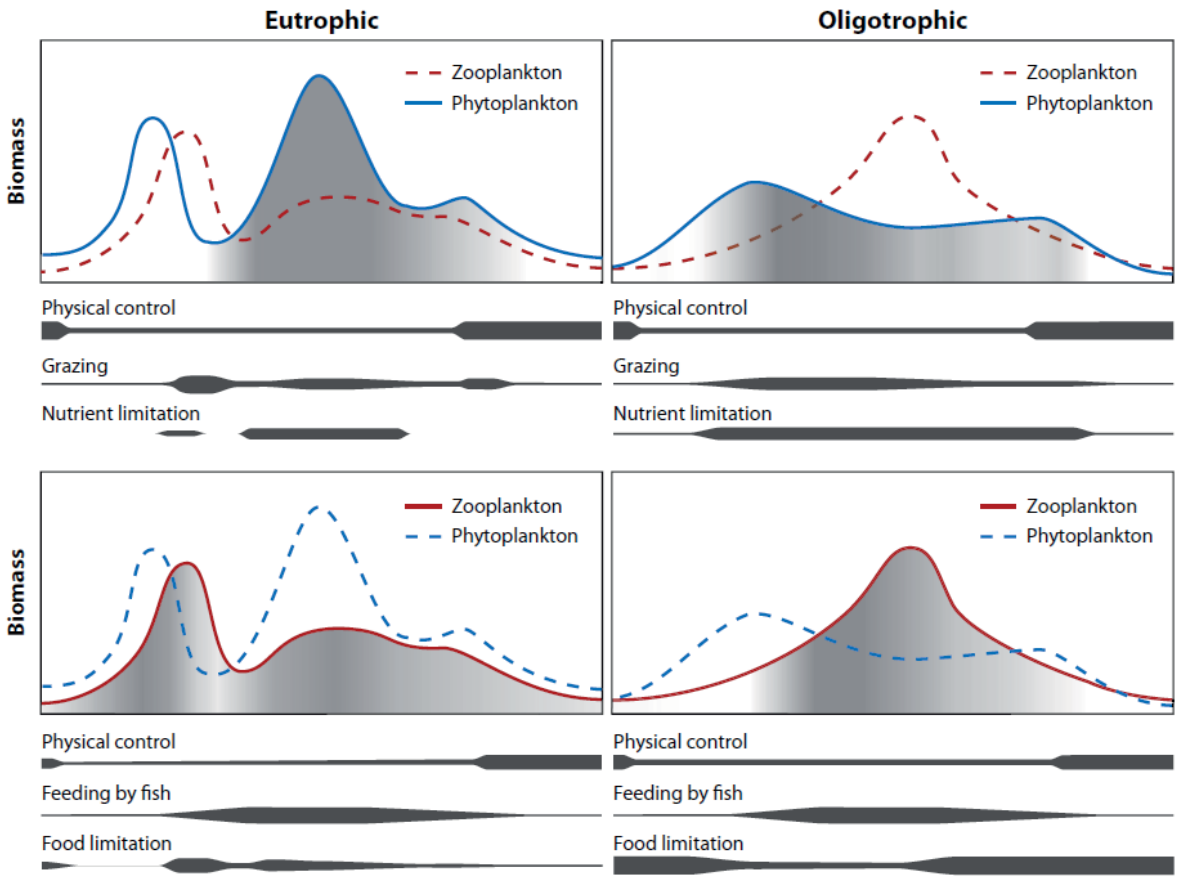

Fig. 1.9 Phytoplankton and zooplankton biomass curve formulated by the PEG model.

Seasonal (winter through autumn) biomass patterns in eutrophic (left) and oligotrophic (right) water bodies. (Top) Focus on phytoplankton (blue solid line) (dark shading, inedible for zooplankton; light shading, edible for zooplankton). (Bottom) Focus on zooplankton (red solid line) (dark shading, small herbivores; light shading, large herbivores). The thickness of the horizontal bars indicates the seasonal change in relative importance of physical factors, grazing, nutrient limitation, fish predation, and food limitation (Sommer *et al.*, 2012).

Since food quality and quantity has an important impact on fitness of organisms by influencing growth, survival and the reproductive output and thus the birth rate and potential abundance of a population (Lampert, 1978; Lampert, 1985; Sommer *et al.*, 1986; Urabe, 1991), it is crucial to determine the degree of food limitation of zooplankton and relate it to measurable food parameters to better understand bottom-up control mechanism.

Daphnia are unselective filter feeders and major herbivorous grazers of algae that play a significant ecological role in the dynamic of the food network (Miner *et al.*, 2012). Of all types of freshwater zooplankton, *Daphnia* have the greatest ability to graze phytoplankton and have the highest proportion of phosphorous (P) of all zooplankton taxa and the lowest nitrogen to phosphorous ratio (N:P) (Fig. 1.10) (Miner *et al.*, 2012). The size of the ingestible food particles ranges from 0.1 µm to 55 µm; it is dependent of the *Daphnia* species and reflects the mean mesh size of the filter combs and the carapace gape (Geller and Müller, 1981; Gophen and Geller, 1984). However, in response to low food concentrations, *Daphnia* can enlarge the area of the screens on its filtering limbs, representing an example of phenotypic plasticity. These increases in screen area also vary strongly among species. Larger filter screens result in higher filtering and feeding rates (Lampert, 1994).

For *Daphnia*, effects of food depend to a great extent on the quality of that food (Sterner *et al.*, 1993; Weers and Gulati, 1997). Thus daphnids show low growth rates, when fed P-limited algae and therefore completely hinges on the quality of the seston, which, besides particle shape and size of algae or detritus, also depends greatly on the biochemical composition of the selected food particles (Ahlgren *et al.*, 1992; Müller-Navarra, 1995; Weers and Gulati, 1997).

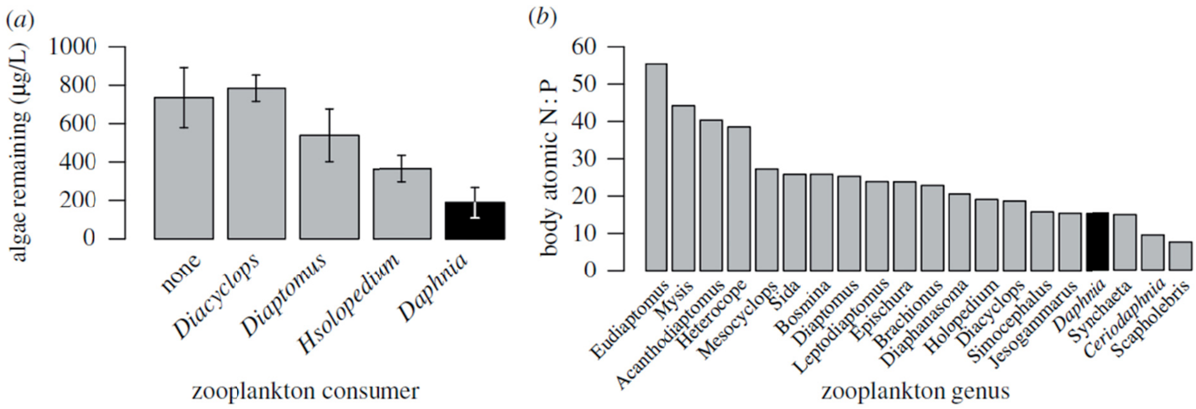

Fig. 1.10 Grazing ability and N:P ratio of *Daphnia*.

Measurements on the grazing effects of common freshwater zooplankton species (a) and N:P ratio in common freshwater zooplankton species (b). Members belonging to the genus *Daphnia* are exceptional among zooplankton because of their (a) high grazing rates on phytoplankton, (b) low N: P ratios that make them a high-quality (P-rich) food source (based on (Brett *et al.*, 1994; Miner *et al.*, 2012).

Consequently, herbivores often face starvation through nutrient limitation. When subjected to severe phosphorus deficiency, consumer growth may cease completely even when food quantity is not limiting, which potentially leads to strong population declines that may even cascade to higher trophic levels. At moderate levels of nutrient deficiency, consumers may partially compensate for the deleterious effects of poor food quality on growth by increasing feeding rates. The C and P balance in the algae food source does affect *Daphnia's* functional genomic response. Since *Daphnia* have especially high P demands, the response of particular

Daphnia species to P limitation influences gene expressions in direct and indirect ways and has considerable bearing on the upward transfer of energy in food webs with broad implications for aquatic ecosystems (Jeyasingh *et al.*, 2011). Within genetically diverse *Daphnia* populations, need of P varies. Animals with higher P requirements will have a higher growth rate and thus succeed in habitats with shorter growth periods. Selection experiments within *Daphnia* clones in the laboratory associated specific alleles of the glucose-6-phosphate isomerase (GPI) locus with variations in growth rate and P requirement (Jeyasingh *et al.*, 2009). In summary, not only shortage of food but also insufficient food quality can be limiting factors for zooplankton growth and reproduction (Sommer *et al.*, 2012). However, as food concentrations decrease, the effect of nutrient limitation, such as P-limitation weakens, while the importance of energetic costs will increase (Bukovinszky *et al.*, 2012).

1.6 Goals of the thesis

The aim of the present study was to investigate the proteome of two *D. pulex* clones differing in thermal tolerance upon the exposure to a) acute heat stress (transfer from 20°C to 30°C), b) acute starvation stress and c) the combination of both in a time-resolved manner (0, 24, and 48 hours of acute stress) to assess, firstly, major differences in clone-specific protein expression and, secondly, the temporal sequence of protein expressions under severe stress conditions. Differentially expressed proteins (DEPs) were identified by 2D gel electrophoresis, mass spectrometry, and subsequent bioinformatic analyses. Protein identification and quantification enabled an analysis of functions and processes under severe stress, with a specific focus on clone-specific differences in stress tolerance and the effects of a combination of stressors. The analysis of cellular adjustments in protein level under stress aimed at an identification of general emergency reactions and clonal differences in stress-induced proteomic responses.

2 Methods

2.1 Animals

The two *Daphnia pulex* clones G and M used for experimentation originated from different habitats. Clone G was isolated from a flooded and eutrophic quarry at Gräfenhain near Dresden, Germany (N50°49’04”, E10°42’02”) in 2002. This wind-sheltered, monomictic quarry with a surface area of 440 m^2 and a mean depth of 7 m is characterized by strong thermal stratification (Sell 1998; Matthes 2004). Clone M was isolated from a highly eutrophic seasonal pond in Münster, Germany (N51°57’48”, E7°34’38”) in 2007. In this temporarily flooded pond with a maximal water depth of 1 m, strong fluctuations in water level and temperature occur. The daphnids were cultured in 1.5 L M4 medium (Elendt and Bias, 1990) under normoxic conditions (T = 20 ± 0.3 °C) and a 16:8 h light:dark photoperiod. The animals were fed *ad libitum* (2.5 mg C/L) with *Desmodesmus subspicatus* (SAG 53.80, Göttingen, Germany) daily. To maintain parthenogenetic reproduction, three-quarters of the medium were changed twice a week, and animals were kept at a density of 50 – 100 individuals per beaker. Any males or ephippial females were removed on appearance. Adult females (2 – 2.5 mm, from the anterior part of the head to the base of the apical spine) were used for experimentation.

2.2 Clone identification by allozyme characterization

Individuals of each *D. pulex* clone were used for allozyme characterisation of the genotype. Cellulose acetate electrophoresis (Hebert and Beaton, 1989; Pinkhaus *et al.*, 2007) was performed for eight different enzyme loci: aldehyde oxidase (AO, EC 1.2.3.1), lactate dehydrogenase (LDH, EC 1.1.1.27), malate dehydrogenase (MDH, EC 1.1.1.37), mannose-6-phosphate isomerase (MPI, EC 5.3.1.8), amino-/dipeptidase (PEP, EC 3.4.11 or 3.4.13), glutamate oxaloacetate transaminase (GOT, EC 2.6.1.1), phosphoglucomutase (PGM, EC 5.4.2.2), and glucose-6-phosphate isomerase (GPI, EC 5.3.1.9). Pictures were adjusted with Ulead PhotoImpact X3 (Corel GmbH, München, Germany).

2.3 Motility and survival assay

For motility-and-survival assays at heat stress (30°C, *ad libitum* food supply) or starvation stress (20°C, no food), five or respectively ten 20°C-acclimated animals each were transferred to pre-tempered M4 medium: T = 20°C (control, starvation stress) or 30°C (heat stress). The media were mildly aerated using a membrane pump. For control and heat stress conditions, the animals were fed *ad libitum* with *Desmodesmus subspicatus* daily, whereas for starvation stress animals were not fed at all. Any freshly hatched juvenile *Daphnia* were removed. The number of regularly swimming *Daphnia* was counted, and immobile animals were removed.

Results were analyzed and Kaplan-Meier survival curves were plotted using *SigmaPlot 11.0* (Systat Software, Erkrath, Germany). Statistically significant differences ($P < 0.05$ and $P < 0.001$, Gehan-Breslow test) were determined with *SigmaPlot 11.0*.

2.4 Long term swimming assay

To determine maximal physiological performance under starvation stress and heat-and-starvation stress (30°C, no food), long-term swimming activity assays were carried out. The swimming activity assay used was derived from the test system described (Zeis *et al.*, 2004). For each assay, ten 20°C-acclimated *D. pulex* were transferred into a 4-mL flow-through cuvette. The cuvette was filled with pre-tempered aerated M4 medium, which was exchanged during the assay at a constant flow rate of 1 mL/min. During the whole experiment, the exchanged medium was kept at experimental temperature and mildly aerated with a membrane pump. Swimming activity was monitored at 580 nm in 5-sec intervals using a photometer. To take into account diurnal rhythms of the animals, each experiment was started at 5 p.m.. Swimming activity indices were calculated as described (Zeis *et al.*, 2004) and standardized to the mean value of the first 10 hours of measurement. Results were analyzed and plotted in *OriginPro 8.5* (OriginLab Corporation, Northampton, MA, USA).

2.5 Stress exposure and protein extraction

For each experiment, 25–30 animals were transferred to pre-incubated M4 medium. Depending on the type of stress, the following temperature and feeding conditions were applied. For control (T = 20°C) and heat stress conditions (T = 30°C for 24 h and 48 h), the animals were fed *ad libitum* with *Desmodesmus subspicatus* during experiments, except for a 12-h period at the end of incubation, during which they were kept in algae-free pre-tempered M4 medium to minimize contributions by algae proteins. During starvation experiments, animals were kept at T = 20°C and not fed during the incubation period (24 h and 48 h). For combined heat-and-starvation stress experiments, animals were not fed and kept at T = 30°C for 24 h and 48 h. Regularly swimming animals were then collected by sieving and after gently drying them on a paper tissue to remove adhering water, their fresh weight was determined, before they were shock-frozen in liquid nitrogen. For the extraction of total soluble protein, rehydration buffer (8 mol/L urea, 2 mol/L thiourea, 4% (w/v) CHAPS (3-((3-Cholamidopropyl)dimethylammonio)-propanesulfonic acid), 65 mmol/L DTT (dithiothreitol), 0.5% (v/v) ampholyte-containing IPG buffer pH 4–7 (Bio-Rad, München, Germany), one tablet of Complete Mini Protease Inhibitor Cocktail (Roche, Mannheim, Germany) per 3.5 mL solution) was added to each sample (1:10 w/v), which was then homogenized on ice using a Teflon® pistil. After centrifugation (17900 g, 4 min, 4°C), the supernatant was mixed 1:2 (v/v) with 25% TCA (trichloroacetic acid) and incubated on ice for 70 min. Proteins were precipitated by centrifugation (17900 g, 15 min, 4°C). The protein pellet was washed ten times by adding ice-cold 80% acetone (containing 0.2% DTT) followed by centrifugations (17900 g, 5 min, 4 °C). The pellet was then resuspended in 110 µL rehydration buffer. Protein concentrations were determined by Bradford assays (Bradford, 1976) using a Multimode Reader LB 941 TriStar (filter, F590/10; Berthold Technologies GmbH & Co. KG, Bad Wildbad, Germany).

For a validation of proteomic data by Western Blot analyses, aliquots from controls (20°C) and samples from heat stress experiments (T = 30°C for 24 h and 48 h) were kept. Prior to isoelectric focusing (IEF), 350 µg protein was diluted in rehydration buffer to an end volume of 110 µL and washed a second time using the ReadyPrepTM 2-D Cleanup Kit (Bio-Rad) according to the manufacturer's protocol. The protein was then dried at room temperature for maximally 5 min and resuspended in rehydration buffer to an end concentration of 1 µg/µL. Samples were kept at -80 °C.

2.6 Evaluation of total protein amount

The total protein content of raw extracts of the samples used for later two-dimensional (2D) gel electrophoreses was determined by Bradford assays. The statistical significance of changes in total protein content was determined with an independent two-sample two-tail Student's t-test ($P < 0.05$; *Microsoft Excel*). Figures were also created with *Microsoft Excel*.

2.7 Two-dimensional gel electrophoresis

For isoelectric focusing, linear IPG strips (17 cm, pH 4 – 7 ReadyStrip™; Bio-Rad) were passively rehydrated for 12 h in 350 µL of rehydration buffer containing brom phenole blue. IEF was performed in a manifold tray (IEF-StripholderEttan™IPGphor™ Cup Loading

Manifold; Amersham, Piscataway, NJ, USA) on an EttanIPGphor II isoelectric focusing unit (Amersham). 120 µg of protein extract was diluted in 150 µL of rehydration buffer and applied in a cup on the cathodic end. IEF was carried out at 15°C. Voltage settings comprised 50 V for 5.5 h, a 50–100 V gradient for 1 min, 100 V for 7 h, a 100–1000 V gradient for 10 min, 1000 V for 2 h, a 1000–4000 V gradient for 1 h, 4000 V for 2 h, a 4000–8000 V gradient for 45 min, and 8000 V until 45000 Vh were reached. Then, IEF Strips were equilibrated for 15 min in 10 mL equilibration buffer (0.05 mol/L Tris (tris(hydroxymethyl)aminomethane), 6 mol/L urea, 30% glycerol, 2% SDS (sodium dodecyl sulfate), pH 8.8) containing 1% DTT, and another 15 min in 10 mL equilibration buffer containing 2.5% iodoacetamide. In the second dimension, protein separation according to molecular mass was carried out using 12% polyacrylamide gels (0.56 mol/L Tris, 0.1% SDS, pH 8.8) in a Protean II xi cell (Bio-Rad). Electrophoresis was performed in a Tris-glycine buffer system (see (Schwerin *et al.*, 2009) at 15 mA for 15 min, and then at 40 mA for 10 h. PageRuler™ Protein Ladder (10–200 kDa; Fermentas, St.-Leon-Rot, Germany) was used for molecular mass calibration. Gels were stained with the fluorescent dye Ruthenium II tris (bathophenantroline disulfonate) (RuBPs) as described in (Lamanda *et al.*, 2004). Fluorescence intensity due to UV light excitation (UVT-20 M/W; Herolab, Wiesloch, Germany) was documented (Olympus E410, 14–42 mm/ F 3.5–5.6) using *Olympus Studio 2* (Olympus, Hamburg, Germany)) and analyzed with *Delta 2D 4.3* (DECODON, Greifswald, Germany). Gels were warped using the exact warp mode and fusion gels were created using the union mode. Pictures were adjusted with *Ulead PhotoImpact X3*.

2.8 Analysis of differential protein expression

Preceding the quantification of protein expression from staining intensities in the gels, a normalization procedure was done setting the total spot quantity to 100% for each gel image. Protein expression was assessed by calculating the individual spot quantity in proportion to the total spot quantity for each 2D gel. Spot quantities were calculated in Delta2D. The statistical significance of changes in protein expression was determined with Student's t-test ($P < 0.05$). Results were processed with *Microsoft Excel*, and graphs were plotted using *OriginPro 8.5*. Differences in protein amounts for different categories (Fig. 3.11, 3.15, 3.19) and in ratio values for different categories and protein families (Fig. 3.20–3.22) were assessed by two-way analysis of variance (ANOVA) using *SigmaPlot 11.0*. In case of statistically significant differences ($P < 0.05$), an "all pairwise multiple comparison" procedure ($P < 0.05$, Student-Newman-Keuls method, SNK) was applied to determine differing pairs of means.

2.9 LC-MS/MS, identification and characterization of proteins

RuBPs-stained protein spots were excised from the gel and subjected to overnight in-gel trypsin digestion according to established protocols (Shevchenko *et al.*, 2007). Peptides were resuspended in eluent A (see below) and analyzed by LC-MS/MS on an Ultimate 3000 Nanoflow HPLC system (*Dionex* Corporation, *Sunnyvale,* CA, USA) coupled to an LTQ Orbitrap XL mass spectrometer (Thermo Finnigan, Bremen, Germany). Eluents were composed of aqueous solutions of 5% (v/v) acetonitrile (JT Baker, *Deventer,* Netherlands)/0.1% (v/v) formic acid (eluent A) and 80% acetonitrile/0.1% formic acid (eluent B). The flow rate was set to 300 nL/min.

The sample (1 µL) was loaded onto a trap column (C18 PepMap100; 300 µm i.d. x 5 mm, 5 µm particle size, 100 Å pore size; Dionex) and desalted using eluent A at 25 µL/min for 4 min. Subsequently, the trap column was switched in series with a capillary column (Atlantis dC18; 75 µm x 150 mm, 3 µm particle size, 100 Å pore size), and the following gradients for eluent B were applied for peptide separation: 0 – 12% (10 min), 12 – 50% (45 min), 50 – 100% (2 min), and 100% (5 min). The column was re-equilibrated with 100% eluent A for 10 min. Peptides eluted directly into the nanospray source of the mass spectrometer.

The mass spectrometer was operated in positive ion mode. Survey scans were obtained by FT-MS (*m/z* 375 – 2000) at a resolution of 60.000 FWHM using internal lock mass calibration on *m/z* 445.120025. The five most intense ions were sequentially subjected to CID-fragmentation (35% normalized collision energy) in the linear ion trap (MS2). Fragment ions were analyzed in the mass analyzer of the ion trap. Dynamic exclusion was enabled with a repeat duration of 60 s, repeat count of 1 and exclusion mass width of ± 5 ppm.

For the identification of peptides, MS2 spectra were matched against the *D. pulex* "Filtered Models v1.1", the "Frozen Gene Catalog protein database v 1.1" (containing all manual revisions as well as automatically annotated models chosen from the "Filtered Models v1.1") (Colbourne *et al.*, 2011) as well as the "allModels of 2007 set" and the *Daphnia*_genes2010_beta3 (*D. pulex* Gene Set 2.0 beta3, 2010 April; http://wfleabase.org/) database (*Daphnia* Genomics, *Daphnia pulex* v1.0; http://genome.jgi-psf.org/Dappu1/Dappu1.home.html) using the SEQUEST® algorithm implemented in Bioworks 3.3.1 SP1 (Thermo Finnigan), OMSSA 2.1.4 (Geer *et al.*, 2004), and X!tandem release CYCLONE (2012.10.01) (X! Tandem, http://www.thegpm.org/TANDEM/index.html; (Craig and Beavis, 2004). Evaluation of the mass spectrometric results, matching and aligning peptides to genes and calculating sequence coverage values were done with Proteomatic (Specht *et al.*, 2011). The maximum number of missed cleavages allowed was two. Mass accuracy was set to 5 ppm for MS1 precursor ions and 0.8 Da for product ions. Oxidation of methionine was included as variable parameter. A minimum of three identified peptides and/or sequence coverage of at least 30% were considered necessary for positive protein identification. If multiple proteins in a spot matched these criteria, either the protein with the highest peptide count (NP) or in case of equal peptide counts that with the highest sequence coverage (SC) and the best match between M_re and M_rp and pI*e* and pI*p* was assigned to the spot (see Table 3.2 for abbreviations). Putative protein functions were identified by the automated blastp search of the Joint Genome Institute (Colbourne *et al.*, 2011). The derived protein sequences were analyzed for putative N-terminal signal sequences using SignalP V4.0 (Petersen *et al.*, 2011). M_rp and pI*p* of the mature proteins (proteins without signal peptide) were determined by the ExPASy proteomic tool “Compute pI/MW” (Gasteiger *et al.*, 2005).

2.10 HSP60 quantification with Western Blots

To validate exemplarily results from the proteomic studies, heat shock protein 60 (HSP60) quantities were determined by Western Blots. Samples containing equal masses of protein (120 µg) were subjected to 10% acrylamide SDS-PAGE along with the protein mass marker PageRuler Plus Prestained (11–250 kDa; Fermentas, St.-Leon-Rot, Germany) and standardized extracts from heat-stressed human HeLa cells as positive control. Separated proteins were blotted (18.5 h, 100 mA; RT) to a nitrocellulose membrane. HSP60 contents was determined by Western Blotting using anti-human primary anti-Hsp60 (SPA-805; BIOTREND, Köln, Germany) as described in (Mikulski *et al.*, 2009) and subseqequently goat anti-rabbit horseradish peroxidase-conjugated secondary antibody solution (Sigma, Germany) as described in (Becker, 2011). Detection of the chemiluminescence upon incubation with luminol (final concentration, 1.25 mmol/L) and p-coumaric acid (final concentration, 0.2 mmol/L) was performed by photography (Amersham Hyperfilm ECL, GE Healthcare, Germany). For each digitized gel image (Epson Perfection V700 Photo; EPSON, Meerbusch, Germany), HSP60 quantities were normalized with respect to the HSP bands of the HeLa cells extracts (Mikulski *et al.*, 2009; Becker, 2011). Intensities were evaluated using *ImageJ* 1.47 m (W. Rasband, National Institutes of Health, USA). Calculation of induction ratios

(*Daphnia* HSP60 vs HeLa HSP60) and statistical analyses (t-tests, $P < 0.05$) were carried out with *Microsoft Excel*. Pictures were adjusted with *Ulead PhotoImpact X3*, and figures were created with *Microsoft Excel.*

3 Results

3.1 Clonal characterization by allozyme analysis

Allozyme analysis was used to characterize two *D. pulex* clones. Fifty-two individuals of clone G and twenty-eight individuals of clone M were analyzed by conducting native cellulose acetate electrophoresis and activity staining at eight enzyme loci: *AO*, *GOT*, *GPI*, *LDH*, *MDH*, *MPI*, *PEP*, and *PGM*. All these enzymes showed homozygous patterns. Clonal differences were observed only in case of three loci: aldehyde oxidase (*AO*, Fig. 3.1A), lactate dehydrogenase (*LDH*, Fig. 3.1B), and malate dehydrogenase (*MDH*, Fig. 3.1C). For *AO*, the clones differed in medium-speed (M) alleles (G: M_1M_1, M: M_2M_2). Clone G showed slow (S) alleles for *LDH* and *MDH*, whereas fast (F) alleles for *LDH* and *MDH* were characteristic for clone M.

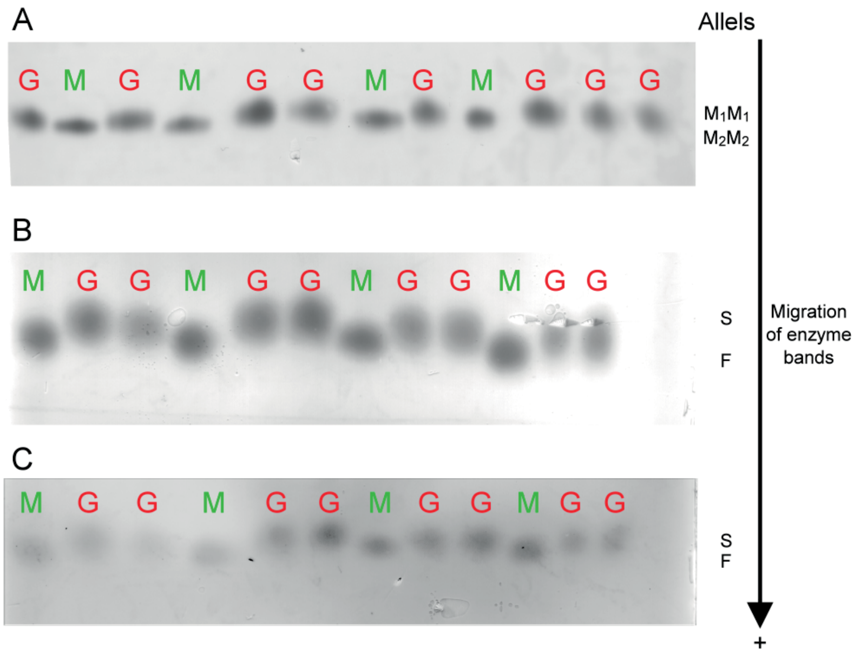

Fig. 3.1 Genotypic differences between clone G and M at three enzyme loci.

The clones differed in allozyme patterns for (**A**) aldehyde oxidase (AO; clone G, M1M1 vs clone M, M2M2), (**B**) lactate dehydrogenase (LDH; clone G, S vs clone M, F), and (**C**) malate dehydrogenase (MDH; clone G, S vs clone M, F). Each band represents a single individual (red letters: clone G; green letters: clone M).

3.2 Temporal changes in motility and long-term survival under control and stress conditions

The two *D. pulex* clones M and G did not significantly differ in motility (i.e., regular swimming activity) and long-term survival at control conditions (20°C, *ad libitum* food supply). There were also no significant differences between the two clones during starvation stress (20°C, no food) (Fig. 3.2).

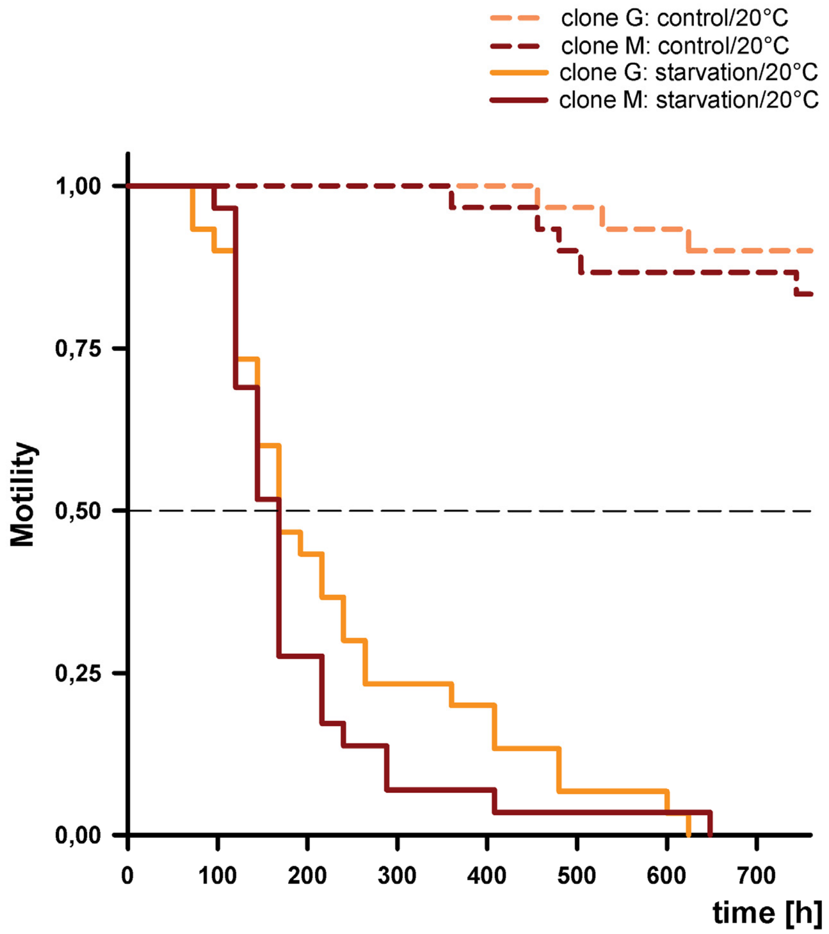

Fig. 3.2 Temporal changes in motility and long-term survival under control conditions and starvation stress.

Kaplan-Meier survival curves for *D. pulex* clone G (orange lines) and M (brown lines) under starvation stress (solid lines; 20°C, no food) and at control conditions (broken lines; 20°C, *ad libitum* food supply) (n = 3 experiments on N = 10 individuals each). Starvation stress and control curves for clone G and M did not differ significantly (Gehan-Breslow test, $P < 0.05$).

In a next step, effects of heat stress (30 °C, food *ad libitum*) were tested in both clones and revealed heat tolerance to be much higher in the *D. pulex* clone M than in clone G (Fig. 3.3).

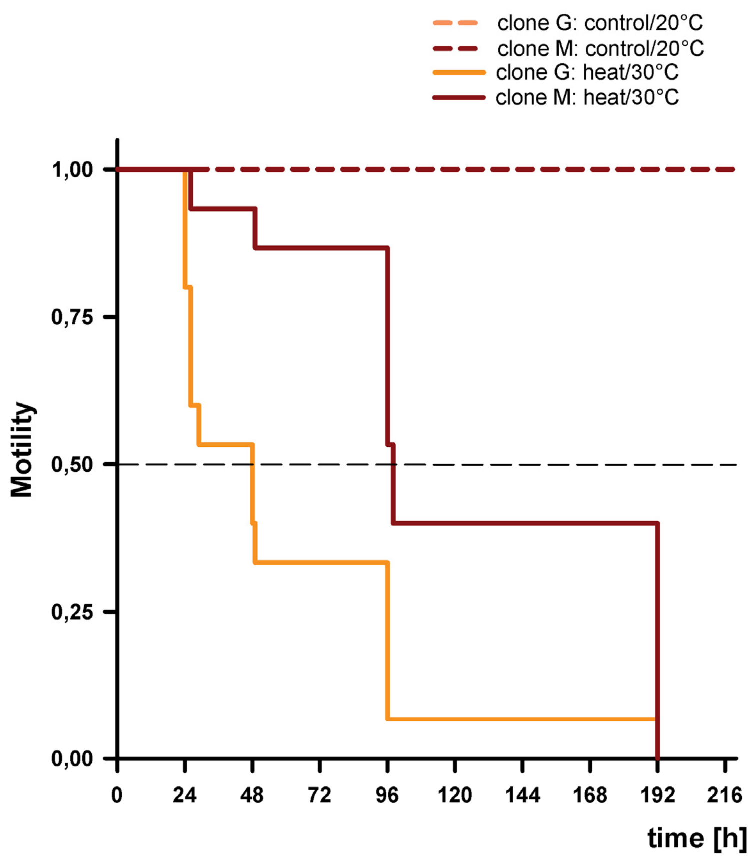

Fig. 3.3 Temporal changes in motility and long-term survival under control conditions and heat stress.

Kaplan-Meier survival curves for the *D. pulex* clone G (orange lines) and M (brown lines) at heat stress (solid lines, 30°C, *ad libitum* food supply) (n = 3 experiments on N = 5 individuals each) and under control conditions (broken lines; 20°C, *ad libitum* food supply) (n = 3 experiments on N = 10 individuals each). Curves for clone G and M at heat stress differed significantly (Gehan-Breslow test; $P < 0.001$).

Regular swimming activity assays under heat-and-starvation stress (30°C, no food) revealed a much higher stress tolerance in clone M than in clone G (Fig. 3.4 B, D). No differences in stress tolerance were detected under pure starvation stress (Fig. 3.4A, C).

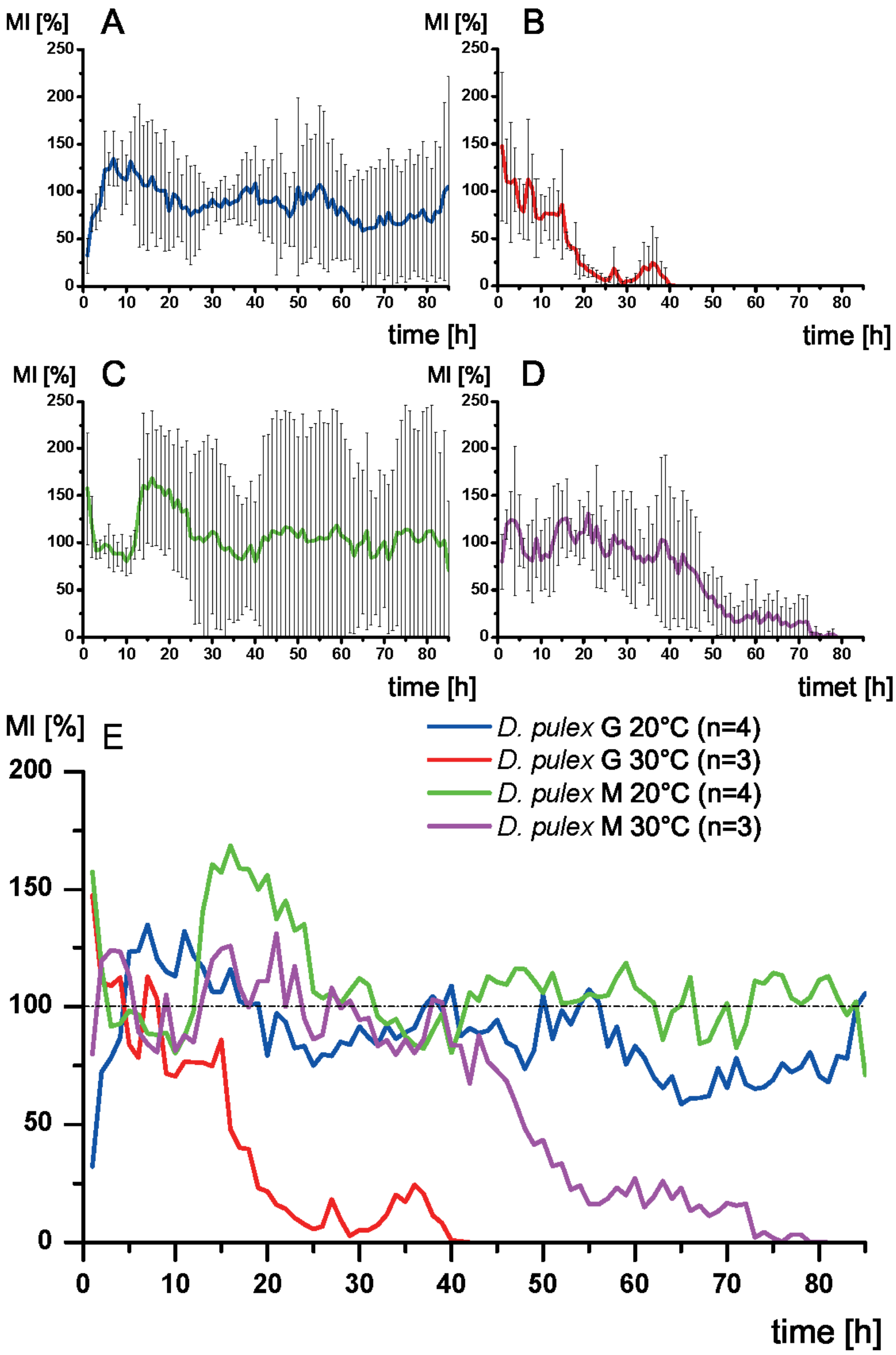

Fig. 3.4 Temporal changes in motility and survival under starvation stress and heat-and-starvation stress.

Motility (motility index, MI; i.e., long-term swimming activity) and survival of (**A**) (n = 4 on N = 10 individuals each) and (**B**) (n = 3 on N = 10 individuals each) *D. pulex* clone G and (**C**, **D**) (n = 4 each on N = 10 individuals each) *D. pulex* clone M under (**A**, **C**) pure starvation stress (20°C, no food) or (**B**, **D**) heat-and-starvation stress (30°C, no food) (means ± S.D. of normalized data; 100%, average of the first ten hours). (**E**) Comparison of all results.

Motility decreased to half-maximal values (MT_{50}) in 167 hours (clone G and M) at starvation stress, 48 hours (clone G) or 98 hours (clone M) at heat stress, and 17 hours (clone G) or 49 hours (clone M) at heat-and-starvation stress (Table 3.1).

Table 3.1 Times for decreases in motility to half-maximal values (MT_{50}) under control and different stress conditions

In motility, survival and long-term-swimming assays evaluated mean time of half-maximal motility (MT_{50}) of *D. pulex* clone G and M.

	control condition	starvation stress	heat stress	starvation-and-heat stress
clone G	> 750 h	167 h	48 h	17 h
clone M	> 750 h	167 h	98 h	49 h

3.3 Protein expression at different environmental conditions

3.3.1 Total protein quantities at different environmental conditions

Prior to two-dimensional (2D) gel electrophoresis and mass spectrometry, the total protein content of raw extracts from animals at different environmental conditions was determined. Under control conditions, the total protein content was almost identical in both clones (clone G vs clone M, 24 vs 25 µg protein/mg fresh weight, FW). In clone G, there was almost no change in total protein content at heat stress. However, 24 and 48 hours of starvation stress or heat-and-starvation stress caused considerable decreases in total protein content (Fig 3.5). Clone M, however, did not show significant changes in total protein content at any stress condition. Protein quantity was always above 18 µg protein/mg FW (Fig 3.5).

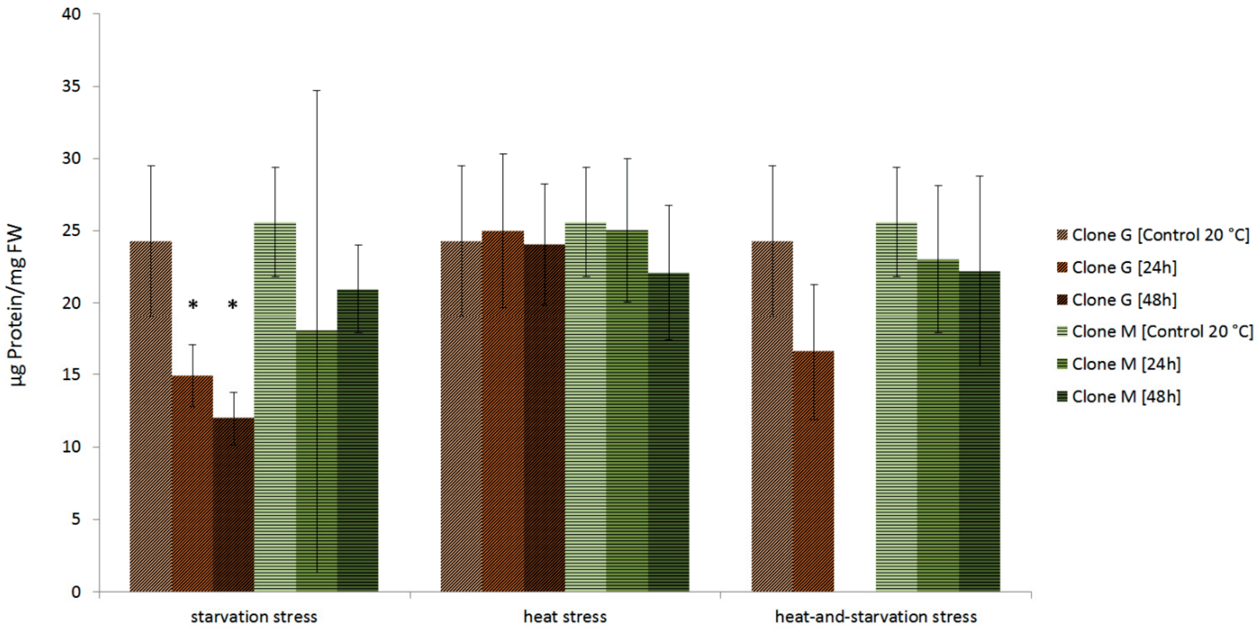

Fig. 3.5 Total protein quantities under control and stress conditions.

Total protein content under control conditions (20°C, *ad libitum* food supply), starvation stress (20°C, no food), heat stress (30°C, *ad libitum* food supply), and heat-and-starvation stress (30°C, no food) in *D. pulex* clone G and clone M. Clone G (means ± S.E.M; control conditions (*n*=5), starvation stress ([24h] *n*=4, [48h] *n*=4), heat stress ([24h] *n*=4, [48h] *n*=6) and heat-and-starvation stress ([24h] *n*=5) determintations on *N* = 25 – 30 animals each) and clone M (means ± S.E.M; control conditions (*n*=4), S-stress ([24h] *n*=4, [48h] *n*=5), H-stress ([24h] *n*=3, [48h] *n*=10) and HS-stress ([24h] *n*=5, [48h] *n*=7) determintations on *N* = 25 – 30 animals each). Asterisks indicate significant differences between acute exposures and control conditions for each experimental setup (two-sample two tail Student's t-test, $P < 0.05$).

3.3.2 Protein expression at control conditions (20 °C, *ad libitum* food supply)

2D gel electrophoresis, mass spectrometry of excised protein spots, and computer-based data evaluation were used to identify and quantify up- and down-regulated proteins and their amounts under various stress conditions. Representative reference gels for each clone under control conditions served as orientation for spot excision (Fig. 3.6, 3.7). A total of 674 protein spots were detected on the fusion (averaged) images of 2D gels from control or stressed animals. 95 spots were excised and analyzed by mass spectrometry, which enabled protein identification in 78 cases, with 34 identified proteins in total. Proteins in the remaining 17 spots did not match with the *D. pulex* database or could not be clearly assigned to specific proteins. The excised spots showed a high staining intensity, which implies that identified proteins were present in large quantities. According to function, identified proteins were assigned to different categories (antioxidative defense/detoxification, ATPase, carbohydrate binding/metabolism, chaperone, cytoskeleton/muscle protein, kinase, proteolytic enzyme, transcription factor, transport protein, ubiquitin/proteasome system).

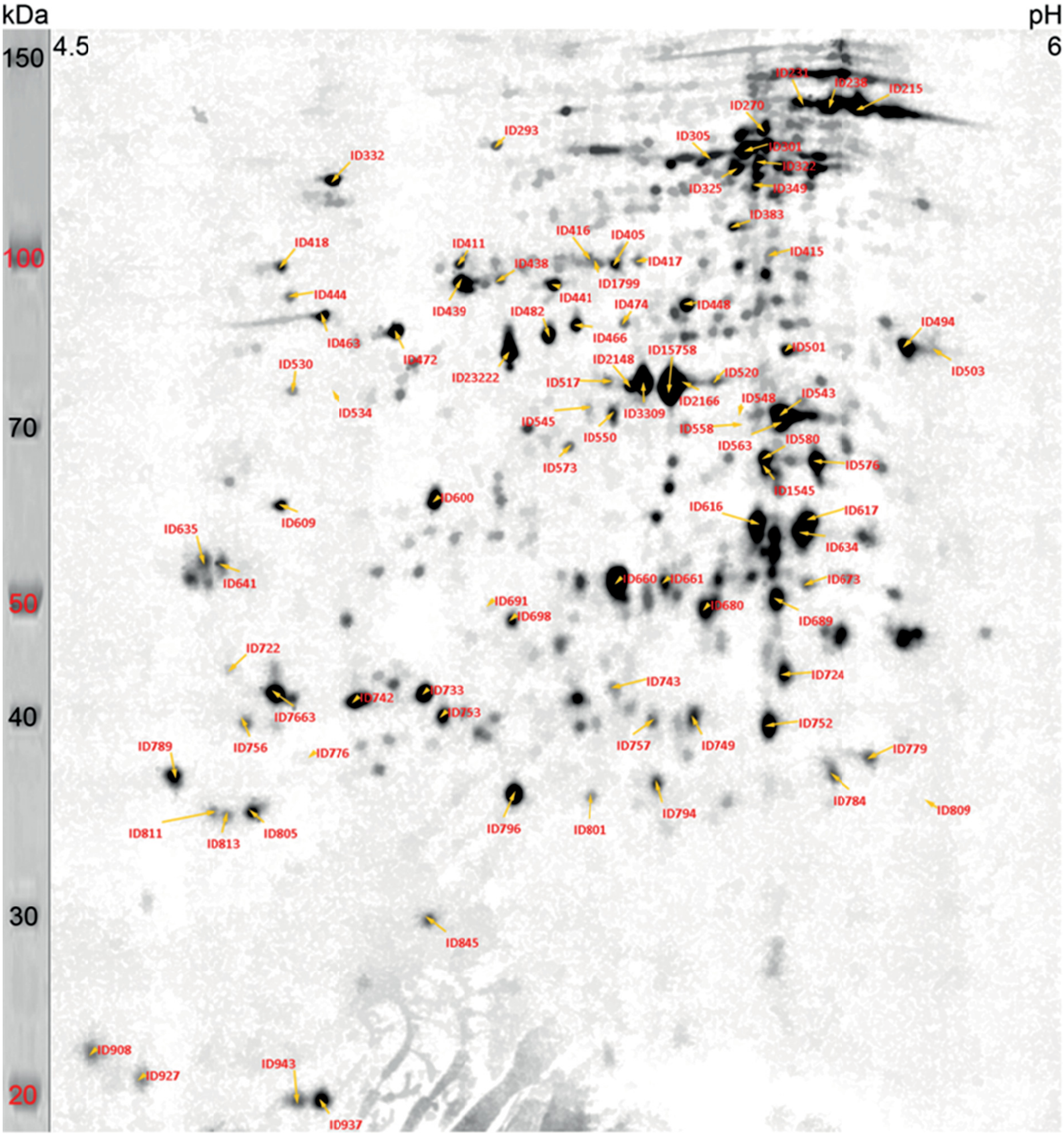

Fig. 3.6 Two-dimensional protein gel from the 20°C-acclimated clone G.

The RuBPs-stained 2D gel served as reference for the excision of protein spots for mass spectrometry (pI: 4.5–6, molecular weight: 20–150 kDa). Red characters are spot identifiers (spot IDs).

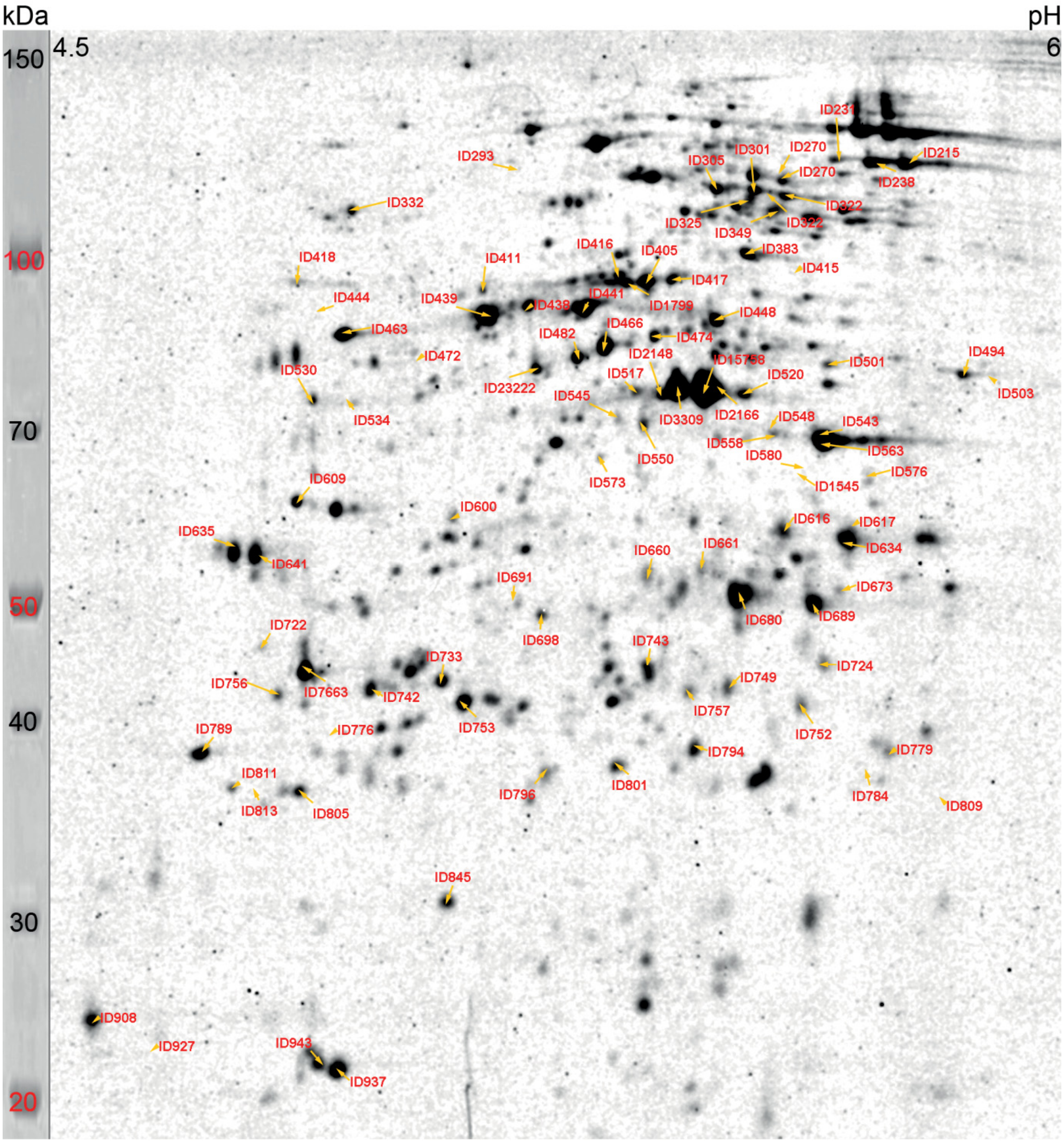

Fig. 3.7 Two-dimensional protein gel from the 20°C-acclimated clone M.

The RuBPs-stained 2D gel served as reference for the excision of protein spots for mass spectrometry (pI: 4.5–6, molecular weight: 20–150 kDa). Red characters are spot identifiers (spot IDs).

3.3.3 Protein expression at heat stress (30 °C, *ad libitum* food supply)

To study acute heat effects on protein expression in clone G and M, they were either kept under control conditions (20°C) or incubated for 24 hours or 48 hours at 30°C. Twenty-two protein spots in case of clone G (Fig. 3.8) and 24 protein spots for clone M (Fig. 3.9) comprised proteins showing significant ($P < 0.05$) differential expression when contrasting 30°C (24-hour or 48-hour incubations) vs 20°C.

Differentally expressed proteins

With regard to the functional category 'antioxidative defense/detoxification', three different isoforms of glutathione transferases were identified in three spots, with one isoform (gene ID: 303282) up-regulated in clone G, another one (305501) up-regulated in clone M, and the third one up-regulated in both clones (Tables 3.2, 3.3). Within the category 'ATPase', two different isoforms of the H^+-transporting two-sector ATPase were identified in eight spots. One isoform (306451) was up-regulated in clone M, and the other one (309746) was mainly up-regulated in clone G. Seven different proteins for 'carbohydrate binding/metabolism' were identified in ten spots. Glycoside hydrolases of the families 7 and 16 were down-regulated (particularly in clone G). In case of the category 'chaperone', four different proteins were detected in four spots. In case of clone M, but not in clone G, heat shock protein 60 (HSP60) was highly up-regulated upon heat stress. Calreticulin was up-regulated in clone G, and protein disulphide isomerase in clone M. Within the category 'cytoskeleton/muscle protein', two different isoforms of alpha tubulin, one beta tubulin and three different isoforms of actin were identified in fourteen spots. Upon heat stress, the quantity of one alpha tubulin isoform (100611) increased only in clone G, whereas that of the other one (301837) increased in both clones, as it was the case for beta tubulin. With respect to actin, one isoform (306442) was up-regulated only in clone G, and another one (305550) only in clone M. Within this category, the expression intensity due to heat stress seemed to be higher in clone G. Two different proteins for the category 'kinase' were detected in eight spots. Only one of them (arginine kinase) was found to be regulated (in clone G), with one (spot ID: 757) showing up-regulation and the other one (spotID: 796) down-regulation. Two of the four different proteolytic enzymes from five spots were down-regulated (particularly in clone M). Most of the corresponding genes coded for a signal peptide sequence, which indicates intestinal digestive functions. The putative transcription factor FOG was up-regulated, more intensely in clone M. The quantity of vitellogenin from the category 'transport protein', which comprised two different proteins from 20 spots, increased particularly in clone M. Again, the quantity of one isoform (308693) increased only in clone G, and that of the other one (219769) only in clone M. The high discrepancy between experimental and predicted molecular weights for vitellogenin (12.1–117 *vs.* 191.9–224.8 kDa) indicates that these proteins were fragments resulting from protein cleavage. A protein within the cytosolic fatty-acid binding category was down-regulated in clone M. Two different proteins from the category ‘ubiquitin/proteasome system’, which were detected in four spots, decreased only in clone G. Ubiquitin was found as a companion protein in several spots, indicating that some proteins were tagged for degradation. The higher experimental molecular weights (18.3–107.3 kDa) than the predicted one (5.7 kDa) indicate attachments to non-identified target proteins.

In summary, acute heat stress affected the *D. pulex* clones G and M differently as evidenced from differing differentially expressed isoforms in most cases as well as frequent differences in expression intensity or regulatory pattern. Altogether, 18 proteins were significantly up-regulated, with five of them up-regulated in both clones. Seven proteins were specifically up-regulated in clone G, and six proteins were up-regulated only in clone M. A total of eleven proteins were significantly down-regulated, with five of them specific for clone G and four for clone M. Two digestive proteins, one carbohydrate processing and one protein degrading enzyme, were down-regulated in both clones.

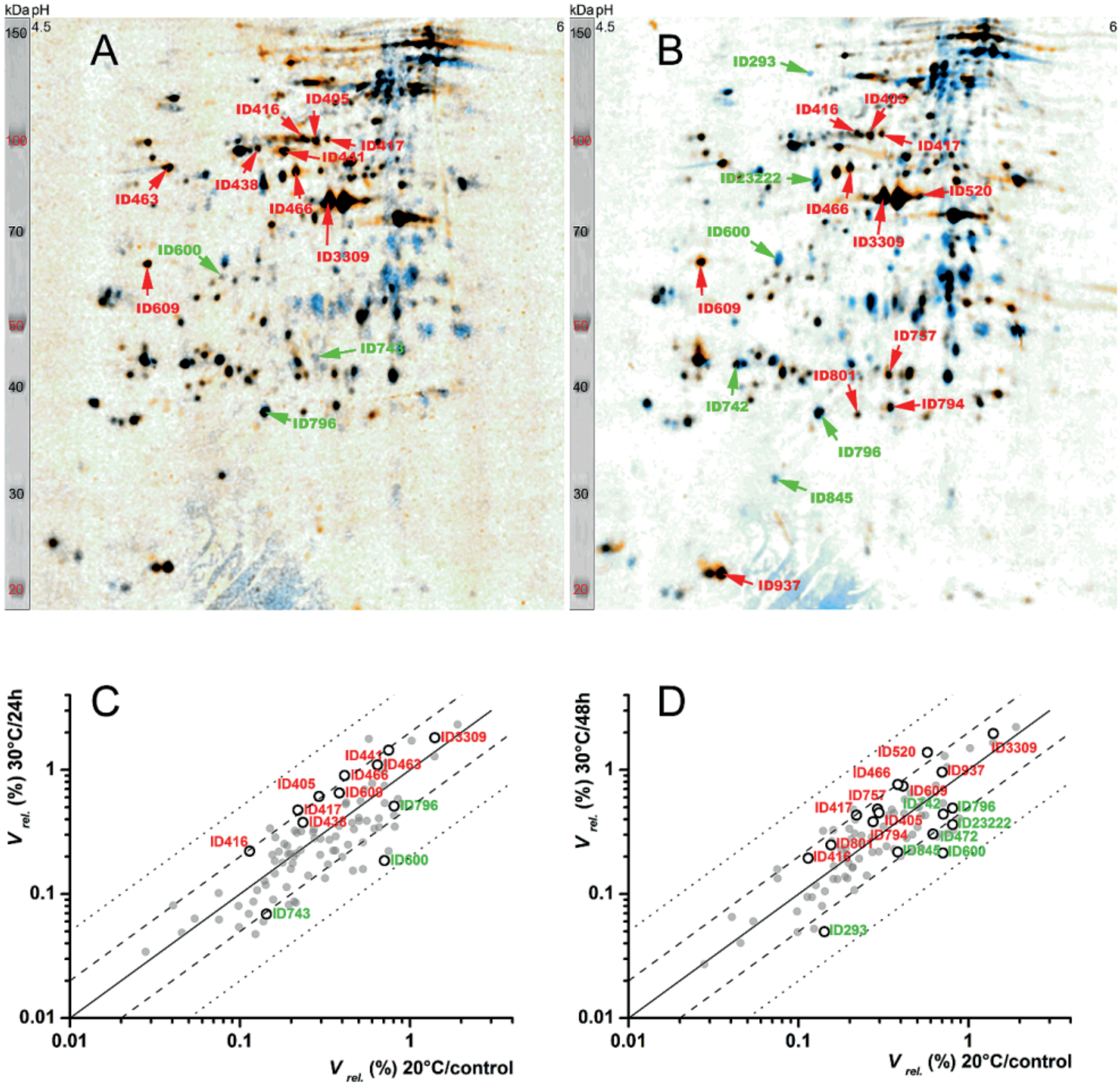

Fig. 3.8 Two-dimensional protein gels from the heat-stressed *Daphnia pulex* clone G.

The 2D gel images are fusion (averaged) images of different numbers (*n*) of biological replicates showing changes in protein expression upon the acute exposure of 20°C acclimated *D. pulex* clone G (blue spots; *n* = 5) to (**A**) 24 hours (orange spots; *n* = 4) or (**B**) 48 hours (orange spots; *n* = 6) of heat stress (30°C). Red spot IDs mark significantly up-regulated proteins, and green spot IDs indicate significantly down-regulated proteins (t-tests, $P < 0.05$; Table 3.2). The scatter plots show changes in expression level ($V_{rel.}$, relative spot volume) between (**C**) 30°C/24 h or (**D**) 30°C/48 h contrasted with 20°C/control (data from the fusion images; open circles, significant regulations; gray circles, non-significant regulations; dashed lines, 2-fold changes; dotted lines, 5-fold changes; heat-induced proteins are found above the solid lines).

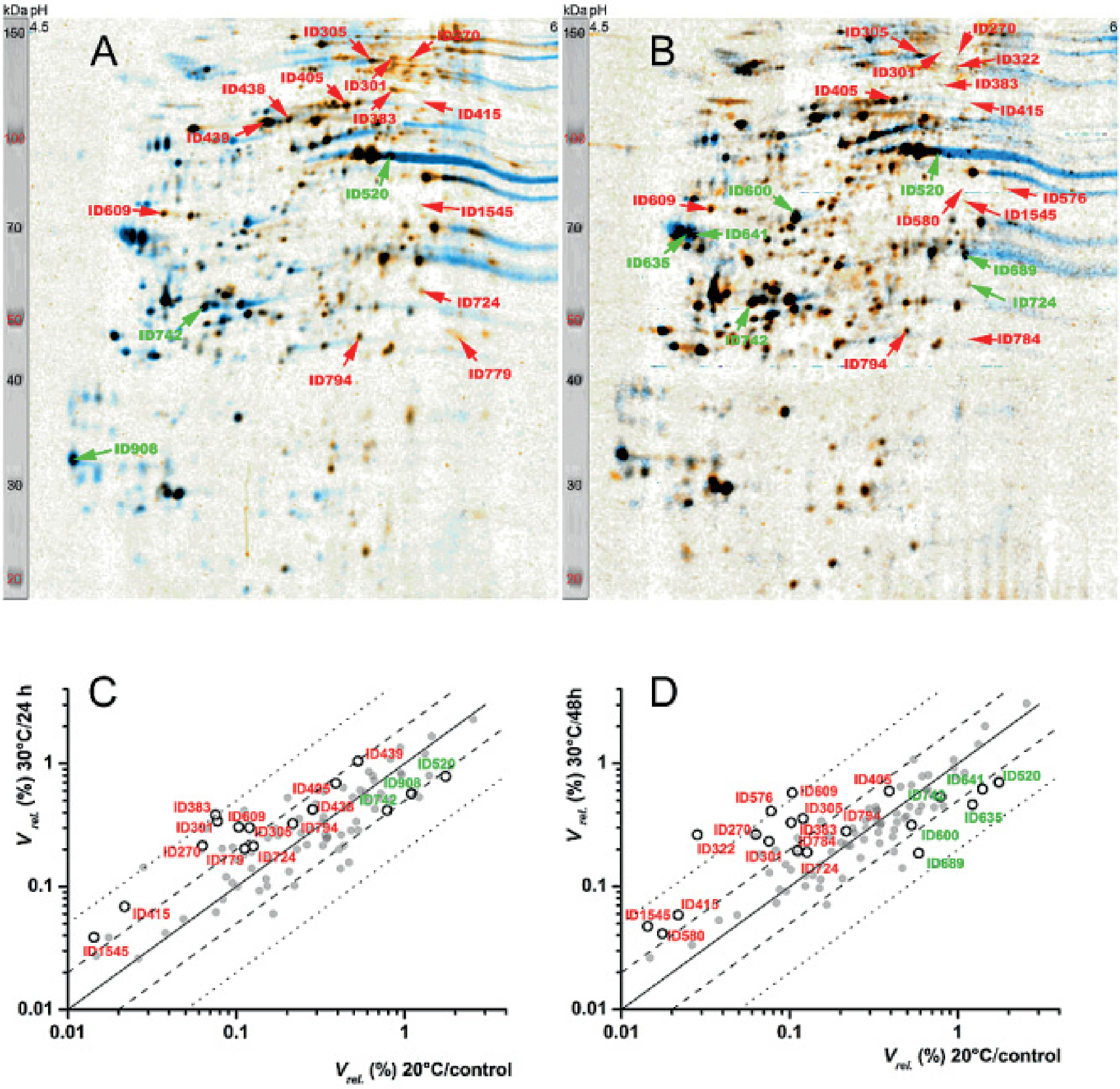

Fig. 3.9 Two-dimensional protein gels from the heat-stressed *Daphnia pulex* clone M.

The 2D gel images are fusion (averaged) images of different numbers (n) of biological replicates showing changes in protein expression upon the acute exposure of 20°C acclimated *D. pulex* clone M (blue spots; n = 4) to (**A**) 24 hours (orange spots; n = 3) or (**B**) 48 hours (orange spots; n = 10) of heat stress (30°C). Red IDs mark significantly up-regulated proteins, and green IDs indicate significantly down-regulated proteins ($p < 0.05$; Table 3.3). The scatter plots show changes in expression level ($V_{rel.}$, relative spot volume) between (**C**) 30°C/24 h or (**D**) 30°C/48 h contrasted with 20°C/control (data from the fusion images; open circles, significant regulations; gray circles, non-significant regulations; dashed lines, 2-fold changes; dotted lines, 5-fold changes; heat-induced proteins are found above the solid lines).

Table 3.2 Proteins from the *D. pulex* clone G after 24 or 48 hours of heat stress (30°C) in comparison to control conditions (C, 20°C).

After applying 2D gel electrophoresis and nano-HPLC ESI-MS/MS analysis of trypsin-digested protein spots, identified peptides were matched against the "Filtered Models_v1.1_fixed-database" of the *D. pulex* protein database. The table shows spot identifying number (spot ID; see Fig. 3.6, 3.7), experimental and predicted molecular weights (M_re, M_rp) and isoelectric points (pI*e*, pI*p*) of the mature protein (without signal peptide), sequence coverage (SC; percentage of the predicted protein sequence covered by fitting peptide sequences), number of fitting peptides (NP), protein function as described in the protein sequence database of the *D. pulex* genome assembly v1.0 (Colbourne *et al.*, 2005), gene ID (JGI_V11_gene id), predicted length of N-terminal signal peptide (SP), expression ratio (R; 30°C/24 h or 30°C/48 h vs. 20°C/control) and associated *P* value (t-test).

	Spot ID	M_re	M_rp	pI*e*	pI*p*	SC (%)	NP	Function	Gene ID	SP	R	*p*	R	*p*
											30°C/24 h *vs.* C		30°C/48 h *vs.* C	
								Antioxidative defense/detoxification						
1	801	24.2	24.8	5.3	5.4	36.8	12	Glutathione transferase	303282	-	1.3	0.074	**1.6**	**0.001**
2	784	25.3	25.2	5.8	5.6	36.2	10	dito	305501	-	0.9	0.674	1.4	0.297
3	794	25.0	25.0	5.4	5.2	67.3	18	dito	317266	-	1.0	0.844	**1.4**	**0.047**
								ATPase						
4	415	66.9	55.5	5.7	5.5	57.6	56	H(+)-transporting two-sector ATPase	306451	-	0.7	0.545	0.8	0.573
5	441	78.1	56.8	5.2	5.5	43.8	16	dito	309746	-	**1.9**	**0.004**	1.4	0.074
6	466	71.4	56.8	5.2	5.5	79.4	56	dito	309746	-	**2.2**	**0.005**	**1.8**	**0.003**
7	482	69.7	56.8	5.2	5.5	80.5	64	dito	309746	-	0.8	0.304	1.4	0.312
8	23222	66.8	56.8	5.1	5.5	65.5	23	dito	309746	-	0.5	0.090	**0.5**	**0.023**
9	545	61.2	56.8	5.3	5.5	9.6	4	dito	309746	-	1.1	0.653	1.1	0.578
10	779	26.5	56.8	5.9	5.5	64.2	20	dito	309746	-	1.2	0.576	2.0	0.143
11	927	12.7	56.8	4.3	5.5	49.3	26	dito	309746	-	1.0	0.977	0.9	0.647
								Carbohydrate binding/metabolism						
12	474	71.5	49.1	5.3	5.2	18.2	6	Glycoside hydrolase, family 9	230437	18	1.8	0.055	1.0	0.889
13	501	83.4	44.2	5.6	5.5	39.4	28	3-phosphoglycerate kinase	299795	-	1.4	0.287	1.8	0.058
14	472	70.2	50.3	4.8	4.7	21.5	8	Glycoside hydrolase, family 7	300366	19	0.5	0.066	**0.5**	**0.018**
15	494	67.7	46.8	5.9	5.7	59.9	36	Enolase	301844	-	0.6	0.318	1.4	0.583
16	503	46.8	46.8	5.7	5.7	43.3	13	dito	301844	-	0.6	0.190	0.8	0.647
17	809	26.1	46.8	6.0	5.7	28.1	8	dito	301844	-	1.2	0.291	1.1	0.730
18	1027	5.0	46.8	6.6	5.7	19.8	6	dito	301844	-	1.1	0.832	0.9	0.758
19	621	43.8	35.6	6.8	5.6	57.1	22	Glyceraldehyde 3-phosphate dehydrogenase	302823	-	0.7	0.388	0.6	0.160
20	600	47.5	40.4	4.9	4.5	30.1	12	Glycoside hydrolase, family 16	303036	19	**0.3**	**0.009**	**0.3**	**0.003**
21	411	81.9	57.1	5.0	4.6	15.5	9	Beta-glucosidase	314456	19	1.1	0.421	0.9	0.463
								Chaperone						
22	463	72.4	46.7	4.7	4.2	48.3	18	Calreticulin	210624	16	**1.7**	**0.026**	1.2	0.439
23	805	23.3	23.4	4.5	4.5	66.7	14	FKBP-type peptidyl-prolyl cis-trans isomerase	231271	17	1.1	0.801	0.8	0.185
24	439	78.1	58.3	5.0	4.8	44.4	22	Protein disulphide isomerase	234212	15	1.3	0.117	1.1	0.675
25	383	89.1	61.4	5.6	5.3	31.2	22	Chaperonin ATPase, Cpn60/HSP60p	301074	-	1.0	0.979	1.4	0.358
								Cytoskeleton/muscle protein						
26	417	82.3	46.1	5.4	5.0	23.8	8	Alpha tubulin	100611	-	**2.2**	**0.018**	**2.0**	**0.005**
27	520	62.6	41.8	5.5	5.3	30.0	8	Actin and related proteins	300012	-	3.1	0.061	**2.4**	**0.044**
28	2148	61.9	41.8	5.3	5.3	20.2	8	dito	300012	-	0.8	0.490	1.7	0.169
29	550	60.5	41.8	5.3	5.3	14.3	4	dito	300012	-	1.2	0.208	1.1	0.654
30	698	36.2	41.8	5.1	5.3	22.8	8	dito	300012	-	1.3	0.253	1.1	0.788
31	752	28.2	41.8	5.6	5.3	36.3	17	dito	300012	-	0.8	0.673	1.0	0.987
32	438	78.8	50.1	5.1	4.6	19.9	10	Beta tubulin	300845	-	**1.6**	**0.009**	1.3	0.094
33	405	81.9	49.9	5.3	4.7	33.0	16	Alpha tubulin	301837	-	**2.1**	**0.001**	**1.7**	**0.006**
34	416	81.9	49.9	5.2	4.7	11.8	6	dito	301837	-	**1.9**	**0.000**	**1.7**	**0.020**
35	517	62.5	41.8	5.3	5.4	24.7	6	Actin and related proteins	305550	-	0.8	0.573	1.3	0.442
36	724	32.0	41.8	5.7	5.4	37.9	12	dito	305550	-	0.7	0.442	0.7	0.414
37	749	29.1	41.8	5.5	5.3	28.9	10	dito	305550	-	0.6	0.062	1.2	0.442
38	3309	62.6	41.9	5.4	5.2	30.8	8	dito	306442	-	**1.3**	**0.026**	**1.4**	**0.001**
39	2166	62.4	41.9	5.5	5.2	34.2	14	dito	306442	-	1.7	0.054	1.5	0.181
								Kinase						
40	7663	116.4	39.9	5.8	5.5	21.2	5	Arginine kinase	220693	-	0.9	0.570	1.2	0.296
41	543	57.6	39.9	5.7	5.5	58.4	32	dito	220693	-	1.6	0.244	1.8	0.109
42	563	57.6	39.9	5.7	5.5	58.4	32	dito	220693	-	1.5	0.489	2.3	0.111
43	757	28.8	39.9	5.4	5.5	36.3	9	dito	220693	-	0.9	0.347	**1.5**	**0.010**

44	756	28.7	39.9	4.5	5.5	18.7	5	dito	220693	-	0.8	0.313	0.6	0.051
45	796	24.4	39.9	5.1	5.5	34.9	10	dito	220693	-	**0.6**	**0.025**	**0.6**	**0.006**
46	943	12.1	39.9	4.6	5.5	32.1	9	dito	220693	-	1.3	0.280	1.4	0.202
47	1029	4.9	17.4	6.3	6.1	49.0	7	Nucleoside-diphosphate kinase	306455	-	1.2	0.489	1.0	0.946
								Proteolytic enzyme						
48	332	99.0	75.4	4.7	4.6	47.9	34	M13 family peptidase	200882	-	0.7	0.222	0.6	0.108
49	722	39.9	30.2	5.5	4.6	22.3	3	Peptidase S1, chymotrypsin	248155	15	1.3	0.265	1.2	0.287
50	635	41.5	39.5	4.4	4.7	12.7	6	Serine endopeptidase	251885	19	0.4	0.268	0.4	0.138
51	641	41.2	39.5	4.5	4.7	12.7	6	dito	251885	19	0.6	0.300	0.4	0.060
52	742	30.0	46.1	4.8	4.9	29.6	14	Carboxypeptidase A2	303899	17	0.8	0.058	**0.6**	**0.008**
								Transcription factor						
53	609	47.2	42.1	4.6	4.4	18.6	7	FOG: Leucine rich repeat	304126	22	**1.7**	**0.003**	**2.0**	**0.001**
								Transport protein						
54	270	110.9	224.8	5.6	6.5	12.3	22	Vitellogenin fused with SOD	219769	17	0.6	0.532	1.7	0.434
55	301	107.0	224.8	5.6	6.5	13.3	34	dito	219769	17	0.4	0.341	1.1	0.868
56	305	104.8	224.8	5.5	6.5	12.5	23	dito	219769	17	1.0	0.997	1.3	0.495
57	322	102.6	224.8	5.6	6.5	12.3	21	dito	219769	17	0.4	0.325	0.6	0.367
58	325	101.9	224.8	5.6	6.5	12.6	29	dito	219769	17	0.4	0.271	0.8	0.654
59	573	53.9	224.8	5.2	6.5	11.5	19	dito	219769	17	0.9	0.643	0.9	0.820
60	576	51.9	224.8	5.7	6.5	7.5	18	dito	219769	17	0.5	0.396	0.7	0.562
61	1545	51.8	224.8	5.6	6.5	9.9	22	dito	219769	17	0.6	0.450	0.5	0.299
62	580	51.8	224.8	5.6	6.5	9.9	22	dito	219769	17	0.4	0.357	0.4	0.285
63	617	45.5	224.8	5.7	6.5	10.9	29	dito	219769	17	0.4	0.330	0.5	0.311
64	616	45.1	224.8	5.6	6.5	8.9	24	dito	219769	17	0.3	0.145	0.4	0.149
65	634	44.1	224.8	5.7	6.5	15.4	30	dito	219769	17	0.3	0.210	0.5	0.216
66	660	40.0	224.8	5.3	6.5	12.8	26	dito	219769	17	0.3	0.234	0.4	0.207
67	661	39.6	224.8	5.4	6.5	11.9	19	dito	219769	17	0.4	0.110	0.7	0.277
68	689	38.1	224.8	5.7	6.5	12.9	25	dito	219769	17	0.5	0.250	0.5	0.145
69	908	26.1	14.8	6.0	5.3	31.1	4	Cytosolic fatty-acid binding protein	300446	-	1.3	0.374	1.0	0.871
70	231	117.0	191.9	5.7	6.4	16.3	47	Vitellogenin	308693	20	0.6	0.460	0.6	0.375
71	238	117.0	191.9	5.8	6.4	18.4	46	dito	308693	20	0.6	0.563	0.7	0.554
72	215	116.7	191.9	5.8	6.4	16.4	41	dito	308693	20	0.5	0.389	0.8	0.753
73	448	74.3	191.9	5.5	6.4	9.8	31	dito	308693	20	0.8	0.334	0.7	0.116
74	937	12.1	191.9	4.7	6.4	11.3	16	dito	308693	20	1.4	0.078	**1.4**	**0.045**
								Ubiquitin/proteasome system						
75	293	107.3	5.7	5.1	5.2	35.3	2	Ubiquitin and ubiquitin-like proteins	9558	-	0.8	0.629	**0.4**	**0.036**
76	444	76.2	5.7	4.6	5.2	35.3	2	dito	9558	-	1.4	0.080	1.1	0.534
77	845	18.3	5.7	4.9	5.2	35.3	2	dito	9558	-	0.9	0.586	**0.6**	**0.011**
78	743	34.3	28.0	5.3	5.3	35.9	8	20S proteasome, A and B subunits	306433	-	**0.5**	**0.004**	0.7	0.135
								Unknown						
79	530	224.8		6.5							0.9	0.531	0.8	0.237
80	811	185.1		6.9							1.0	0.875	0.8	0.214
81	776	148.9		5.7							0.8	0.446	0.7	0.272
82	349	97.5		5.6							0.6	0.284	0.7	0.395
83	1799	82.3		5.3							**2.2**	**0.016**	**1.6**	**0.026**
84	418	81.3		4.6							1.2	0.345	0.8	0.257
85	15758	61.7		5.4							1.2	0.341	1.2	0.406
86	534	56.8		5.5							**2.0**	**0.007**	1.6	0.245
87	673	56.8		5.5							0.9	0.684	2.3	0.071
88	680	40.8		5.5							**0.5**	**0.047**	**0.5**	**0.005**
89	548	39.9		5.5							0.8	0.734	1.8	0.421
90	558	39.9		5.5							1.4	0.605	2.1	0.428
91	691	37.4		5.0							1.4	0.238	1.1	0.884
92	813	33.2		5.4							1.3	0.462	0.8	0.320
93	733	30.7		4.9							**0.6**	**0.032**	**0.5**	**0.002**
94	753	28.9		4.9							1.1	0.614	1.0	0.821
95	789	25.5		4.4							**0.7**	**0.008**	0.8	0.136

Table 3.3 Proteins from the *D. pulex* clone M after 24 or 48 hours of heat stress (30°C) in comparison to control conditions (C, 20°C).

See Table 3.2 for detailed explanations.

	Spot ID	Function	Gene ID	R	*p*	R	*p*
				30°C/24 h *vs.* C		30°C/48 h *vs.* C	
		Antioxidative defense/detoxification					
1	801	Glutathione transferase	303282	1.1	0.565	1.1	0.572
2	784	dito	305501	1.6	0.065	**1.8**	**0.031**
3	794	dito	317266	**1.5**	**0.028**	**1.3**	**0.023**
		ATPase					
4	415	H(+)-transporting two-sector ATPase.	306451	**3.2**	**0.032**	**2.7**	**0.017**
5	441	dito	309746	1.4	0.104	1.1	0.338
6	466	dito	309746	1.4	0.113	1.3	0.095
7	482	dito	309746	0.6	0.412	1.2	0.496
8	23222	dito	309746	1.5	0.181	0.9	0.464
9	545	dito	309746	1.0	0.935	0.9	0.661
10	779	dito	309746	**1.8**	**0.006**	1.6	0.103
11	927	dito	309746	0.6	0.378	0.6	0.068
		Carbohydrate binding/metabolism					
12	474	Glycoside hydrolase, family 9	230437	0.8	0.604	0.7	0.079
13	501	3-phosphoglycerate kinase	299795	1.1	0.748	1.3	0.215
14	472	Glycoside hydrolase, family 7	300366	0.6	0.139	0.7	0.179
15	494	Enolase	301844	1.5	0.180	1.2	0.411
16	503	dito	301844	0.8	0.524	0.6	0.125
17	809	dito	301844	1.1	0.391	1.4	0.087
18	1027	dito	301844	1.0	0.977	1.3	0.300
19	621	Glyceraldehyde 3-phosphate dehydrogenase	302823	0.7	0.287	0.9	0.732
20	600	Glycoside hydrolase, family 16	303036	0.5	0.143	**0.6**	**0.027**
21	411	Beta-glucosidase	314456	1.5	0.309	1.1	0.695
		Chaperone					
22	463	Calreticulin	210624	1.2	0.294	0.9	0.605
23	805	FKBP-type peptidyl-prolyl cis-trans isomerase	231271	0.8	0.263	0.8	0.271
24	439	Protein disulphide isomerase	234212	**2.0**	**0.001**	1.3	0.232
25	383	Chaperonin ATPase, Cpn60/HSP60p	301074	**5.1**	**0.015**	**3.1**	**0.038**
		Cytoskeleton/muscle protein					
26	417	Alpha tubulin	100611	1.8	0.121	1.3	0.315
27	520	Actin and related proteins	300012	**0.5**	**0.044**	**0.4**	**0.001**
28	2148	dito	300012	1.6	0.324	2.2	0.077
29	550	dito	300012	0.7	0.432	0.7	0.115
30	698	dito	300012	0.6	0.151	0.7	0.107
31	752	dito	300012	0.7	0.077	0.9	0.651
32	438	Beta tubulin	300845	**1.5**	**0.013**	1.0	0.802
33	405	Alpha tubulin	301837	**1.8**	**0.007**	**1.5**	**0.011**
34	416	dito	301837	1.7	0.185	1.5	0.127
35	517	Actin and related proteins	305550	1.0	0.932	1.4	0.409
36	724	dito	305550	**1.7**	**0.015**	**1.5**	**0.042**
37	749	dito	305550	0.7	0.443	1.1	0.734
38	3309	dito	306442	1.2	0.672	1.4	0.100
39	2166	dito	306442	0.9	0.786	1.0	0.926
		Kinase					
40	7663	Arginine kinase	220693	0.9	0.763	1.1	0.730
41	543	dito	220693	1.1	0.809	2.0	0.182
42	563	dito	220693	1.1	0.714	0.9	0.823
43	757	dito	220693	0.7	0.254	0.9	0.582
44	756	dito	220693	0.5	0.057	0.8	0.327
45	796	dito	220693	0.8	0.513	1.0	0.921
46	943	dito	220693	0.8	0.538	0.6	0.064
47	1029	Nucleoside-diphosphate kinase	306455	1.9	0.134	1.8	0.104
		Proteolytic enzyme					
48	332	M13 family peptidase	200882	0.5	0.070	0.6	0.079
49	722	Peptidase S1, chymotrypsin	248155	0.5	0.232	1.0	0.910
50	635	Serine endopeptidase	251885	0.4	0.159	**0.4**	**0.005**
51	641	dito	251885	0.6	0.206	**0.4**	**0.006**
52	742	Carboxypeptidase A2	303899	**0.5**	**0.030**	**0.7**	**0.048**
		Transcription factor					
53	609	FOG: Leucine rich repeat	304126	**3.0**	**0.002**	**5.6**	**0.000**
		Transport protein					
54	270	Vitellogenin fused with SOD	219769	**3.4**	**0.050**	**4.2**	**0.017**
55	301	dito	219769	**4.4**	**0.018**	**5.3**	**0.001**

56	305	dito	219769	**2.5**	**0.044**	**3.0**	**0.003**
57	322	dito	219769	5.1	0.058	**9.3**	**0.007**
58	325	dito	219769	4.5	0.060	2.8	0.058
59	573	dito	219769	0.7	0.556	0.8	0.410
60	576	dito	219769	1.6	0.313	**3.2**	**0.047**
61	1545	dito	219769	**2.7**	**0.045**	**3.3**	**0.005**
62	580	dito	219769	2.2	0.126	**2.4**	**0.040**
63	617	dito	219769	1.6	0.275	1.0	0.974
64	616	dito	219769	1.4	0.383	1.0	0.922
65	634	dito	219769	1.0	0.999	0.7	0.259
66	660	dito	219769	1.0	0.955	1.4	0.101
67	661	dito	219769	1.1	0.765	0.8	0.489
68	689	dito	219769	0.9	0.874	**0.3**	**0.013**
69	908	Cytosolic fatty-acid binding protein	300446	**0.5**	**0.039**	0.8	0.254
70	231	Vitellogenin	308693	3.2	0.072	4.0	0.053
71	238	dito	308693	3.7	0.053	2.2	0.196
72	215	dito	308693	2.6	0.100	1.1	0.747
73	448	dito	308693	1.6	0.237	1.4	0.171
74	937	dito	308693	0.8	0.701	0.8	0.426
		Ubiquitin/proteasome system					
75	293	Ubiquitin and ubiquitin-like proteins	9558	0.9	0.895	0.9	0.772
76	444	dito	9558	1.1	0.586	1.6	0.169
77	845	dito	9558	1.0	0.787	0.8	0.336
78	743	20S proteasome, A and B subunits	306433	2.2	0.075	1.0	0.763
		Unknown					
79	530			0.9	0.722	0.9	0.793
80	811			**0.3**	**0.008**	**0.5**	**0.001**
81	776			0.4	0.121	**0.4**	**0.014**
82	349			2.5	0.109	2.4	0.283
83	1799			1.5	0.097	1.3	0.323
84	418			1.4	0.190	1.1	0.820
85	15758			0.9	0.804	1.2	0.409
86	534			1.1	0.647	1.2	0.427
87	673			0.3	0.253	**0.3**	**0.020**
88	680			1.3	0.513	0.7	0.084
89	548			0.8	0.707	1.7	0.323
90	558			1.0	0.975	1.3	0.535
91	691			1.1	0.598	1.0	0.943
92	813			0.7	0.282	0.9	0.709
93	733			0.6	0.104	**0.6**	**0.007**
94	753			1.1	0.175	0.8	0.120
95	789			0.8	0.345	0.7	0.314

Temporal patterns of differentially expressed proteins

Proteins, which showed significant differential expression (30°C vs 20°C) at least once during acute heat stress (24 and/or 48 h), were grouped in accordance with their specific time course: maximal expression after a) 24 hours ('early' up-regulation) or b) 48 hours ('late' up-regulation) of heat stress or c) down-regulation upon heat stress (Fig. 3.10). The first group was mainly represented by chaperones, cytoskeleton/muscle proteins, and H^+-transporting ATPases (Fig. 3.10A, B). Vitellogenins mainly represented the second group in case of clone M (Fig. 3.10D), whereas only a few proteins from clone G belonged to this group (e.g., FOG transcription factor, glutathione transferases) (Fig. 3.10C). The third group was mainly represented by metabolic enzymes and, additionally in case of clone G, arginine kinases and proteins related to the ubiquitin/proteasome system (Fig. 3.10E, F). Maximal induction rates (expression ratios, R) of up-regulated proteins were frequently higher in case of clone M (Fig. 3.10B, D), and the number of down-regulated proteins was higher in case of clone G (Fig. 3.10E).

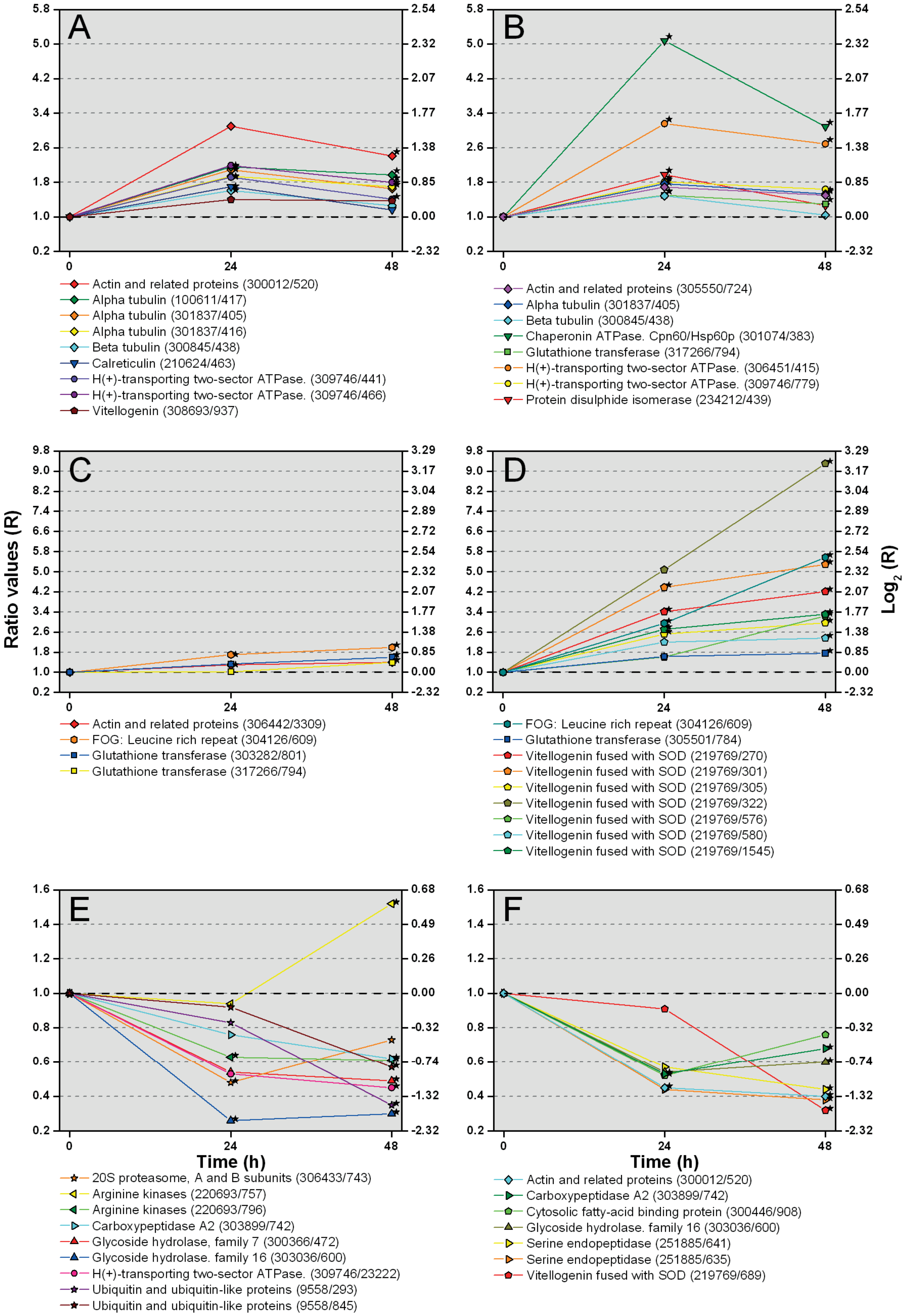
A
Actin and related proteins (300012/520)
Alpha tubulin (100611/417)
Alpha tubulin (301837/405)
Alpha tubulin (301837/416)
Beta tubulin (300845/438)
Calreticulin (210624/463)
H(+)-transporting two-sector ATPase. (309746/441)
H(+)-transporting two-sector ATPase. (309746/466)
Vitellogenin (308693/937)
B
Actin and related proteins (305550/724)
Alpha tubulin (301837/405)
Beta tubulin (300845/438)
Chaperonin ATPase. Cpn60/Hsp60p (301074/383)
Glutathione transferase (317266/794)
H(+)-transporting two-sector ATPase. (306451/415)
H(+)-transporting two-sector ATPase. (309746/779)
Protein disulphide isomerase (234212/439)
C
Ratio values (R)
Actin and related proteins (306442/3309)
FOG: Leucine rich repeat (304126/609)
Glutathione transferase (303282/801)
Glutathione transferase (317266/794)
D
Log2 (R)
FOG: Leucine rich repeat (304126/609)
Glutathione transferase (305501/784)
Vitellogenin fused with SOD (219769/270)
Vitellogenin fused with SOD (219769/301)
Vitellogenin fused with SOD (219769/305)
Vitellogenin fused with SOD (219769/322)
Vitellogenin fused with SOD (219769/576)
Vitellogenin fused with SOD (219769/580)
Vitellogenin fused with SOD (219769/1545)
E
Time (h)
20S proteasome, A and B subunits (306433/743)
Arginine kinases (220693/757)
Arginine kinases (220693/796)
Carboxypeptidase A2 (303899/742)
Glycoside hydrolase, family 7 (300366/472)
Glycoside hydrolase. family 16 (303036/600)
H(+)-transporting two-sector ATPase. (309746/23222)
Ubiquitin and ubiquitin-like proteins (9558/293)
Ubiquitin and ubiquitin-like proteins (9558/845)
F
Time (h)
Actin and related proteins (300012/520)
Carboxypeptidase A2 (303899/742)
Cytosolic fatty-acid binding protein (300446/908)
Glycoside hydrolase. family 16 (303036/600)
Serine endopeptidase (251885/641)
Serine endopeptidase (251885/635)
Vitellogenin fused with SOD (219769/689)

Fig. 3.10 Temporal changes in differential protein expression upon acute heat stress.

Temporal changes in expression ratio (R) of significantly (asterisks; t-tests, $P < 0.05$) up- or down-regulated proteins (see Tables 3.2, 3.3), after exposing 20°C-acclimated individuals (time, 0 hours) from *D. pulex* clones G (**A**, **C**, **E**) and M (**B**, **D**, **F**) to 24 hours or 48 hours of acute heat stress (30°C). Proteins were either up-regulated and showed maxima after (**A**, **B**) 24 hours or (**C**, **D**) 48 hours, or were (**E**, **F**) down-regulated. Linear (R) and logarithmic ($\log_2$[R]) y-axes are shown. Numbers in parentheses (after the protein functions) are gene and spot IDs.

Protein regulation within different categories

To assess for all clones (G, M) and experimental conditions (20°C/control, 30°C/24h, 30°C/48h) the total protein amount within each category, the spot volumes ($V_{rel.}$) of proteins, which belonged to a specific category, were added up for all analyzed 2D gels and then divided by the number of gels (Fig. 3.11). Significant clone-specific differences were primarily detected in case of two categories, with higher protein amounts upon heat stress in clone G for ‘cytoskeleton/muscle proteins’ and the FOG transcription factor (Fig. 3.11B–C). Significant condition-specific differences were found in case of five categories (carbohydrate binding/metabolism, chaperone, cytoskeleton/muscle protein, proteolytic enzyme, transcription factor) for the contrast 30°C/24h vs 20°C/control (Fig. 3.11B; small letter *a*), and also five categories (antioxidant defense/detoxification, carbohydrate binding/metabolism, cytoskeleton/muscle protein, proteolytic enzyme, transcription factor) for the contrast 30°C/48h vs 20°C/control (Fig. 3.11C; small letter *b*). For the contrast 30°C/24h vs 30°C/48h (Fig. 3.11B, C; small letter *c*), three categories differed significantly in total protein amount (antioxidant defense/detoxification, chaperone, transcription factor). Clone G showed significantly higher protein amounts under heat stress (red lines) in case of four categories (antioxidant defense/detoxification, chaperone, cytoskeleton/muscle protein, and transcription factor) and a significantly lower protein amount (green line) in case of one category (carbohydrate binding/metabolism). Clone M exhibited higher protein amounts at 30°C in case of two categories (chaperone, transcription factor) and a lower protein amount in case of one category (proteolytic enzyme).

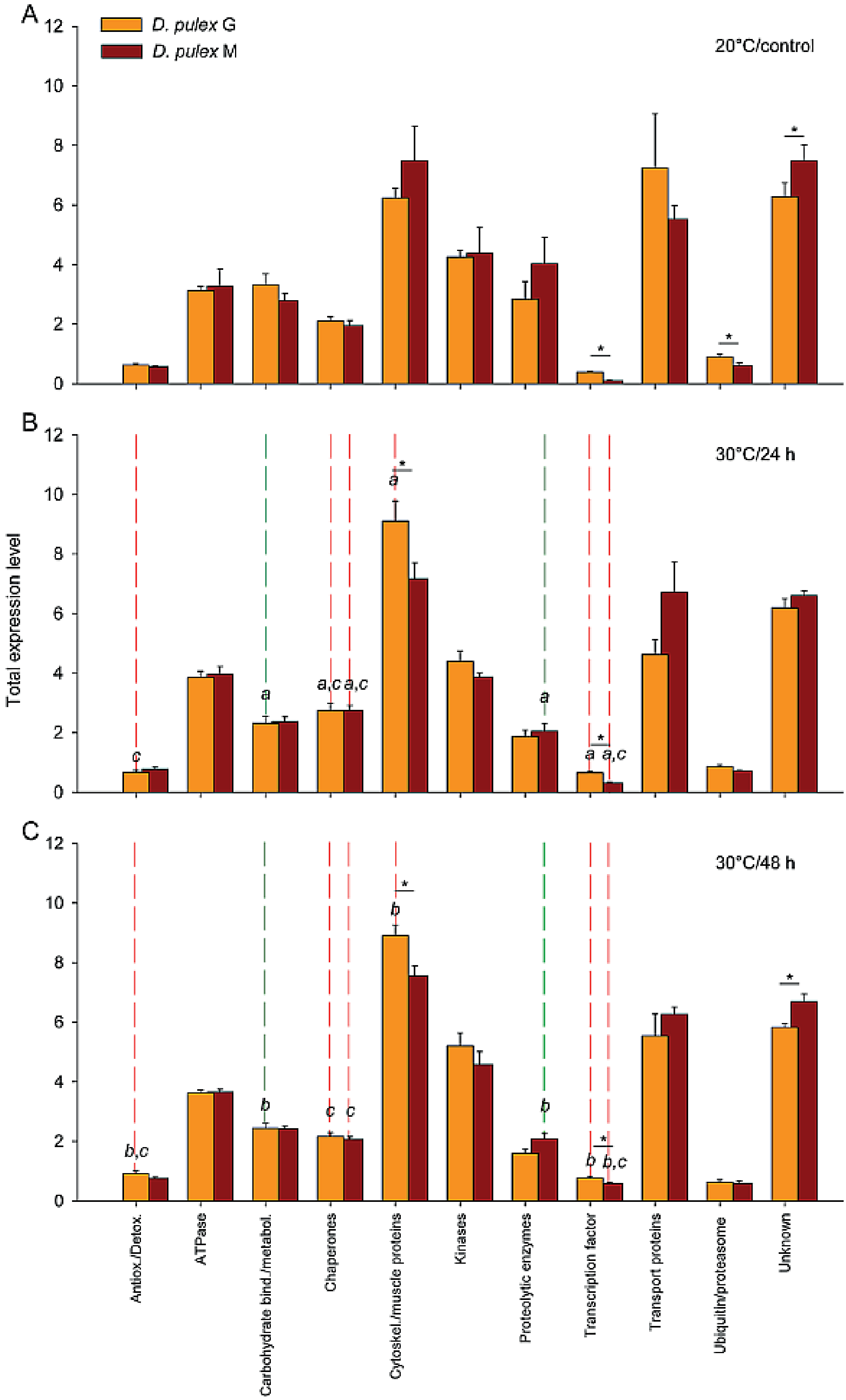
A
B
C
D. pulex G
D. pulex M
20°C/control
30°C/24 h
30°C/48 h
Total expression level
0
2
4
6
8
10
12
*
a
c
a,c
a,c
a,c
a
b
b,c
b
c
c
b
b
b,c
Antiox./Detox.
ATPase
Carbohydrate bind./metabol.
Chaperones
Cytoskel./muscle proteins
Kinases
Proteolytic enzymes
Transcription factor
Transport proteins
Ubiquitin/proteasome
Unknown

Fig. 3.11 Protein regulation within different functional categories upon acute heat stress (30°C).

Total expression levels (summed spot volumes; means ± S.E.M.) of identified proteins within different categories (see Tables 3.2, 3.3) for clone G (orange bars) and M (brown bars) (**A**) under control conditions (20°C; clone G, n = 5 biological replicates [b.r.]; clone M, n = 4 b.r.) and after (**B**) 24 hours (clone G, n = 4 b.r.; clone M, n = 3 b.r.) or (**C**) 48 hours (clone G, n = 6 b.r.; clone M, n = 5 b.r.) of heat stress (30°C). Asterisks and bars indicate significant differences between clones; small letters (*a*, 30°C/24 h vs 20°C/control; *b*, 30°C/48 h vs 20°C/control; *c*, 30°C/24 h vs 30°C/48 h) and dashed lines (red, up-regulation; green, down-regulation) denote significant differences between experimental conditions (two-way ANOVA and SNK analyses; $P < 0.05$).

3.3.4 Protein expression in two *D. pulex* clones at starvation stress

To study starvation effects on protein expression, both 20°C acclimated clones were kept either at control conditions (20°C; *ad libitum* food supply) or incubated for 24 hours or 48 hours under starvation stress (20°C; no food). Nineteen protein spots in case of clone G (Fig. 3.12) and 31 protein spots for clone M (Fig. 3.13) comprised proteins that were differentially expressed ($P < 0.05$) between starvation (24 h or 48 h incubations) and control conditions.

Differentially expressed proteins

One glutathione transferase isoform (gene ID: 317266) was up-regulated in both clones, and the other two isoforms (303282, 305501) were up-regulated only in clone M (Tables 3.4, 3.5). One isoform of the H^+-transporting two-sector ATPase (306451) showed a tendency towards up-regulation in clone M, whereas the other isoform (309746) was down-regulated (spot ID: 441). However, one spot (779) conversely indicated an up-regulation of the latter isoform in both clones. Within the category ‘carbohydrate metabolism’, 3-phosphoglycerate kinase (clone G) and enolase (clone M) were up-regulated, but glycoside hydrolase, family 9 was down-regulated (clone M). Concerning the category ‘chaperone’, Hsp60 was highly up-regulated in clone M, calreticulin was down-regulated in both clones, and FKBP-type peptidyl-prolyl cis-trans isomerase was down-regulated only in clone G. Within the category ‘cytoskeleton/muscle protein’, alpha tubulins were up-regulated in clone G, whereas alpha and beta tubulins were down-regulated in clone M. Concerning actin, one isoform (306442) showed up-regulation in clone G, and another one (305550) exhibited up-regulation in clone M, but down-regulation in clone G. Several protein spots indicated up-regulation of a third actin isoform (300012) in both clones at least after 24 hours of starvation. Arginine kinase (220693) was up-regulated in both clones. Concerning the category ‘proteolytic enzymes’, a chymotrypsin was up-regulated (clone G), whereas carboxypeptidase A2 (clone G) and a serine endopeptidase (clone M) were down-regulated. The transcription factor FOG was up-regulated in clone M. Within the category ‘transport protein’, the vitellogenin isoform containing a SOD subunit (219769) was more intensely up-regulated in clone M. A cytosolic fatty-acid binding protein, member of the category ‘transport protein’ was down-regulated in clone G. Ubiquitin was down-regulated in both clones.

In summary, acute starvation stress affected the clones G and M differently. Altogether, sixteen proteins were significantly up-regulated, with five of them specific for clone G and six specific for clone M. A total of thirteen proteins were significantly down-regulated, with four of them specific for clone G and six specific for clone M.

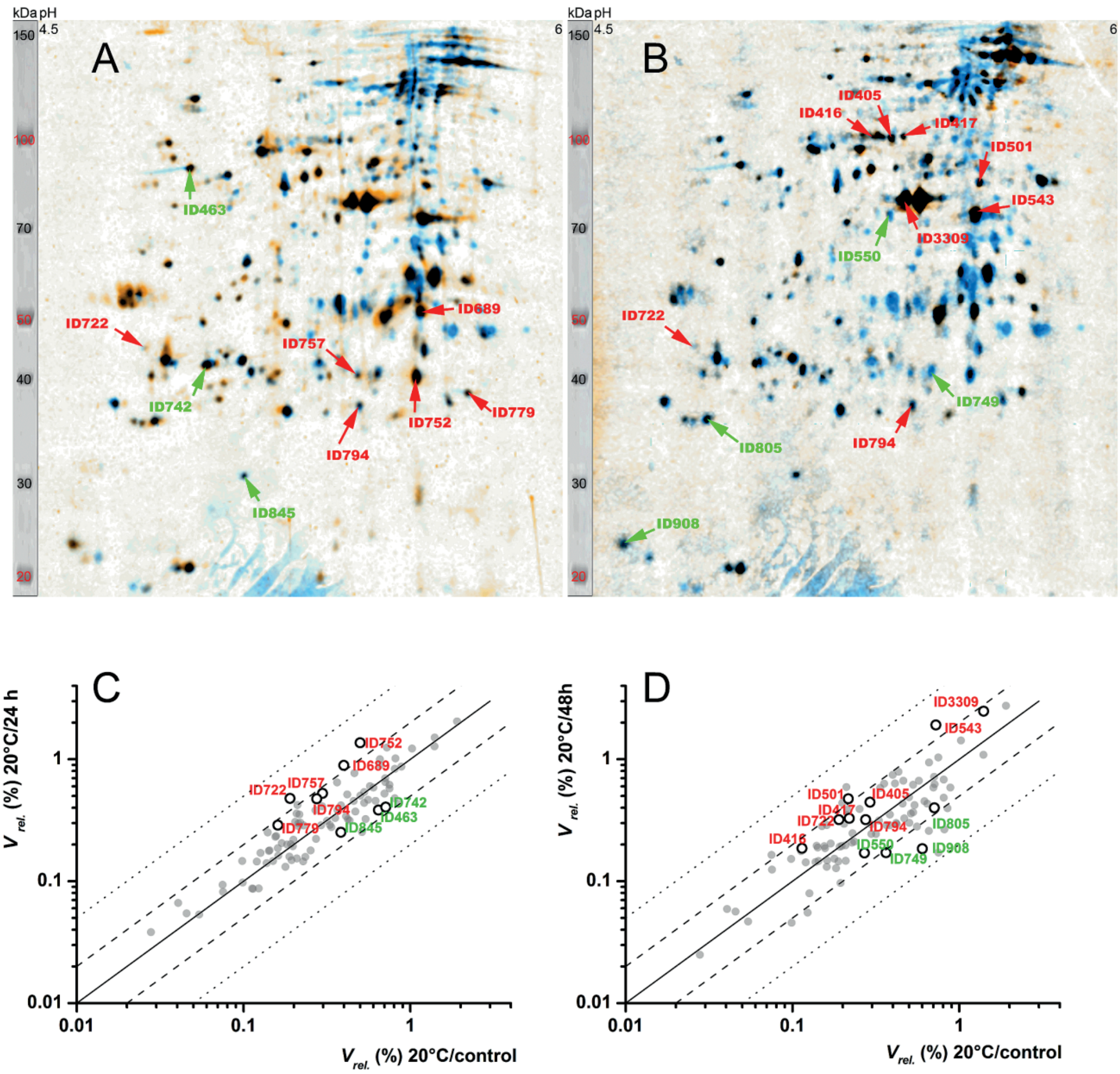

Fig. 3.12 Two-dimensional protein gels from starved *Daphnia pulex* clone G.

The 2D gel images are fusion (averaged) images of different numbers (n) of biological replicates showing changes in protein expression upon the acute exposure of 20°C acclimated *D. pulex* clone G (blue spots; n = 5) to (**A**) 24 hours (orange spots; n = 4) or (**B**) 48 hours (orange spots; n =

4) of starvation stress (S; 20°C). Red IDs mark significantly up-regulated proteins, and green IDs indicate significantly down-regulated proteins ($P < 0.05$; Table 3.4). The scatter plots show changes in expression level between (**C**) S/24 h or (**D**) S/48 h and control (food *ad libitum*) of significantly (open circles) or non-significantly (gray circles) up- or down-regulated proteins. See Fig. 3.8 for detailed information.

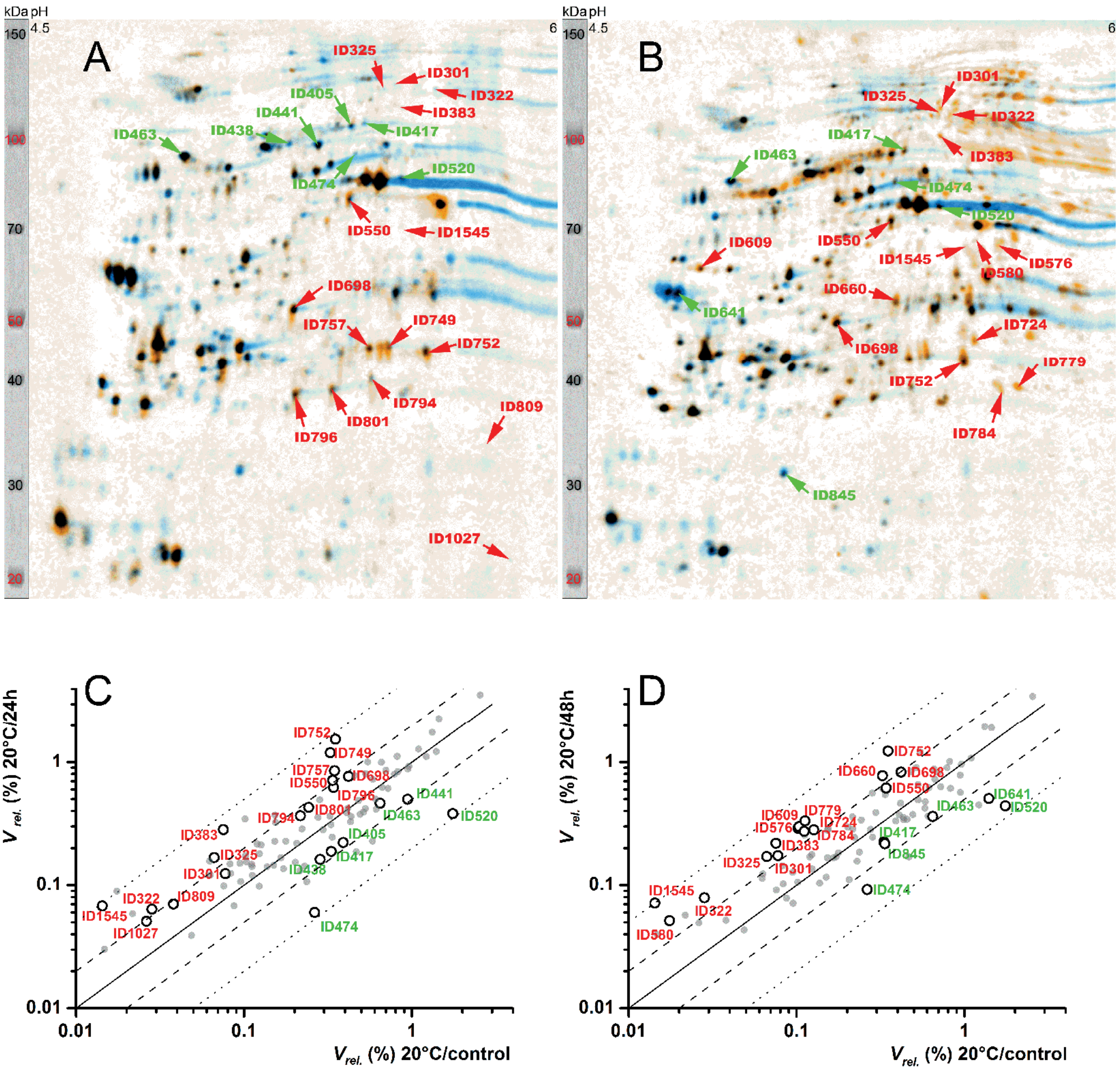

Fig. 3.13 Two-dimensional protein gels from the starvation-stressed *D. pulex* clone M.

The 2D gel images are fusion (averaged) images of different numbers (n) of biological replicates showing changes in protein expression upon the acute exposure of 20°C acclimated *D. pulex* clone M (blue spots; n = 4) to (**A**) 24 hours (orange spots; n = 4) or (**B**) 48 hours (orange spots; n = 5) of starvation stress (S; 20°C). Red IDs mark significantly up-regulated proteins, and green IDs indicate significantly down-regulated proteins ($P < 0.05$; Table 3.5). The scatter plots show changes in expression level between (**C**) S/24 h or (**D**) S/48 h and control (food *ad libitum*) of significantly (open circles) or non-significantly (gray circles) up- or down-regulated proteins. See Fig. 3.8 for detailed information.

Table 3.4 Proteins from the *D. pulex* clone G after 24 or 48 hours of starvation stress (S; 20°C) in comparison to control conditions (C; 20°C).

See Table 3.2 for detailed explanations.

N	Spot ID	M_re	M_rp	p*Ie*	p*Ip*	SC (%)	NP	Function	Gene ID	SP	R	*p*	R	*p*
											S/24 h *vs.* C		S/48 h *vs.* C	
								Antioxidative defense & detoxification						
1	801	24.2	24.8	5.3	5.4	36.8	12	Glutathione transferase	303282	-	1.5	0.157	1.2	0.195
2	784	25.3	25.2	5.8	5.6	36.2	10	dito	305501	-	1.5	0.134	1.4	0.148
3	794	25.0	25.0	5.4	5.2	67.3	18	dito	317266	-	**1.7**	**0.023**	**1.2**	**0.027**
								ATPase						
4	415	66.9	55.5	5.7	5.5	57.6	56	H(+)-transporting two-sector ATPase.	306451	-	1.2	0.651	1.2	0.684
5	441	78.1	56.8	5.2	5.5	43.8	16	dito	309746	-	0.8	0.457	1.4	0.173
6	466	71.4	56.8	5.2	5.5	79.4	56	dito	309746	-	0.8	0.563	1.5	0.058
7	482	69.7	56.8	5.2	5.5	80.5	64	dito	309746	-	1.0	0.984	0.9	0.787
8	23222	66.8	56.8	5.1	5.5	65.5	23	dito	309746	-	0.6	0.143	0.6	0.172
9	545	61.2	56.8	5.3	5.5	9.6	4	dito	309746	-	1.0	0.795	1.0	0.989
10	779	26.5	56.8	5.9	5.5	64.2	20	dito	309746	-	**1.8**	**0.037**	1.8	0.074
11	927	12.7	56.8	4.3	5.5	49.3	26	dito	309746	-	0.6	0.253	0.9	0.879
								Carbohydrate metabolism						
12	474	71.5	47.3	5.3	4.8	18.2	6	Glycoside hydrolase, family 9	230437	18	1.0	0.995	0.9	0.744
13	501	83.4	44.2	5.6	5.5	39.4	28	3-phosphoglycerate kinase	299795	-	1.6	0.120	**2.2**	**0.003**
14	472	70.2	48.2	4.8	4.7	21.5	8	Glycoside hydrolase, family 7	300366	19	0.7	0.261	0.7	0.273
15	494	67.7	46.8	5.9	5.7	59.9	36	Enolase	301844	-	0.9	0.864	1.8	0.163
16	503	46.8	46.8	5.7	5.7	43.3	13	dito	301844	-	0.8	0.390	1.6	0.328
17	809	26.1	46.8	6.0	5.7	28.1	8	dito	301844	-	1.0	0.932	0.9	0.518
18	1027	5.0	46.8	6.6	5.7	19.8	6	dito	301844	-	1.2	0.519	1.2	0.504
19	621	43.8	32.6	6.8	5.6	57.1	22	Glyceraldehyde 3-phosphate dehydrogenase	302823	-	0.5	0.146	0.5	0.137
20	600	47.5	38.5	4.9	4.5	30.1	12	Glycoside hydrolase, family 16	303036	19	1.0	0.973	1.0	0.956
21	411	81.9	55.0	5.0	4.6	15.5	9	Beta-glucosidase	314456	19	1.0	0.892	1.0	0.892
								Chaperones						
22	463	72.4	45.1	4.7	4.2	48.3	18	Calreticulin	210624	16	**0.6**	**0.047**	0.7	0.061
23	805	23.3	23.4	4.5	4.5	66.7	14	FKBP-type peptidyl-prolyl cis-trans isomerase	231271	17	0.9	0.810	**0.6**	**0.032**
24	439	78.1	56.6	5.0	4.8	44.4	22	Protein disulphide isomerase	234212	15	0.6	0.054	0.8	0.144
25	383	89.1	55.8	5.6	5.3	31.2	22	Chaperonin ATPase. Cpn60/Hsp60p	301074	-	1.3	0.366	1.6	0.064
								Cytoskeleton & muscle proteins						
26	417	82.3	41.6	5.4	5.0	23.8	8	Alpha tubulin	100611	-	1.4	0.165	**1.5**	**0.011**
27	520	62.6	41.8	5.5	5.3	30.0	8	Actin and related proteins	300012	-	1.1	0.832	1.2	0.590
28	2148	61.9	41.8	5.3	5.3	20.2	8	dito	300012	-	1.1	0.730	2.2	0.111
29	550	60.5	41.8	5.3	5.3	14.3	4	dito	300012	-	1.4	0.082	**0.6**	**0.019**
30	698	36.2	41.8	5.1	5.3	22.8	8	dito	300012	-	1.2	0.362	0.7	0.099
31	752	28.2	41.8	5.6	5.3	36.3	17	dito	300012	-	**2.7**	**0.036**	1.0	0.956
32	438	78.8	41.8	5.1	4.6	19.9	10	Beta tubulin	300845	-	0.7	0.084	0.9	0.577
33	405	81.9	47.9	5.3	4.7	33.0	16	Alpha tubulin	301837	-	1.0	0.948	**1.5**	**0.028**
34	416	81.9	47.9	5.2	4.7	11.8	6	dito	301837	-	0.8	0.167	**1.6**	**0.041**
35	517	62.5	39.8	5.3	5.4	24.7	6	Actin and related proteins	305550	-	0.8	0.621	1.7	0.386
36	724	32.0	39.8	5.7	5.4	37.9	12	dito	305550	-	1.4	0.332	1.0	0.973
37	749	29.1	41.8	5.5	5.3	28.9	10	dito	305550	-	1.8	0.176	**0.5**	**0.020**
38	3309	62.6	41.9	5.4	5.2	30.8	8	dito	306442	-	1.1	0.303	**1.8**	**0.008**
39	2166	62.4	41.9	5.5	5.2	34.2	14	dito	306442	-	1.2	0.491	1.4	0.242
								Kinases						
40	7663	116.4	39.9	5.8	5.5	21.2	5	Arginine kinase	220693	-	0.9	0.641	0.8	0.225
41	543	57.6	39.9	5.7	5.5	58.4	32	dito	220693	-	1.7	0.094	**2.6**	**0.003**
42	563	57.6	39.9	5.7	5.5	58.4	32	dito	220693	-	2.0	0.210	2.8	0.120
43	757	28.8	39.9	5.4	5.5	36.3	9	dito	220693	-	**1.8**	**0.039**	0.8	0.064
44	756	28.7	39.9	4.5	5.5	18.7	5	dito	220693	-	1.0	0.833	0.8	0.282
45	796	24.4	39.9	5.1	5.5	34.9	10	dito	220693	-	1.0	0.848	0.8	0.310
46	943	12.1	39.9	4.6	5.5	32.1	9	dito	220693	-	0.8	0.189	0.7	0.144
47	1029	4.9	17.4	6.3	6.1	49.0	7	Nucleoside-diphosphate kinase	306455	-	1.4	0.420	0.9	0.700
								Proteolytic enzymes						
48	332	99.0	75.4	4.7	4.6	47.9	34	M13 family peptidase	200882	-	0.8	0.370	0.7	0.250
49	722	39.9	28.6	5.5	4.6	22.3	3	Peptidase S1, chymotrypsin	248155	15	**2.5**	**0.038**	**1.7**	**0.025**
50	635	41.5	37.7	4.4	4.7	12.7	6	Serine endopeptidase	251885	19	1.2	0.645	0.3	0.188
51	641	41.2	37.7	4.5	4.7	12.7	6	dito	251885	19	1.5	0.273	0.4	0.096
52	742	30.0	44.3	4.8	4.9	29.6	14	Carboxypeptidase A2	303899	17	**0.6**	**0.032**	0.9	0.305
								Transcription factor						
53	609	47.2	39.8	4.6	4.4	18.6	7	FOG: Leucine rich repeat	304126	22	1.1	0.648	0.9	0.568

								Transport proteins						
54	270	110.9	223.0	5.6	6.5	12.3	22	Vitellogenin fused with SOD	219769	17	1.5	0.506	1.2	0.797
55	301	107.0	223.0	5.6	6.5	13.3	34	dito	219769	17	1.0	0.982	0.8	0.691
56	305	104.8	223.0	5.5	6.5	12.5	23	dito	219769	17	0.7	0.559	0.9	0.736
57	322	102.6	223.0	5.6	6.5	12.3	21	dito	219769	17	1.0	0.969	1.0	0.940
58	325	101.9	223.0	5.6	6.5	12.6	29	dito	219769	17	0.7	0.624	0.7	0.570
59	573	53.9	223.0	5.2	6.5	11.5	19	dito	219769	17	1.3	0.329	0.6	0.211
60	576	51.9	223.0	5.7	6.5	7.5	18	dito	219769	17	0.9	0.825	1.0	0.934
61	1545	51.8	223.0	5.6	6.5	9.9	22	dito	219769	17	1.0	0.982	0.5	0.374
62	580	51.8	223.0	5.6	6.5	9.9	22	dito	219769	17	0.7	0.658	0.4	0.408
63	617	45.5	223.0	5.7	6.5	10.9	29	dito	219769	17	1.4	0.561	1.8	0.267
64	616	45.1	223.0	5.6	6.5	8.9	24	dito	219769	17	0.8	0.724	0.7	0.500
65	634	44.1	223.0	5.7	6.5	15.4	30	dito	219769	17	1.7	0.347	1.4	0.444
66	660	40.0	223.0	5.3	6.5	12.8	26	dito	219769	17	0.8	0.685	0.2	0.198
67	661	39.6	223.0	5.4	6.5	11.9	19	dito	219769	17	0.8	0.497	0.5	0.159
68	689	38.1	223.0	5.7	6.5	12.9	25	dito	219769	17	**2.2**	**0.039**	1.9	0.063
69	908	26.1	14.8	6.0	5.3	31.1	4	Cytosolic fatty-acid binding protein	300446	-	1.0	0.929	**0.3**	**0.030**
70	231	117.0	189.9	5.7	6.4	16.3	47	Vitellogenin	308693	20	0.7	0.623	1.5	0.470
71	238	117.0	189.9	5.8	6.4	18.4	46	dito	308693	20	0.7	0.702	1.8	0.326
72	215	116.7	189.9	5.8	6.4	16.4	41	dito	308693	20	1.0	0.978	1.2	0.812
73	448	74.3	189.9	5.5	6.4	9.8	31	dito	308693	20	1.0	0.988	0.6	0.053
74	937	12.1	189.9	4.7	6.4	11.3	16	dito	308693	20	0.7	0.144	0.8	0.334
								Proteins of the ubiquitin proteasome system						
75	293	107.3	5.7	5.1	5.2	35.3	2	Ubiquitin and ubiquitin-like proteins	9558	-	1.2	0.506	1.3	0.364
76	444	76.2	5.7	4.6	5.2	35.3	2	dito	9558	-	1.3	0.220	1.1	0.742
77	845	18.3	5.7	4.9	5.2	35.3	2	dito	9558	-	**0.7**	**0.043**	0.7	0.081
78	743	34.3	28.0	5.3	5.3	35.9	8	20S proteasome, A and B subunits	306433	-	1.3	0.271	1.0	0.801
								Unknown						
79	530	224.8		6.5							1.2	0.361	0.8	0.253
80	811	185.1		6.9							1.7	0.060	0.9	0.760
81	776	148.9		5.7							1.5	0.104	1.6	0.056
82	349	97.5		5.6							0.8	0.660	0.8	0.524
83	1799	82.3		5.3							1.0	0.927	**1.9**	**0.032**
84	418	81.3		4.6							0.8	0.386	0.6	0.088
85	15758	61.7		5.4							1.1	0.725	1.4	0.075
86	534	56.8		5.5							**1.6**	**0.039**	1.5	0.153
87	673	56.8		5.5							**1.8**	**0.018**	1.4	0.125
88	680	40.8		5.5							1.4	0.262	1.4	0.079
89	548	39.9		5.5							1.1	0.857	1.6	0.365
90	558	39.9		5.5							1.2	0.441	2.2	0.131
91	691	37.4		5.0							1.1	0.742	0.7	0.252
92	813	33.2		5.4							1.2	0.500	1.2	0.577
93	733	30.7		4.9							1.0	0.942	0.7	0.073
94	753	28.9		4.9							**0.5**	**0.003**	**0.7**	**0.015**
95	789	25.5		4.4							0.8	0.234	**0.5**	**0.021**

Table 3.5 Proteins from the *D. pulex* clone M after 24 or 48 hours of starvation stress (S; 20°C) in comparison to control conditions (C; 20°C).

See Table 3.2 for detailed explanations.

N	Spot ID	Function	Gene ID	R	*p*	R	*p*
				S/24 h *vs.* C		S/48 h *vs.* C	
		Antioxidative defense & detoxification					
1	801	Glutathione transferase	303282	**1.8**	**0.009**	1.4	0.115
2	784	dito	305501	1.3	0.163	**2.5**	**0.037**
3	794	dito	317266	**1.7**	**0.005**	1.3	0.265
		ATPase					
4	415	H(+)-transporting two-sector ATPase.	306451	2.7	0.053	2.6	0.202
5	441	dito	309746	**0.5**	**0.032**	0.8	0.341
6	466	dito	309746	0.7	0.096	1.0	0.970
7	482	dito	309746	0.9	0.853	1.1	0.772
8	23222	dito	309746	0.8	0.156	0.8	0.368
9	545	dito	309746	1.3	0.512	1.0	0.940
10	779	dito	309746	1.1	0.729	**3.0**	**0.028**
11	927	dito	309746	1.1	0.875	0.5	0.153
		Carbohydrate metabolism					
12	474	Glycoside hydrolase, family 9	230437	**0.2**	**0.023**	**0.4**	**0.025**
13	501	3-phosphoglycerate kinase	299795	0.9	0.795	0.7	0.100
14	472	Glycoside hydrolase, family 7	300366	1.0	0.964	1.8	0.201

15	494	Enolase	301844	1.7	0.272	2.0	0.171
16	503	dito	301844	1.0	0.938	0.8	0.462
17	809	dito	301844	**1.9**	**0.004**	1.4	0.423
18	1027	dito	301844	**1.9**	**0.044**	1.9	0.261
19	621	Glyceraldehyde 3-phosphate dehydrogenase	302823	0.8	0.527	1.7	0.254
20	600	Glycoside hydrolase, family 16	303036	1.5	0.058	0.9	0.749
21	411	Beta-glucosidase	314456	1.3	0.343	1.0	0.891
		Chaperones					
22	463	Calreticulin	210624	**0.7**	**0.034**	**0.6**	**0.021**
23	805	FKBP-type peptidyl-prolyl cis-trans isomerase	231271	1.2	0.366	1.2	0.474
24	439	Protein disulphide isomerase	234212	0.8	0.276	1.2	0.238
25	383	Chaperonin ATPase. Cpn60/Hsp60p	301074	**3.8**	**0.005**	**2.9**	**0.001**
		Cytoskeleton & muscle proteins					
26	417	Alpha tubulin	100611	**0.6**	**0.021**	**0.7**	**0.037**
27	520	Actin and related proteins	300012	**0.2**	**0.002**	**0.3**	**0.001**
28	2148	dito	300012	2.1	0.060	1.8	0.147
29	550	dito	300012	**1.8**	**0.030**	**1.8**	**0.010**
30	698	dito	300012	**1.8**	**0.014**	**2.0**	**0.004**
31	752	dito	300012	**4.4**	**0.001**	**3.5**	**0.027**
32	438	Beta tubulin	300845	**0.6**	**0.008**	0.9	0.720
33	405	Alpha tubulin	301837	**0.6**	**0.033**	0.9	0.450
34	416	dito	301837	0.8	0.548	1.0	0.978
35	517	Actin and related proteins	305550	1.7	0.169	0.8	0.394
36	724	dito	305550	1.7	0.061	**2.2**	**0.018**
37	749	dito	305550	**3.7**	**0.003**	1.9	0.101
38	3309	dito	306442	1.6	0.076	1.3	0.292
39	2166	dito	306442	0.9	0.831	0.6	0.207
		Kinases					
40	7663	Arginine kinase	220693	1.3	0.438	1.5	0.087
41	543	dito	220693	1.8	0.075	2.2	0.081
42	563	dito	220693	1.5	0.194	1.3	0.402
43	757	dito	220693	**2.5**	**0.005**	1.7	0.060
44	756	dito	220693	0.8	0.494	0.8	0.354
45	796	dito	220693	**2.1**	**0.026**	1.6	0.083
46	943	dito	220693	0.8	0.649	0.9	0.692
47	1029	Nucleoside-diphosphate kinase	306455	2.0	0.057	2.7	0.076
		Proteolytic enzymes					
48	332	M13 family peptidase	200882	0.9	0.799	0.9	0.679
49	722	Peptidase S1, chymotrypsin	248155	1.3	0.439	1.1	0.764
50	635	Serine endopeptidase	251885	0.9	0.799	0.4	0.055
51	641	dito	251885	0.9	0.654	**0.4**	**0.028**
52	742	Carboxypeptidase A2	303899	1.0	0.924	1.1	0.331
		Transcription factor					
53	609	FOG: Leucine rich repeat	304126	1.5	0.071	**2.9**	**0.013**
		Transport proteins					
54	270	Vitellogenin fused with SOD	219769	1.9	0.093	2.0	0.120
55	301	dito	219769	**1.6**	**0.041**	**2.2**	**0.028**
56	305	dito	219769	1.8	0.142	1.4	0.240
57	322	dito	219769	**2.3**	**0.029**	**2.8**	**0.032**
58	325	dito	219769	**2.5**	**0.013**	**2.6**	**0.038**
59	573	dito	219769	2.4	0.051	1.1	0.839
60	576	dito	219769	1.7	0.148	**2.8**	**0.012**
61	1545	dito	219769	**4.7**	**0.005**	**5.0**	**0.002**
62	580	dito	219769	5.1	0.055	**2.9**	**0.007**
63	617	dito	219769	0.8	0.509	1.4	0.411
64	616	dito	219769	0.6	0.224	1.7	0.130
65	634	dito	219769	0.4	0.186	0.7	0.510
66	660	dito	219769	1.1	0.699	**2.4**	**0.002**
67	661	dito	219769	1.5	0.371	1.1	0.808
68	689	dito	219769	1.2	0.596	0.8	0.638
69	908	Cytosolic fatty-acid binding protein	300446	1.2	0.597	1.0	0.943
70	231	Vitellogenin	308693	2.5	0.108	1.8	0.140
71	238	dito	308693	1.3	0.653	2.3	0.135
72	215	dito	308693	0.8	0.600	1.5	0.426
73	448	dito	308693	1.0	0.870	1.3	0.437
74	937	dito	308693	1.0	0.926	1.0	0.994
		Proteins of the ubiquitin proteasome system					
75	293	Ubiquitin and ubiquitin-like proteins	9558	1.5	0.340	1.2	0.552
76	444	dito	9558	1.6	0.065	1.3	0.348
77	845	dito	9558	0.7	0.319	**0.6**	**0.044**
78	743	20S proteasome, A and B subunits	306433	1.1	0.740	0.7	0.224
		Unknown					
79	530			0.6	0.230	0.7	0.300
80	811			1.0	0.957	1.1	0.622

81	776			1.0	0.986	1.0	0.977
82	349			1.8	0.068	1.7	0.069
83	1799			**0.5**	**0.036**	0.8	0.569
84	418			0.8	0.248	0.9	0.702
85	15758			1.4	0.278	1.4	0.324
86	534			0.8	0.321	0.9	0.675
87	673			0.4	0.215	0.4	0.141
88	680			1.0	0.959	0.7	0.391
89	548			1.3	0.518	1.2	0.721
90	558			3.4	0.209	1.0	0.922
91	691			1.5	0.107	**1.8**	**0.012**
92	813			1.0	0.918	0.8	0.263
93	733			1.4	0.072	1.2	0.207
94	753			0.8	0.089	**0.8**	**0.002**
95	789			0.8	0.346	**0.6**	**0.039**

Temporal courses of differential protein expression

Proteins, which showed significant differential expression (starvation vs no starvation) at least once during starvation stress (24 and/or 48 h), were grouped in accordance with their specific time pattern (maximum after 24 h, maximum after 48 h, down-regulation) (Fig. 3.14). Specific differences were detected between the protein groups from clone G and M. The first pattern was mainly represented by actins, arginine kinase and glutathione transferases (Fig. 3.14 A, B). Both clones differed in the induction of peptidase S1 in clone G and HSP60 and enolase in clone M. The second pattern was mainly represented in clone M by vitellogenin, whereas only a few proteins from clone G belonged to this pattern (Fig. 3.14 C, D). The third pattern was mainly due to tubulins, chaperones other than HSP60, and metabolic enzymes (Fig. 3.14 E, F). For all three patterns, numbers of proteins and maximal increase in expression intensities were higher in case of clone M.

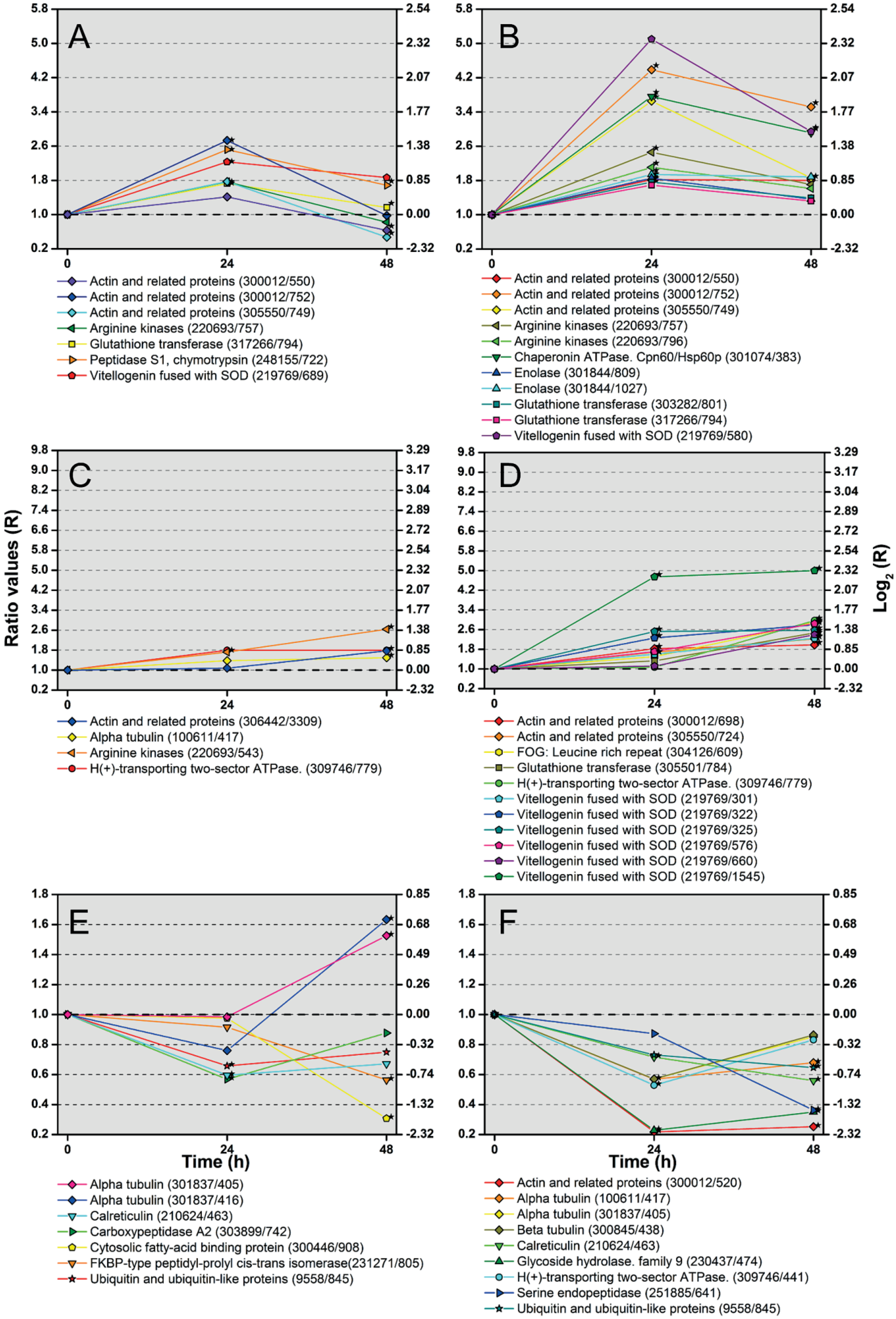
A
Actin and related proteins (300012/550)
Actin and related proteins (300012/752)
Actin and related proteins (305550/749)
Arginine kinases (220693/757)
Glutathione transferase (317266/794)
Peptidase S1, chymotrypsin (248155/722)
Vitellogenin fused with SOD (219769/689)
B
Actin and related proteins (300012/550)
Actin and related proteins (300012/752)
Actin and related proteins (305550/749)
Arginine kinases (220693/757)
Arginine kinases (220693/796)
Chaperonin ATPase. Cpn60/Hsp60p (301074/383)
Enolase (301844/809)
Enolase (301844/1027)
Glutathione transferase (303282/801)
Glutathione transferase (317266/794)
Vitellogenin fused with SOD (219769/580)
C
Actin and related proteins (306442/3309)
Alpha tubulin (100611/417)
Arginine kinases (220693/543)
H(+)-transporting two-sector ATPase. (309746/779)
D
Actin and related proteins (300012/698)
Actin and related proteins (305550/724)
FOG: Leucine rich repeat (304126/609)
Glutathione transferase (305501/784)
H(+)-transporting two-sector ATPase. (309746/779)
Vitellogenin fused with SOD (219769/301)
Vitellogenin fused with SOD (219769/322)
Vitellogenin fused with SOD (219769/325)
Vitellogenin fused with SOD (219769/576)
Vitellogenin fused with SOD (219769/660)
Vitellogenin fused with SOD (219769/1545)
E
Alpha tubulin (301837/405)
Alpha tubulin (301837/416)
Calreticulin (210624/463)
Carboxypeptidase A2 (303899/742)
Cytosolic fatty-acid binding protein (300446/908)
FKBP-type peptidyl-prolyl cis-trans isomerase(231271/805)
Ubiquitin and ubiquitin-like proteins (9558/845)
F
Actin and related proteins (300012/520)
Alpha tubulin (100611/417)
Alpha tubulin (301837/405)
Beta tubulin (300845/438)
Calreticulin (210624/463)
Glycoside hydrolase. family 9 (230437/474)
H(+)-transporting two-sector ATPase. (309746/441)
Serine endopeptidase (251885/641)
Ubiquitin and ubiquitin-like proteins (9558/845)
Ratio values (R)
Log2 (R)
Time (h)

Fig. 3.14 Temporal changes in differential protein expression upon acute starvation stress.

Temporal changes in expression ratios (R) in the *D. pulex* clones G (**A**, **C**, **E**) and M (**B**, **D**, **F**) of significantly (asterisks; t-tests, $P < 0.05$; see Tables 3.4, 3.5) up- or down-regulated proteins after the acute exposure (time, 0 hours) of 20°C acclimated individuals to 24 hours or 48 hours at starvation stress (20°C). The ratio values either increased under starvation, with maxima after (**A**, B) 24 hours or (**C**, **D**) 48 hours, or (**E**, **F**) decreased. Both linear (R) and logarithmic ($\log_2$[R]) y-axes are shown. Numbers in parentheses (after protein functions) are gene and spot IDs.

Regulation of proteins from different categories

Calculating the total expression intensities of all proteins from one functional category (Fig. 3.15) at three different experimental conditions (*ad libitum* food supply/control, starvation/24 h, and starvation/48 h; 20°C) revealed mostly higher protein amounts in clone G for the FOG transcription factor and proteins of the category 'ubiquitin/proteasome system'. At one condition (Fig. 3.15C), chaperone amounts were higher in clone M than in clone G. Proteins of the category 'antioxidant defense/detoxification' were frequently up-regulated (both clones), and those of the category 'kinase' as well as the FOG transcription factor were up-regulated only in clone M.

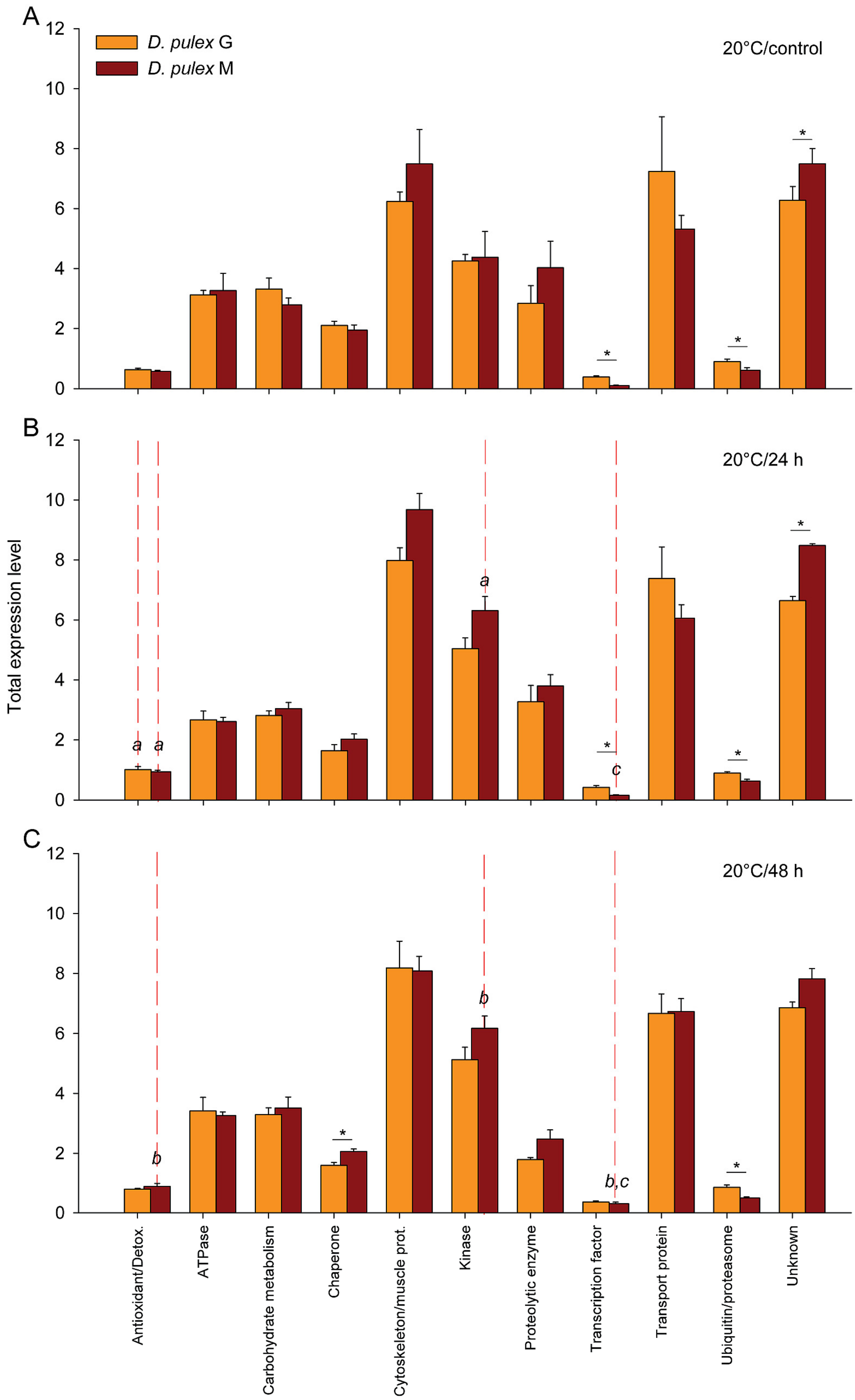
A
B
C
D. pulex G
D. pulex M
20°C/control
20°C/24 h
20°C/48 h
Total expression level
Antioxidant/Detox.
ATPase
Carbohydrate metabolism
Chaperone
Cytoskeleton/muscle prot.
Kinase
Proteolytic enzyme
Transcription factor
Transport protein
Ubiquitin/proteasome
Unknown

Fig. 3.15 Protein regulation within different functional categories upon acute starvation stress.

Total expression levels (summed spot volumes; means ± S.E.M.) of identified proteins within different functional categories (see Tables 3.4, 3.5) plotted for the 20°C acclimated *D. pulex* clones G (orange bars) and M (brown bars) (**A**) at control condition (food *ad libitum*, 20°C; clone G, *n* = 5 biological replicates [b.r.]; clone M, *n* = 4 b.r.), and (**B**) after 24 hours (clone G, *n* = 4 b.r.; clone M, *n* = 4 b.r.) or (**C**) 48 hours (clone G, *n* = 4 b.r.; clone M, *n* = 5 b.r.) at starvation stress (S; 20°C). Asterisks and bars indicate significant differences between clones; small letters (*a*, S/24 h *vs.* C; *b*, S/48 h *vs.* C; *c*, S/24 h *vs.* S/48 h) and dashed lines (red, up-regulation; green, down-regulation) denote significant differences between experimental conditions (two-way ANOVA and SNK analyses; $P < 0.05$).

3.3.5 Protein expression at heat-and-starvation stress (30 °C, no food)

To study the combined effects of heat and starvation on protein expression, both 20°C acclimated clones were kept either at control conditions (20°C, *ad libitum* food supply) or incubated for 24 hours or 48 hours under heat (30°C) and starvation stress. Sixteen protein spots in case of clone G (Fig. 3.16) and 41 protein spots for clone M (Fig. 3.17) comprised proteins that were differentially expressed ($P < 0.05$) between heat and starvation stress (24-h or 48-h incubations) and control conditions.

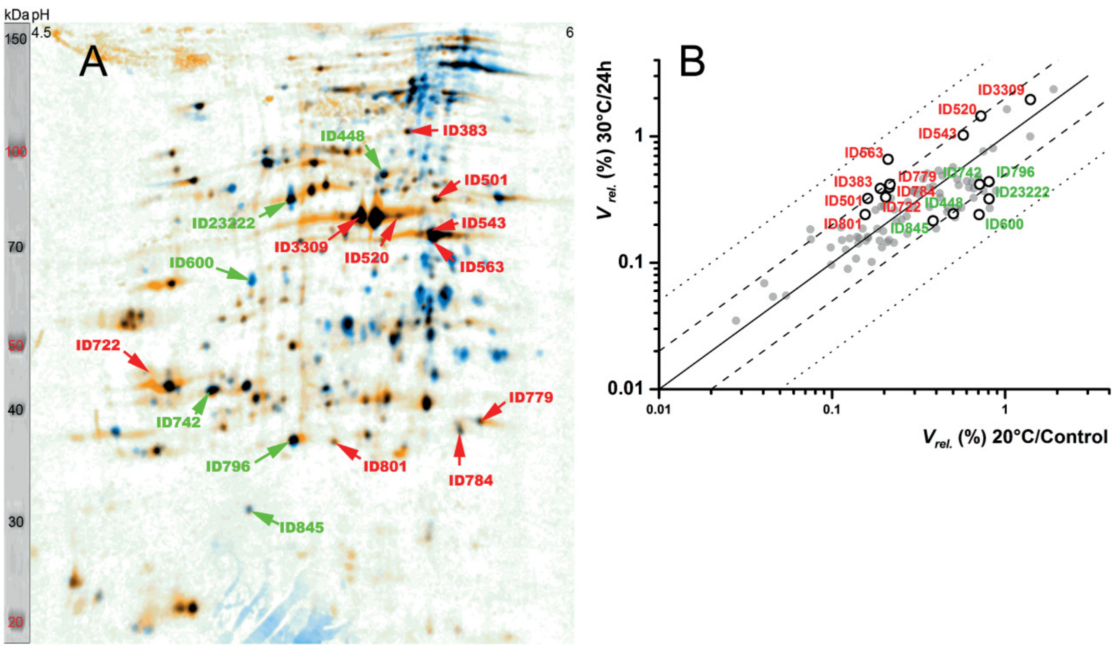

Fig. 3.16 Two-dimensional protein gel from the heat-and-starvation stressed *Daphnia pulex* clone G.

The (**A**) 2D gel image is a fusion (averaged) image of different numbers (*n*) of biological replicates showing changes in protein expression upon the acute exposure of 20°C acclimated *D. pulex* clone G (blue spots; *n* = 5) to 24 hours (orange spots; *n* = 5) of heat-and-starvation stress (S;

30°C). Red IDs mark significantly up-regulated proteins and green spot IDs indicate significantly down-regulated proteins (t-tests, $P < 0.05$; Table 3.6). The scatter plot show changes in expression level between (**B**) 30°C/S/24 h and 20°C/control of significantly (open circles) or non-significantly (gray circles) up- or down-regulated proteins. See Fig. 3.8 for detailed information.

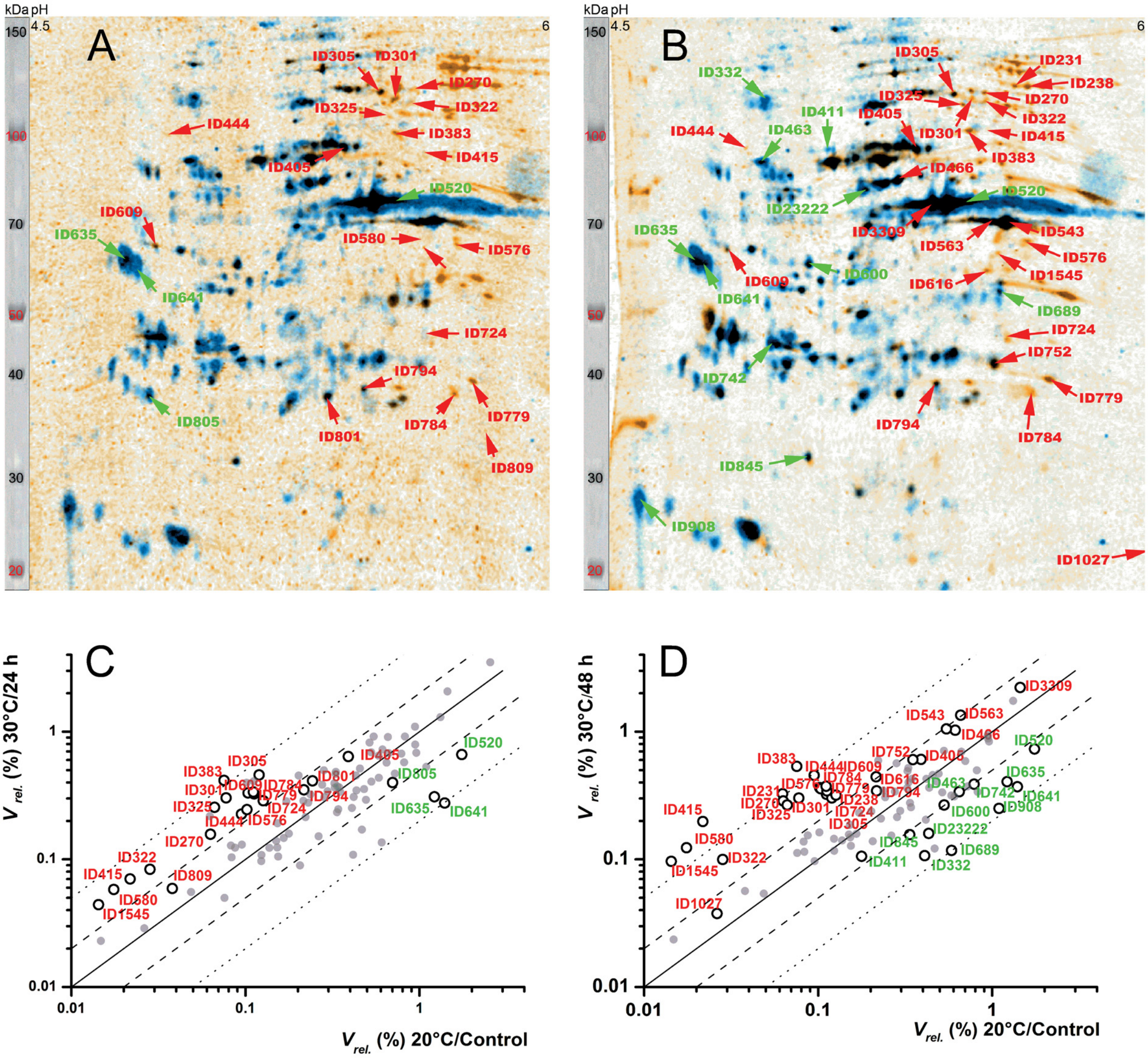

Fig. 3.17 Two-dimensional protein gels from the heat- and starvation-stressed *Daphnia pulex* clone M.

The 2D gel images are fusion (averaged) images of different numbers (n) of biological replicates showing changes in protein expression upon the acute exposure of 20°C acclimated *D. pulex* clone M (blue spots; $n = 4$) to (**A**) 24 hours (orange spots; $n = 5$) or (**B**) 48 hours (orange spots; $n = 7$) of heat-and-starvation stress (S; 30°C). Red spot IDs mark significantly up-regulated proteins, and green spot IDs indicate significantly down-regulated proteins (t-tests, $P < 0.05$; Table 3.7). The scatter plots show changes in expression level between (**C**) 30°C/S/24 h or (**D**) 30°C/S/48 h and 20°C/control of significantly (open circles) or non-significantly (gray circles) up- or down-regulated proteins. See Fig. 3.8 for detailed information.

Differentially expressed proteins

Two (clone G) or all three (clone M) glutathione transferase isoforms were up-regulated under combinded heat-and-starvation stress (Tables 3.6, 3.7). One isoform of the H^+-transporting two-sector ATPase (306451) was up-regulated in clone M, and another isoform (309746) was up-regulated in both clones. However, one spot (23222) conversely indicated a down-regulation of the latter isoform in both clones. For the category ‘carbohydrate metabolism’, 3-phosphoglycerate kinase (clone G) and enolase (clone M) were up-regulated, whereas glycoside hydrolase, family 16 (both clones) and beta-glucosidase (clone M) were down-regulated. Within the category ‘chaperone’, Hsp60 was up-regulated in both clones (particularly in clone M), but calreticulin and FKBP-type peptidyl-prolyl cis-trans isomerase were down-regulated only in clone M. Concerning the category ‘cytoskeleton/muscle protein’, alpha tubulin was up-regulated in clone M. Two (clone G) and three (clone M) actin isoforms also showed up-regulation. Arginine kinase was up-regulated in both clones (only spot 796 indicated down-regulation in case of clone G). Except for peptidase S1 in clone G, proteolytic enzymes were down-regulated. The transcription factor FOG was up-regulated in clone M. Within the category ‘transport proteins’, both vitellogenin isoforms were highly up-regulated in clone M, whereas a cytosolic fatty-acid binding protein was down-regulated. One spot (444) containing ubiquitin increased in clone M, whereas another spot (845) decreased in volume in both clones.

In summary, the combined heat and starvation stress affected protein expression differently in both clones and that of clone M particularly strongly. From the eighteen significantly up-regulated proteins were three specific for clone G and nine specific for clone M. From the fourteen significantly down-regulated proteins were three specific for clone G and eight specific for clone M.

Table 3.6 Proteins from the *D. pulex* clone G after 24 or 48 hours of heat-and-starvation stress (S; 30°C) in comparison to control conditions (C; 20°C, *ad libitum* food supply).

See Table 3.2 for detailed explanations.

	Spot ID	M_re	M_rp	pI*e*	pI*p*	SC (%)	NP	Function	Gene ID	SP	R	*p*	R	*p*
											30°C+S/24h *vs.* C		30°C+S/48h *vs.* C	
								Antioxidative defense & detoxification						
1	801	24.2	24.8	5.3	5.4	36.8	12	Glutathione transferase	303282	-	**1.6**	**0.002**	-	-
2	784	25.3	25.2	5.8	5.6	36.2	10	dito	305501	-	**1.6**	**0.027**	-	-
3	794	25.0	25.0	5.4	5.2	67.3	18	dito	317266	-	1.1	0.379	-	-
								ATPase						
4	415	66.9	55.5	5.7	5.5	57.6	56	H(+)-transporting two-sector ATPase.	306451	-	1.1	0.888	-	-

5	441	78.1	56.8	5.2	5.5	43.8	16	dito	309746	-	1.0	0.957	-	-
6	466	71.4	56.8	5.2	5.5	79.4	56	dito	309746	-	1.3	0.322	-	-
7	482	69.7	56.8	5.2	5.5	80.5	64	dito	309746	-	1.1	0.489	-	-
8	23222	66.8	56.8	5.1	5.5	65.5	23	dito	309746	-	**0.4**	**0.027**	-	-
9	545	61.2	56.8	5.3	5.5	9.6	4	dito	309746	-	1.4	0.175	-	-
10	779	26.5	56.8	5.9	5.5	64.2	20	dito	309746	-	**2.0**	**0.002**	-	-
11	927	12.7	56.8	4.3	5.5	49.3	26	dito	309746	-	0.6	0.131	-	-
								Carbohydrate metabolism						
12	474	71.5	47.3	5.3	4.8	18.2	6	Glycoside hydrolase. family 9	230437	18	1.0	0.911	-	-
13	501	83.4	44.2	5.6	5.5	39.4	28	3-phosphoglycerate kinase	299795	-	**1.9**	**0.004**	-	-
14	472	70.2	48.2	4.8	4.7	21.5	8	Glycoside hydrolase, family 7	300366	19	0.6	0.102	-	-
15	494	67.7	46.8	5.9	5.7	59.9	36	Enolase	301844	-	1.4	0.268	-	-
16	503	46.8	46.8	5.7	5.7	43.3	13	dito	301844	-	1.7	0.061	-	-
17	809	26.1	46.8	6.0	5.7	28.1	8	dito	301844	-	1.0	0.945	-	-
18	1027	5.0	46.8	6.6	5.7	19.8	6	dito	301844	-	1.2	0.693	-	-
19	621	43.8	32.6	6.8	5.6	57.1	22	Glyceraldehyde 3-phosphate dehydrogenase	302823	-	0.9	0.850	-	-
20	600	47.5	38.5	4.9	4.5	30.1	12	Glycoside hydrolase. family 16	303036	19	**0.3**	**0.008**	-	-
21	411	81.9	55.0	5.0	4.6	15.5	9	Beta-glucosidase	314456	19	0.9	0.534	-	-
								Chaperones						
22	463	72.4	45.1	4.7	4.2	48.3	18	Calreticulin	210624	16	0.7	0.065	-	-
23	805	23.3	23.4	4.5	4.5	66.7	14	FKBP-type peptidyl-prolyl cis-trans isomerase	231271	17	0.6	0.066	-	-
24	439	78.1	56.6	5.0	4.8	44.4	22	Protein disulphide isomerase	234212	15	0.8	0.065	-	-
25	383	89.1	55.8	5.6	5.3	31.2	22	Chaperonin ATPase. Cpn60/Hsp60p	301074	-	**1.8**	**0.029**	-	-
								Cytoskeleton & muscle proteins						
26	417	82.3	41.6	5.4	5.0	23.8	8	Alpha tubulin	100611	-	1.5	0.051	-	-
27	520	62.6	41.8	5.5	5.3	30.0	8	Actin and related proteins	300012	-	**1.8**	**0.048**	-	-
28	2148	61.9	41.8	5.3	5.3	20.2	8	dito	300012	-	1.4	0.220	-	-
29	550	60.5	41.8	5.3	5.3	14.3	4	dito	300012	-	0.9	0.353	-	-
30	698	36.2	41.8	5.1	5.3	22.8	8	dito	300012	-	0.8	0.385	-	-
31	752	28.2	41.8	5.6	5.3	36.3	17	dito	300012	-	1.1	0.724	-	-
32	438	78.8	41.8	5.1	4.6	19.9	10	Beta tubulin	300845	-	0.9	0.637	-	-
33	405	81.9	47.9	5.3	4.7	33.0	16	Alpha tubulin	301837	-	1.3	0.303	-	-
34	416	81.9	47.9	5.2	4.7	11.8	6	dito	301837	-	1.3	0.154	-	-
35	517	62.5	39.8	5.3	5.4	24.7	6	Actin and related proteins	305550	-	1.4	0.399	-	-
36	724	32.0	39.8	5.7	5.4	37.9	12	dito	305550	-	0.9	0.826	-	-
37	749	29.1	41.8	5.5	5.3	28.9	10	dito	305550	-	1.1	0.795	-	-
38	3309	62.6	41.9	5.4	5.2	30.8	8	dito	306442	-	**1.4**	**0.016**	-	-
39	2166	62.4	41.9	5.5	5.2	34.2	14	dito	306442	-	1.6	0.069	-	-
								Kinases						
40	7663	116.4	39.9	5.8	5.5	21.2	5	Arginine kinase	220693	-	0.7	0.287	-	-
41	543	57.6	39.9	5.7	5.5	58.4	32	dito	220693	-	**2.0**	**0.029**	-	-
42	563	57.6	39.9	5.7	5.5	58.4	32	dito	220693	-	**3.1**	**0.030**	-	-
43	757	28.8	39.9	5.4	5.5	36.3	9	dito	220693	-	1.2	0.120	-	-
44	756	28.7	39.9	4.5	5.5	18.7	5	dito	220693	-	0.8	0.281	-	-
45	796	24.4	39.9	5.1	5.5	34.9	10	dito	220693	-	**0.5**	**0.025**	-	-
46	943	12.1	39.9	4.6	5.5	32.1	9	dito	220693	-	0.8	0.443	-	-
47	1029	4.9	17.4	6.3	6.1	49.0	7	Nucleoside-diphosphate kinase	306455	-	1.2	0.460	-	-
								Proteolytic enzymes						
48	332	99.0	75.4	4.7	4.6	47.9	34	M13 family peptidase	200882	-	0.6	0.057	-	-
49	722	39.9	28.6	5.5	4.6	22.3	3	Peptidase S1, chymotrypsin	248155	15	**2.0**	**0.022**	-	-
50	635	41.5	37.7	4.4	4.7	12.7	6	Serine endopeptidase	251885	19	0.3	0.140	-	-
51	641	41.2	37.7	4.5	4.7	12.7	6	dito	251885	19	0.5	0.118	-	-
52	742	30.0	44.3	4.8	4.9	29.6	14	Carboxypeptidase A2	303899	17	**0.6**	**0.016**	-	-
								Transcription factor						
53	609	47.2	39.8	4.6	4.4	18.6	7	FOG: Leucine rich repeat	304126	22	1.1	0.867	-	-
								Transport proteins						
54	270	110.9	223.0	5.6	6.5	12.3	22	Vitellogenin fused with SOD	219769	17	1.0	0.934	-	-
55	301	107.0	223.0	5.6	6.5	13.3	34	dito	219769	17	1.1	0.851	-	-
56	305	104.8	223.0	5.5	6.5	12.5	23	dito	219769	17	1.5	0.256	-	-
57	322	102.6	223.0	5.6	6.5	12.3	21	dito	219769	17	0.8	0.643	-	-
58	325	101.9	223.0	5.6	6.5	12.6	29	dito	219769	17	1.5	0.324	-	-
59	573	53.9	223.0	5.2	6.5	11.5	19	dito	219769	17	1.2	0.544	-	-
60	576	51.9	223.0	5.7	6.5	7.5	18	dito	219769	17	1.1	0.767	-	-
61	1545	51.8	223.0	5.6	6.5	9.9	22	dito	219769	17	1.0	0.962	-	-
62	580	51.8	223.0	5.6	6.5	9.9	22	dito	219769	17	0.7	0.634	-	-
63	617	45.5	223.0	5.7	6.5	10.9	29	dito	219769	17	0.7	0.579	-	-
64	616	45.1	223.0	5.6	6.5	8.9	24	dito	219769	17	0.5	0.232	-	-
65	634	44.1	223.0	5.7	6.5	15.4	30	dito	219769	17	0.5	0.332	-	-
66	660	40.0	223.0	5.3	6.5	12.8	26	dito	219769	17	0.5	0.325	-	-
67	661	39.6	223.0	5.4	6.5	11.9	19	dito	219769	17	0.7	0.325	-	-
68	689	38.1	223.0	5.7	6.5	12.9	25	dito	219769	17	0.5	0.169	-	-
69	908	26.1	14.8	6.0	5.3	31.1	4	Cytosolic fatty-acid binding protein	300446	-	0.7	0.432	-	-
70	231	117.0	189.9	5.7	6.4	16.3	47	Vitellogenin	308693	20	0.9	0.810	-	-

71	238	117.0	189.9	5.8	6.4	18.4	46	dito	308693	20	1.1	0.826	-	-
72	215	116.7	189.9	5.8	6.4	16.4	41	dito	308693	20	0.9	0.790	-	-
73	448	74.3	189.9	5.5	6.4	9.8	31	dito	308693	20	**0.5**	**0.006**	-	-
74	937	12.1	189.9	4.7	6.4	11.3	16	dito	308693	20	0.7	0.191	-	-
Proteins of the ubiquitin proteasome system														
75	293	107.3	5.7	5.1	5.2	35.3	2	Ubiquitin and ubiquitin-like proteins	9558	-	1.0	0.997	-	-
76	444	76.2	5.7	4.6	5.2	35.3	2	dito	9558	-	1.1	0.298	-	-
77	845	18.3	5.7	4.9	5.2	35.3	2	dito	9558	-	**0.6**	**0.011**	-	-
78	743	34.3	28.0	5.3	5.3	35.9	8	20S proteasome, A and B subunits	306433	-	1.1	0.640	-	-
Unknown														
79	530	224.8		6.5							1.0	0.994	-	-
80	811	185.1		6.9							0.7	0.075	-	-
81	776	148.9		5.7							1.3	0.347	-	-
82	349	97.5		5.6							0.8	0.570	-	-
83	1799	82.3		5.3							1.2	0.419	-	-
84	418	81.3		4.6							**0.6**	**0.049**	-	-
85	15758	61.7		5.4							1.2	0.267	-	-
86	534	56.8		5.5							1.7	0.085	-	-
87	673	56.8		5.5							1.2	0.589	-	-
88	680	40.8		5.5							0.6	0.060	-	-
89	548	39.9		5.5							2.0	0.155	-	-
90	558	39.9		5.5							2.5	0.245	-	-
91	691	37.4		5.0							1.0	0.949	-	-
92	813	33.2		5.4							0.6	0.085	-	-
93	733	30.7		4.9							**0.4**	**0.008**	-	-
94	753	28.9		4.9							**0.4**	**0.005**	-	-
95	789	25.5		4.4							**0.5**	**0.000**	-	-

Table 3.7 Proteins from the *D. pulex* clone M after 24 and 48 hours of heat-and-starvation stress (S; 30°C) in comparison to control conditions (C; 20°C, *ad libitum* food supply).

See Table 3.2 for detailed explanations.

	Spot ID	Function	Gene ID	R	*p*	R	*p*
				30°C+S/24 h *vs.* C		30°C+S/48 h *vs.* C	
Antioxidative defense & detoxification							
1	801	Glutathione transferase	303282	**1.7**	**0.043**	1.3	0.132
2	784	dito	305501	**3.0**	**0.004**	**3.4**	**0.003**
3	794	dito	317266	**1.6**	**0.020**	**1.6**	**0.039**
ATPase							
4	415	H(+)-transporting two-sector ATPase.	306451	**3.2**	**0.005**	**9.1**	**0.000**
5	441	dito	309746	1.2	0.501	1.0	0.988
6	466	dito	309746	1.2	0.388	**1.7**	**0.018**
7	482	dito	309746	1.0	0.950	1.0	0.856
8	23222	dito	309746	1.0	0.799	**0.4**	**0.000**
9	545	dito	309746	1.4	0.284	1.2	0.593
10	779	dito	309746	**2.9**	**0.020**	**3.1**	**0.010**
11	927	dito	309746	0.4	0.094	0.7	0.250
Carbohydrate metabolism							
12	474	Glycoside hydrolase. family 9	230437	0.6	0.102	0.6	0.084
13	501	3-phosphoglycerate kinase	299795	1.4	0.238	1.6	0.056
14	472	Glycoside hydrolase, family 7	300366	0.7	0.174	0.8	0.333
15	494	Enolase	301844	1.8	0.230	2.0	0.071
16	503	dito	301844	0.9	0.841	1.0	0.893
17	809	dito	301844	**1.6**	**0.024**	1.5	0.256
18	1027	dito	301844	1.1	0.527	**1.4**	**0.048**
19	621	Glyceraldehyde 3-phosphate dehydrogenase	302823	1.6	0.345	0.6	0.144
20	600	Glycoside hydrolase. family 16	303036	0.8	0.353	**0.5**	**0.013**
21	411	Beta-glucosidase	314456	0.9	0.694	**0.6**	**0.032**
Chaperones							
22	463	Calreticulin	210624	0.9	0.491	**0.5**	**0.002**
23	805	FKBP-type peptidyl-prolyl cis-trans isomerase	231271	**0.6**	**0.032**	0.8	0.347
24	439	Protein disulphide isomerase	234212	1.3	0.093	1.3	0.184
25	383	Chaperonin ATPase. Cpn60/Hsp60p	301074	**5.5**	**0.000**	**7.1**	**0.000**
Cytoskeleton & muscle proteins							
26	417	Alpha tubulin	100611	1.5	0.070	1.2	0.328
27	520	Actin and related proteins	300012	**0.4**	**0.003**	**0.4**	**0.001**

28	2148	dito	300012	0.7	0.337	0.8	0.684
29	550	dito	300012	0.7	0.265	0.7	0.210
30	698	dito	300012	0.7	0.327	1.0	0.945
31	752	dito	300012	1.0	0.733	**1.7**	**0.011**
32	438	Beta tubulin	300845	1.1	0.637	0.8	0.188
33	405	Alpha tubulin	301837	**1.6**	**0.018**	**1.6**	**0.043**
34	416	dito	301837	1.7	0.132	1.3	0.289
35	517	Actin and related proteins	305550	1.1	0.641	1.0	0.988
36	724	dito	305550	**2.3**	**0.012**	**2.5**	**0.000**
37	749	dito	305550	1.1	0.731	1.5	0.154
38	3309	dito	306442	1.4	0.185	**1.5**	**0.033**
39	2166	dito	306442	0.8	0.619	0.9	0.814
		Kinases					
40	7663	Arginine kinase	220693	1.0	0.955	1.3	0.345
41	543	dito	220693	1.7	0.056	**1.9**	**0.028**
42	563	dito	220693	1.4	0.110	**2.0**	**0.000**
43	757	dito	220693	1.1	0.798	1.2	0.260
44	756	dito	220693	0.8	0.270	0.8	0.494
45	796	dito	220693	1.1	0.691	0.8	0.422
46	943	dito	220693	0.6	0.241	0.5	0.065
47	1029	Nucleoside-diphosphate kinase	306455	1.6	0.126	1.6	0.227
		Proteolytic enzymes					
48	332	M13 family peptidase	200882	0.6	0.068	**0.3**	**0.000**
49	722	Peptidase S1, chymotrypsin	248155	1.0	0.922	2.7	0.219
50	635	Serine endopeptidase	251885	**0.3**	**0.022**	**0.3**	**0.011**
51	641	dito	251885	**0.2**	**0.007**	**0.3**	**0.002**
52	742	Carboxypeptidase A2	303899	0.9	0.514	**0.5**	**0.002**
		Transcription factor					
53	609	FOG: Leucine rich repeat	304126	**3.2**	**0.018**	**3.5**	**0.000**
		Transport proteins					
54	270	Vitellogenin fused with SOD	219769	**2.5**	**0.015**	**4.6**	**0.018**
55	301	dito	219769	**3.9**	**0.011**	**3.9**	**0.002**
56	305	dito	219769	**3.8**	**0.000**	**2.5**	**0.009**
57	322	dito	219769	**3.0**	**0.013**	**3.5**	**0.000**
58	325	dito	219769	**3.8**	**0.001**	**4.0**	**0.001**
59	573	dito	219769	1.3	0.579	1.0	0.935
60	576	dito	219769	**2.4**	**0.010**	**3.6**	**0.002**
61	1545	dito	219769	**3.1**	**0.019**	**6.7**	**0.016**
62	580	dito	219769	**3.3**	**0.004**	**7.0**	**0.000**
63	617	dito	219769	0.8	0.450	1.2	0.573
64	616	dito	219769	1.3	0.318	**2.1**	**0.006**
65	634	dito	219769	1.1	0.817	0.5	0.158
66	660	dito	219769	1.2	0.476	1.1	0.641
67	661	dito	219769	0.9	0.711	0.9	0.843
68	689	dito	219769	0.7	0.554	**0.2**	**0.017**
69	908	Cytosolic fatty-acid binding protein	300446	0.5	0.051	**0.2**	**0.000**
70	231	Vitellogenin	308693	3.5	0.078	**5.2**	**0.009**
71	238	dito	308693	3.7	0.133	**2.9**	**0.042**
72	215	dito	308693	2.2	0.255	1.2	0.682
73	448	dito	308693	1.2	0.681	0.8	0.464
74	937	dito	308693	0.7	0.378	0.9	0.604
		Proteins of the ubiquitin proteasome system					
75	293	Ubiquitin and ubiquitin-like proteins	9558	1.2	0.384	1.4	0.273
76	444	dito	9558	**2.4**	**0.000**	**4.8**	**0.001**
77	845	dito	9558	0.7	0.089	**0.5**	**0.002**
78	743	20S proteasome, A and B subunits	306433	1.4	0.279	1.0	0.933
		Unknown					
79	530			1.2	0.629	0.9	0.680
80	811			**0.3**	**0.001**	**0.5**	**0.002**
81	776			0.9	0.716	1.0	0.863
82	349			1.6	0.199	**1.7**	**0.023**
83	1799			1.4	0.148	1.5	0.086
84	418			1.4	0.229	**1.8**	**0.029**
85	15758			1.4	0.263	**1.7**	**0.027**
86	534			1.1	0.601	1.1	0.518
87	673			0.4	0.137	**0.3**	**0.041**
88	680			1.1	0.669	**0.4**	**0.010**
89	548			0.7	0.322	1.5	0.260
90	558			**3.9**	**0.005**	1.6	0.108
91	691			0.8	0.429	1.2	0.406
92	813			0.9	0.715	1.0	0.910
93	733			0.7	0.143	**0.6**	**0.036**
94	753			**0.6**	**0.004**	0.9	0.573
95	789			**0.2**	**0.001**	**0.5**	**0.022**

Temporal pattern of differentially expressed proteins

The temporal courses of proteins with significant differential expression under heat-and-starvation stress at at least one point in time (24 and/or 48 h) were separated in three temporal patterns (maximum after 24 h, maximum after 48 h, down-regulation) (Fig. 3.18). Specific differences were detected between the protein groups from clone G and M. The first temporal pattern was represented by glutathione transferases and H^+-transporting ATPases in both clones (Fig. 3.18 A, C), but considerable differences existed regarding the expression of 3-phosphoglycerate kinase, actins, arginine kinase, Hsp60, and peptidase S1 (clone G) and alpha tubulin, enolase and vitellogenins (clone M). The second temporal pattern (only in clone M; Fig. 3.18 D) was mainly represented by vitellogenins, H^+-transporting ATPases, actins, and arginine kinase. The third temporal pattern (down-regulation) was mainly represented by proteins of the carbohydrate metabolism, proteolytic enzymes, or non-Hsp60 chaperones in case of clone M (Fig. 3.18 B, E). Numbers of expressed proteins and maximal increase in expression intensities were higher in case of clone M.

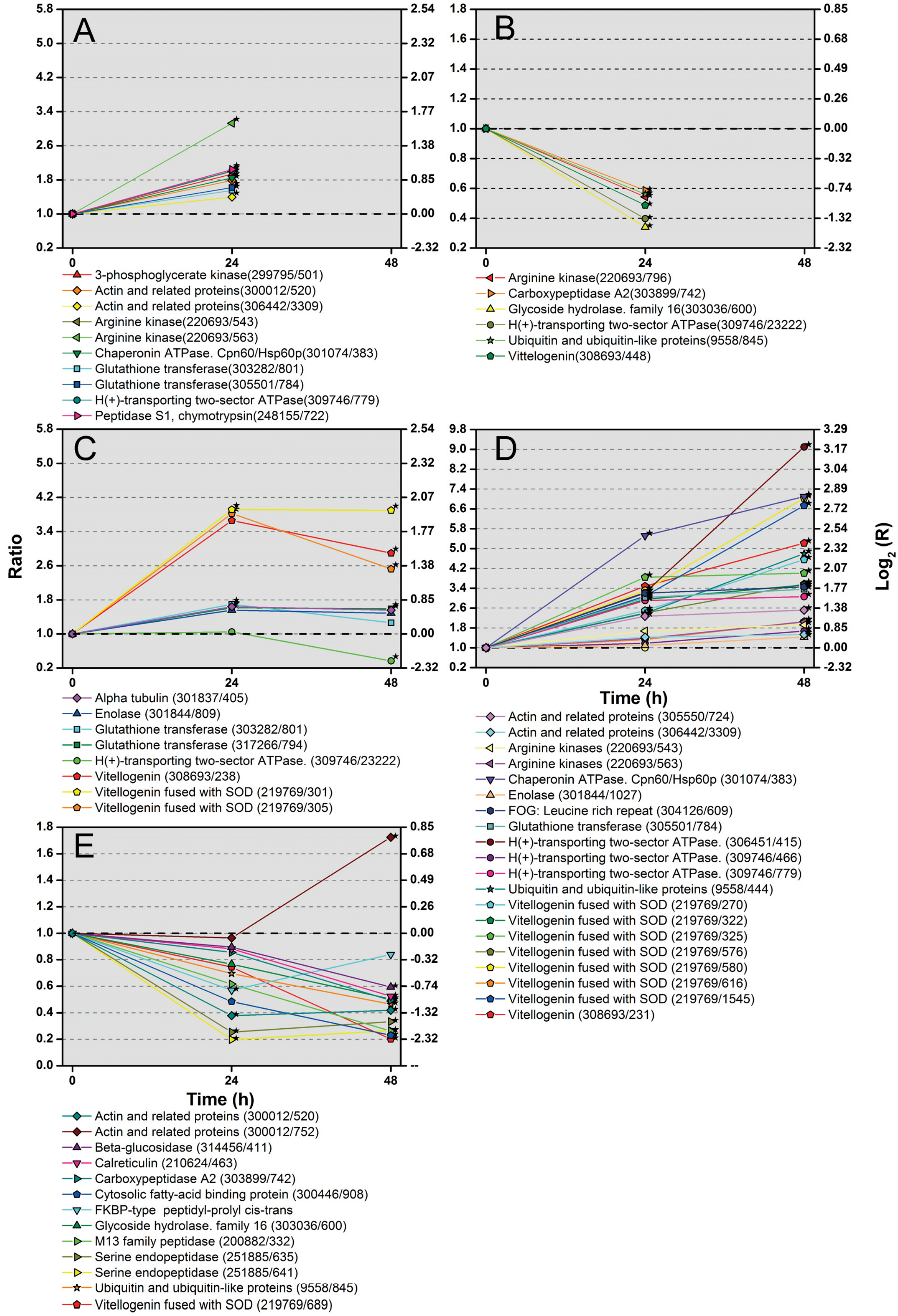
A
3-phosphoglycerate kinase(299795/501)
Actin and related proteins(300012/520)
Actin and related proteins(306442/3309)
Arginine kinase(220693/543)
Arginine kinase(220693/563)
Chaperonin ATPase. Cpn60/Hsp60p(301074/383)
Glutathione transferase(303282/801)
Glutathione transferase(305501/784)
H(+)-transporting two-sector ATPase(309746/779)
Peptidase S1, chymotrypsin(248155/722)
B
Arginine kinase(220693/796)
Carboxypeptidase A2(303899/742)
Glycoside hydrolase. family 16(303036/600)
H(+)-transporting two-sector ATPase(309746/23222)
Ubiquitin and ubiquitin-like proteins(9558/845)
Vittelogenin(308693/448)
C
Ratio
Alpha tubulin (301837/405)
Enolase (301844/809)
Glutathione transferase (303282/801)
Glutathione transferase (317266/794)
H(+)-transporting two-sector ATPase. (309746/23222)
Vitellogenin (308693/238)
Vitellogenin fused with SOD (219769/301)
Vitellogenin fused with SOD (219769/305)
D
Log2 (R)
Time (h)
Actin and related proteins (305550/724)
Actin and related proteins (306442/3309)
Arginine kinases (220693/543)
Arginine kinases (220693/563)
Chaperonin ATPase. Cpn60/Hsp60p (301074/383)
Enolase (301844/1027)
FOG: Leucine rich repeat (304126/609)
Glutathione transferase (305501/784)
H(+)-transporting two-sector ATPase. (306451/415)
H(+)-transporting two-sector ATPase. (309746/466)
H(+)-transporting two-sector ATPase. (309746/779)
Ubiquitin and ubiquitin-like proteins (9558/444)
Vitellogenin fused with SOD (219769/270)
Vitellogenin fused with SOD (219769/322)
Vitellogenin fused with SOD (219769/325)
Vitellogenin fused with SOD (219769/576)
Vitellogenin fused with SOD (219769/580)
Vitellogenin fused with SOD (219769/616)
Vitellogenin fused with SOD (219769/1545)
Vitellogenin (308693/231)
E
Time (h)
Actin and related proteins (300012/520)
Actin and related proteins (300012/752)
Beta-glucosidase (314456/411)
Calreticulin (210624/463)
Carboxypeptidase A2 (303899/742)
Cytosolic fatty-acid binding protein (300446/908)
FKBP-type peptidyl-prolyl cis-trans
Glycoside hydrolase. family 16 (303036/600)
M13 family peptidase (200882/332)
Serine endopeptidase (251885/635)
Serine endopeptidase (251885/641)
Ubiquitin and ubiquitin-like proteins (9558/845)
Vitellogenin fused with SOD (219769/689)

Fig. 3.18 Temporal changes in protein expression of the *D. pulex* clones G and M upon acute heat and starvation stress.

Temporal changes in expression ratios (R; see Tables 3.6, 3.7) in the *D. pulex* clones G (A, B) and M (C, D, E) of significantly (*; t-tests, $p < 0.05$; see Tables 3.6, 3.7) up- or down-regulated proteins after the acute exposure (time, 0 hours) of 20°C acclimated individuals to 24 hours or 48 hours at heat (30°C) and starvation stress (HS-stress). The ratio values either increased under heat and starvation stress, with maxima after (A, C) 24 hours or (D) 48 hours, or (B, E) decreased. Both linear (left) and logarithmic (log2; right) y-axes are shown. Numbers in parentheses (after protein functions) are gene and spot IDs.

Regulation of proteins from different categories

Calculating expression intensities of all proteins from one category (Fig. 3.19) at three different experimental conditions (control, 20°C, *ad libitum* food supply; 30°C, starvation for 24 hours, and 30°C, starvation for 48 hours) in clone G in comparison to clone M revealed higher protein amounts at control conditions for the FOG transcription factor and proteins of the category 'ubiquitin/proteasome system' (Fig. 3.19A), and lower proteins amounts within the category 'antioxidant defense/detoxification' after 24 hours of stress (Fig. 3.19B). Proteins of the category 'antioxidant defense/detoxification' and the FOG transcription factor were up-regulated with increasing stress period, whereas proteolytic enzymes were down-regulated. Cytoskeleton/muscle proteins were up-regulated only in clone G.

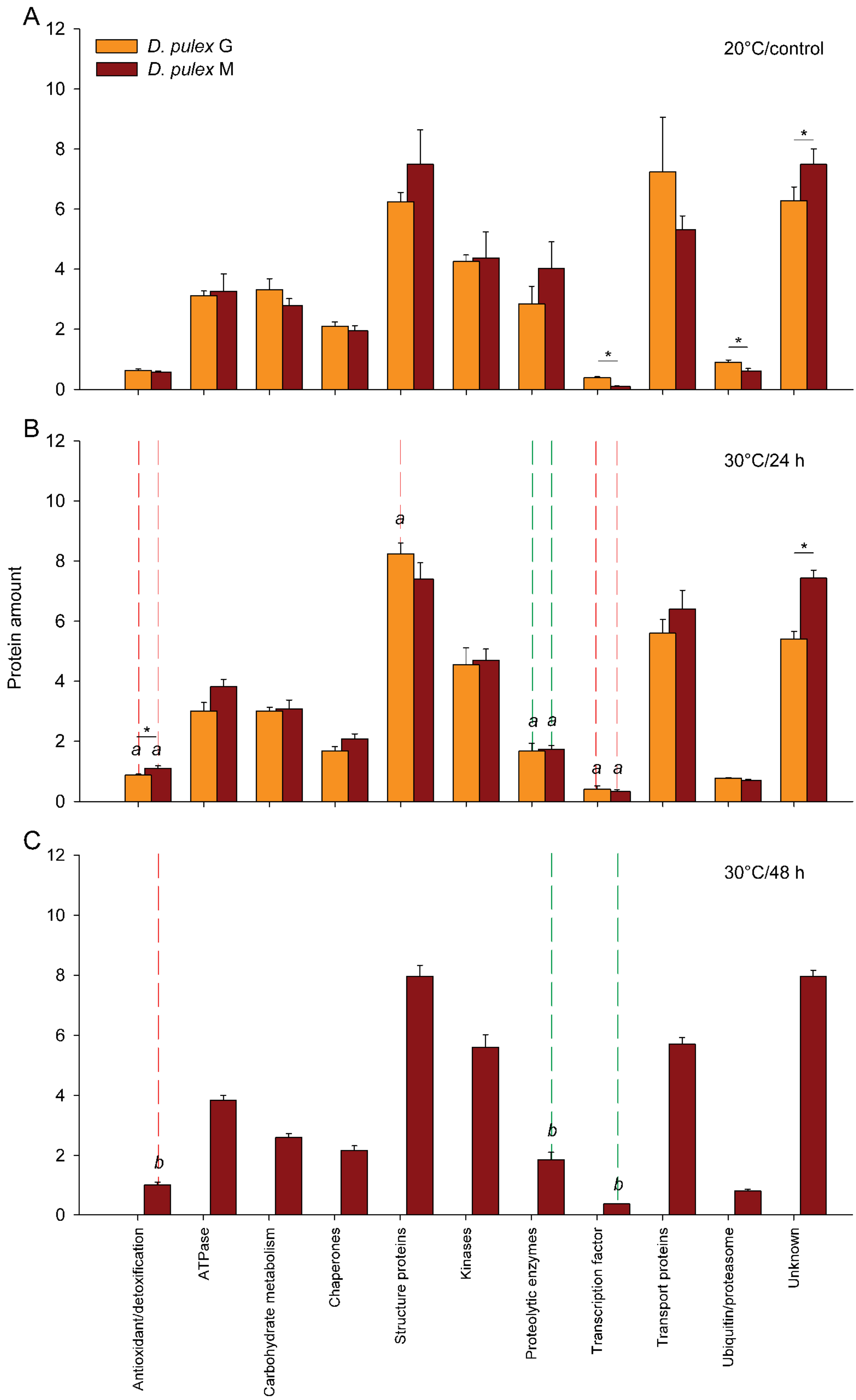
A
B
C
D. pulex G
D. pulex M
20°C/control
30°C/24 h
30°C/48 h
Protein amount
0
2
4
6
8
10
12
*
a
b
Antioxidant/detoxification
ATPase
Carbohydrate metabolism
Chaperones
Structure proteins
Kinases
Proteolytic enzymes
Transcription factor
Transport proteins
Ubiquitin/proteasome
Unknown

Fig. 3.19 Protein regulation within different categories upon acute heat-and-starvation stress.

Total expression levels (summed spot volumes; means ± S.E.M.) of identified proteins within different functional categories (see Tables 3.6, 3.7) for *D. pulex* clones G (orange bars) and M (brown bars) (**A**) at control condition (20°C, food *ad libitum*; clone G, $n = 5$ biological replicates [b.r.]; clone M, $n = 4$ b.r.), and (**B**) after 24 hours (clone G, $n = 5$ b.r.; clone M, $n = 5$ b.r.) or (**C**) 48 hours (clone M, $n = 7$ b.r.) of heat-and-starvation stress (S; 30°C). Asterisks and bars indicate significant differences between clones; small letters (*a*, 30°C/S/24 h vs 20°C/control; *b*, 30°C/S/48 h vs 20°C/control; *c*, 30°C/S/24 h vs 30°C/S/48 h) and dashed lines (red, up-regulation; green, down-regulation) denote significant differences between experimental conditions (two-way ANOVA and SNK analyses; $P < 0.05$).

3.3.6 Summary of differential protein expressions

To gain an overview of differential protein expressions in clone G and M at heat, starvation, and heat-and-starvation stress, the ratio (R) values from the 95 analyzed protein spots were plotted (Fig. 3.20 – 3.22) in the same order as in the Tables 3.2–3.7, and statistical analyses were carried out to identify significant differences between clones and experimental conditions with respect to category and protein family. Under heat stress, clone G and M differed in ratio values for the categories “chaperone” and “transport protein” (24 h; Fig. 3.20A – B: a, c) as well as “transcription factor” and “transport protein” (48 h; Fig. 3.20C – D: b, c). With respect to protein families, clone G and M differed in ratio values for HSP60, vitellogenin fused with SOD, and vitellogenin (24 h; Fig. 3.20A – B, asterisks). For the contrast heat stress vs heat-and-starvation stress, HSP60 and vitellogenin fused with SOD differed significantly (Fig. 3.20, 3.22: α, β). Under starvation stress, clone G and M differed in ratio values for the categories “transcription factor” and “transport protein” (48 h; Fig. 3.21C – D: b, c). With respect to protein families, clone G and M differed in ratio values for FOG and vitellogenin fused with SOD (48 h; Fig. 3.21C – D, asterisks). For the contrast starvation stress vs heat-and-starvation stress, HSP60, actin, and serin endopeptidase differed significantly (Fig. 3.21, 3.22: i, ii, iii). Under heat-and-starvation stress, clone G and M differed in ratio values for the categories “chaperone”, “transcription factor”, and “transport protein” (24 h; Fig. 3.22A – B: a, b, c). With respect to protein families, clone G and M differed in ratio values for HSP60, FOG, vitellogenin fused with SOD, and vitellogenin (24 h; Fig. 3.20A – B, asterisks).

Thus, significant differences existed between clone G and M including a higher up-regulation of chaperone/HSP60 in clone M both during heat and heat-and-starvation stress as well as higher up-regulations of transcription factor/FOG and transport protein/vitellogenin fused with SOD/vitellogenin in clone M during heat, starvation, and heat-and-starvation stress. Starvation promoted under heat stress conditions the expression of HSP60 and vitellogenin fused with SOD. Heat promoted under starvation conditions the expression of HSP60, but caused a reduced expression of actin and serine endopeptidase.

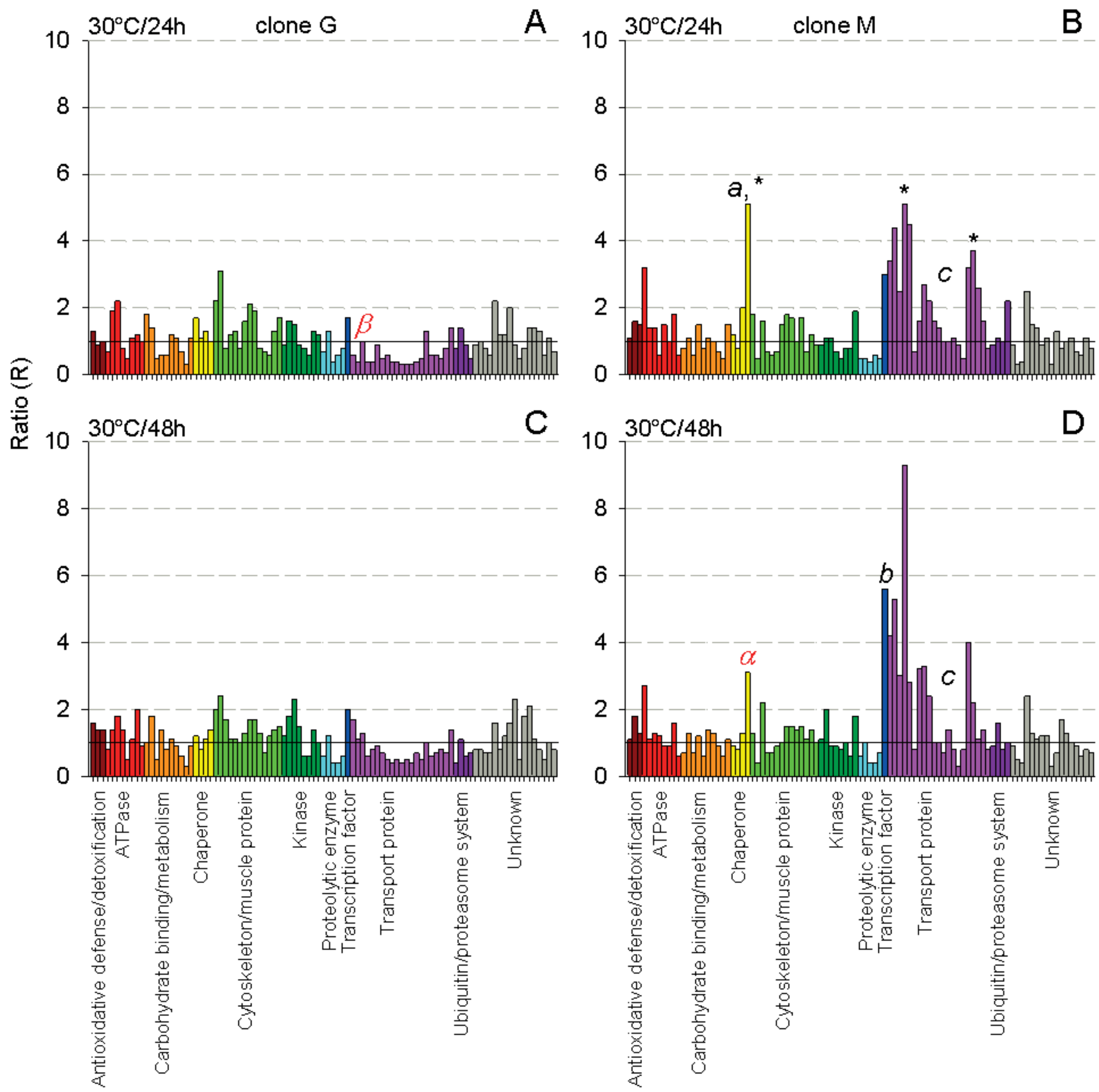

Fig. 3.20 Differential protein expression in clone G and M at heat stress.

Expression ratios (R) of proteins within different categories (data from Tables 3.2 and 3.3) for (**A**, **C**) clone G and (**B**, **D**) clone M after (**A**, **B**) 24 hours or (**C**, **D**) 48 hours of heat stress (30°C). Small letters for categories and asterisks for protein families indicate significant differences between clone G and M. Greek letters indicate significant differences between heat stress (*ad libitum* food supply) and heat-and-starvation stress (see Fig. 3.22) (two-way ANOVA and SNK analyses; $P < 0.05$).

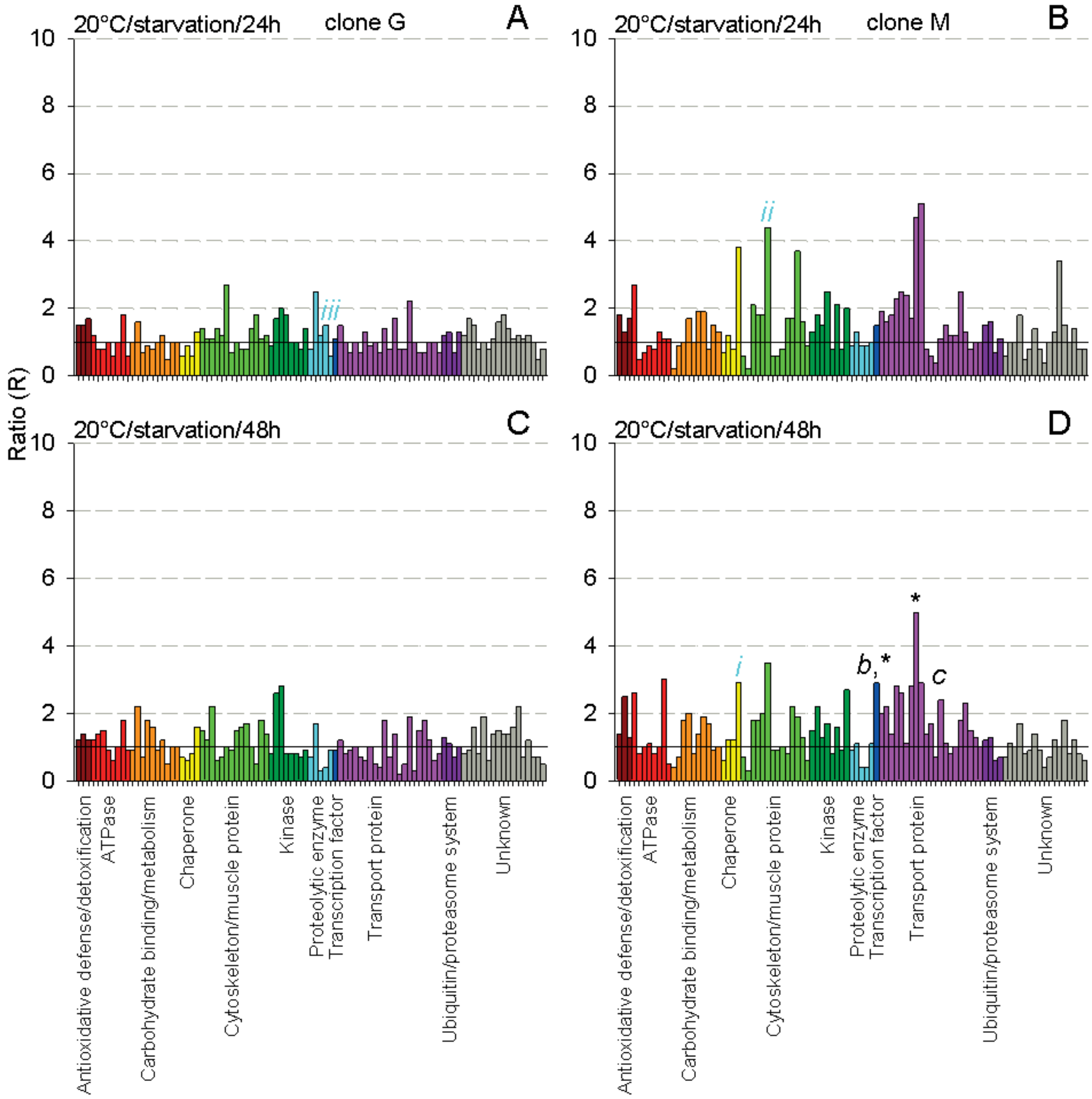

Fig. 3.21 Differential protein expression in clone G and M at starvation stress.

Expression ratios (R) of proteins within different categories (data from Tables 3.4 and 3.5) for (**A**, **C**) clone G and (**B**, **D**) clone M after (**A**–**B**) 24 hours or (**C**–**D**) 48 hours of starvation stress (20°C; no food). Small letters for categories and asterisks for protein families indicate significant differences between clone G and M. Roman numbers indicate significant differences between starvation stress at T = 20°C and heat-and-starvation stress (see Fig. 3.22) (two-way ANOVA and SNK analyses; $P < 0.05$).

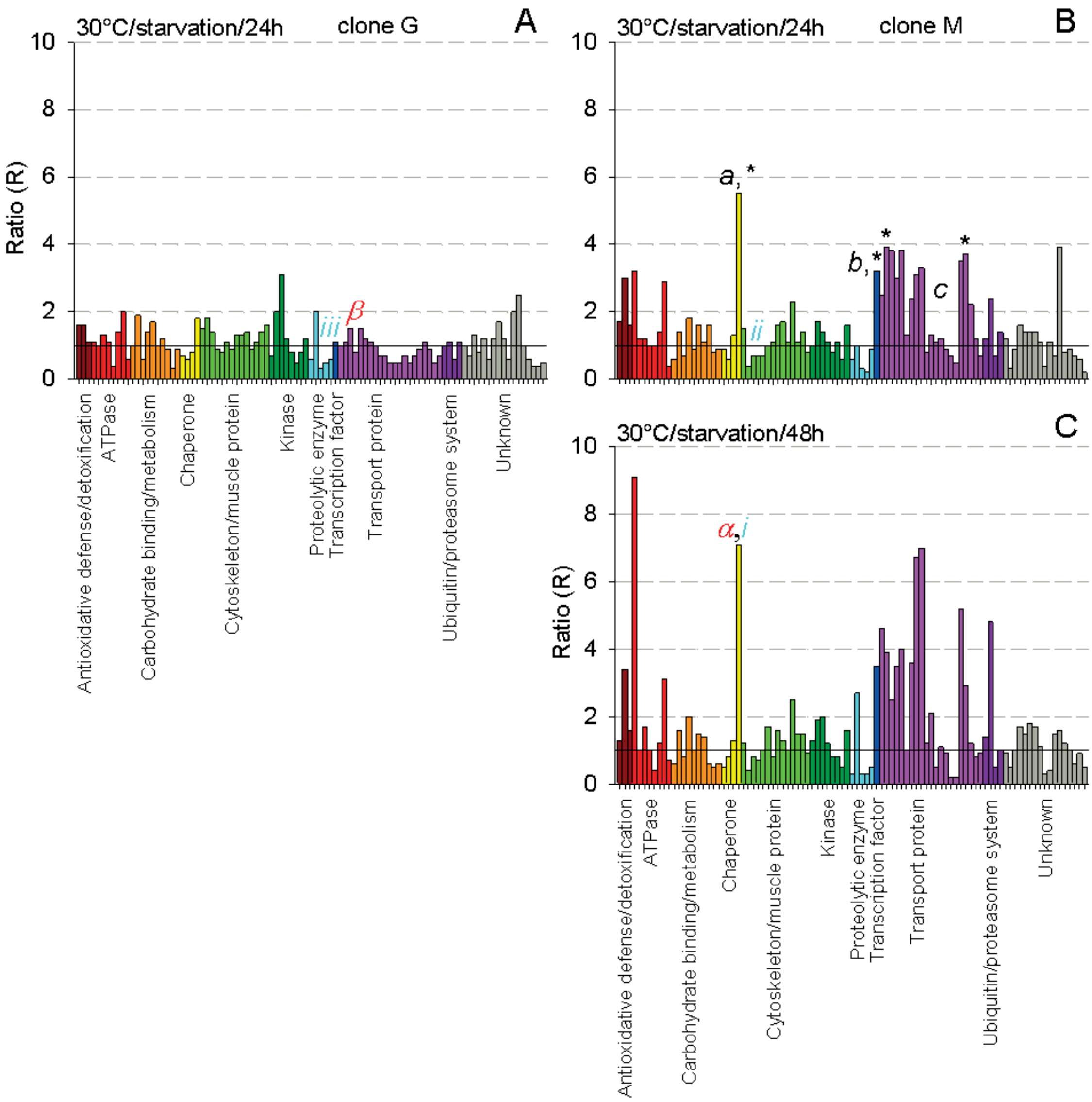

Fig. 3.22 Differential protein expression in clone G and M at heat-and-starvation stress.

Expression ratios (R) of proteins within different categories (data from Tables 3.6 and 3.7) for (**A**) clone G and (**B**–**C**) clone M after (**A**–**B**) 24 hours or (**C**) 48 hours of heat-and-starvation stress (30°C; no food). Small letters for categories and asterisks for protein families indicate significant differences between clone G and M. Greek letters indicate significant differences between heat stress (*ad libitum* food supply; Fig. 3.20) and heat-and-starvation stress. Roman numbers indicate significant differences between starvation stress at T = 20°C (Fig. 3.21) and heat-and-starvation stress. (Two-way ANOVA and SNK analyses; $P < 0.05$).

3.4 Validation of the protein expression changes: HSP60

As quality check of the proteomic data, heat-induced (30°C for 24 h and 48 h) changes in the quantity of a prominent protein example, namely HSP60, was determined in clone G and M by a method other than two-dimensional (2D) gel electrophoresis and computer-based volume quantification. Applying Western Blot analysis on the same samples, which had already been studied using 2D gels and had been kept frozen at -80°C, revealed two distinct lanes at ~73.8 and ~60.4 kDa (Fig 3.23A). The expression of HSP60 (60.4 kDa protein) increased with the period of heat stress and was markedly higher in clone M than in clone G (Fig. 3.23A, B), which fits quite well with the results obtained with the 2D gels (Fig. 3.20). The protein from the 73.8 kDa lane did not show significant changes in quantity upon acute heat stress (Fig. 3.23B).

In both *Daphnia* clones measured intensity on Western Blots showed that expressions of the identified HSP60 isoforms in *D. pulex* clone M were stronger, under control conditions as well as under H-stress, than in clone G. In both clones the expression of the two HSP60 isoforms were enhanced during acute heat stress and expression levels of the 60 kDa protein were higher than for the 74 kDa isoform. The induction pattern for HSP60 measured on the 2D Gels was confirmed in the Western Blot analysis of the bands at ~60.4 kDa, even though the observed induction pattern on the Western Blot showed differences in quality and quantity. To clarify the appearance of two distinct HSP60 bands (Fig. 3.23) and the deviations in mass between Western Blot (73.8 and 60.4 kDa) and 2D gel analyses (Table 3.2; $M_r e$, 89.1 kDa), bioinformatic studies were carried out (see Supplement) which resulted in eleven identified HSP60 genes containing the HSP60 specific Cpn60_TCP1 domain (PF00118) (Fig. 3.24). The HSP60 identified by 2D gel electrophoresis and mass spectrometry belongs to group 3 with its encoding gene located on scaffold 12 (Fig. 3.24 and supplement).

A)

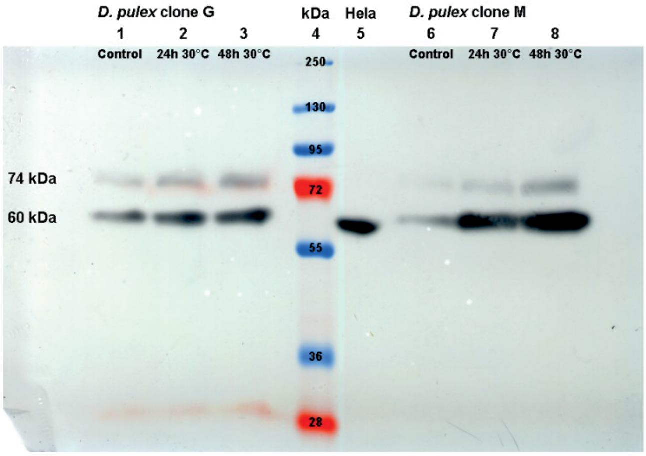

B)

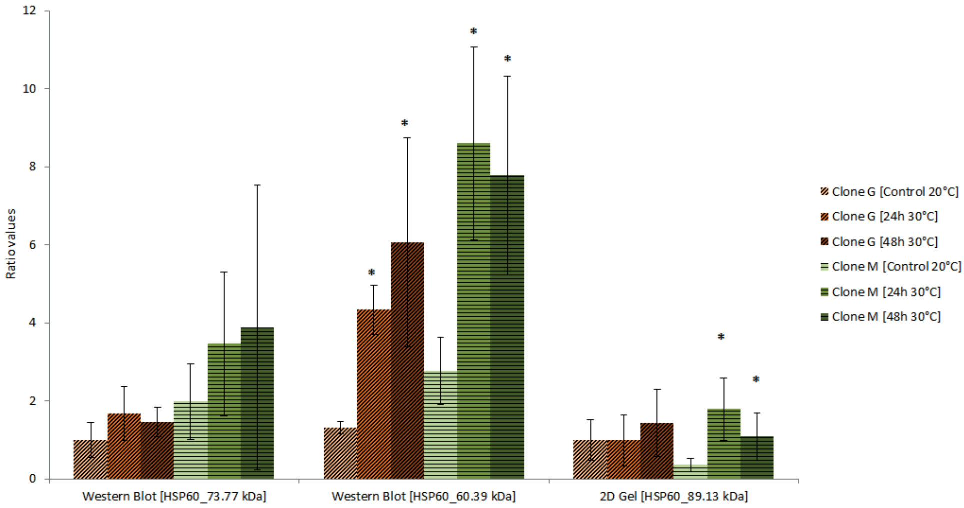

Fig. 3.23 Effect of acute heat stress at 30 °C on HSP60 in *Daphnia pulex* clone G and M.

(**A**) Representative Western Blot of HSP60 expression. From left to right: clone G, control/20°C, 30°C/24 h, 30°C/48 h; protein mass marker; heat-shocked HeLa cells (positive control); clone M, control/20°C, 30°C/24 h, 30°C/48 h.) B) Quantification of induced HSP60 levels. Values for Western Blot intensities were calculated relative to the positive control (heat shocked Hela cells lane 5 in A). To compare results obtained from Western Blots to 2D Gels, ratio values were calculated relative to the control of *D. pulex* clone G [HSP60_73.77 kDA]. Measured protein levels in 2D Gels were also added to identify induction patterns. For 2D Gels, ratio values were calculated relative to the control of *D. pulex* clone G. Mean ± SEM of three independent samples. *P < 0.05 compared to control conditions, t-tests.

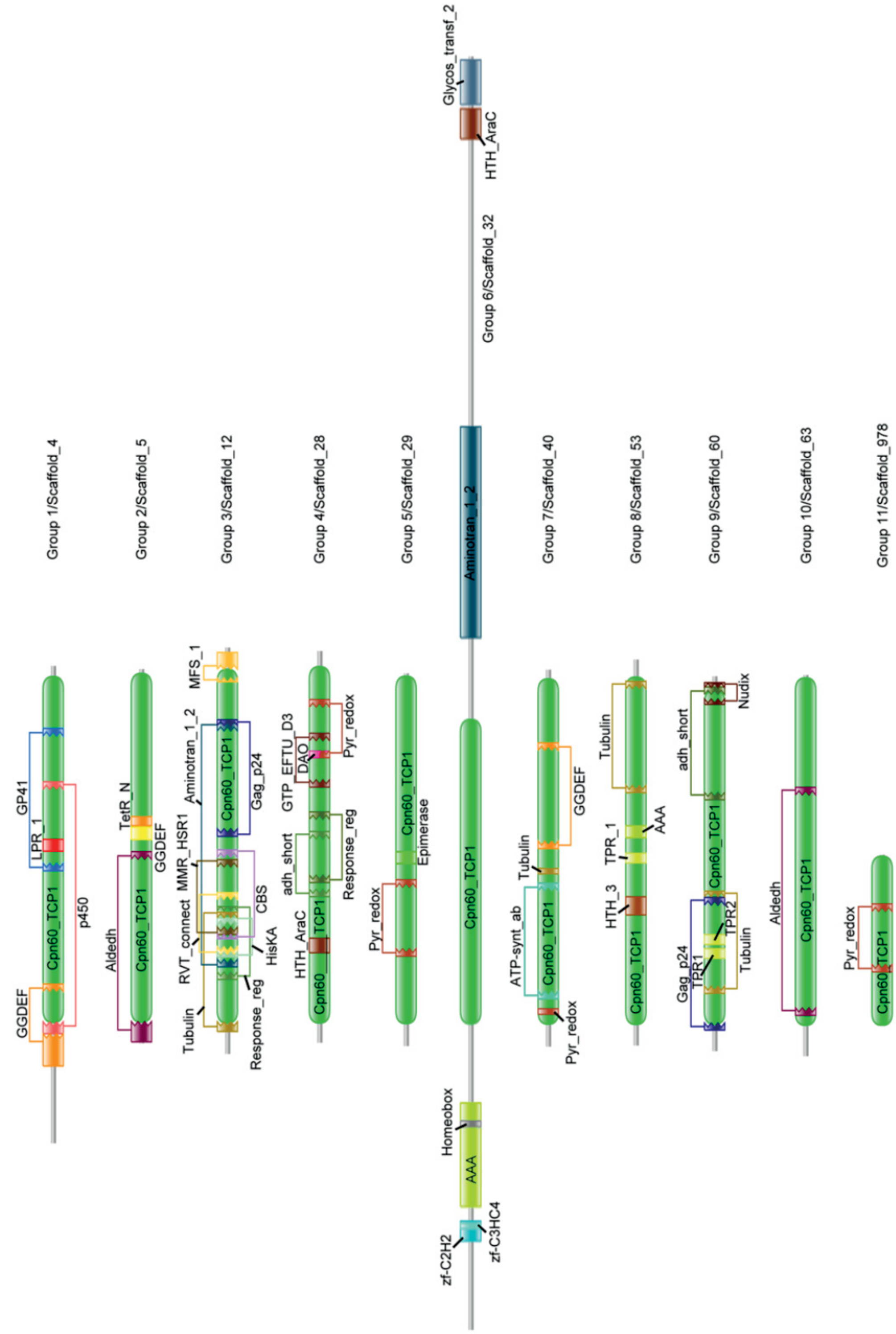

Fig. 3.24 Identified domain organisations or architectures in putative HSP60 proteins.

For each identified group and scaffold, the characteristic domain organization and architecture of the putative encoded HSP60 protein was determined. The sequence is represented as a grey bar. As of release 22.0, Pfam 100 identifies 32 domains. The HSP60 specific Cpn60_TCP1 domain (PF00118) is coloured in green. Protein length, start and end position for each identified domain as well as the corresponding Pfam accession number were evaluated by *CLC Genomics Workbench* and can be found in Table 5.2 in the supplement.

4 Discussion

2D gel electrophoresis and mass spectrometry were used to study effects of heat stress (30°C), starvation stress, and the combination of both on the proteomes of two *D. pulex* clones (clone G and M). To determine the time of the initial stress responses of both clones, survival- and long term swimming-assays were applied. The proteomes were assessed in 20°C-acclimated animals (control condition) and after 24 and 48 hours of stress.

As only dominant spots were picked for mass spectrometry, the 34 identified proteins were present in high copy numbers. The *D. pulex* clone G was already subject of previous investigations (Gerke *et al.*, 2011) including two proteomic studies on animals long-term-acclimated to 10°C and 20°C (Schwerin *et al.*, 2009) or normoxia and hypoxia (Zeis *et al.*, 2009). Improved sample preparation (prevention of proteolysis by rapid protein precipitation using trichloroacetic acid) caused changes in the protein spot pattern in comparison to the two previous studies (Schwerin *et al.*, 2009; Zeis *et al.*, 2009) Also the identified proteins were mostly different in the previous work and the present study, which may partly be related to differences in environmental conditions and partly to the improvements in sample preparation. The common set of differentially expressed proteins (DEPs) from the three proteomic studies comprised a total of five proteins, with one belonging to the category 'proteolytic enzyme' (M13 family peptidase) and four of them to the category 'carbohydrate binding/metabolism' (enolase and the three glycoside hydrolases, families 7, 9, and 16). The common set from the two temperature-related proteomic studies comprised a total of ten proteins, which included four proteins from the category 'carbohydrate binding/metabolism' (enolase and the three glycoside hydrolases, families 7, 9, and 16), the three actin isoforms, one proteolytic enzyme (M13 family peptidase) and the two vitellogenin isoforms (see Table 3.2). From the minimal stress proteome (MSP) defined by (Kültz, 2005), four proteins were also identified in this study, which were enolase (glycolysis, energy metabolism), a HSP60 chaperone, a nucleoside-diphosphate kinase (exchange of phosphate groups between different nucleoside diphosphates), and a FKBP-type peptidyl-prolyl cis-trans isomerase (cyclophilin-like function). Investigations of the common set of DEPs of the two temperature-related proteomic studies (Schwerin *et al.*, 2009 and this study) revealed, that in 10°C-acclimated *D. pulex* clone G, actin isoforms as well as the vitellogenin isoforms were cold-induced, whereas Carbohydrate-modifying enzymes were constitutively expressed or down-regulated (e.g. enolase) in the cold (Schwerin *et al.*, 2009). From the four identified proteins of the MSP, enolase (glycolysis, energy metabolism), a HSP60 chaperone, a nucleoside-diphosphate kinase (exchange of phosphate groups between different nucleoside diphosphates), and a FKBP-type peptidyl-prolyl cis-trans isomerase (cyclophilin-like function), the first three types of proteins were significantly (HSP60) or tendentiously more strongly up-regulated in clone M than in clone G (Tables 3.2, 3.3).

The two *D. pulex* clones G and M were chosen for experimentation because of significant differences in heat tolerance, with clone M performing much better than clone G at heat stress (Fig. 3.3) or at heat-and-starvation stress (Fig. 3.4). Under pure starvation stress in case of both clones, 50% mortality was reached after 167 hours and after 600 – 700 hours all animals were dead (Table 3.1, Fig. 3.2). Under pure heat stress, 100% mortality was found after 192 hours in case of both clones, and 50% mortality occurred after 48 hours (clone G) or 98 hours (clone M) (Table 3.1). Applying heat-and-starvation stress caused 50% mortalities after 17 hours (clone G) and 49 hours (clone M) and 100% mortality in clone G after 40 hours and in clone M after 80 hours (Table 3.1). The heat stress of 30°C turned out to be the thermal limit of these organisms, particularly in case of the *D. pulex* clone G (Fig. 3.3). Mortality was even significantly higher, if both stress conditions were imposed at the same time (Fig. 3.4).Thus, the combination of heat and starvation particularly impaired clone G. This result fits to the significant decrease in protein content only in clone G during starvation stress (Fig. 3.5). These results are in accordance with other observations in *Daphnia*. Starvation significantly decreases the body weight and body content of energy, protein, and lipids (Han *et al.*, 2012), and in *D. magna* and *D. galeata-hyalina* low food concentration caused a reduction of total protein content (Guisande *et al.*, 1991; Schwerin *et al.*, 2010). Under starvation and normoxia conditions, protein demand in *D. magna* will first be met by breaking down hemolymph proteins (including hemoglobin), if available, and then breaking down cellular proteins, and expression of proteins involved in carbohydrate binding and metabolism or proteolytic processes were mostly down-regulated (Schwerin *et al.*, 2010). Under acute heat stress no significant changes in protein content were observed. Research on *D. galeata-hyalina* showed, that protein stores are only used, if there is not sufficient protein available from food (Schwerin *et al.*, 2010). Under acute heat-and-starvation stress, the protein amount did not change significantly for *D. pulex* clone G and clone M, and it was less than the observed reduction under pure starvation stress. With rising temperature, oxygen availability in the water diminishes, while the need for energy supply and therefore cellular oxygen demand rises (Pörtner, 2001; Pörtner, 2002). However, under starvation conditions, nutrient and energy storages will be depleted in order to maintain essential physiological functions (Han *et al.*, 2012). Therefore it is very probable, that the weaker decline of total protein amount in *D. pulex* clone G under heat-and-starvation stress is due to the fact, that hemolymph protein concentration, especially hemoglobin concentration, has to be maintained constant to ensure oxygen transport from oxygen-poor water. Also the shorter lifespan could be an indication for depletion of cellular protein stores by macroautophagy. This would be consistent with results for *D. magna* exposed to starvation and hypoxia, were the hemolymph protein store remained unchanged, whereas the cellular protein store was broken down, since hemoglobin concentration had to be maintained to ensure cellular oxygen demands (Schwerin *et al.*, 2010). The animals of clone G, which were exposed to heat-and-starvation stress for the later determination of protein content and proteome, were all dead after 40 hours of stress (Fig. 3.4, 3.5).

It is therefore clear, that clone G is less heat-tolerant and to a certain extent also less tolerant to starvation than clone M, which fits to the different enviromental conditions in the habitats of both clones (section 2.1). Furthermore, the points in time for proteome determinations (24 and 48 hours of stress) approached the temporal stress limits of both clones, although it is essential to point out, that only actively and regularly swimming animals, which indicated that they were still in good health, were chosen for proteomics.

4.1 Major differences in stress-induced proteomic responses between the *D. pulex* clones G and M

Main differences between clone G and M in the proteomic responses to stress concerned chaperones and vitellogenins (Fig. 3.20–3.22, letters ‘*a*’, ‘*b*’, ‘*c*’, and asterisks). With respect to chaperones, particularly HSP60 was highly up-regulated in clone M at any kind of stress (Tables 3.3, 3.5, 3.7), whereas only heat-and-starvation stress induced a significant up-regulation of HSP60 in clone G (Table 3.6). In *D. magna,* also interclonal differences in the constitutive level of Hsp60 as well as in the increase in Hsp60 upon exposure to stress were demonstrated (Pauwels *et al.*, 2005). Concerning HSP60 functions, mitochondrial HSP60 supports protein import and folding (Koll *et al.* 1992) and DNA metabolism (Kaufmann *et al.* 2003), and cytoplasmic HSP60 counteracts apoptosis (Itoh *et al.* 2002). HSP60 induction is also part of the cellular stress response (Martin *et al.* 1992; Vargas-Parada and Solis 2001). Under heat stress, HSP60 function is presumably related to protein repair, whereas starvation stress may require other functions of this chaperone than maintaining/repairing the cellular protein pool. Transmembrane protein transports (Koll *et al.* 1992) and/or mitochondrial DNA metabolism (Kaufmann *et al.* 2003) could become key functions of HSP60 under starvation stress. Whatever the case, it is likely that (particularly in clone M) other heat shock proteins were also up-regulated aside from HSP60, which were not detected in the current proteomic study. Maximal HSP60 concentration was usually reached early (after 24 hours of stress; Fig. 3.10B, 3.14B, 3.18A). This result fits to a recent transcriptomic study on clone G (D. Becker, unpublished data) showing an immediate gene expression response of all HSP genes upon acute heat stress (tranfer from 20°C to 30°C) with maximal mRNA levels after two hours of stress. Only heat-and-starvation stress evoked an ongoing increase in HSP60 level in clone M (Fig. 3.18D).

The clearly higher up-regulation of vitellogenins in clone M than in clone G is more difficult to explain. There were two types of vitellogenins (VTG) up-regulated, with one fused with a superoxide dismutase (SOD) domain (VTG-SOD). VTG is a precursor of the yolk protein vitellin. It is a lipoglycoprotein, that is employed as a vehicle to provide the developing embryo with proteins, lipids, carbohydrates, and other essential resources (Schwerin *et al.* 2009). SOD is a major ROS-scavenging enzyme, which converts superoxide into the less harmful hydrogen peroxide which is then degraded by catalase (Storey 1996). Until now, a VTG-SOD type of vitellogenin has been reported for only two other crustaceans, *Daphnia magna* (Kato *et al.* 2004) and *Artemia parthenogenetica* (Chen *et al.* 2011). The SOD-like domain shows strong phylogenetic relationships to viral and bacterial Cu/Zn SODs, whereas the VTG domain is related rather to insect VTGs than to decapod VTGs (Chen *et al.* 2011; Tokishita *et al.* 2006). In *D. magna*, SOD activity of the fusion protein was suggested to be low due to amino acid substitutions or deletions (Tokishita *et al.* 2006), whereas in *A. parthenogenetica*, SOD activity was proposed to be high (Chen *et al.* 2011). *Daphnia* and *Artemia* release ephippia or diapause cysts (encysted embryos) to withstand environmental stress, and it was suggested, that the SOD domains of both VTGs are important during the development of ephippia/diapause cysts (Chen *et al.* 2011). Since this VTG type was (highly) up-regulated only in clone M, this may indicate the production of ephippia as an emergency response upon acute heat stress, whereas clone G may have been too stressed to be able to invest resources in reproductive processes. The previous study on long-term-acclimated animals of clone G (Schwerin *et al.* 2009) showed vitellogenins to be cold-induced at 10°C acclimation. An enhanced VTG content at 10°C may indicate an improved supply and better resources of pregnable eggs in the cold, whereas the induction of VTG under acute heat stress may result from an induced formation of ephippia. Maximal VTG levels were usually reached in clone M only after 48 hours of stress (Fig. 3.10D, 3.14D, 3.18D).

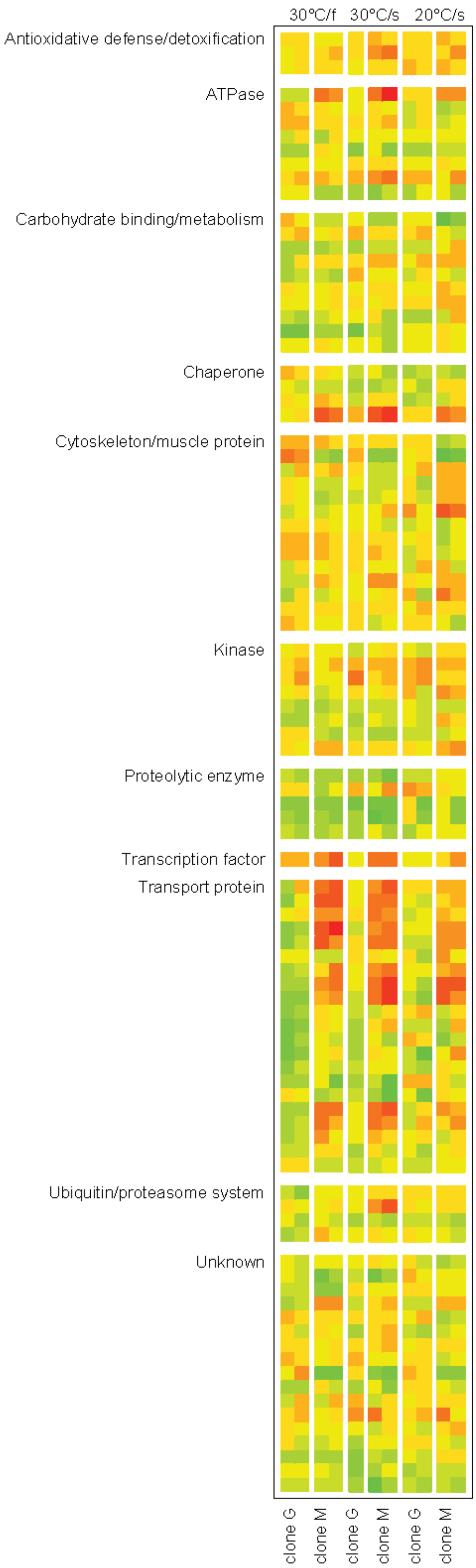

A third protein, a FOG ('friend of GATA') transcription factor, was also differently expressed in clone G and M under stress (Fig. 3.20–3.22). FOG transcription factors, which interact with members of the GATA family of zinc finger transcription factors, are highly represented in the *D. pulex* genome. Thus, a specific function of the identified FOG protein cannot be suggested yet. According to arthropod orthology (ARP2; arthropod orthologous gene group ID, version 2; http://arthropods.eugenes.org/arthropods/), however, this protein may also be a membrane glycoprotein (LIG-1), for which a participation in cell growth processes has been reported (Suzuki *et al.* 2002). The similarity in clone-specific expression of 'FOG' and VTG (higher expression in clone M) and their similar time course (Fig. 3.10D, 3.14D, 3.18D), together with a possible participation of 'FOG' in cell growth processes may be considered as an indication of an involvement of 'FOG' during the development of ephippia/diapause cysts.

Fig. 4.1 Ratio values (R) of protein expression under different stress conditions encoded in spectral pseudo colours.

From left to right: 30°C at *ad libitum* food supply (30°C/f), 30°C without food supply (30°C/s), 20°C without food supply (20°C/s), with clone G at 24 and 48 hours of stress alternating with clone M at 24 and 48 hours of stress (red, up-regulation; blue, down-regulation). Data from Tables 3.2–3.7.

4.2 Differences in heat-induced proteomic responses between the fed and non-fed *D. pulex* clones G and M

Two different heat stress conditions (30°C) were applied, one without food restriction and the other one combined with starvation. The latter type of stress caused already 50% mortality after 17 hours of exposure in animals of clone G. Contrasting protein expression at both conditions (Fig. 3.20, 3.22) revealed major differences in protein regulation for chaperones/HSP60 (clone M; letter 'α' in the graphs) and vitellogenins (clone G; letter 'β'). For both stress conditions, protein expression was induced in clone M, while in clone G vitellogenin expression was repressed. In clone M, chaperones/HSP60 were more intensely expressed under the double-stress conditions. Both heat and starvation evidently induced stress, which further promoted chaperone/HSP60 expression in the clone that exhibited this type of stress response already under 'pure' heat stress conditions (clone M) and reduces, in contrast to heat stress alone, VTG repression in clone G. In clone M, VTG expression may have already reached its limit.

Significant heat-induced proteomic responses were detected in all categories (Fig. 4.1; Tables 3.2, 3.3, 3.6, 3.7). More markedly in clone M than in clone G (see also Fig. 4.2), glutathione transferase (GST) isoforms from the category 'antioxidative defense/detoxification' were significantly up-regulated which, according to ARP2, belong either to the Sigma (gene ID: 305501) or Theta classes of glutathione S-transferases (GSTs). GSTs catalyze conjugations of reduced glutathione with many substrates such as xenobiotics or toxins to contribute in this way to their detoxification (Sheehan *et al.* 2001). Previous studies have already shown increases in GST mRNA level upon heat stress, which suggests a participation of GSTs in heat tolerance mechanisms (Yao *et al.* 2011). Since heat stress is linked with the formation of reactive oxygen species (ROS) (Pörtner 2002; Pörtner and Knust, 2007; Pörtner and Farrell, 2008), the heat-induced GST proteins may have been involved in the detoxification of ROS-damaged cellular components (Storey 1996). Heat-and-starvation stress caused GST expression (Sigma-GST in particular) to further increase, which adds starvation stress to other types of stress (e.g., heavy metal, osmotic, and temperature stress or drought stress) that cause increases in GST activity and induction (Hogue *et al.* 2007; Haluskova *et al.* 2009).

Again more markedly in clone M than in clone G (see also Fig. 4.2), the two proteins from the category 'ATPase' were significantly up-regulated which, according to ARP2, are subunits of the vacuolar-type of proton-pumping ATPase (V-ATPase) that energize, for instance, apical membrane transports of monomers from nutrients (Wieczorek, 1992; Harvey and Wieczorek 1997). They are also involved in the regulation of acidity within intracellular compartments (Forgac 2007) and autophagy (von Schwarzenberg *et al.*, 2012), which is part of the cellular stress response (Platini *et al.* 2010), or they contribute to non-apoptotic programmed cell death (PCD) under ER (endoplasmic reticulum) stress (Kim *et al.* 2012).

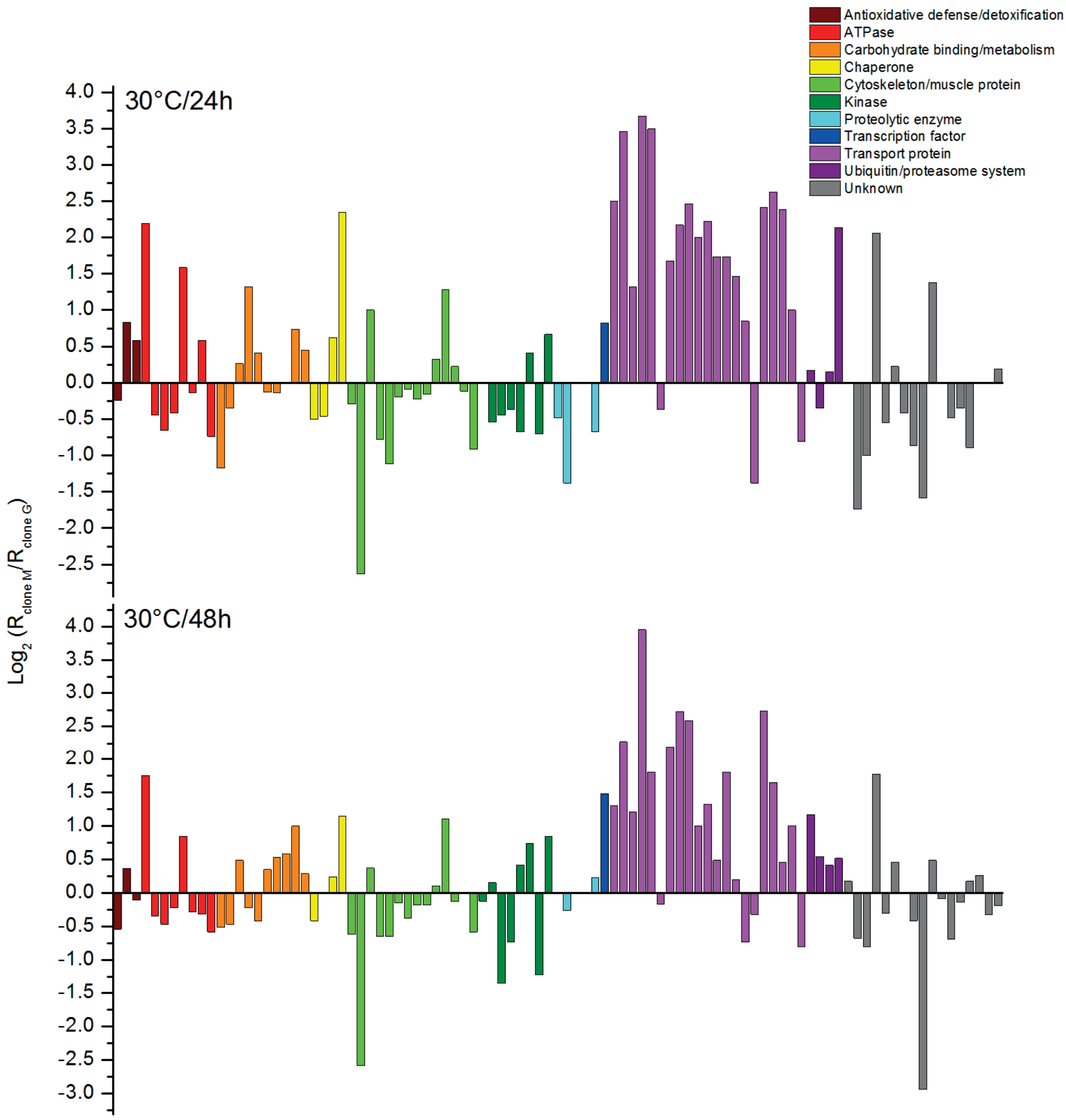

Fig. 4.2 Differences in ratio values (R) of protein expression between clone M and G at heat stress.

Differences in the ratio values of protein expression were calculated between clone M and G for the condition 30°C, *ad libitum* food supply (top, 24 h of stress; bottom, 48 h of stress; data from Tables 3.2–3.3).

It is difficult to say, why V-ATPase subunits are up-regulated in both *D. pulex* clones, but the regulation of pH and autophagy may be most important under heat stress and even more under heat-and-starvation stress.

Within the category ‘carbohydrate binding/metabolism’, glycoside hydrolases were significantly down-regulated at elevated temperature (the glycoside hydrolase family 7 and particularly family 16 in clone G and clone M) (see also Fig. 4.1). According to ARP2, the glycoside hydrolase, family 7 encodes endoglucanases, which are involved in cellulose degradation (Davies and Henrissat, 1995). The glycoside hydrolase family 16 codes for a β-1,3-glucan binding protein (gram-negative bacteria binding protein, GNBP), which is a pattern recognition receptor protein involved in immune responses (Roux *et al.* 2002). Enolase, however, was up-regulated in clone M during heat-and-starvation stress. Besides its glycolytic function, enolase was identified as Hsp48p, found in association with the cell wall (Edwards *et al.* 1999) and identified as cofactor of tRNA targeting toward the mitochondria (Entelis *et al.* 2006). However, there was a predominant down-regulation of proteins for ‘carbohydrate binding/metabolism’ under heat stress (Fig. 3.11, 3.19 and 4.1), which was possibly the result of a strategy to focus on stress protein expression, while disregarding protein expressions for metabolic and other more common processes (see also the discussion of proteolytic enzymes below).

Within the category ‘chaperone’, three proteins were significantly up-regulated upon acute heat stress (clone G, calreticulin; clone M, HSP60 and protein disulphide isomerase). Under acute heat and starvation stress HSP 60 was upregulated in both strains. Calreticulin (CRT) prevents misfolded proteins in the ER from proceeding to the Golgi apparatus, which finally causes their degradation, and it is also involved in the regulation of Ca^{2+} homeostasis (Gelebart *et al.* 2005). In addition, CRT mRNA expression increases upon acute cellular stress (Conway *et al.* 1995), and CRT proteins interact with other chaperones during the recovery from acute stress (Jethmalani and Henle 1998). Furthermore, CRT accumulation and function is linked with apoptotic processes (Prasad *et al.* 1999; Tarr *et al.* 2010). In clone M, however, CRT and, additionally, a FKBP-type peptidyl-prolyl cis-trans isomerase (FKBP) were down-regulated during heat-and-starvation stress. FK506-binding protein (FKBP) is one of two major immunophilins, an ancient and ubiquitous protein family of highly conserved proteins binding immunosuppressive drugs such as FK506, rapamycin and cyclosporin A. Most of FKBP family members bind FK506 and share a characteristic peptidyl-prolyl cis-trans isomerase domain with protein folding as key feature (Granzin *et al.*, 2006; Kang *et al.*, 2008). Small size FKBP family members contain only FK506-binding domain, while FKBPs with large molecular weights possess extra domains, such as tetratricopeptide repeat domains, calmodulin binding and transmembrane motifs. FKBPs are involved in several biochemical processes including protein folding, receptor signaling, protein trafficking, protein assembly and transcription; they participate in protein transportation and protect cells from apoptosis through their molecular interactions with receptors or proteins (Shirane and Nakayama 2003; Kang *et al.* 2008). Some FKBPs (FKBP38 and FKBP12-rapamycin complex) also function as inhibitors of mTOR, a central regulator of cell growth. In response to growth factor stimulation and nutrient availability, mTOR activity is regulated through FKBP and a Ras-like small GTPase (RHEB) interaction. RHEB prevents the association of FKBP with mTOR (Bai *et al.*, 2007). Protein disulfide isomerases, which were also reported to be involved in apoptotic processes (Prasad *et al.* 1999), support protein folding within the ER by catalyzing thiol-disulfide exchanges (formation of disulfide bonds between cysteine residues; Hatahet and Ruddock 2007). The heat-induced expression of CRT in clone G may indicate misfolded proteins in the ER and apoptotic processes, whereas the strong expression of HSP60 in clone M can be interpreted as an indicator of a reasonably well working protein protection and repair machinery to prevent apoptosis upon acute heat stress.

Alpha/beta tubulins but also actins from the category ‘cytoskeleton/muscle proteins’ were frequently up-regulated upon acute heat stress (particularly in clone G). At lower (acclimation) temperatures, it was the exact opposite in clone G, with a down-regulation of actins between 10°C and 20°C acclimation (Schwerin *et al.*, 2009). As heat stress is known to have detrimental effects on the cytoskeleton and its constituents (Richter *et al.* 2010), possibly resulting in a disturbance of cytoplasmic organization and a collapse and aggregation of the intermediate filament cytoskeleton around the nucleus (Welch and Suhan, 1985; Leicht *et al.*, 1986; Walter *et al.*, 1990; Kuwahara, 1991; Coss and Linnemans, 1996; Podrabsky and Somero, 2004; Serafini *et al.*, 2011), the stronger expression of cytoskeleton proteins in clone G may indicate more severe cell damage and increased efforts to re-construct this highly sensitive cellular organization system.

Arginine kinase (AK) from the category ‘kinase’ was mainly regulated in clone G. AK is a phosphotransferase playing a key role in cellular energy metabolism by catalysing the reversible transfer of a phosphate between ATP and guanidine compounds (Jarilla and Agatsuma 2010). The phosphorylated high-energy guanidine is referred to as a phosphagen (Uda *et al.* 2006). Phosphagens serve for the replenishment of the ATP pool in cells with high

ATP turnover rates. The simultaneous up- and down-regulation of arginine kinase in two spots (ID757, ID796) may be due to activity control (reversible phosphorylation; Dawson and Storey 2011) or other post-translational processes.

Proteins of the category ‘proteolytic enzymes’ were predominantly down-regulated upon heat stress (particularly in clone M), with down-regulation even more marked during heat-and-starvation stress (see also Fig. 3.11, 3.19 and 4.1). Similar to the down-regulation of proteins from the category ‘carbohydrate binding/metabolism’, it is very likely that that these down-regulations served to save energy. Surviving stressful conditions requires an adequate energy supply, and the highly energy consuming protein biosyntheses have to be restricted to the necessary minimum, which is the expression of stress proteins (Spriggs *et al.* 2010). Mammalian cells, for instance, show a highly coordinated up-regulation of genes for heat shock proteins upon acute heat stress and a general decrease in the rate of biosynthesis (Shalgi *et al.* 2013). However, mRNA down-regulation does not necessarily imply protein down-regulation (Lackner *et al.* 2012). In contrast to the strong correlation between up-regulated transcript levels and protein expression, reductions in mRNA level may only serve to redirect the ribosomal machinery to newly synthesized transcripts (Lee *et al.* 2011), with the existing long-lived protein equipment not much affected by reduced mRNA levels.

The predominant up-regulation of the FOG transcription factor and vitellogenins (VTGs) in clone M (and down-regulation of VTGs in clone G) have already been discussed (see above). A cytosolic fatty acid binding protein down-regulated in clone M likely serves for the transport of fatty acids between intracellular membranes (Weisiger 2002).

Within the category ‘ubiquitin/proteasome system’, the quantity of ubiquitin or an ubiquitin-like protein (possibly an ubiquitin/ribosomal fusion protein according to ARP2) as well as a subunit of the 20S proteasome endopeptidase complex decreased in clone G but increased in clone M at least during heat-and-starvation stress (see also Fig. 4.1). The proteasome degrades damaged proteins or proteins no longer required, with such proteins tagged with ubiquitin for proteasomal degradation (Peters 1994). The decreasing protein quantities for proteasomal degradation in clone G might be a survival mechanism, which, however, could result in higher cellular amounts of damaged protein and possibly in apoptotic induction (Adams *et al.* 1999). Interestingly, a recent report on (amino acid starvation-induced) autophagy, which in the long term causes autophagic (type II) PCD, showed protein degradation to happen in an ordered fashion (Kristensen *et al.* 2008), with cytosolic and proteasomal proteins degraded first. The multiple detection of these proteins and the large discrepancies between the experimental (18.3–107.3 kDa) and predicted $M_r p$ values (Ubiquitin: 5.7 kDa) indicate, that the excised spots contained more than one protein. Since under acute stress conditions protein damage occurs, it is highly possible, that these non-identified proteins were damaged and therefore tagged with ubiquitin for degradation. Another possible reason for the change of protein amount from the category 'ubiquitin/proteasome system' could be, that the synthesis of the tagged protein is reduced, since ubiquitinylation is also used in non-proteolytic regulatory mechanisms (Hochstrasser, 2009).

In summary, there are several indications that heat-induced stress effects were higher in clone G, which included up-regulated CRT expression (indicating misfolded ER proteins and apoptotic processes), up-regulated expression of cytoskeleton/muscle proteins (possibly for re-constructing elements of the cytoskeleton), and down-regulated expression of proteins for the 'ubiquitin/proteasome system' (likely resulting in higher amounts of damaged protein and possibly in apoptotic induction). In contrast, clone M exhibited a strong expression of HSP60 (likely for refolding denatured proteins and preventing apoptosis) and VTG/VTG-SOD (possibly indicating ephippia production). In both clones (but frequently to a higher extent in clone M), up-regulation was found for GSTs (likely for detoxifying ROS-damaged molecules), V-ATPases (regulation of pH and autophagy), and unnecessary energy-consuming biosyntheses (proteins for carbohydrate binding/metabolism or proteolytic processes) were down-regulated probably to save energy for specific stress responses.

The expression of all these proteins showed specific temporal patterns, with particularly the H(+)-transporting ATPases, cytoskeleton/muscle proteins, and chaperones reaching maximal values after 24 hours of heat stress, the vitellogenin-SOD fusion proteins reaching maximal values after 48 hours of heat stress in clone M, and the proteins related to carbohydrates or protein metabolism down-regulated (Fig. 3.10). These temporal patterns reflect the dynamics of stress-related processes. Proteins and protein groups showing maximal values already after 24 hours of heat stress can be supposed to be most important for survival mechanisms under severe heat stress. Interestingly, one highly up-regulated glutathione S-transferase isoform also belonged to these rapidly regulated proteins in case of clone M. Heat-and-starvation stress caused time delays in clone M, with several proteins now reaching maximal values only after 48 hours of stress ($H^{(+)}$-transporting ATPases, actins, HSP60) (Fig. 3.18C, D). It also resulted in definitely more proteins up- or down-regulated than in case of heat stress alone.

Adding up protein amounts in a category-specific manner (Fig. 3.11) confirmed the existence of clone-specific differences in protein expression, with this type of evaluation showing a higher up-regulation of proteins from the category ‘cytoskeleton/muscle proteins’ in clone G than in clone M. Results of this type of analysis also included the a) up-regulation of proteins within the categories ‘antioxidant defense/detoxification’ (clone G) and ‘chaperone’ (clone G and M) and the b) down-regulation of proteins related to carbohydrate (clone G) and protein metabolism (clone M). In case of heat-and-starvation stress, this evaluation type showed a) up-regulations of proteins within the categories ‘antioxidant defense/detoxification’ (higher in clone M than in clone G) and ‘cytoskeleton/muscle proteins’ (clone G) and b) down-regulations for ‘proteolytic enzymes’ (Fig. 3.19).

4.3 Differences in starvation-induced proteomic responses between the *D. pulex* clones G and M at 20°C and 30°C

Two different starvation conditions were applied, one at moderate temperature (20°C) and the other one combined with heat (30°C). The latter type of stress caused a 100% mortality in clone G after 40 hours of exposure. Contrasting protein expression at both conditions (Fig. 3.21, 3.22) revealed major differences for chaperones (small Roman number ‘*i*’) (clone M), cytoskeleton/muscle proteins (‘*ii*’) (clone M), and proteolytic enzymes (‘*iii*’) (clone G). In starving animals, heat stress strongly promoted the expression of HSP60 in clone M (Fig. 3.21D, 3.22C) and caused reduced expressions of actin in clone M (Fig. 3.21B, 3.22B) and proteolytic enzymes in clone G (Fig. 3.21A, 3.22A).

Significant starvation-induced proteomic responses were detected in all categories beside proteins of the ubiquitin proteasome system (Fig. 4.1; Tables 3.4, 3.5, 3.6, 3.7). More markedly in clone M than in clone G (see also Fig. 4.3), glutathione S-transferases were up-regulated during starvation stress. Starvation stimulates the formation of mitochondria-generated ROS (hydrogen peroxide, H_2O_2 and superoxide, $O_2^{\cdot-}$; Scherz-Shouval *et al.* 2007; Li *et al.* 2013). Mitochondria-generated ROS are linked to autophagy by the AMP-activated protein kinase (AMPK) and the target of rapamycin (TOR) pathways, with starvation-induced autophagy being physiologically important in regulating cell survival (Li *et al.* 2013). As cellular stress signal, starvation-induced ROS may also trigger other cellular stress responses such as the induction of GSTs, which are involved in the detoxification of ROS-damaged cellular components (Storey 1996) and a variety of radicals (Qin *et al.* 2011, Qin *et al.* 2012). Surprisingly, even though survival and maximal physiological performance assays under acute heat stress (Fig. 3.3, Fig. 3.4) and under acute starvation (Fig. 3.2, Fig. 3.4) suggest that exposure to a temperature of 30°C represents a more stressful environment to the animals than acute starvation stress, the increase in GST expression level due to starvation stress was even higher than that to heat stress alone. Additional heat stress further enhanced the expression of GSTs.

Being higher in clone M after 48 h of starvation stress than in clone G (see also Fig. 4.3), expression of the two V-ATPase subunits from the category 'ATPase' was enhanced by starvation stress and further elevated by heat stress. As a link between V-ATPases and starvation, it is known that V-ATPases disassemble into the V0 and V1 subunits upon glucose withdrawal, which results in a disconnection of V1 from vacuolar membranes and a shut down of V-ATPase activity (Forgac 2007). The starvation-induced increase in expression of V-ATPase subunits may be part of a compensatory mechanism to maintain V-ATPase-dependent membrane transports, for instance, for embryogenesis and yolk transfer (Choi *et al.* 2003).

Proteins from the category 'carbohydrate binding/metabolism' showed either a constitutive or reduced expression under starvation stress (particularly glycoside hydrolase, family 9, in clone M) (see also Fig. 4.1). However, 3-phosphoglycerate kinase, an enzyme required to generate ATP during glycolysis (Zerrad *et al.* 2011), in clone G and enolase, which catalyzes the conversion of 2-phosphoglycerate to phosphoenolpyruvate during glycolysis (Zhang *et al.* 1997), in clone M were significantly up-regulated. The lack of food may in general negatively affect protein expression for carbohydrate binding/metabolism as an energy-saving strategy (down-regulation of unnecessary protein biosyntheses), whereas the induction of enzymes involved in glycolysis is possibly maintained/up-regulated to maintain adequate levels of energy supply under acute starvation stress.

Starvation stress forced a down-regulation of calreticulin (clone G and M) and FKBP (clone G) and an up-regulation of HSP60 (clone M). The down-regulation of CRT (and FKBP) indicates that misfolded proteins in the ER and apoptotic processes are not a problem during starvation stress. The up-regulation of HSP60 in clone M may be related to other HSP60 functions than protein repair, which include transmembrane protein transports (Koll *et al.* 1992) and/or mitochondrial DNA metabolism (Kaufmann *et al.* 2003).

Proteins of the category 'cytoskeleton/muscle proteins' were up-/down-regulated upon starvation stress, with clone M showing such regulations on a much larger scale. In this case, alpha and beta tubulins were down-regulated, and actins were mostly up-regulated. The response of clone M to 'pure' starvation stress was even more intense than those to heat or heat-and-starvation stress (see also Fig. 4.1). While a reorganization of the cytoskeleton as a response to nutrient starvation has already been reported (Gresham *et al.* 2011), a detailed explanation of the prevailing processes in *D. pulex* is not possible yet (but see below).

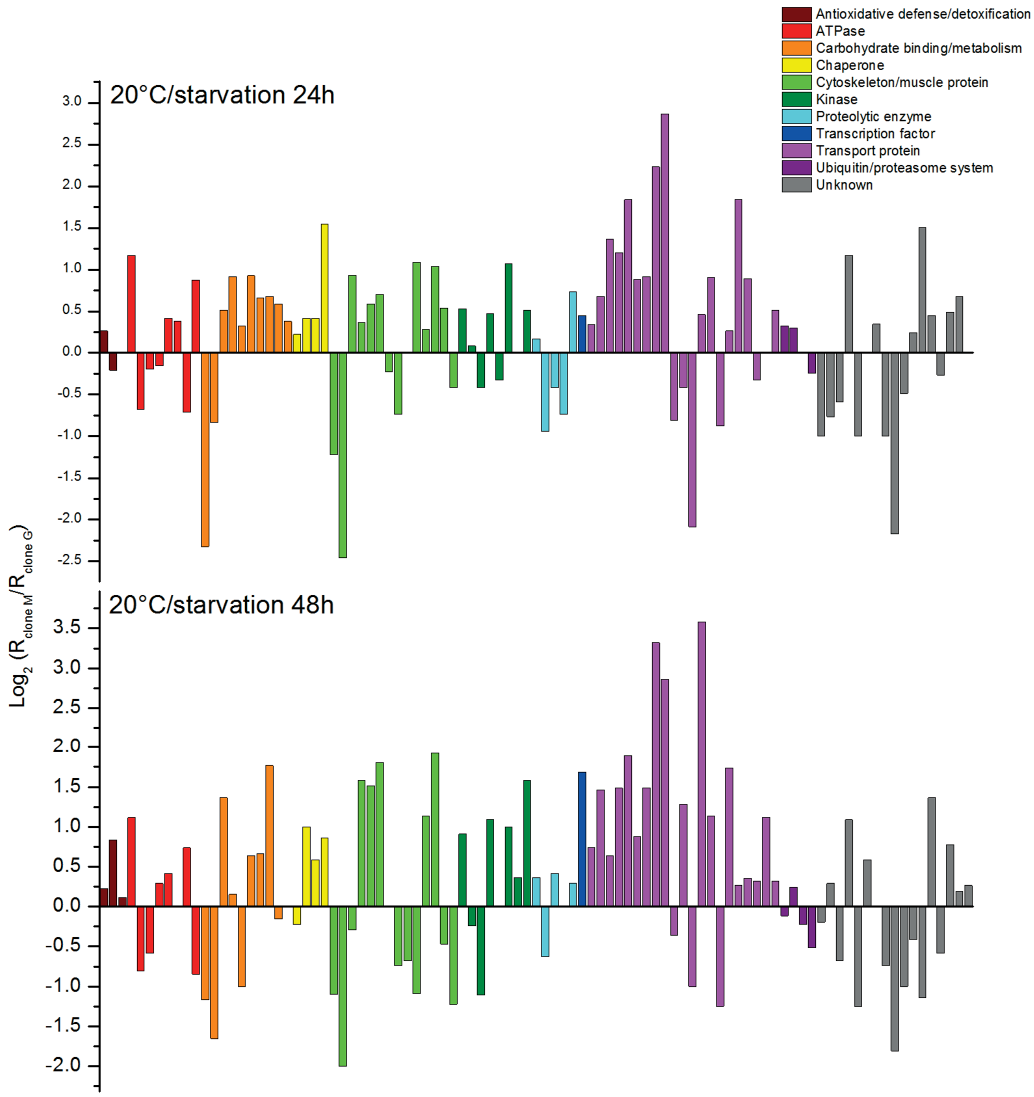

Fig. 4.3 Differences in ratio values (R) of protein expression between clone M and G at starvation stress.

Differences in the ratio values of protein expression were calculated between clone M and G for the condition 20°C, no food (top, 24 h of stress; bottom, 48 h of stress; data from Tables 3.4–3.5).

Both *D. pulex* clones increased the expression of arginine kinase (AK) (from the category 'kinase') under starvation stress. AK catalyzes synthesis of the transient energy buffer phosphoarginine, which helps to stabilize the intracellular ATP level. Previous studies already identified AK as a possible modulator of energetic reserves during starvation stress (Alonso *et al.* 2001), and overexpression of this enzyme has been shown to improve survival capabilities under nutritional stress (Pereira *et al.* 2002).

As observed during acute heat-stress, the serine endopeptidase (strain M) with similarity to placental protein 11, for which, however, a recent report demonstrated endoribonuclease activity (Laneve *et al.*, 2008) as well as the carboxypeptidase A2 (strain G), which is likely involved in digestive processes, were down-regulated during acute starvation stress. However chymotrypsin, a serine protease within the group of proteolytic enzymes, was strongly up-regulated in strain G (see also Fig. 4.1). Chymotrypsin, besides of Trypsin, represents one of the most important digestive proteases in the gut of *Daphnia* (von Elert *et al.*, 2004). Low food quality due to the presence of protease inhibitors causes a reduction of somatic growth and a remodelling of chymotrypsin in *D. magna* (von Elert *et al.*, 2012). It could be possible that the up-regulation of the identified chymotrypsin isoform in strain G is a result of the remodeling of chymotrypsin in response to the reduced availability of nutrients, whereas the reason for down-regulation of the other proteolytic enzymes is likely the same reason as under acute heat stress, which is to minimize unnecessary energy-consuming processes.

Similar to heat stress, the vitellogenin (VTG) fused with a superoxide dismutase (SOD) domain (gene ID: 219769) was up-regulated in clone G and M as well as the FOG transcription factor expression (clone M) was induced. The similarity, especially for clone M, in expression patterns in the categories ‘transcription factor’, ‘transport protein’, and others (e.g., ‘antioxidative defense/detoxification’, ‘ATPase’) during heat, heat-and-starvation, and starvation stress represents strong evidence for heat stress and starvation stress acting frequently in the same direction resulting in an enhanced regulation, when heat and starvation stress were combined (see Fig. 4.1).

Proteins from the category ‘ubiquitin/proteasome system’ remained more or less constant or decreased in quantity during starvation stress, which possibly reflects autophagic processes, because a recent report on autophagy induced by amino acid starvation (Kristensen *et al.* 2008) showed protein degradation to occur in an ordered fashion, with cytosolic and proteasomal proteins degraded first.

In summary, the proteomic data indicate that starvation stress induced stronger cell responses in clone M than in clone G (see Fig. 4.3) as was partly also the case for heat stress (Fig. 4.2). This involved proteins in the categories ‘antioxidative defense/detoxification’, ‘ATPase’, ‘carbohydrate binding/metabolism’, ‘chaperone’, ‘cytoskeleton/muscle proteins’, ‘kinase’, ‘transcription factor’, and ‘transport protein’. In clone G, besides of proteins in the categories ‘antioxidative and ROS detoxification response’, ‘proteolytic enzymes’ and ‘cytoskeleton/muscle proteins’ which were up-regulated under starvation, protein expression levels frequently remained unchanged or decreased (Fig. 3.21 and Fig. 4.1), which fits to the overall decrease in protein level of this clone under starvation stress (Fig. 3.5). Starvation stress as well as heat stress induced GST expression in both clones.The increased GST levels under acute starvation-stress might be linked to a change of cellular metabolism and amino acid starvation (Zhao *et al.*, 1998). The need of maintaining cellular energy levels to ensure survival during starvation and amino acid deprivation is met by the breakdown of cellular proteins via autophagy. Autophagy is a process by which cytoplasmic material is sequestered in a double-membrane vesicle destined for degradation (Sterner *et al.*, 1993; Lin *et al.* 2013). Actin is necessary for starvation-mediated autophagy and seems to participate in the initial membrane remodeling stage, when cells require an enhanced rate of autophagosome formation (Aguilera *et al.* 2012). This fact may explain the enhanced expression of actins in both clones during starvation. All in all, gene expressions and translations seem to occur more frequently in clone M than in clone G under starvation stress. Both clones likely use autophagy to maintain the cellular energy balance and to obtain the raw material (amino acids) for necessary biosyntheses. As the breakdown of endogeneous proteins is limited in both amount and rate, the stronger cell responses (protein biosyntheses) in clone M may have resulted from higher endogeneous protein resources and a more developed autophagic system and/or clone M is able to utilize another food source, namely bacteria, more efficiently than clone G, which were, in contrast to algae, still available during the starvation experiments. This implies a more advanced or specialized filtering system for food particles and/or a higher expression level for digestive enzymes, which are able to degrade bacterial compounds such as the bacterial cell wall.

The expression of proteins from the different categories showed specific temporal patterns under starvation stress. Particularly, arginine kinases, glutathione transferases, HSP60, and partly cytoskeleton/muscle proteins reached maximal values after 24 hours of starvation stress, whereas $H^{(+)}$-transporting ATPases, and vitellogenins reached maximal levels mostly later (Fig. 3.14).

Adding up protein amounts in a category-specific manner (Fig. 3.15) confirmed the existence of clone-specific differences in protein expression, with this type of evaluation showing for clone M (in comparison to clone G) a higher protein level within the category 'chaperone' and a lower one for 'ubiquitin/proteasome'. The observed induction of proteins of the categories 'antioxidant defense/detoxification' (clone G and M) or 'kinase' and 'transcription factor' (clone M) are surprising, especially since under starvation rates of growth, reproduction and metabolism decrease (Ingle *et al.*, 1937; Sterner *et al.*, 1993) which supports the explanation of another food source, such as bacteria or autophagy, to obtain energy and the raw material (amino acids) for necessary biosyntheses (see above).

4.4 Stress responses in the *D. pulex* clones G and M: conclusions and short outlook

The physiological assays as well as the proteomic data showed negative stress effects to be higher in clone G than in clone M. Clone G did not survive heat-and-starvation stress for more than 24 hours; it was more susceptible to heat, showed a breakdown of protein stores during starvation, and exhibited a rather limited cell response spectrum to stress at the level of protein expressions. Differences in autophagic resources and mechanisms and/or differences in food availability (bacterial food) likely contributed to these clone-specific differences. This means that food (protein) availability and the nutronal status of an animal are of prime importance for the survival of acute stress situations. Actually, 50%-survival rates were 48 hours (clone G) and 98 hours (clone M) when food was provided during heat stress, and decreased to 17 hours (clone G) and 49 hours (clone M) in case of heat and starvation. Furthermore, the energy saving measures undertaken under stress such as the down-regulation of carbohydrate and protein metabolism also indicates that nutronal limitations strongly contribute to stress intolerances. Interestingly, it applies in reverse that a slight undernourishment promotes stress tolerance (and lifespan) via distinct stress signaling pathways (FoxO/DAF-16- and Nrf2/SKN-1-mediated stress responses; (Kenyon, 2010). Thus, future studies should focus on differences in the nutronal status of clone G and M to test this hypothesis. In any case, starvation and heat stress acted frequently in the same direction, resulting in the necessity to further enhance gene expression and regulation, when heat and starvation stress were combined. Heat exposure in starving animals of clone M required further increases (e.g., GSTs, HSP60) or decreases (e.g., proteolytic enzymes) in protein expression (see also Fig. 4.1, 30°C/s vs 20°C/s). In clone G, regulatory processes at the level of protein expression were rather limited. Starvation in heat-exposed animals of clone M caused again marked adjustments in protein expression (e.g., GSTs, H(+)-transporting ATPases, HSP60, proteolytic enzymes; Fig. 4.1, 30°C/f vs 30°C/s), whereas clone G showed again only modest cell reponses. Of course, there were also differences in protein expression between heat stress and starvation stress, which were mainly detected in clone M and concerned, in particular, cytoskeleton/muscle proteins (higher regulatory activity under starvation stress) and vitellogenins (higher expression intensity under heat stress). The changes in protein expression were frequently based on changes in mRNA expression (Fig. 4.4), which suggests including transcriptome data for comprehensive meta-analyses of *Daphnia*'s adjustments to changes in temperature and food availability.

4.5 Validation of the protein pattern by Western Blot analysis

To confirm protein expressions measured in 2D gel analysis for both clones, Western Blot analysis of HSP 60 were performed. Earlier studies on *D. magna* using two commercial Anti-Hsp60 antibodies revealed multiple immunoreactive protein bands of different molecular weights. These bands were described as separate proteins and for *D. magna*, a total of four different HSP 60 could be identified. Anti-Hsp60 antibody SPA-807 revealed two distinct proteins at ~50 and ~56 kDa and Anti-Hsp60 antibody SPA-805 revealed two distinct proteins one at ~60 kDa and the second protein at ~103 kDa (Mikulski *et al.*, 2009). Since on the 2D gel, HSP60 identified the by mass-spectrometry has an estimated experimental molecular weight (M_re) of ~89.1 kDa, anti-Hsp60 antibody SPA-805 was used for our Western Blot analysis. For both clones, two distinct HSP60 bands were revealed, one at ~60.4 and a second at ~73.8 kDa (Fig 3.23-A). Thus the measured molecular weight in Western Blot analysis diverges considerably from the observed molecular weight on the 2D gels as well as from the result described by Mikulski et al., (2009). The identified protein at ~60.4 kDa was slightly larger than the corresponding human HSP (~57.7 kDa) but seems to match with the results observed for *D. magna* HSP (~60 kDa). The second protein (~73.8 kDa) was considerably larger than the human HSP and much smaller than the second one observed for *D. magna* (~103 kDa). In between both *D. pulex* clones, no differences in the measurements of molecular weight could be observed. The theoretical molecular weight (M_rp) of the HSP60 (301074) identified in the 2D gels corresponds to a protein sequence of 61.4 kDa. The higher experimental molecular weight measured on the 2D gel could indicate binding to another protein. In the performed Western Blots, this protein could well contribute to the lower band.

Since none of the evaluated molecular weights in Western Blotting experiments confirmed the results from 2D gel analysis, further bioinformatics analysis were performed on the *D. pulex* genome assembly v1.0 all models (*Daphnia pulex* v1.0 - Home). For 196 protein database entries, the Cpn_TCP1 domain (PF00118), which is characteristic for HSP60, could be identified. They could be merged to a total of 11 distinct proteins (Fig. 3.24) with theoretical molecular weight ranges from ~25.2 to ~201.8 kDa, with the largest share of the identified proteins to be found in a range of ~57 to ~61.5 kDa (see supplement Table 5.1 and Fig. 5.1).

Since the HSP60 detected at ~73.8 kDa differed from the anticipated molecular weights, the measured molecular weight might be the product of posttranslational modifications of a protein from the Hsp60 family (e.g., a fusion with another polypeptide) as already suggested (Mikulski *et al.*, 2009).

In the two investigated clones, thermal stress enhanced the expression of both *D. pulex* HSP60 proteins. Induction of HSP 60 under heat stress was also observed in *D. magna* (Mikulski *et al.*, 2009; Mikulski *et al.*, 2011). The observed expression patterns were different in both clones. In the Western Blot analysis, expression patterns for the protein at ~60.4 kDa, were similar to the time course observed in the 2D Gel analysis, confirming the results obtained by 2D Gel analysis. Total expression levels of HSP60 as well as induction under acute H-stress were higher in clone M than in clone G. The observed results are a further explanation of the higher stress tolerance of *D. pulex* clone M compared to *D. pulex* clone G.

4.6 Comparison of transcriptome and proteome

A recent transcriptome study on clone G upon acute heat stress (transfer of 20°C-acclimated animals to either 30°C or 20°C/control, and contrasting 30°C vs 20°C after 2, 4, and 8 hours of heat stress; Becker 2011) allowed to compare the temporal courses of differentially expressed mRNA and protein levels (Fig. 4.4). In most cases, the polarity of regulations was identical for both gene products (Fig.4.4A–D), which is another proof of the quality of the proteomic data.

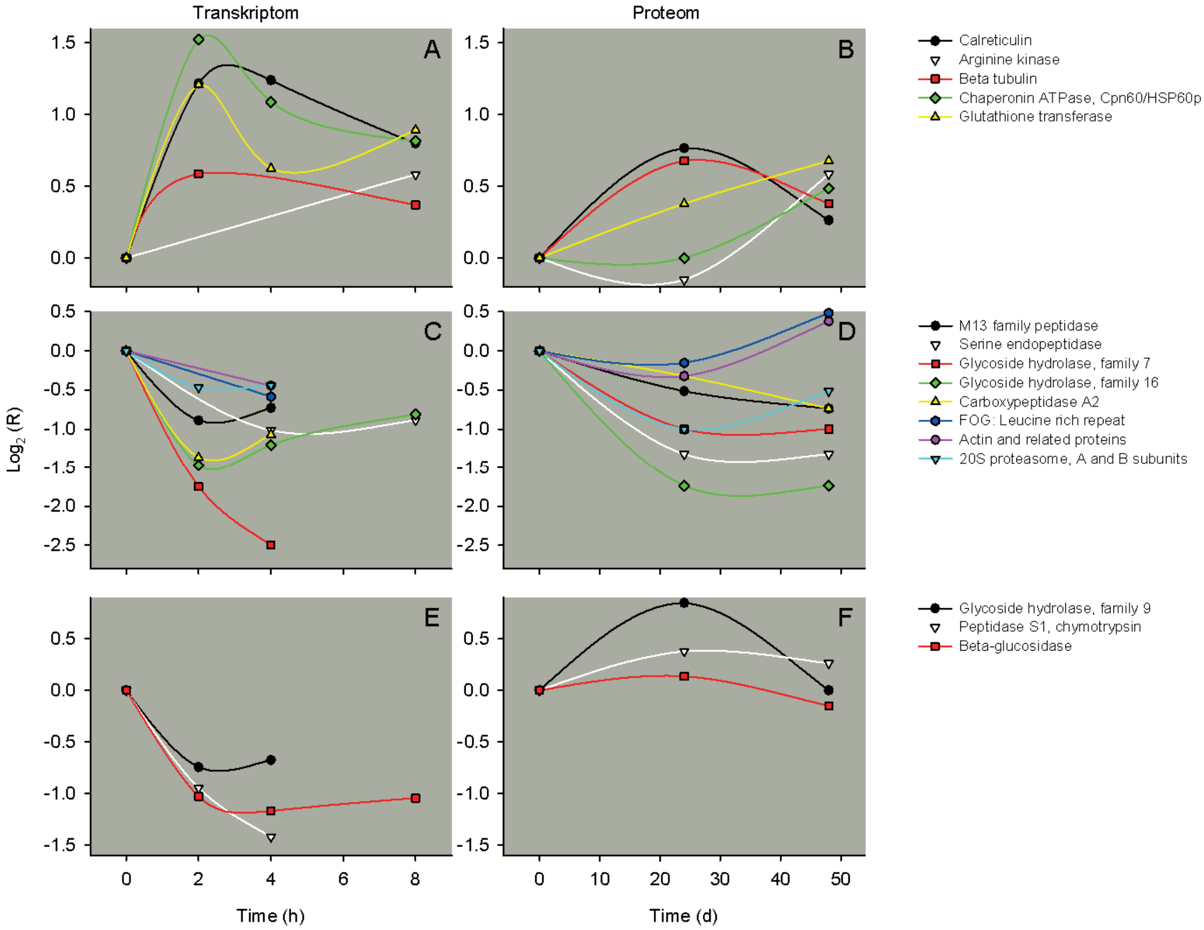

Fig. 4.4 Temporal patterns of mRNA and protein quantities in clone G upon acute heat stress.

Time-resolved transcriptomic (Becker 2011) and proteomic data (this study) were used to contrast temporal changes in differentially expressed (**A**, **C**, **E**) mRNA and (**B**, **D**, **F**) protein quantities ($\log_2$-ratios of quantities at 30°C and 20°C) originating from common genes of clone G upon acute heat stress (transfer from 20°C to 30°C). The number of depicted (**A**–**B**) up-regulations, (**C**–**D**) down-regulations, and (**E**–**F**) opposed regulations was limited by the constraint of significance in false discovery rate (FDR) for differential mRNA expression. Thus, only ratio values with FDR < 0.05 are shown (symbols in **A**, **C**, **E**).

5 Supplement

5.1 Validation of the protein expression changes: HSP60

A total of putative 169 database entries for HSP60 gene and protein sequences were extracted from the *D. pulex* genome assembly v1.0 all models (*Daphnia pulex* v1.0 - Home) and analyzed via *CLC Genomic Workbench*. For the 169 protein sequences, the HSP60 specific Cpn60_TCP1 domain (PF00118) could be predicted by CLC Genomics Workbench version 3.6.5 (Tables 5.1). In order to find double database entries an alignment tree was performed by *CLC Genomics*. A total of eleven different HSP60s could be identified by aligning and grouping the protein sequences (Fig 5.1) and then verifying for each protein sequence the location of the coding gen (Tables 5.1). Each of the eleven identified HSP60s in *D. pulex* revealed a characteristic domain organization and architecture and all together a total of 31 additional domains or domain fragments associated with the HSP60 specific Cpn60_TCP1 domain (PF00118) could be identified by *CLC Genomics* using PFAM100 Version 22.0 (Fig. 3.24 and Table 5.2). Comparisons of bioinformatics results revealed that these proteins can be categorized into five sections as a function of the theoretical molecular weight. For the three main sections an average molecular weight of about 56.95 kDa, 59.4 kDa and 61.46 kDa is predicted, and for the two smaller sections, a molecular weight of about 25.16 kDa and 201.8 kDa is calculated.

Table 5.1 Identified putative genes encoding HSP60 proteins.

Protein ID (JGI_V11_gene id) and the corresponding gene location were retrieved of the database of the *Daphnia pulex* genome assembly v1.0 (Colbourne et al., 2005). For each protein, the length, predicted molecular weight (M_rp) and predicted isoelectric point (pIp) were evaluated by CLC Genomics Workbench.

Protein ID	Scaffold	Gene Location	Length	Mean Length	M_rp	Max M_rp	Min M_rp	Mean M_rp	pIp	Max pIp	Min pIp	Mean pIp
Group 1												
2210	4	1415614-1417654 (+)	531	**527**	57.99	75.11	54.18	**57.79**	5.65	6.10	5.65	**5.90**
22718	4	1415614-1417663 (+)	534		58.36				5.80			
22727	4	1415614-1417663 (+)	534		58.36				5.80			
42351	4	1415614-1417669 (+)	536		58.64				5.99			
42535	4	1415614-1417669 (+)	536		58.64				5.99			
42617	4	1415614-1417669 (+)	536		58.64				5.99			
96135	4	1415245-1417669 (+)	537		58.77				5.99			
127024	4	1415245-1417669 (+)	537		58.77				5.99			
191724	4	1415614-1417832 (+)	494		54.18				5.88			
191725	4	1415614-1417832 (+)	494		54.18				5.88			
191726	4	1415614-1417832 (+)	494		54.18				5.88			
206860	4	1415614-1417832 (+)	494		54.18				5.88			

206861	4	1415614-1417832 (+)	494		54.18				5.88			
206862	4	1415614-1417832 (+)	494		54.18				5.88			
234605	4	1406054-1417669 (+)	678		75.11				5.78			
305644	4	1415614-1417842 (+)	494		54.18				5.88			
311479	4	1415245-1417833 (+)	546		59.85				6.10			
Group 2												
22706	5	847146-849430 (+)	530	**555**	58.15	112.10	58.15	**61.08**	6.43	9.70	6.43	**6.70**
22707	5	847146-849430 (+)	530		58.15				6.43			
31022	5	847146-849430 (+)	530		58.15				6.43			
42850	5	847146-849433 (+)	531		58.26				6.56			
43235	5	847146-849433 (+)	531		58.26				6.56			
43297	5	847146-849433 (+)	531		58.26				6.56			
96599	5	847146-849433 (+)	531		58.26				6.56			
127117	5	847146-849433 (+)	531		58.26				6.56			
187326	5	846975-849594 (+)	531		58.26				6.56			
192149	5	846975-849594 (+)	531		58.26				6.56			
192150	5	846975-849594 (+)	531		58.26				6.56			
192151	5	846975-849594 (+)	531		58.26				6.56			
207281	5	846975-849594 (+)	531		58.26				6.56			
207282	5	846975-849594 (+)	531		58.26				6.56			
207283	5	846975-849594 (+)	531		58.26				6.56			
221466	5	846975-849594 (+)	531		58.26				6.56			
235153	5	847146-849433 (+)	531		58.26				6.56			
306375	5	846975-849594 (+)	531		58.26				6.56			
311926	5	846975-849594 (+)	993		112.10				9.70			
Group 3												
22521	12	879554-881449 (+)	552	**578**	58.57	66.06	58.57	**61.55**	5.65	6.24	5.65	**6.19**
22569	12	879485-881452 (+)	576		61.38				6.07			
22576	12	879485-881443 (+)	573		61.06				6.07			
46835	12	879485-881455 (+)	577		61.50				6.24			
46850	12	879485-881455 (+)	577		61.50				6.24			
47090	12	879485-881455 (+)	577		61.50				6.24			
99546	12	879485-881455 (+)	577		61.50				6.24			
127762	12	879485-881455 (+)	577		61.50				6.24			
187757	12	879212-881888 (+)	577		61.50				6.24			
194406	12	879212-881888 (+)	577		61.50				6.24			
194407	12	879212-881888 (+)	577		61.50				6.24			
194408	12	879212-881888 (+)	577		61.50				6.24			
209509	12	879212-881888 (+)	577		61.50				6.24			
209510	12	879212-881888 (+)	577		61.50				6.24			
209511	12	879212-881888 (+)	577		61.50				6.24			
222944	12	879212-881888 (+)	577		61.50				6.24			
238728	12	878717-881455 (+)	618		66.06				6.17			
301074	**12**	**879212-881890 (+)**	**577**		**61.50**				**6.24**			
314723	12	879212-881890 (+)	577		61.50				6.24			
443017	12	879212-881890 (+)	577		61.50				6.24			
Group 4												
2081	28	556020-558277 (-)	552	**555**	59.20	59.71	59.00	**59.63**	6.78	7.08	6.57	**6.78**
22581	28	556017-558277 (-)	553		59.32				6.57			
22591	28	556023-558274 (-)	550		59.00				7.08			
51919	28	556014-558283 (-)	556		59.71				6.78			
51982	28	556014-558283 (-)	556		59.71				6.78			
52015	28	556014-558283 (-)	556		59.71				6.78			
103996	28	556014-558283 (-)	556		59.71				6.78			

128465	28	556014-558283 (-)	556		59.71				6.78			
188247	28	555452-558378 (-)	556		59.71				6.78			
197227	28	555452-558378 (-)	556		59.71				6.78			
197228	28	555452-558378 (-)	556		59.71				6.78			
197229	28	555452-558378 (-)	556		59.71				6.78			
212297	28	555452-558378 (-)	556		59.71				6.78			
212298	28	555452-558378 (-)	556		59.71				6.78			
212299	28	555452-558378 (-)	556		59.71				6.78			
224919	28	555452-558378 (-)	556		59.71				6.78			
244455	28	556014-558283 (-)	556		59.71				6.78			
304295	28	555452-558378 (-)	556		59.71				6.78			
319199	28	555452-558378 (-)	556		59.71				6.78			
Group 5												
2206	29	1080181-1082486 (+)	524	**521**	56.38	95.19	27.14	**56.37**	7.14	9.14	6.62	**7.72**
22664	29	1080208-1082486 (+)	515		55.39				6.62			
31016	29	1080172-1082486 (+)	527		56.74				7.14			
52120	29	1080178-1082609 (+)	566		61.18				8.74			
52226	29	1080202-1082609 (+)	558		60.31				8.60			
52332	29	1080172-1082609 (+)	568		61.40				8.76			
104310	29	1080372-1081438 (+)	252		27.14				6.88			
128522	29	1080372-1081438 (+)	252		27.14				6.88			
188288	29	1080031-1082686 (+)	529		57.01				7.68			
197435	29	1080031-1082686 (+)	529		57.01				7.68			
197436	29	1080031-1082686 (+)	529		57.01				7.68			
197437	29	1080031-1082686 (+)	529		57.01				7.68			
212502	29	1080031-1082686 (+)	529		57.01				7.68			
212503	29	1080031-1082686 (+)	529		57.01				7.68			
212504	29	1080031-1082686 (+)	529		57.01				7.68			
225077	29	1080031-1082686 (+)	529		57.01				7.68			
244798	29	1080178-1082565 (+)	529		57.01				7.68			
304509	29	1080030-1082686 (+)	855		95.19				9.14			
319480	29	1080030-1082866 (+)	529		57.01				7.68			
Group 6												
219	32	661691-667241 (+)	1630	**1808**	182.58	212.91	182.58	**201.80**	6.54	6.65	6.48	**6.54**
20169	32	660817-667241 (+)	1874		209.18				6.62			
20234	32	661691-667241 (+)	1630		182.58				6.54			
104778	32	660817-667337 (+)	1855		206.87				6.48			
225292	32	660817-667681 (+)	1855		206.87				6.48			
245420	32	660817-667324 (+)	1852		206.54				6.55			
305043	32	660817-667683 (+)	1855		206.87				6.48			
319941	32	660817-667683 (+)	1909		212.91				6.65			
Group 7												
2224	40	255859-258059 (+)	533	**567**	57.82	118.20	57.82	**61.76**	6.01	9.88	6.01	**6.33**
22683	40	255859-258059 (+)	533		57.82				6.01			
22717	40	255859-258059 (+)	533		57.82				6.01			
54097	40	255859-258062 (+)	534		57.94				6.11			
54145	40	255859-258062 (+)	534		57.94				6.11			
54273	40	255859-258062 (+)	534		57.94				6.11			
106017	40	255619-258062 (+)	535		58.07				6.11			
128760	40	255619-258062 (+)	535		58.07				6.11			
198330	40	255520-258230 (+)	535		58.07				6.11			
198331	40	255520-258230 (+)	535		58.07				6.11			
198332	40	255520-258230 (+)	535		58.07				6.11			
213377	40	255520-258230 (+)	535		58.07				6.11			

213378	40	255520-258230 (+)	535		58.07				6.11			
213379	40	255520-258230 (+)	535		58.07				6.11			
247480	40	255428-258292 (+)	566		61.73				6.43			
305762	40	255520-258508 (+)	1065		118.20				9.88			
321299	40	255526-258508 (+)	535		58.07				6.11			
Group 8												
2213	53	630006-632385 (+)	538	**541**	58.91	60.06	55.51	**59.28**	6.16	6.31	5.75	**6.14**
11838	53	630006-632394 (+)	541		59.33				6.16			
11843	53	630006-632385 (+)	538		58.91				6.16			
55967	53	630006-632397 (+)	542		59.45				6.31			
56065	53	630006-632397 (+)	542		59.45				6.31			
56104	53	630006-632397 (+)	542		59.45				6.31			
107930	53	630376-632397 (+)	505		55.51				5.75			
129032	53	630376-632397 (+)	505		55.51				5.75			
188654	53	629857-632608 (+)	548		60.06				6.16			
199431	53	629857-632608 (+)	548		60.06				6.16			
199432	53	629857-632608 (+)	548		60.06				6.16			
199433	53	629857-632608 (+)	548		60.06				6.16			
214456	53	629857-632608 (+)	548		60.06				6.16			
214457	53	629857-632608 (+)	548		60.06				6.16			
214458	53	629857-632608 (+)	548		60.06				6.16			
226374	53	629857-632608 (+)	548		60.06				6.16			
250472	53	629919-632397 (+)	548		60.06				6.16			
306806	53	629857-632609 (+)	548		60.06				6.16			
Group 9												
2200	60	570287-572424 (-)	539	**521**	58.46	60.02	45.79	**56.69**	5.50	8.84	5.40	**5.85**
11821	60	570287-572424 (-)	539		58.46				5.50			
11897	60	570278-572424 (-)	542		58.77				5.40			
108749	60	570272-572424 (-)	532		57.62				5.45			
129163	60	570272-572424 (-)	532		57.62				5.45			
188746	60	570131-572521 (-)	494		54.18				5.88			
226650	60	570131-572521 (-)	532		57.62				5.45			
251754	60	570272-572424 (-)	540		58.42				5.44			
307226	60	570130-572524 (-)	417		45.79				5.55			
324227	60	570130-572524 (-)	543		60.02				8.84			
Group 10												
2068	63	68440-71094 (-)	536	**540**	58.80	59.37	58.80	**59.28**	6.17	6.17	6.07	**6.10**
11739	63	68440-71094 (-)	536		58.80				6.17			
30953	63	68440-71094 (-)	536		58.80				6.17			
57451	63	68425-71094 (-)	541		59.37				6.09			
57470	63	68425-71094 (-)	541		59.37				6.09			
57538	63	68425-71094 (-)	541		59.37				6.09			
109119	63	68425-71094 (-)	541		59.37				6.09			
129255	63	68425-71094 (-)	541		59.37				6.09			
188811	63	68276-71212 (-)	541		59.37				6.09			
200181	63	68276-71212 (-)	541		59.37				6.09			
200182	63	68276-71212 (-)	541		59.37				6.09			
200183	63	68276-71212 (-)	541		59.37				6.09			
215193	63	68276-71212 (-)	541		59.37				6.09			
215194	63	68276-71212 (-)	541		59.37				6.09			
215195	63	68276-71212 (-)	541		59.37				6.09			
226852	63	68276-71212 (-)	541		59.37				6.09			
252142	63	68425-71094 (-)	541		59.37				6.09			
307416	63	68276-71212 (-)	541		59.37				6.07			

324554	63	68276-71212 (-)	541		59.37				6.09			
Group 11												
16512	987	11182-12091 (-)	222	**234**	23.86	25.89	23.86	**25.16**	5.45	5.87	5.45	**5.68**
33375	987	11125-12091 (-)	241		25.89				5.87			
33907	987	11125-12088 (-)	240		25.73				5.71			

Table 5.2 Identified domain organisations or architectures in putative HSP60 proteins.

For each identified group, the characteristic domain organization and architecture was determined. Protein length, start and end position for each identified domain as well as the corresponding Pfam accession number were evaluated identified by *CLC Genomics* using PFAM100 Version 22.0. Results were visualized in Fig. 3.24.

Scaffold	Length	Domain	Acession	Start	End
Group 1					
4	678	GGDEF	PF00990	111	226
		p450	PF00067	156	515
		Cpn60_TCP1	PF00118	172	664
		GP41	PF00517	298	590
		LRR_1	PF00560	417	433
Group 2					
5	531	Aldedh	PF00171	2	272
		Cpn60_TCP1	PF00118	30	526
		TetR_N	PF00440	291	308
		GGDEF	PF00990	311	323
Group 3					
12	577	Tubulin	PF00091	32	202
		Cpn60_TCP1	PF00118	45	548
		Response_reg	PF00072	107	210
		Aminotran_1_2	PF00155	124	470
		HisKA	PF00512	139	194
		RVT_connect	PF06815	142	229
		CBS	PF00571	165	290
		MMR_HSR1	PF01926	170	277
		Gag_p24	PF00607	310	475
		MFS_1	PF07690	530	571
Group 4					
28	556	Cpn60_TCP1	PF00118	29	536
		HTH_AraC	PF00165	128	148
		adh_short	PF00106	208	329
		Response_reg	PF00072	208	301
		GTP_EFTU_D3	PF03143	365	440
		DAO	PF01266	407	416
		Pyr_redox	PF00070	407	488
Group 5					
29	529	Cpn60_TCP1	PF00118	32	526
		Pyr_redox	PF00070	128	236
		Epimerase	PF01370	260	276

Scaffold	Length	Domain	Acession	Start	End
Group 6					
32	1852	zf-C2H2	PF00096	131	159
		zf-C3HC4	PF00097	149	156
		AAA	PF00004	180	330
		Homeobox	PF00046	297	305
		Cpn60_TCP1	PF00118	447	899
		Aminotran_1_2	PF00155	1008	1314
		HTH_AraC	PF00165	1734	1777
		Glycos_transf_2	PF00535	1785	1849
Group 7					
40	535	Cpn60_TCP1	PF00118	33	524
		Pyr_redox	PF00070	47	54
		ATP-synt_ab	PF00006	68	232
		Tubulin	PF00091	246	253
		GGDEF	PF00990	282	432
Group 8					
53	548	Cpn60_TCP1	PF00118	31	525
		HTH_3	PF01381	186	211
		TPR_1	PF00515	260	273
		AAA	PF00004	296	312
		Tubulin	PF00091	361	519
Group 9					
60	532	Gag_p24	PF00607	30	219
		Cpn60_TCP1	PF00118	39	514
		Tubulin	PF00091	83	227
		TPR_1	PF00515	115	146
		TPR_2	PF07719	133	146
		adh_short	PF00106	359	518
		NUDIX	PF00293	495	524
Group 10					
63	541	Cpn60_TCP1	PF00118	44	538
		Aldedh	PF00171	59	383
Group 11					
987	241	Cpn60_TCP1	PF00118	1	241
		Pyr_redox	PF00070	76	173

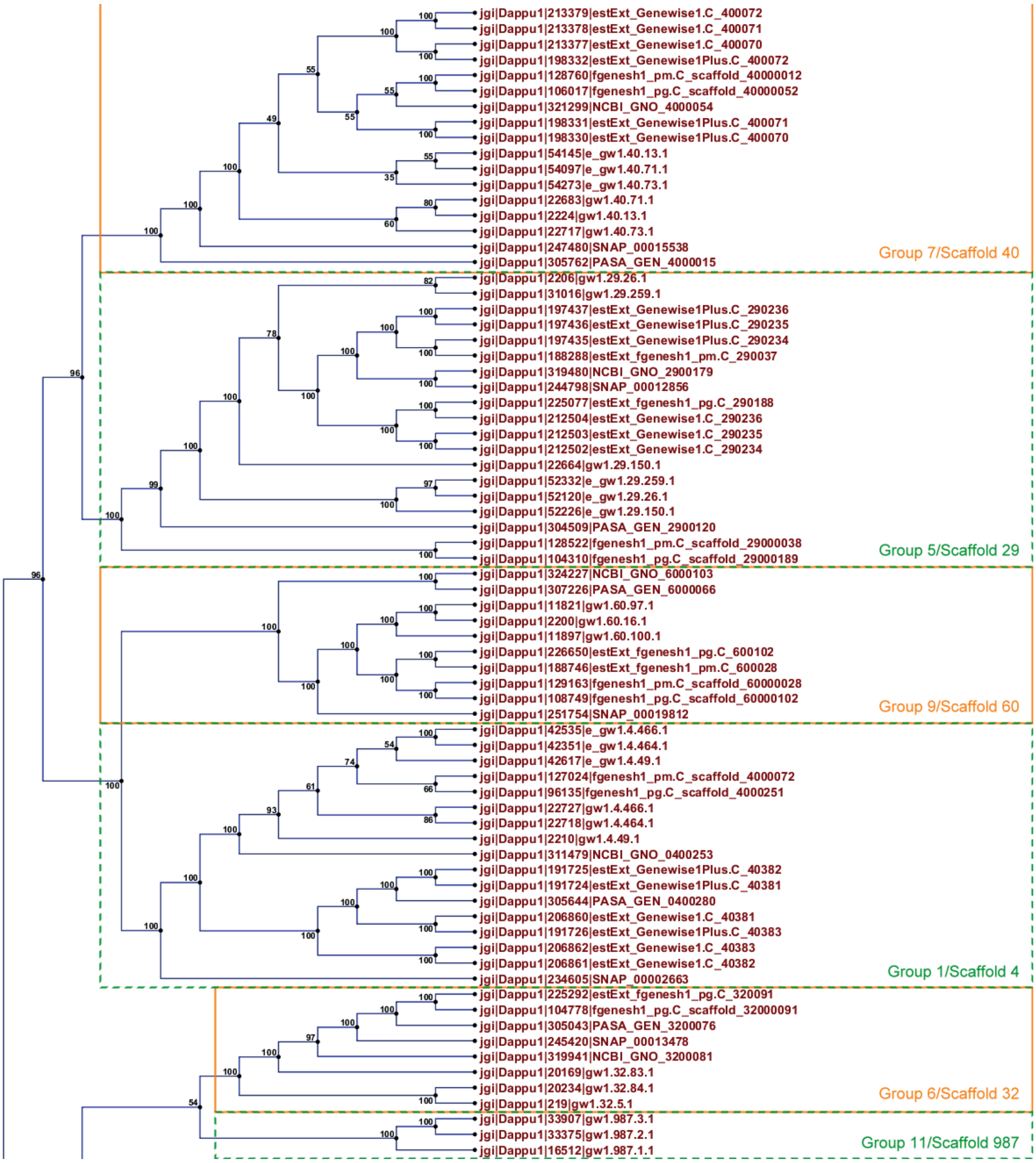
jgi|Dappu1|213379|estExt_Genewise1.C_400072
jgi|Dappu1|213378|estExt_Genewise1.C_400071
jgi|Dappu1|213377|estExt_Genewise1.C_400070
jgi|Dappu1|198332|estExt_Genewise1Plus.C_400072
jgi|Dappu1|128760|fgenesh1_pm.C_scaffold_40000012
jgi|Dappu1|106017|fgenesh1_pg.C_scaffold_40000052
jgi|Dappu1|321299|NCBI_GNO_4000054
jgi|Dappu1|198331|estExt_Genewise1Plus.C_400071
jgi|Dappu1|198330|estExt_Genewise1Plus.C_400070
jgi|Dappu1|54145|e_gw1.40.13.1
jgi|Dappu1|54097|e_gw1.40.71.1
jgi|Dappu1|54273|e_gw1.40.73.1
jgi|Dappu1|22683|gw1.40.71.1
jgi|Dappu1|2224|gw1.40.13.1
jgi|Dappu1|22717|gw1.40.73.1
jgi|Dappu1|247480|SNAP_00015538
jgi|Dappu1|305762|PASA_GEN_4000015
Group 7/Scaffold 40
jgi|Dappu1|2206|gw1.29.26.1
jgi|Dappu1|31016|gw1.29.259.1
jgi|Dappu1|197437|estExt_Genewise1Plus.C_290236
jgi|Dappu1|197436|estExt_Genewise1Plus.C_290235
jgi|Dappu1|197435|estExt_Genewise1Plus.C_290234
jgi|Dappu1|188288|estExt_fgenesh1_pm.C_290037
jgi|Dappu1|319480|NCBI_GNO_2900179
jgi|Dappu1|244798|SNAP_00012856
jgi|Dappu1|225077|estExt_fgenesh1_pg.C_290188
jgi|Dappu1|212504|estExt_Genewise1.C_290236
jgi|Dappu1|212503|estExt_Genewise1.C_290235
jgi|Dappu1|212502|estExt_Genewise1.C_290234
jgi|Dappu1|22664|gw1.29.150.1
jgi|Dappu1|52332|e_gw1.29.259.1
jgi|Dappu1|52120|e_gw1.29.26.1
jgi|Dappu1|52226|e_gw1.29.150.1
jgi|Dappu1|304509|PASA_GEN_2900120
jgi|Dappu1|128522|fgenesh1_pm.C_scaffold_29000038
jgi|Dappu1|104310|fgenesh1_pg.C_scaffold_29000189
Group 5/Scaffold 29
jgi|Dappu1|324227|NCBI_GNO_6000103
jgi|Dappu1|307226|PASA_GEN_6000066
jgi|Dappu1|11821|gw1.60.97.1
jgi|Dappu1|2200|gw1.60.16.1
jgi|Dappu1|11897|gw1.60.100.1
jgi|Dappu1|226650|estExt_fgenesh1_pg.C_600102
jgi|Dappu1|188746|estExt_fgenesh1_pm.C_600028
jgi|Dappu1|129163|fgenesh1_pm.C_scaffold_60000028
jgi|Dappu1|108749|fgenesh1_pg.C_scaffold_60000102
jgi|Dappu1|251754|SNAP_00019812
Group 9/Scaffold 60
jgi|Dappu1|42535|e_gw1.4.466.1
jgi|Dappu1|42351|e_gw1.4.464.1
jgi|Dappu1|42617|e_gw1.4.49.1
jgi|Dappu1|127024|fgenesh1_pm.C_scaffold_4000072
jgi|Dappu1|96135|fgenesh1_pg.C_scaffold_4000251
jgi|Dappu1|22727|gw1.4.466.1
jgi|Dappu1|22718|gw1.4.464.1
jgi|Dappu1|2210|gw1.4.49.1
jgi|Dappu1|311479|NCBI_GNO_0400253
jgi|Dappu1|191725|estExt_Genewise1Plus.C_40382
jgi|Dappu1|191724|estExt_Genewise1Plus.C_40381
jgi|Dappu1|305644|PASA_GEN_0400280
jgi|Dappu1|206860|estExt_Genewise1.C_40381
jgi|Dappu1|191726|estExt_Genewise1Plus.C_40383
jgi|Dappu1|206862|estExt_Genewise1.C_40383
jgi|Dappu1|206861|estExt_Genewise1.C_40382
jgi|Dappu1|234605|SNAP_00002663
Group 1/Scaffold 4
jgi|Dappu1|225292|estExt_fgenesh1_pg.C_320091
jgi|Dappu1|104778|fgenesh1_pg.C_scaffold_32000091
jgi|Dappu1|305043|PASA_GEN_3200076
jgi|Dappu1|245420|SNAP_00013478
jgi|Dappu1|319941|NCBI_GNO_3200081
jgi|Dappu1|20169|gw1.32.83.1
jgi|Dappu1|20234|gw1.32.84.1
jgi|Dappu1|219|gw1.32.5.1
Group 6/Scaffold 32
jgi|Dappu1|33907|gw1.987.3.1
jgi|Dappu1|33375|gw1.987.2.1
jgi|Dappu1|16512|gw1.987.1.1
Group 11/Scaffold 987

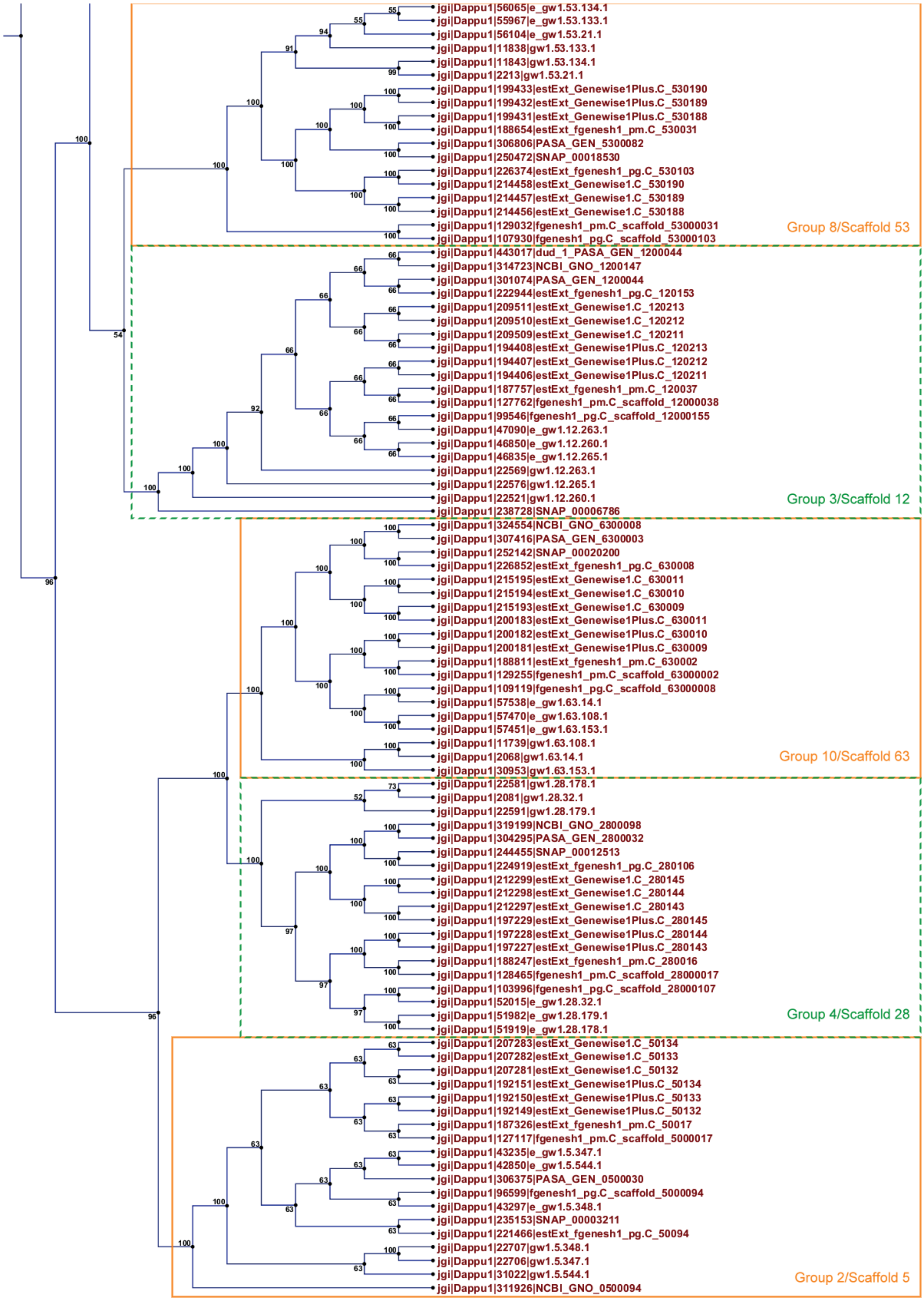

Fig. 5.1 Alignment tree of 169 putative HSP60 database entries.

Alignment tree was performed by *CLC Genomics Workbench* and 11 distinct groups were identified. Each Group represents a single HSP60 (Table 3.8 and Table 3.9).

5.2 Validation of the protein pattern by Western Blot analysis

Bioinformatic analysis on the *D. pulex* genome assembly v1.0 all models (*Daphnia pulex* v1.0 - Home) identified a total of 196 protein database entries containing the Cpn_TCP1 domain (PF00118), which is characteristic for HSP60. TCP-1/cpn60 chaperonin family is a family of evolutionarily related proteins that includes members from the HSP60 chaperone family and the TCP-1 (T-complex protein) family (Gupta, 1995; Punta *et al.*, 2012). The results could be merged to a total of 11 distinct proteins with theoretical molecular weight ranges from ~25.2 to ~201.8 kDa. The largest share of the identified proteins could be found in a range of ~57 to ~61.5 kDa. The unambiguous assignment was possible by the characteristic domain structure of the individual HSP60 proteins (Table 5.2 and Fig. 3.24). Additional to the Cpn_TCP1 domain, 31 further domains could be identified. Of these the two most abundant identified domain structures were Tubulin (PF00091) and Pyr_redox (PF00070). The identified Tubulin domain (PF00091) is a GTPase of the tubulin/Fts7 family found in all tubulin chains, such as tubulin alpha, beta and gamma chains, and some bacterial FtsZ proteins (Nogales *et al.*, 1998) and was found in HSP60s encoded by genes on scaffold 12, 40, 53 and 60 (Table 5.2 and Fig. 3.24). The identified Pyr_redox (PF00070) domain is a small NADH binding domain within a larger FAD binding domain that is included in both class I and class II oxidoreductases and also NADH oxidases and peroxidases (Mande *et al.*, 1996). HSP60s encoded by genes on scaffolds 28, 29, 40 and 987 contained this type of domain (Table 5.2 and Fig. 3.24). The second most abundant identified domain encoded on HSP60s by genes on scaffolds 4, 5 and 40 is GGDEF (PF00990) a domain that is reported to be ubiquitous in bacteria and is often linked to a regulatory domain, such as a phosphorylation receiver or oxygen sensing domain (Ryjenkov *et al.*, 2005). The domains AAA (PF00004), adh_short (PF00106), Aldedh (PF00171), Aminotran_1_2 (PF00155), Gag_p24 (PF00607), HTH_AraC (PF00165), Response_reg (PF0072) and TPR_1 (PF00515) are found in two different HSP60s (Table 5.2 and Fig. 3.24). HSP60 proteins encoded by genes on scaffolds 32 and 53 contained AAA domains of the ATPase family associated with various cellular activities. Proteins of this large family often perform chaperone-like functions that assist in the assembly, operation, or disassembly of protein complexes (Neuwald *et al.*, 1999). HSP60s encoded by genes on scaffold 5 and 63 containt Aldedh (PF00171) domains. These domains belong to the aldehyde dehydrogenase family which implies enzymes that oxidize a wide variety of aliphatic and aromatic aldehydes using NADP as a cofactor (Steinmetz *et al.*, 1997). Genes on scaffold 28 and 60 encoded for HSP60 proteins containing adh_short domains. The adh_short domain belongs to the short-chain dehydrogenases/reductases family (SDR), that is a very large family of enzymes that ar mostly NAD- or NADP-dependetnt oxidoreductases (Jörnvall *et al.*, 1995). HTH_AraC (PF00165) is a major protein structural motif capable to bind to the DNA. This domain belongs to the Bacterial regulatory helix-turn-helix proteins, AraC family and is found in the domain structure of two HSP60s protein encoded by genes on scaffold 28 and 32. The tetratrico peptide repeat TPR_1 (PF00515) and TPR_2 (PF07719) are also structural motifs that are found in a huge part of proteins and that asssist in protein-protein interactions and the assembly of multiprotein complexes (Das *et al.*, 1998; D'Andrea and Regan, 2003). The HSP60 protein encoded on scaffold 53 contains a TPR_1 motif, and the HSP60 protein encoded on scaffold 60 contains both identified TPR motifs. The family of Aminotransferase class I an II (Aminotran_1_2 (PF00155)) contains Aminotransferases and other pyridoxal-phosphate dependent enzymes, that share sequence similarities (Sung *et al.*, 1991). HSP60s encoded on scaffold 12 and 32 contain this motif. The response regulator reciver domain (Response_reg (PF00072)) is a two-component signal transduction system found in bacteria. In bacteria this system helps to sense, respond and adapt to a wide range of enviroments and stress conditions (Pao and Saier, 1995; Skerker *et al.*, 2005). These domains are found in HSP60 proteins encoded on scaffold 12 and 28. The Gag protein (Gag_p24 (PF00607)), also known as p24, is reported as structure protein of retroviruses that forms the inner protein layer of the nucleocapsid (Wehrly and Chesebro, 1997). The Gag_p24 motif could be observed in two HSP60s encoded on scaffold 12 and 9. The HSP60 protein of group 1 is encoded on scaffold 4 and contains, besides the Cpn60_TCP1 and the GGDEF domain, a GP41 (PF00517), a LRR_1 (PF00560) and a p450 (PF00067) domain (Table 5.2 and Fig. 3.24). Gp41, also known as glycoprotein 41, is a subunit of the envelope protein complex and is part of a family that includes envelope proteins from a variety of retroviruses (Malashkevich *et al.*, 1998). The leucine-rich repeat (LRR_1) is a protein structural motif that generally forms an arc or horseshoe (Enkhbayar *et al.*, 2004) and p450 is a domain of Cytochrome P450s enzymes, a superfamily of haem-containing mono-oxygenases that are involved in the oxidative degradation of various compounds (Werck-Reichhart and Feyereisen, 2000) (Table 5.2 and Fig. 3.24). The HSP60 protein of group 2 is encoded on scaffold 5. Its domain structure contains an Aldedh, a Cpn60_TCP1, a GGDEF domain and a TetR_N (PF00440) domain. TetR_N belongs to the bacterial regulatory proteins, tetR family (Chattoraj *et al.*, 2011).

The HSP60 (Protein ID 301074) identified on the 2D gels, belongs to group 3 and is encoded on scaffold 12. With 10 different domains involved in the characteristic domain structure, this HSP60 has the most complex domain architecture of all identified HSP60s. Beside of the already described domains Aminotran_1_2, Cpn60_TCP1, Gag_p24, Response_reg and Tubulin, the domains CBS (PF00571), HisKA (PF00512), MFS_1 (PF07690), MMR_HSR1 (PF01926) and RVT_connect (PF06815) could be identified (Table 5.2 and Fig. 3.24). CBS (cystathionine-beta-synthase) domains are small intracellular modules that pair together, forming a globular domain. They are mostly found in two or four copies within a protein, that occur in a variety of proteins in bacteria, archaea, and eukaryotes (Ignoul and Eggermont, 2005). The His Kinase A (phospho-acceptor) domain (HisKA) is a two-component signal transduction system, that enables bacteria to sense, respond, and adapt to a wide range of environments, stressors, and growth conditions (West and Stock, 2001). MFS_1 domain is characteristique for transporters of the Major Facilitator Superfamily (MFS). They are single-polypeptide secondary carriers capable only of transporting small solutes in response to chemiosmotic ion gradients (Pao *et al.*, 1998). MMR_HSR1 belongs to the 50S ribosome-binding GTPase family. For a complete activity of the protein to interact with the 50S ribosome, the full-length GTPase protein is required. Recently it was shown that several proteins contain structural motifs characteristic of GTP-binding proteins (Sazuka *et al.*, 1992). The connection domain (RVT_connect) is reported to lie between thumb and palm domain (Kohlstaedt *et al.*, 1992). The HSP60 protein of group 4 that is encoded on a gene of scaffold 28 contains in its structure beside the adh_short, Cpn60_TCP1, HTH_AraC, Pyr_redox and Response_reg domain two further domains DAO (PF01266) and GTP_EFTU_D3 (PF03143) (Table 5.2 and Fig. 3.24). D-amino acid oxidase (DAO) is a domain of the FAD dependent oxidoreductase family, which catalyzes the oxidation of neutral and basic D-amino acids into their corresponding keto acids (Negri *et al.*, 1992). GTP_EFTU_D3 is a domain that belongs to the GTP-binding elongation factor family, EF-Tu/EF-1A subfamily. Proteins of this family consist of three structural domains, a GTP-binding domain, and two oligonucleotide binding domains that are often referred to as domain 2 and domain 3. The C-terminally located GTP_EFTU_D3 is the third domain and adopts a beta-barrel structure. GTP_EFTU_D3 is involved in binding to both charged tRNA and to EF1B (or EF-Ts) (Wang *et al.*, 1997). The domain structure of the HSP60, encoded on scaffold 29 (Group 5) contains beside of a Cpn60_TCP1 and a Pyr_redox domain also an Epimerase (PF01370) domain (Table 5.2 and Fig. 3.24). The Epimerase domain is present in proteins of the NAD dependent epimerase/dehydratase family and uses nucleotide-sugar substrates for a variety of chemical reactions, with NAD as a cofactor (Thoden *et al.*, 1997). The domain architecture of the identified HSP60 of group 6, encoded on scaffold 32 contained additional to the above described domains AAA, Aminotran_1_2, Cpn60_TCP1 and HTH_AraC a Glycos_transf_2 (PF00535), a homeobox (PF00046), a zf-C2H2 (PF00096) and a zf-C3HC4 (PF00097) domain (Table 5.2 and Fig. 3.24). Glycosyl transferase family 2 (Glycos_transf_2) is a domain that is found in a diverse family of glycosyl transferases that transfer the sugar from UDP-glucose, UDP-N-acetyl-galactosamine, GDP-mannose or CDP-abequose, to a range of substrates including cellulose, dolichol phosphate and teichoic acids (Campbell *et al.*, 1997). The identiefied HSP60 protein in group 7 is encoded on scaffold 40 and presented a domain architecture containing beside the already described domains Cpn60_TCP1, GGDEF, Pyr_redox and Tubulin an additional ATP-syn_ab (PF00006) domain (Table 5.2 and Fig. 3.24). The ATP-syn_ab domain, a nucleotide-binding domain, belongs to the ATP synthase alpha/beta family that includes the ATP synthase alpha and beta subunits (Shirakihara *et al.*, 1997). In group 8 a HSP60 was identified, which contains AAA, Cpn60_TCP1, TPR_1, Tubulin (see above) as well as HTH_3 (PF01381) in its domain structure (Table 5.2 and Fig. 3.24). The described HTH_3 domain belongs to the large family of DNA binding helix-turn-helix proteins (Ren *et al.*, 2010). The HSP60 of group 8 is encoded on scaffold 53. Scaffold 60 encoded a HSP60 protein (group 9) that revealed a domain architecture containing six of the already described domains (adh_short, Cpn60_TCP1, Gag_p24, TPR 1 + 2 and Tubulin) and a additional NUDIX (PF00293) domain (Table 5.2 and Fig. 3.24). NUDIX (Nucleoside Diphosphate linked to X) forms a protein family of phosphohydrolases, which creates two products by breaking a phosphate bond in their substrate through water-mediated catalysis (McLennan, 2006).

5.3 Regulation of gene expression

Multicellular organisms have the capacity of maintaining an internal homeostasis. They consist of specific cell types which are regularly exposed to sudden changes in extracellular environment, having the ability to quickly overcome these changes. Sophisticated sensing mechanisms and signal transduction systems respond to cellular stress in a variety of accurate dynamic ways ranging from activation of CSR pathways that promote survival to eliciting programmed cell death that eliminates damaged cells (Hochachka, 2000; Fulda *et al.*, 2010; De Nadal *et al.*, 2011). These activated signaling pathways control almost every aspect of cellular physiology and changes in gene expressions are an essential part of the CSR. These changes in gene expression include general responses that are common for many stresses (CSR) as well as stress specific adaptive responses (CHR) that are essential for the slower, long-term adaptation and recovery phases. For the most adaptive responses, control of the gene expression has a fast reversible response kinetic, leading to changes of the cellular transcription state within minutes in stressful conditions, and will return to its basal state after the stress is removed. However, if the harmful stress situation cannot be coped with, then activation of death signaling pathways by the cell is the consequence (Fulda *et al.*, 2010; De Nadal *et al.*, 2011). Gene expression is regulated by combined interaction of different *cis*-regulatory elements such as core promoters, enhancers, silencers, insulators and tethering elements. For the transcription initiation by RNA polymerases II (RNA pol II), multiple basal transcription factors (TFs) are required (Fig 5.2). This way, enhancers and their associated TFs have a leading part in the initiation of gene expression (Shilatifard *et al.*, 1997; Spitz and Furlong, 2012).

5.4 Regulation of gene expression via core promoters

The core promoters consist of a special type of enhancer elements that can activate transcription only when located in proximity of the transcription start site (TSS). There are two known modes of transcription initiation, a focused one and a dispersed one. Focused transcription initiation will start at a specific TSS, whereas in the dispersed mode of transcription initiation, there are multiple weak TSSs over a broad region of around 50 to 100 nucleotides. In all organisms, focused transcription initiation takes place and appears to be predominant in simpler organisms, whereas 70 % of the vertebrate genes possess dispersed promoters. Some core promoters present a combination of focused and dispersed promoters. In general, it seems that regulated genes are equipped with focused promoters while constitutively expressed genes are associated with dispersed promoters (Juven-Gershon and Kadonaga, 2010). Research for transcription factor binding sites on focused core promoters has led to the discovery of sequence motifs such as the TATA box, BRE*u* and BRE*d* (*up*- and *down*stream TFII*B* *R*ecognition *E*lement), Inr (initiator), sINR (strict initiator), DPE (*D*ownstream *P*romoter *E*lement), DCE (*D*ownstream *C*ore *E*lement), MTE (*M*otif *T*en *E*lement) as well as XPCE1 and 2 (*X* *C*ore *P*romoter *E*lement 1 and 2) (Fig. 5.3). Dispersed promoters in general lack BRE, TATA, DPE and MTE motifs but might contain CGI (*CG* *I*slands also called CpG islands (*C*ytosin-*p*hosphatidyl-*G*uanin islands)). The mechanisms of focused versus dispersed mode of transcription initiation are likely to be very different. For this study I will mainly lay emphasis on focused core promoters (FCP). The FCP are diverse in structure and function and are generally located at -100 to +40 relative to the TSS. Since there are no universal regulatory core elements, different regulatory elements can contribute to FCP activity and will serve as location at which the RNA pol II machinery starts transcriptions. Basal transcription factors (BTFs) and RNA pol II will bind to these regulatory sequence elements that serve as docking site and form a pre-initiation complex (PIC).

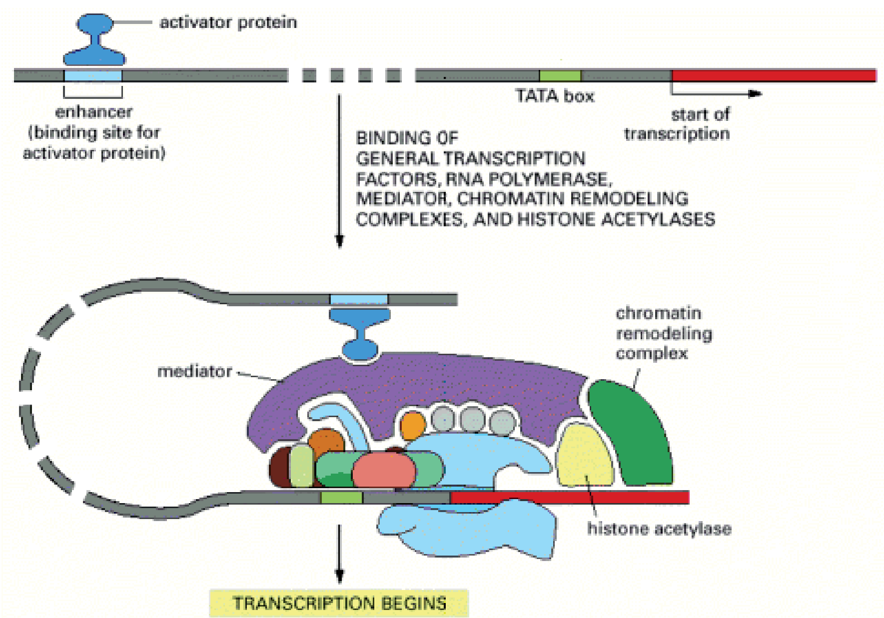

Fig. 5.2 Transcription initiation by RNA pol II in eukaryotic cells

Transcription initiation requires the presence of transcription factors, which bind to specific binding sites of the DNA. Although only one is shown here, a typical eucaryotic gene has many activator proteins, which together determine its rate and pattern of transcription. Sometimes acting from a distance of several thousand nucleotide pairs (indicated by the dashed DNA molecule), these gene regulatory proteins help RNA polymerase, the general factors, and the mediator all to assemble at the promoter. In addition, activators attract ATP-dependent chromatin-remodeling complexes and histone acetylases (Alberts *et al.*, 2002).

Transcription factor binding sites will contain different types of BTFs such as TFIIA (*T*ranscription *F*actor for Polymerase *II A*), TFIIB, TFIID, TFIIE, TFIIF or TFIIH, with TFIID being the major core promoter-binding factor (Juven-Gershon and Kadonaga, 2010; Dikstein, 2011). Therefore, depending on the regulatory motifs of the core promoter, different sets of combinations of BTFs will act in the initiation of the transcription. Since the binding strength of the RNA pol II and the different sets of combinations of BTFs vary, the composition of the FCP may have an impact on the intensity of transcription (Juven-Gershon and Kadonaga, 2010; Dikstein, 2011). The upstream T of the TATA box of the highly conserved element is usually located at -45 to -15 relative to TSS (Fig. 5.3) (Yang *et al.*, 2007; Juven-Gershon and Kadonaga, 2010). The TATA box element is recognized and bound by TBP and will form a multi protein complex to which RNA pol II will bind along with various other transcription factors to initiate transcription (Alberts *et al.*, 2002). Once the TATA box was considered to be a universal core promoter element, but today's data reveal that most genes lack a TATA box and do instead possess alternative core promoter elements such as Inr or DCE. For example the fraction of TATA-dependent promoters in *Drosophila* is approximatly 30%, in yeast between 20 – 46% and in humans around 35% (Dikstein, 2011).

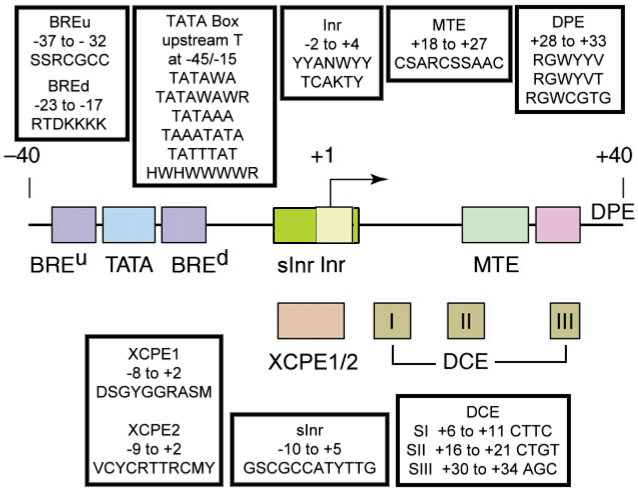

Fig. 5.3 Some of the known core promoter motifs for transcription by RNA polymerase II

Some of the typically found motifs in focused core promoters. It is likely that additional core promoter motifs remain to be discovered. The presence or absence of specific core promoter elements determines the characteristics of any particular core promoter and therefore the type of the transcription regulation based on (Juven-Gershon and Kadonaga, 2010).

The Initiator (Inr) as well as the strict Initiator (sInr) are strictly located around the TSS (Fig. 5.3). The Inr itself can be recognized and bound by RNA pol II (Dikstein, 2011), also the direct bond of RNA pol II is weak, it might assist the correct positioning of the polymerase on the promoter. Inr can be bound by RNA pol II more strongly if the RNA pol II is part of a protein complex. The Inr is probably the most commonly occurring sequence motif in focused core promoters and can function alone, together with the TATA box or in combination with DPE or MTE (Juven-Gershon *et al.*, 2008; Dikstein, 2011). sInr on the other hand is specifically enriched in TATA-less promoters and functions in combination with a nearby Sp1 site (Dikstein, 2011).

The downstream promoter element (DPE) is located precisely at +28 to +32 to the TSS (Fig. 5.3). It was discovered as a downstream TFIID recognition sequence in *Drosophila melanogaster*. But it is also present in other species including humans and excluding *Saccharomyces cerevisiae* (Burke and Kadonaga, 1996). It appears to be as common as the TATA box. While a lot of promoters containing DPE do not contain a TATA box, there are also promoters that contain both a TATA box and a DPE (Butler and Kadonaga, 2002; Juven-Gershon *et al.*, 2008; Dikstein, 2011).

The motive ten element (MTE) is a downstream core promoter element that promotes transcription by RNA pol II when it is located precisely at positions +18 to +27. Like DPE, the MTE functions in cooperation with Inr with a strict Inr-MTE spacing requirement and can act independently of the DPE as well as the TATA box. However synergies between MTE and DPE as well as the TATA box were observed, leading to the concept of a super core promoter (SCP) that contains a TATA box, Inr, MTE and DPE. The SCP in conjunction with transcriptional enhancers is the strongest core promoter yielding high levels of transcription observed in vitro and cultured cells (Juven-Gershon and Kadonaga, 2010).

The downstream core element (DCE) consists of three consensus elements referred to as sub-elements: SI (CTTC), SII (CTGT) and SIII (AGC) (Fig. 5.3). DCE occurs with the TATA box, and appears to be distinct from the DPE (Juven-Gershon *et al.*, 2008). The BREu was initially identified as a TFIIB binding sequence immediately upstream to the TATA box. BREd is a second TFIIB binding site, that is located downstream (Fig. 5.3). Both of these elements function in conjunction with a TATA box and are known to raise or lower the level of basal transcription (Juven-Gershon and Kadonaga, 2010).

Despite the fact that a large number of promoters lack both TATA-box and Inr, the number of characterized core elements that function without the presence of a TATA box or an Inr sequence is limited. XCPE1 and XCPE2 are directing activator-, mediator-, protein-dependent transcription from TATA box and Inr less promoters. Whereas XCPE1 is acting TFIID-independently, XPCE1 is dependent on TBP and the mediator to drive transcription. XCPE1 is present in about 1% of human core promoters, particularly in poorly characterized TATA-less genes (Dikstein, 2011). A large subclass of RNA pol II promoters lacks both TATA box and CAAT box sequence motifs but contains Cytosin-phosphatidyl-Guanin islands (CpG islands) which generally range in size from 0.5 to 2 kbp. In these promoters, transcription start sites may be single and specific, or there may be multiple weak start sites. GC box motifs are one of the most common regulatory DNA elements of eukaryotic genes and recognized by the Spl and related transcription factors (Butler and Kadonaga, 2002).

The core promoter elements do not only serve as elements to properly place the RNA pol II transcription machinery, but are also target of the action of sequence-specific transcription factors and coregulators, and therefore *cis*-acting regulatory elements. This is achieved by the diversity of the core promoter structure, which plays a particular role in enhancer-promoter communication (Fig. 5.4) (Butler and Kadonaga, 2002). Beside of enhancer proximal promoter elements also play an important role in the activity of promoters. Sp1-Binding sites as well as the binding sites of other well-known transcription factors such as Ets-1, NRF1, NRF2 and CREB are over-represented motifs close to the TSS (Dikstein, 2011).

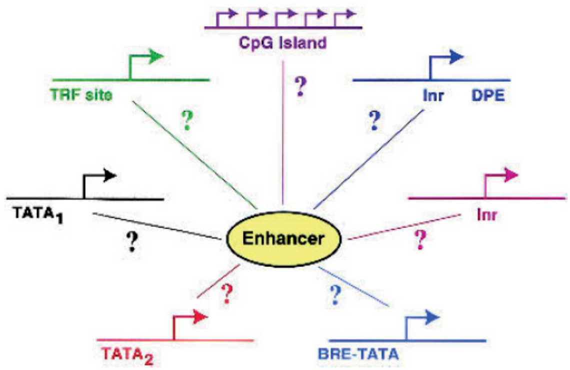

Fig. 5.4 Variety of different core promoter elements in enhancer-promoter communication

Transcriptional enhancers are confronted with a wide variety of core promoters. Core promoters not only direct the initiation of transcription, but also participate in the specificity of enhancer function (Butler and Kadonaga, 2002).

Even though our understanding of eukaryotic gene regulation has advanced considerably, the emerging picture of transcriptional regulation reveals the incredible complexity of the system. It is therefore essential to increase the breadth and depth of our current knowledge to illuminate the molecular mechanisms as well as to uncover novel modes of gene regulation. Gene regulation modes and molecular mechanisms through core promoter elements and enhancers can be studied in model organisms of known genomic information such as *Daphnia*.

5.5 Bioinformatical analysis for specific promoters and highly conserved protein domains

In addition to the performed proteomic analysis, for all identified proteins via LC-MS/MS, gene sequences with an extension of 4 kbp up– and downstream, were retrieved from the gene catalog of *D. pulex* at the JGI Genome Portal (http://genome.jgi.doe.gov) (Grigoriev *et al.*, 2012). The drawn genome regions were screened for different promoters using *rVista* (http://genome.lbl.gov/vista/index.shtml) (Loots *et al.*, 2002). Consensus sequences of IUPAC motifs for core promoters and enhancer (Table 5.3) were searched in sense and antisense strands up- and downstream of the transcriptional start sites (TSS). The exon (coding regions (CR)), intron (IN), untranslated regions (UTRs), estimated core promoter region (ECPRs) and potential core promoter structure of each gene was visualized by *CLC Genomics Workbench 3* and the graphical figures were adjusted with *Ulead PhotoImpact X3*.

Potential genome and protein sequences of HSP60s were detected by database research and obtained from the JGI *Daphnia* pulex genome portal (Colbourne *et al.*, 2011). The theoretical molecular mass (M_rp) and isoelectric point (pI*p*) of mature proteins were determined by *CLC Genomics Workbench 3*. Phylogenetic tree and alignments were done by *CLC Genomics Workbench 3* and highly conserved Pfam protein domains of the HSP60-family were searched within the 100 most frequent domains were via Pfam Domain Search in *CLC Genomics* using PFAM100 Version 22.0. Visualisation and graphical representation of domain organisations or architectures were done by the domain graphics generator using a JSON string to describe the domain graphic (http:// http://pfam.sanger.ac.uk/generate_graphic) (Mistry and Finn, 2007; Finn *et al.*, 2010; Punta *et al.*, 2012). The graphical figures were adjustes with *Ulead PhotoImpact X3*.

Table 5.3 Analyzed core promoter and enhancer motifs

[a] Consensus sequences of IUPAC motifs (R=A/G, Y=C/T, K=G/T, M=A/C, B=C/G/T, H=A/C/T, D=A/G/T, N=A/C/G/T) [b] Position of the first nucleotide of the motifs relevant to TSS (transcription starting site) Referenz: (Briggs *et al.*, 1986; El-Deiry *et al.*, 1992; Friling *et al.*, 1992; Carter *et al.*, 1992; Hanson *et al.*, 1993; Ko and Engel, 1993; Kim *et al.*, 1995; Burke and Kadonaga, 1996; Mantovani, 1998; Lagrange *et al.*, 1998; Segal *et al.*, 1999; Butler and Kadonaga, 2002; GuhaThakurta *et al.*, 2002; Kadonaga, 2002; Morrish *et al.*, 2003; Cha-Molstad *et al.*, 2004; Lim *et al.*, 2004; Deng and Roberts, 2005; Doi, 2005; Lee *et al.*, 2005; Perry, 2005; Xie *et al.*, 2005; Zhang *et al.*, 2005; Murphy, 2006; Tokishita *et al.*, 2006; Aldridge *et al.*, 2007; Yang *et al.*, 2007; Roy and Tamuli, 2008; Elfakess and Dikstein, 2008; Hollenhorst *et al.*, 2009; Yarden *et al.*, 2009; Isern *et al.*, 2010; Parry *et al.*, 2010; Winklmayr *et al.*, 2010; Zeng *et al.*, 2010; Ferguson *et al.*, 2010; Dikstein, 2011; Gerke *et al.*, 2011; Seitz *et al.*, 2011; Chorley *et al.*, 2012; Odrowaz and Sharrocks, 2012).

Motif	Motif Sequence[a]	Known Factor	Position[b]	Referenz
Core Promoter				
Estimated Core Promoter Region (ECPR)			**-125 .. 34**	
TATA box	*TATAWA*	TBP subunit of TFIID	-31 .. -30	Dikstein 2011
	TATAWAWR		-35 .. -25	Dikstein 2011
	TATAAA		-35 .. -25	Dikstein 2011
	TAAATATA		-35 .. -25	Butler and Kadonaga 2002
	TATTTAT		-35 .. -25	Butler and Kadonaga 2002
	HWHWWWWR		-45 .. -15	Yang *et al.* 2007
Inr	*YYANWYY*	RNA pol II, YY1	-2 .. 4	Dikstein 2011
	TCAKTY	TAF1 and TAF2 subunits of TFIID	-2 .. 4	Burke and Kadonaga 1996
sINR	*GSCGCCATYTTG*	YY1, TAF1 subunit of TFIID	-10 .. 5	Yarden *et al.* 2009
TCT	*YCTYTYY*		-1 .. 5	Parry *et al.* 2010
	YYCTTTYY		-2 .. 5	Parry *et al.* 2010
TOP	*YYCTYTTYYY*		-2 .. 7	Perry 2005
DPE	*RGWYYV*	TAF6 and TAF9 subunits of TFIID	28 .. 33	Kadonaga 2002
	RGWYVT		28 .. 33	Lim *et al.* 2004
	RGWCGTG		28 .. 33	Burke and Kadonaga 1996
DCE-SI	*CTTC*	TAF1/TAF_{II}250 subunits of TFIID	6 .. 11	Lee *et al.* 2005
DCE-SII	*CTGT*		16 .. 21	Lee *et al.* 2005
DCE-SIII	*AGC*		30 .. 34	Lee *et al.*2005
BREu	*SSRCGCC*	TFIIB	-37 .. -32	Lagrange *et al.* 1998
BREd	*RTDKKKK*	TFIIB	-23 .. -17	Deng and Roberts 2005
MTE	*CSARCSSAAC*	TFIID	18 .. 27	Lim *et al.* 2004
XCPE1	*DSGYGGRASM*		-8 .. 2	Dikstein 2011
XCPE2	*VCYCRTTRCMY*	TBP subunit of TFIID	-9 .. 2	Dikstein 2011
TISU	*AAGATGGC*	YY1	5 .. 30	Elfakess and Dikstein 2008
CAAT-box	*CCAAT*	C/EBP, CTF/NF-I, NF-Y, Y Box factors,	-100 .. -80	Mantovani 1998
	ATTGG	CDP, CTF1/NF1	-100 .. -80	Mantovani 1998
ets-binding-motif	*CGGAAR*	ETS family of transcription factors	6 .. 33	Carter *et al.* 1992
	GGAW		6 .. 33	Hollenhorst *et al.* 2009
	CCGGAAGT		6 .. 33	Odrowaz and Sharrocks 2012
M1	*YGCGCAYGCGCR*	NRF-1	-63 .. -61	Morrish *et al.* 2003
	RCGCANGCGY		-63 .. -61	Xie *et al.* 2005
	TGCGCATGCGCA		-63 .. -61	Roy and Tamuli 2008
M2	*CACGTG*	MYC	-63 .. -61	Seitz *et al.* 2011
	VCNBKTK		-63 .. -61	Seitz *et al.* 2011
	CAYGCG		-63 .. -61	Morrish *et al.* 2003
M3	*SCGGAAGY*	ELK-1	-25 .. -23	Xie *et al.* 2005
M6	*KGGGCGGRRY*	Sp1	-75 .. -35	Segal *et al.* 1999
	RYYCCGCCCM		-125 .. -34	Carter *et al.* 1992
M18	*TCACNCCAC*	SREBPs	-65 .. -63	Kim *et al.* 1995
	TCANNTGAY		-65 .. -63	Xie *et al.* 2005
M22	*TGCGCANK*	-	-18 .. -16	Xie *et al.* 2005
GpC box	*KRGGCGKRRY*	Sp1		Briggs *et al.* 1986
GATA	*WGATAR*	GATA-binding protein	-114 .. 0	Ko and Engel 1993/Doi 2005
	AGATCTTA		-114 .. 0	Ko and Engel 1993

	HGATAR		-114 .. 0	Tokishita *et al.* 2006
	YTATCD		-114 .. 0	Tokishita *et al.*2006
Enhancer				
CRE	*TGACGTCA*	carbohydrate response element-binding protein (ChREBP)		Cha-Molstad *et al.* 2004
	RGACGTCA	CREB		Hanson *et al.* 1993
	TGACSGTCA			Zhang *et al.* 2005
DAE	*CTTATCA*	DAF-16/FOXO		Murphy, 2006
DBE	*TRTTTAC*	DAF-16/FOXO		Murphy, 2006
E74 binding site	*CATCAGGAAGC*	E74		Tokishita *et al.* 2006
	GCTTCCTGATG			Tokishita *et al.* 2006
E75 binding site	*ATATGGGGCA*	E75		Tokishita *et al.* 2006
	TGCCCCATATT			Tokishita *et al.* 2006
EcRE	*RGKTCANTGAMCY*	ecdysone		Tokishita *et al.* 2006
GATA	*WGATAR*	GATA-binding protein	-1000 .. -114	Ko and Engel 1993
	AGATCTTA	GATA-binding protein	-1000 .. -114	Ko and Engel 1993
	HGATAR	GATA-binding protein	-1000 .. -114	Tokishita *et al.* 2006
	YTATCD	GATA-binding protein	-1000 .. -114	Tokishita *et al.* 2006
GLI-binding site	*GACCWCCCA*	GLI transcription factors		Winklmayr *et al.* 2010
HRE	*BRCGTGVB*	HIF-1		Gerke *et al.* 2011
HSAS	*GGGTYWCT*	heat shock transcription factors?		GuhaThakurta *et al.* 2002
HSE	*TTCYMGAA*	heat shock transcription factors		GuhaThakurta *et al.* 2002
JHRE	*RGRNYANNNNRGRNYA*	FKBP39, Chd64		Tokishita *et al.* 2006
	TRNYCYNNNNTRNYCY			Tokishita *et al.* 2006
XBP-1 binding site	*TGCA*	XBP1		Zeng *et al.* 2010
IRF binding site	*TTGARARGGAAACT*	IRF		Zeng *et al.* 2010
AP-1	*TGASTCA*	Jun, FOS, ATF, CREB,		Isern *et al.* 2010
	TGASTMA	PMA response elements		Friling *et al.* 1992
EpRE	*TGACAWW*	Jun, Fos		Friling *et al.* 1992
CHOP site	*GRTTGCA*	CHOP		Aldridge *et al.* 2007
MURE1	*AGAATBGCT*	?		Aldridge *et al.* 2007
MURE2	*GYACBCSAG*	?		Aldridge *et al.* 2007
NRF2 binding site	*TGASTCA*	NRF2		Chorley *et al.* 2012
p53 binding site	*RRRCWWGYYY*	p53		El-Deiry *et al.* 1992
skn-1 binding site	*WWTRTCAT*	skn-1		Ferguson *et al.* 2010
UAS2	*TNRTTGGT*	HAP2, HAP3		Carter *et al.* 1992
	TTCTCGGT			Carter *et al.* 1992

5.6 Bioinformatic analysis of promotor regions and enhancers

Bioinformatic analysis of the estimated core promoter region (ECPR) from the protein encoding gene sequences of the 34 identified proteins (see above), revealed ten different core promoter schemes (Fig. 5.5). Ten analyzed genes did not reveal any of the surveyed core promoter elements. This includes protein-encoding genes of proteins from the protein families

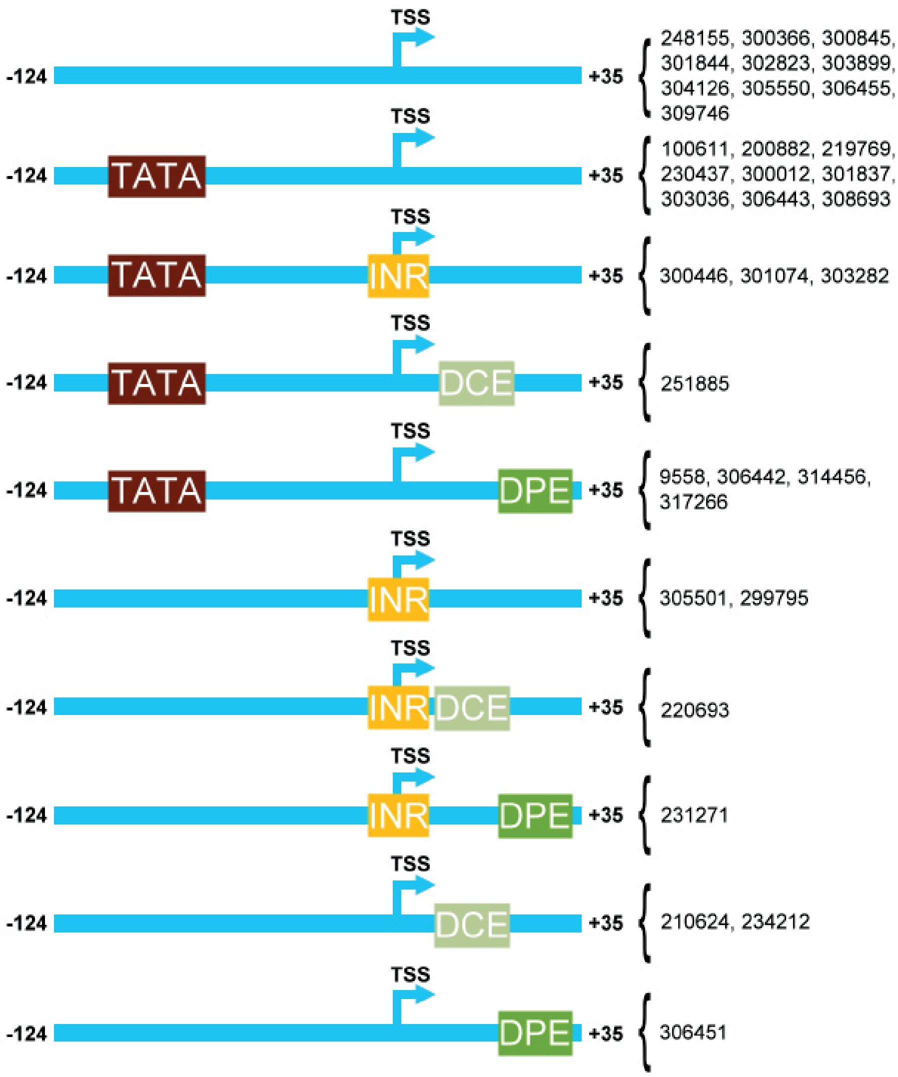

Fig. 5.5 Identified core promoter schemes in D. pulex

For all identified proteins, the upstream regions and coding genes were analyzed for core promoter elements. Identified core promoter elements were assigned to score promoter schemes. Blue areas represent the estimated core promoter Region, TSS (Transcription start side), TATA (Tata-Box), INR (Initiator), DCE (Downstream Core Element) and DPE (Downstream Promoter Element). On the right side, the associated Protein IDs are matched to the identified core promoter scheme.

ATPase, Carbohydrate metabolism, cytoskeleton and muscle proteins, kinases, proteolytic enzymes and transcription factors (Fig. 5.5). Nine of these protein encoding genes comprised only a TATA box. These genes encode proteins that are assigned to six different categories (Carboyhdrate metabolism, cytoskeleton and muscle proteins, proteolytic enzymes, transport proteins and proteins of the ubiquitin proteasome system). Core promoter regions for the encoding genes of three proteins contained a TATA-Box sequence together with the initiator (INR). These proteins belonged to the group of the antioxidative defense and detoxification, chaperones and transport proteins. Only the encoding gene of the serine endopeptidase (251885), a proteolytic enzyme, contained a core promoter sequence with a TATA-box combinded with downstream core element sequences (DCE). Core promoter elements of four genes, encoding proteins for the antioxidative defense and detoxification, carbohydrate metabolism, cytoskeleton and muscle proteins and proteins of the ubiquitin proteasome system, contained a TATA-box combined with a downstream promoter element (DPE) (Fig. 5.5). Core promoter elements containing only INR were detected in two genes coding for proteins of the carbohydrate metabolism and the antioxidative defense and detoxification. The encoding gene of the identified Arginine kinase (220693) implies INR and DCE sequence in the core promoter region. For the core promoter region of the encoding gene for the FKBP-type peptidyl-prolyl cis-trans isomerase (231271) an INR and DPE could be identified. In the core promoter element of the encoding gene for Calreticulin (210624) and protein disulphide isomerase (234212), DCE was characterized. In the core promoter region of the gene for the H+-transporting two-sector ATPase (309746) DPE was identified (Fig. 5.5).

In addition to the identified RNAPol II binding sites, five proximal core promoter elements were identified in the core promoter of the coding genes of the identified proteins. A CAAT-box element was identified for the gene encoding Nucleoside-diphosphate kinase (306455). EBS was found in four protein encoding genes for Glycoside hydrolase family 9 (230437), Alpha tubulin (100611), Actin (306422) and M13 family peptidase (200882). GATA was identified in the genes encoding for the Glutathione transferases (305501 and 317266), the H+-transporting two-sector ATPase (306451), Glycoside hydrolase family 9 (230437) and family 16 (303036), 3-phosphoglycerate kinase (299795), beta-glucosidase (314456), Actin (306442), Peptidase S1 (248155), Vitellogenin fused with SOD (219769) and Ubiquitin (9558). For the encoding gene of Glutathione transferases (317266), the H^+-transporting two-sector ATPase (306451), 3-phosphoglycerate kinase (299795), enolase (301844), HSP60p (301074), Actin (300012), Nucleoside-diphosphate kinase (306455),

Table 5.4 Identified core promoter schemes in *D. pulex*

Genes of those proteins identified in 2D gels were analysed for RNAPolymerase II (RNAPolII) binding sites as well was proximal core promoter elements. Presence of RNAPol II Binding sites as well as proximal core promoter elements in the analysed gene are marked by X. Additional to the core promoter shemes, protein expression under different applied stresses and duration are indicatd (0 no change, + significant induction and - significant reduction of protein expression – nD no data avaiable).

Spot ID	Function	Gene ID	RNAPol II Binding sites					Proximal Core Promoter Elements					*D. pulex* Clone G			*D. pulex* Clone M		
			TATA Box	Inr	DPE	DCE SI	DCE SII	CAAT box	EBS	GATA	GpC box	M2	H-stress 24h/48h	S-stress 24h/48h	HS-stress 24h/nD	H-stress 24h/48h	S-stress 24h/48h	HS-stress 24h/48h
Antioxidative defense & detoxification																		
801	Glutathione transferase	303282	X	X									0/+	0/0	+/nD	0/0	+/0	+/0
784	Glutathione transferase	305501		X						X			0/0	0/0	+/nD	0/+	0/+	+/+
794	Glutathione transferase	317266	X		X					X	X		0/+	+/+	0/nD	+/+	+/0	+/+
ATPase																		
415	H(+)-transporting two-sector ATPase.	306451			X					X	X		0/0	0/0	0/nD	+/+	0/0	+/+
441	H(+)-transporting two-sector ATPase.	309746											+/0	0/0	0/nD	0/0	-/0	0/0
466	H(+)-transporting two-sector ATPase.	309746											+/+	0/0	0/nD	0/0	0/0	0/+
482	H(+)-transporting two-sector ATPase.	309746											0/0	0/0	0/nD	0/0	0/0	0/0
23222	H(+)-transporting two-sector ATPase.	309746											0/-	0/0	-/nD	0/0	0/0	0/-
545	H(+)-transporting two-sector ATPase.	309746											0/0	0/0	0/nD	0/0	0/0	0/0
779	H(+)-transporting two-sector ATPase.	309746											0/0	+/0	+/nD	+/0	0/+	+/+
927	H(+)-transporting two-sector ATPase.	309746											0/0	0/0	0/nD	0/0	0/0	0/0
Carbohydrate metabolism																		
474	Glycoside hydrolase, family 9	230437	X						X	X			0/0	0/0	0/nD	0/0	-/-	0/0
501	3-phosphoglycerate kinase	299795		X						X	X		0/0	0/+	+/nD	0/0	0/0	0/0
472	Glycoside hydrolase, family 7	300366											0/-	0/0	0/nD	0/0	0/0	0/0
494	Enolase	301844									X		0/0	0/0	0/nD	0/0	0/0	0/0
503	Enolase	301844									X		0/0	0/0	0/nD	0/0	0/0	0/0
809	Enolase	301844									X		0/0	0/0	0/nD	0/0	+/0	+/0
1027	Enolase	301844									X		0/0	0/0	0/nD	0/0	+/0	0/+

621	Glyceraldehyde 3-phosphate dehydrogenase	302823										0/0	0/0	0/nD	0/0	0/0	0/0
600	Glycoside hydrolase, family 16	303036	X						X			-/-	0/0	-/nD	0/-	0/0	0/-
411	Beta-glucosidase	314456	X		X				X		X	0/0	0/0	0/nD	0/0	0/0	0/-
Chaperones																	
463	Calreticulin	210624				X						+/0	-/0	0/nD	0/0	-/-	0/-
805	FKBP-type peptidyl-prolyl cis-trans isomerase	231271		X	X							0/0	0/-	0/nD	0/0	0/0	-/0
439	Protein disulphide isomerase	234212					X					0/0	0/0	0/nD	+/0	0/0	0/0
383	Chaperonin ATPase. Cpn60/Hsp60p	301074	X	X						X		0/0	0/0	+/nD	+/+	+/+	+/+
Cytoskeleton & muscle proteins																	
417	Alpha tubulin	100611	X					X				+/+	0/+	0/nD	0/0	-/-	0/0
520	Actin and related proteins	300012	X							X		0/+	0/0	+/nD	-/-	-/-	-/-
2148	Actin and related proteins	300012	X							X		0/0	0/0	0/nD	0/0	0/0	0/0
550	Actin and related proteins	300012	X							X		0/0	0/-	0/nD	0/0	+/+	0/0
698	Actin and related proteins	300012	X							X		0/0	0/0	0/nD	0/0	+/+	0/0
752	Actin and related proteins	300012	X							X		0/0	+/0	0/nD	0/0	+/+	0/+
438	Beta tubulin	300845										+/0	0/0	0/nD	+/0	-/0	0/0
405	Alpha tubulin	301837	X									+/+	0/+	0/nD	+/+	-/0	+/+
416	Alpha tubulin	301837	X									+/+	0/+	0/nD	0/0	0/0	0/0
517	Actin and related proteins	305550										0/0	0/0	0/nD	0/0	0/0	0/0
724	Actin and related proteins	305550										0/0	0/0	0/nD	+/+	0/+	+/+
749	Actin and related proteins	305550										0/0	0/-	0/nD	0/0	+/0	0/0
3309	Actin and related proteins	306442	X		X			X	X			+/+	0/+	+/nD	0/0	0/0	0/+
2166	Actin and related proteins	306442	X		X			X	X			0/0	0/0	0/nD	0/0	0/0	0/0
Kinases																	
7663	Arginine kinases	220693		X			X					0/0	0/0	0/nD	0/0	0/0	0/0
543	Arginine kinases	220693		X			X					0/0	0/+	+/nD	0/0	0/0	0/+
563	Arginine kinases	220693		X			X					0/0	0/0	+/nD	0/0	0/0	0/+
757	Arginine kinases	220693		X			X					0/+	+/0	0/nD	0/0	+/0	0/0
756	Arginine kinases	220693		X			X					0/0	0/0	0/nD	0/0	0/0	0/0

796	Arginine kinases	220693		X		X					-/-	0/0	-/nD	0/0	+/0	0/0
943	Arginine kinases	220693		X		X					0/0	0/0	0/nD	0/0	0/0	0/0
1029	Nucleoside-diphosphate kinase	306455					X			X	0/0	0/0	0/nD	0/0	0/0	0/0
Proteolytic enzymes																
332	M13 family peptidase	200882	X					X			0/0	0/0	0/nD	0/0	0/0	0/-
722	Peptidase S1, chymotrypsin	248155							X		0/0	+/+	+/nD	0/0	0/0	0/0
635	Serine endopeptidase	251885	X		X					X	0/0	0/0	0/nD	0/-	0/0	-/-
641	Serine endopeptidase	251885	X		X					X	0/0	0/0	0/nD	0/-	0/-	-/-
742	Carboxypeptidase A2	303899								X	0/-	-/0	-/nD	-/-	0/0	0/-
Transcription factor																
609	FOG: Leucine rich repeat	304126									+/+	0/0	0/nD	+/+	0/+	+/+
Transport proteins																
270	Vitellogenin fused with SOD	219769	X						X		0/0	0/0	0/nD	+/+	0/0	+/+
301	Vitellogenin fused with SOD	219769	X						X		0/0	0/0	0/nD	+/+	+/+	+/+
305	Vitellogenin fused with SOD	219769	X						X		0/0	0/0	0/nD	+/+	0/0	+/+
322	Vitellogenin fused with SOD	219769	X						X		0/0	0/0	0/nD	0/+	+/+	+/+
325	Vitellogenin fused with SOD	219769	X						X		0/0	0/0	0/nD	0/0	+/+	+/+
573	Vitellogenin fused with SOD	219769	X						X		0/0	0/0	0/nD	0/0	0/0	0/0
576	Vitellogenin fused with SOD	219769	X						X		0/0	0/0	0/nD	0/+	0/+	+/+
1545	Vitellogenin fused with SOD	219769	X						X		0/0	0/0	0/nD	+/+	+/+	+/+
580	Vitellogenin fused with SOD	219769	X						X		0/0	0/0	0/nD	0/+	0/+	+/+
617	Vitellogenin fused with SOD	219769	X						X		0/0	0/0	0/nD	0/0	0/0	0/0
616	Vitellogenin fused with SOD	219769	X						X		0/0	0/0	0/nD	0/0	0/0	0/+
634	Vitellogenin fused with SOD	219769	X						X		0/0	0/0	0/nD	0/0	0/0	0/0
660	Vitellogenin fused with SOD	219769	X						X		0/0	0/0	0/nD	0/0	0/+	0/0
661	Vitellogenin fused with SOD	219769	X						X		0/0	0/0	0/nD	0/0	0/0	0/0
689	Vitellogenin fused with SOD	219769	X						X		0/0	+/0	0/nD	0/-	0/0	0/-
908	Cytosolic fatty-acid binding protein	300446	X	X						X	0/0	0/-	0/nD	-/0	0/0	0/-
231	Vitellogenin	308693	X								0/0	0/0	0/nD	0/0	0/0	0/+

238	Vitellogenin	308693	X				0/0	0/0	0/nD	0/0	0/0	0/+
215	Vitellogenin	308693	X				0/0	0/0	0/nD	0/0	0/0	0/0
448	Vitellogenin	308693	X				0/0	0/0	-/nD	0/0	0/0	0/0
937	Vitellogenin	308693	X				0/+	0/0	0/nD	0/0	0/0	0/0
Proteins of the ubiquitin proteasome system												
293	Ubiquitin and ubiquitin-like proteins	9558	X	X	X	X	0/-	0/0	0/nD	0/0	0/0	0/0
444	Ubiquitin and ubiquitin-like proteins	9558	X	X	X	X	0/0	0/0	0/nD	0/0	0/0	+/+
845	Ubiquitin and ubiquitin-like proteins	9558	X	X	X	X	0/-	-/0	-/nD	0/0	0/-	0/-
743	20S proteasome, A and B subunits	306433	X				-/0	0/0	0/nD	0/0	0/0	0/0

Serine endopeptidase (251885), Carboxypeptidase A2 (303899), cytosolic fatty-acid binding protein (300446) and Ubiquitin (9558), GpC-box elements were detected. The encoding protein gene for the Beta-glucosidase (314456) also included a M2 sequence (Table 5.4).

Examinations of 23 enhancer patterns (Table 5.5) in the up- and downstream regions of the protein encoding genes for the 34 identified proteins identified a total of 20 enhancers. The most common enhancers were the GATA-binding site with a total of 2803 identified binding sites and the XBP1 binding site, which was identified 2708 times. HRE was identified 312 times, EpRE was identified 261 times and AP-1 was identified 225 times. p53 binding site was identified 184 times, DBE was detected 161 times, UAS2 was discovered 146 times, the skn-1 binding side 135 times and the CHOP binding site 90 times. HSE was identified in a total 81 times, NRF2 binding sites 66 times, DAE 57 times and CRE 51 times. JHRE was characterized 38 times and HSAS was identified 33 times. The less common identified enhancers were MURE1, 10 times and MURE2, 10 times. E75 binding site was identified two times and the GLI binding site only one time (Table 5.5).

Table 5.5 Identified enhancers in *D. pulex*

Genes of those proteins identified in 2D gels were analysed for enhancer patterns in the up- and downstream regions. Presence of enhancer patterns in the analysed genes were counted and noted. Additional to the core promoter shemes, protein expression under different applied stresses and duration are indicatd (0 no change, + significant induction and - significant reduction of protein expression – nD no data avaiable).

Spot ID	Function	Gene ID	Enhancer																				*D. pulex* Clone G			*D. pulex* Clone M		
			AP-1	CHOP site	CRE	DAE	DBE	E75 BS	EpRE	GATA	GLI BS	HRE	HSAS	HSE	JHRE	MURE 1	MURE 2	NRF2 BS	p53 BS	skn-1 BS	UAS2	XBP-1 BS	H-Stress 24h/48h	S-Stress 24h/48h	HS-Stress 24h/nD	H-Stress 24h/48h	S-Stress 24h/48h	HS-Stress 24h/48h
Antioxidative defense & detoxification																												
801	Glutathione transferase	303282	2	1	1	1	6		8	87		9	1	3						3	5	68	0/+	0/0	+/nD	0/0	+/0	+/0
784	Glutathione transferase	305501	7	3		4	1		6	92		5	3	1			1	2	4	5	2	56	0/0	0/0	+/nD	0/+	0/+	+/+
794	Glutathione transferase	317266	3		3	1	3		4	87		11	2	3					4	1	5	68	0/+	+/+	0/nD	+/+	+/0	+/+
ATPase																												
415	H(+)-transporting two-sector ATPase	306451	8			1	5		5	71		8	2	1		1	1	2	12	3	7	88	0/0	0/0	0/nD	+/+	0/0	+/+
441		309746																					+/0	0/0	0/nD	0/0	-/0	0/0
466		309746																					+/+	0/0	0/nD	0/0	0/0	0/+
482		309746																					0/0	0/0	0/nD	0/0	0/0	0/0
###	H(+)-transporting two-sector ATPase	309746	5	2	2	1	10		5	73		15	1	5	4		1	2	6	2	5	68	0/-	0/0	-/nD	0/0	0/0	0/-
545		309746																					0/0	0/0	0/nD	0/0	0/0	0/0
779		309746																					0/0	+/0	+/nD	+/0	0/+	+/+
927		309746																					0/0	0/0	0/nD	0/0	0/0	0/0
Carbohydrate metabolism																												
474	Glycoside hydrolase, family 9	230437	11	2	2	1	11		8	82		8		1	2	1		2	6	4	9	88	0/0	0/0	0/nD	0/0	-/-	0/0
501	3-phosphoglycerate kinase	299795	1	4	2	2	6		5	111		6	1	5	2				4	1	5	82	0/0	0/+	+/nD	0/0	0/0	0/0
472	Glycoside hydrolase, family 7	300366	5	3	1	2	9		14	82		7	3		2			2	2	8	4	52	0/-	0/0	0/nD	0/0	0/0	0/0
494	Enolase	301844	2	3			5		8	78		7	1				1		8	2	3	104	0/0	0/0	0/nD	0/0	0/0	0/0
503		301844																					0/0	0/0	0/nD	0/0	0/0	0/0

809		301844																					0/0	0/0	0/nD	0/0	+/0	+/0
1027		301844																					0/0	0/0	0/nD	0/0	+/0	0/+
621	Glyceraldehyde 3-phosphate dehydrogenase	302823	11	3	4	1	3		8	74		13		2	4			4	4	6	4	70	0/0	0/0	0/nD	0/0	0/0	0/0
600	Glycoside hydrolase, family 16	303036	6	1		1	6		5	66		14		2		1		2	8	3	3	76	-/-	0/0	-/nD	0/-	0/0	0/-
411	Beta-glucosidase	314456	10	4		2	4		5	96		10	1	4				4	4	2	2	100	0/0	0/0	0/nD	0/0	0/0	0/-
Chaperones																												
463	Calreticulin	210624	7	2		2	5		5	87		9	2	3		1			2	3	10	92	+/0	-/0	0/nD	0/0	-/-	0/-
805	FKBP-type peptidyl-prolyl cis-trans isomerase	231271	15	2	1		3	1	8	74		5	1		2	1		6		5	4	62	0/0	0/-	0/nD	0/0	0/0	-/0
439	Protein disulphide isomerase	234212	13	1		2	3		11	110		5			2	1		4	6	3	7	84	0/0	0/0	0/nD	+/0	0/0	0/0
383	Chaperonin ATPase Cpn60/Hsp60p	301074	11	3			4		3	49		7		8	2		1	4	8	4	2	90	0/0	0/0	+/nD	+/+	+/+	+/+
Cytoskeleton & muscle proteins																												
417	Alpha tubulin	100611	1	1	2	4	4		7	91		9	1	2					4	4	4	60	+/+	0/+	0/nD	0/0	-/-	0/0
520	Actin and related proteins	300012																					0/+	0/0	+/nD	-/-	-/-	-/-
2148		300012																					0/0	0/0	0/nD	0/0	0/0	0/0
550		300012	6	3	6	2	4		9	80		9	1	3				2	6	6	1	98	0/0	0/-	0/nD	0/0	+/+	0/0
698		300012																					0/0	0/0	0/nD	0/0	+/+	0/0
752		300012																					0/0	+/0	0/nD	0/0	+/+	0/+
438	Beta tubulin	300845	13	1		4	5		8	90		8	1	3				4		3	5	70	+/0	0/0	0/nD	+/0	-/0	0/0
405	Alpha tubulin	301837	15	4		1	6		9	56		5	1		2		1	6	8	5	8	66	+/+	0/+	0/nD	+/+	-/0	+/+
416		301837																					+/+	0/+	0/nD	0/0	0/0	0/0
517	Actin and related proteins	305550																					0/0	0/0	0/nD	0/0	0/0	0/0
724		305550	6	4	2	4	1		6	103		11		6	2		1	2	8	3	3	68	0/0	0/0	0/nD	+/+	0/+	+/+
749		305550																					0/0	0/-	0/nD	0/0	+/0	0/0
###	Actin and related proteins	306442	16	1	7		6		5	60		10	2	3			1	8	6	2	2	62	+/+	0/+	+/nD	0/0	0/0	0/+
2166		306442																					0/0	0/0	0/nD	0/0	0/0	0/0
Kinases																												

7663	Arginine kinases	220693																					0/0	0/0	0/nD	0/0	0/0	0/0
543		220693																					0/0	0/+	+/nD	0/0	0/0	0/+
563		220693																					0/0	0/0	+/nD	0/0	0/0	0/+
757		220693	1		2		4		4	53		13		3		2			4	4	5	70	0/+	+/0	0/nD	0/0	+/0	0/0
756		220693																					0/0	0/0	0/nD	0/0	0/0	0/0
796		220693																					-/-	0/0	-/nD	0/0	+/0	0/0
943		220693																					0/0	0/0	0/nD	0/0	0/0	0/0
1029	Nucleoside-diphosphate kinase	306455	10	2	4	1	2		6	76		12	2	5	2			4	10	7	1	60	0/0	0/0	0/nD	0/0	0/0	0/0
Proteolytic enzymes																												
332	M13 family peptidase	200882	3	4		1	4		18	66		6	2	2					4	5	7	80	0/0	0/0	0/nD	0/0	0/0	0/-
722	Peptidase S1, chymotrypsin	248155	5	5	1	4	7		10	89		6		3			1		2	11	5	72	0/0	+/+	+/nD	0/0	0/0	0/0
635	Serine endopeptidase	251885	1	3		4	2	1	13	135		30	1	2	6		1		4	5	6	160	0/0	0/0	0/nD	0/-	0/0	-/-
641		251885																					0/0	0/0	0/nD	0/-	0/-	-/-
742	Carboxypeptidase A2	303899	8	5	2	1	9		2	75		9		3	2			2	6		1	96	0/-	-/0	-/nD	-/-	0/0	0/-
Transcription factor																												
609	FOG: Leucine rich repeat	304126	5	2	2	4	3		7	93		4						2	2	4	1	60	+/+	0/0	0/nD	+/+	0/+	+/+
Transport proteins																												
270	Vitellogenin fused with SOD	219769																					0/0	0/0	0/nD	+/+	0/0	+/+
301		219769																					0/0	0/0	0/nD	+/+	+/+	+/+
305		219769																					0/0	0/0	0/nD	+/+	0/0	+/+
322		219769																					0/0	0/0	0/nD	0/+	+/+	+/+
325		219769																					0/0	0/0	0/nD	0/0	+/+	+/+
573		219769	1	11	2	2	2		12	123		5	1	2					14	2	5	80	0/0	0/0	0/nD	0/0	0/0	0/0
576		219769																					0/0	0/0	0/nD	0/+	0/+	+/+
1545		219769																					0/0	0/0	0/nD	+/+	+/+	+/+
580		219769																					0/0	0/0	0/nD	0/+	0/+	+/+
617		219769																					0/0	0/0	0/nD	0/0	0/0	0/0
616		219769																					0/0	0/0	0/nD	0/0	0/0	0/+

634		219769																					0/0	0/0	0/nD	0/0	0/0	0/0
660		219769																					0/0	0/0	0/nD	0/0	0/+	0/0
661		219769																					0/0	0/0	0/nD	0/0	0/0	0/0
689		219769																					0/0	+/0	0/nD	0/-	0/0	0/-
908	Cytosolic fatty-acid binding protein	300446	5	2		1	7		7	63	1	11	1						4	1	5	72	0/0	0/-	0/nD	-/0	0/0	0/-
231		308693																					0/0	0/0	0/nD	0/0	0/0	0/+
238		308693																					0/0	0/0	0/nD	0/0	0/0	0/+
215	Vitellogenin	308693	6	5	1	2	4		14	103		13	1	3	2	1		2	6	6	7	130	0/0	0/0	0/nD	0/0	0/0	0/0
448		308693																					0/0	0/0	-/nD	0/0	0/0	0/0
937		308693																					0/+	0/0	0/nD	0/0	0/0	0/0
Proteins of the ubiquitin proteasome system																												
293		9558																					0/-	0/0	0/nD	0/0	0/0	0/0
444	Ubiquitin and ubiquitin-like proteins	9558	3	1	3	1	5		7	67		6		3					4	2	1	86	0/0	0/0	0/nD	0/0	0/0	+/+
845		9558																					0/-	-/0	-/nD	0/0	0/-	0/-
743	20S proteasome, A and B subunits	306433	3	2	1		2		9	61		6	1		2	1			14	10	2	70	-/0	0/0	0/nD	0/0	0/0	0/0

5.7 Bioinformatic analysis of promotor and enhancer regions

Research for core promoter elements on the protein encoding gene sequences of the 34 identified proteins (e.g. Table 3.2) revealed ten different core promoter patterns (Fig. 5.5). Ten of the analyzed genes showed none of the analyzed promoter elements within the estimated core promoter region (ECPR) and therefore are probably regulated by dispersed transcription initiation or possess an alternate promoter. All other investigates genes showed at least one of the core promoter elements (Fig. 5.5) and will most probably be regulated by focused transcription initiation. In eukaryotes, two different ways of transcription initiation have been observed. The focused initiation occurs with core promoter elements at specific locations within the ECPR, whereas in the dispersed initiation, the transcription initiation will occur at multiple start sites over a broad region. Dispersed initiation is mostly connected to CpG islands and associated with constitutive genes whereas focused transcription initiation is typically found in regulated genes (Butler and Kadonaga, 2002; Juven-Gershon *et al.*, 2006; Juven-Gershon *et al.*, 2008; Juven-Gershon and Kadonaga, 2010; Dikstein, 2011). Some promoters present a combination of both, focused and dispersed transcription initiation sites (Juven-Gershon and Kadonaga, 2010). However not all genes are regulated via focused or dispersed transcription initiation. Besides the core promoter, alternate promoters exist and are typically located hundreds or thousands of nucleotides apart the from transcription start site (TSS) (Juven-Gershon *et al.*, 2008). Enolase (301844), Nucleotide-diphosphate kinase (306455) and Carboxypeptidase A2 (303899) are probably regulated by dispersed transcription initiation through the GpC-box (Table 5.4). Since dispersed transcription initiation is related to constitutive genes, the assumption that these genes are transcribed at a relatively constant level can be made. For one of the identified H^+-transporting two-sector ATPases (309746), glycoside hydrolase, family 7 (300366), glyceraldhyde 3-phosphate dehydrogenase (302823), beta tubulin (300845), one actin (305550) and the transcription factor FOG: leucine rich repeat (304126), no core promoter elements or proximal core promoter elements were identified at all, indicating that transcription of these genes is probably regulated via an alternate promoters (Table 5.4). ECPRs of the genes coding for the glutathione transferase (317266), the V-ATPase (306451), the 3-phosphoglycerate kinase (299795), the chaperone HSP60 (301074), one of the identified actins (300012), the serine endopeptidase (251885), the cytosolic fatty-acid binding protein (300446) and the ubiquitin (9558) contained GpC-boxes combined with another RNAPol II binding site (Table 5.4) indicating combined qualities of focused and dispersed promoters. For all other identified proteins, the encoding gene sequence revealed patterns of a focused transcription initiation and therefore they seem to be inducible genes. Focused transcription initiation occurs in all organisms and seems to be predominant or the exclusive mode of transcription in simpler organism (Juven-Gershon and Kadonaga, 2010). Even though most eukaryotic core promoters are of the focused type, in vertebrates 70% of all genes have dispersed promoters (Juven-Gershon *et al.*, 2008; Juven-Gershon and Kadonaga, 2010).

Transcription is not only regulated by the diversity in the core promoter elements, but also by the diversity and quantity of associated enhancers (Butler and Kadonaga, 2002). For that reason, a broad overview of possible associated enhancers of the studied genes is given (Table 5.5).

The most abundant enhancer identified was the GATA-box element, which is highly represented in the *D. pulex* genome. GATA transcription factors (TF) bind to the GATA box. GATA-TFs are members of the Friend of GATA (FOG) family (Fossett *et al.*, 2001), related by their high degree of amino acid identity throughout the two-zinc-finger DNA-binding domain. They were originally identified as an erythroid cell-specific DNA-binding protein that bound to consensus sequences found in the regulatory regions of many globin and nonglobin erythroid-specific genes (Ko and Engel, 1993) and are also known to regulate gene expression during the development of a variety of tissues (Fossett *et al.*, 2001). All genes that correspond to the identified proteins in this work contained 53 to 135 GATA binding sites. Genes of the two identified Vitellogenins (219769 and 308693) showed a relatively high amount of GATA-TFs binding sites (Table 5.5).

The second most frequently associated enhancer was the XBP1 binding site (Table 5.5). XBP1-TF regulates genes involved in maintaining ER homeostasis and binds to the XBP1 binding site. XBP1-TF is a critical effector of the mammalian unfolded protein response (UPR). The UPR is an evolutionarily conserved signaling pathway that responds to perturbations in endoplasmic reticulum (ER) homeostasis (Acosta-Alvear *et al.*, 2007). All genes encoding the identified proteins in this work contained from 52 up to 160 XBP1 binding sites. The genes corresponding to the four identified chaperones conatained 92 XBP1 binding sites for calreticulin, 62 XBP1 binding sites for the FKBP-type peptidyl-prolyl cis-trans isomerase, 84 for the protein disulphide isomerase (PDI) and 90 TF binding sites for the HSP60p protein. Both Calreticulin and PDI are involved in maintaining ER homeostasis (Prasad *et al.*, 1999; Gelebart *et al.*, 2005).

HRE, EpRE and p53 was another common group of identified TF-binding sites. HRE (hypoxia-responsive element) induces gene expression under hypoxia stress and is reported to regulate hemoglobin gene expression in *Daphnia* (Tokishita *et al.*, 1997; Gorr *et al.*, 2004; Gerke *et al.*, 2011). The glutathione-S-transferase (GST) (317266) in clone M that was induced in all three investigated stress conditions, is encoded by a gene with eleven HREs. Two of the three identified actins (305550 and 306442) were induced in both clones under all stress conditions. These actins correspond to genes with eleven and ten HREs, respectively. The gene encoding the identified vitellogenin fused with SOD carries twelve HREs and was induced in clone M at all three stress conditions. EpRE (electrophile responsive element) is reported to be involved in the gene regulation and expression under oxidative stress and plays an important role in transcription regulation for the GST (Moinova and Mulcahy, 1998; Miller *et al.*, 2000). The GSTs induced here by H-, S- and HS-stress correspond to genes with four to eight EpR elements. Increase in steady-state GST levels are related to an increased activity of ϒ-glutamylcysteine synthase (GCS), which catalyzes the rate-limiting step in the de novo synthesis of GSH from its constituent amino acids. It was demonstrated that basal and β-NF-inducible expression of the GCS gene is mediated by a consensus EpRE sequence (Moinova and Mulcahy, 1998). The TF AP-1 (activator protein 1) is a heterodimeric protein regulating gene expression in response to stress, controlling a number of cellular processes including differentiation, proliferation, and apoptosis. AP-1 will bind to the consensus sequence of AP-1 binding sites and is composed of proteins belonging to the c-Fos, c-Jun, ATF and JDP families (Friling *et al.*, 1992; Hess *et al.*, 2004; Isern *et al.*, 2010). Genes corresponding to all the identified chaperones as well as the identified cytoskeleton and muscle proteins represented an increased number of AP-1 binding sites. P53-bindings site is a consensus sequence. At least two copys of the motif are necessary for a successful binding of P53 TF (El-Deiry *et al.*, 1992). P53 is reported to be involved in apoptotic suppression (Hershberger *et al.*, 1994) and is present in the genes encoding identified chaperones that are involved in cellular apoptosis, such as the HSP60p (301074), the PDI (234212) and calreticulin (210624) (Table 5.5).

Two DAF-16 binding sites (DAE and DBE) were identified in the performed bioinformatics analysis. DAE and DBE are binding sites of the *Caenorhabditis elegans* FOXO transcription factor, DAF-16. DAF-16 expression is regulated via the insulin/IGF-1 receptor (IIR)/FOXO pathway and activated by different stress stimuli. DAF-16 is controlled by the activity of the DAF-2 insulin receptor, repressing DAF-16 activity by phosphorylation and cytoplasmic retention. In the absence of DAF-2/insulin receptor signaling, DAF-16/FOXO translocates into the nucleus and regulates transcription of its targets (Murphy, 2006). The presence of these motifs in mostly all proteins of the set of DEPs identified here suggests a regulation of their genes by insulin like peptides. Only on the gene corresponding to the identified enolase (301844), no DAF-16 binding sites could be identified (Table 5.5).

The identified TF-binding site, UAS2 a CCAAT-box-related motif is a transcription activating element first characterized in yeast, that regulates a number of respiratory genes. CCAAT-box-related motifs have been identified in the promoters of a variety of vertebrate genes. In Yeast, UAS2 will be activated by the HAP complex, which appears to control expression of genes important for mitochondrial biogenesis. In vertebrates, direct homologs of the yeast HAP complex (called NF-Y, CP1, or CBF) have been identified and shown to bind to different CCAAT boxes, with varying levels of specificity (Carter *et al.*, 1992; Edwards *et al.*, 1998). The presence of these motifs in all proteins of the set of DEPs identified here suggests an involvement of some homologs of the HAP complex in gene regulation (Table 5.5).

CHOP (CCAAT-enhancer-binding protein homologous protein) will bind to the investigated consensus sequence of the CHOP binding site and is activated through the CHOP pathway. The CHOP pathway is involved in the response to ER stress, mtUPR or erUPR (mitochondrial and endoplasmatic unfolded protein response) malfunction and will activate apoptosis signaling (Aldridge *et al.*, 2007; Nishitoh, 2011). Transcription regulation with CHOP might depend on MURE1 and MURE2. It could be demonstrated, that in some cases three promoter elements MURE1, CHOP and MURE2 are required for the activation of mtUPR response and that the specificity of the mtUPR response resides in the MURE1 and MURE2 transcription factors (Aldridge *et al.*, 2007). All genes encoding the identified chaperones contained at least one CHOP binding site and one MURE1 motif on the genes corresponding to calreticulin, FKBP-type peptidyl-prolyl cis-trans isomerase and the PDI and one MURE2 motif for the gene corresponding to the HSP60p.

The identified HSE (heat shock element) is the binding site for heat shock factors. Heat shock factor 1 (HSF-1), the major TF in eukaryotes to activate transcription of heat shock genes, is activated through multiple cellular stresses. Cellular stresses, such as heat, will cause protein denaturation. These misfolded proteins will bind to heat shock proteins (HSP) that will dissociate from HSF-1. Free HSF-1 can translocate into the nucleus and activate transcription (GuhaThakurta *et al.*, 2002; Richter *et al.*, 2010). The highest number of HSE motifs was identified on the gene encoding the HSP60p (301074) protein, that showed an increased expression under all three sress conditions in *D. pulex* clone M. HSAS (heat shock associated site), a regulatory motif that plays also a significant role in the transcriptional regulation of heat shock genes (GuhaThakurta *et al.*, 2002), was identified as enhancer sequence in several genes encoding the identified DPEs. Genes corresponding to the identified proteins that were upregulated under H-stress such as GSTs, the V-ATPases (306451), the 3-phosphoglycerate kinase (299795), enolase (301844), Alpha tubulin (301837), Actin (305550), HSP60p, FOG: Leucine rich repeat (304126) and the vitellogenin fused with SOD (219769) contained HSAS motifs.

The two identified enhancers, JHRE (juvenile hormone-responsive element) and the E-75 binding site for the E75-TF are involved in the transcription activation of the vitellogenin gene in *D. magna* (Tokishita *et al.*, 2006). JHRE could also be identified in the gene of Vitellogenin (308693) of *D. pulex*. CRE (cAMP-response element) is an enhancer activated by the interaction with cAMP-response element binding protein (CREB). Hormones and nutrients induce the activation of the cAMP pathway, that stimulates the gene expressions through phosphorylation of CREB (Zhang *et al.*, 2006). CREs could be identified in genes corresponding to proteins throughout all protein classes of the identified DEPs. Copy numbers of the motif ranged from one to seven per gene. The highest copynumber was identified in the genes corresponding to Actin (306442 and 300012) (Table 5.5). Protective responses to cellular oxidative and electrophilic stress are reported to be regulated by the TF NRF2. NRF2 will bind to the identified desoxyribonucleic acid-regulatory sequences (NRF2 binding sites) near stress-responsive genes (Chorley *et al.*, 2012). NRF2 binding sites are present in genes encoding GST (305501), all of the genes corresponding to the identified V-ATPases, genes corresponding to the identified proteins of the carbohydrate metabolism such as Glycoside hydrolase family 7, 9 and 16, glyceraldehyde 3-phosphate dehydrogenase and beta-glucosidase, all identified chaperones involved in the regulation of apoptosis such as calreticulin, PDI and HSP60p, all identified cytoskeleton and muscle proteins beside of alpha tubulin (100611), the nucleoside-diphosphate kinase (306455), the carboxypeptidase A2 (303899), the FOG: Leucine rich repeat and vitellogenin (308693).

The GLI transcription factors are mediators of the hedgehog signal pathways and binds with high affinity to the investigated consensus sequence of the GLI-binding site. The hedgehog signaling pathway is a key regulator of animal development transmitting information to embryonic cells. It is present in all bilaterians (Winklmayr *et al.*, 2010). Only one GLI binding site could be identified in all the genes coresponding the investigated DEPs. The gene encoding the cytosolic fatty-acid binding protein implies one GLI-binding site.

References

Acosta-Alvear D, Zhou Y, Blais A, Tsikitis M, Lents NH, Arias C, Lennon CJ, Kluger Y and Dynlacht BD. (2007) XBP1 controls diverse cell type- and condition-specific transcriptional regulatory networks. *Mol.Cell* 27: 1: 53-66.

Adams V, Jiang H, Yu J, Mobius-Winkler S, Fiehn E, Linke A, Weigl C, Schuler G and Hambrecht R. (1999) Apoptosis in skeletal myocytes of patients with chronic heart failure is associated with exercise intolerance. *J.Am.Coll.Cardiol.* 33: 4: 959-965.

Aguilera MO, Beron W and Colombo MI. (2012) The actin cytoskeleton participates in the early events of autophagosome formation upon starvation induced autophagy. *Autophagy* 8: 11: 1590-1603.

Ahlgren G, Gustafsson I and Boberg M. (1992) Fatty acid content and chemical composition of freshwater microalgae. *J.Phycol.* 28: 1: 37-50.

Aldridge JE, Horibe T and Hoogenraad NJ. (2007) Discovery of genes activated by the mitochondrial unfolded protein response (mtUPR) and cognate promoter elements. *PLoS One* 2: 9: e874.

Alonso GD, Pereira CA, Remedi MS, Paveto MC, Cochella L, Ivaldi MS, Gerez de Burgos NM, Torres HN and Flawia MM. (2001) Arginine kinase of the flagellate protozoa *Trypanosoma cruzi*. Regulation of its expression and catalytic activity. *FEBS Lett.* 498: 1: 22-25.

Altermatt F and Ebert D. (2007) The genotype specific competitive ability does not correlate with infection in natural *Daphnia magna* populations. *PLoS One* 2: 12: e1280.

Bai X, Ma D, Liu A, Shen X, Wang QJ, Liu Y and Jiang Y. (2007) Rheb activates mTOR by antagonizing its endogenous inhibitor, FKBP38. *Science* 318: 5852: 977-980.

Barata C, Varo I, Navarro JC, Arun S and Porte C. (2005) Antioxidant enzyme activities and lipid peroxidation in the freshwater cladoceran Daphnia magna exposed to redox cycling compounds. *Comp.Biochem.Physiol.C.Toxicol.Pharmacol.* 140: 2: 175-186.

Becker D. (2011) Analyse der mit der Signalgebung verbundenen Prozesse bei Sauerstoff- und Temperaturstress beim Kleinkrebs *Daphnia*.

Bednarska and Dawidowicz P. (2007) Change in filter-screen morphology and depth selection : Uncoupled responses of *Daphnia* to the presence of filamentous cyanobacteria. *Limnology and Oceanography* 52: 6: 2358-2363.

Benzie JAH. (2005) *Cladocera: The Genius Daphnia (including Daphniopsis).* Ghent, Belgium: .

Boersma M, De Meester L and Spaak P. (1999) Environmental stress and local adaptation in *Daphnia magna*. *Limnology and Oceanography* 44: 2: 393-402.

Boersma M, Spaak P and De Meester L. (1998) Predator-mediated plasticity in morphology, life history, and behavior of *Daphnia*: the uncoupling of responses. *Am.Nat.* 152: 2: 237-248.

Bradford MM. (1976) A rapid and sensitive method for the quantitation of microgram quantities of protein utilizing the principle of protein-dye binding. *Analytical Biochemistry,* 72: 1-2: 248-254.

Brett MT, Wiackowski K, Lubnow FS, Mueller-Solger A, Elser JJ and Goldman CR. (1994) Species-Dependent Effects of Zooplankton on Planktonic Ecosystem Processes in Castle Lake, California. *Ecology* 75: 8: 2243.

Briggs MR, Kadonaga JT, Bell SP and Tjian R. (1986) Purification and biochemical characterization of the promoter-specific transcription factor, Sp1. *Science* 234: 4772: 47-52.

Brooks JL and Dodson SI. (1965) Predation, Body Size, and Composition of Plankton. *Science* 150: 3692: 28-35.

Bukovinszky T, Verschoor AM, Helmsing NR, Bezemer TM, Bakker ES, Vos M and de Senerpont Domis LN. (2012) The good, the bad and the plenty: interactive effects of food quality and quantity on the growth of different *Daphnia* species. *PLoS One* 7: 9: e42966.

Burke TW and Kadonaga JT. (1996) Drosophila TFIID binds to a conserved downstream basal promoter element that is present in many TATA-box-deficient promoters. *Genes Dev.* 10: 6: 711-724.

Butler JE and Kadonaga JT. (2002) The RNA polymerase II core promoter: a key component in the regulation of gene expression. *Genes Dev.* 16: 20: 2583-2592.

Campbell JA, Davies GJ, Bulone V and Henrissat B. (1997) A classification of nucleotide-diphospho-sugar glycosyltransferases based on amino acid sequence similarities. *Biochem.J.* 326 (Pt 3): Pt 3: 929-939.

Carter RS, Bhat NK, Basu A and Avadhani NG. (1992) The basal promoter elements of murine cytochrome c oxidase subunit IV gene consist of tandemly duplicated ets motifs that bind to GABP-related transcription factors. *J.Biol.Chem.* 267: 32: 23418-23426.

Carvalho GR and Crisp DJ. (1987) The Clonal Ecology of *Daphnia magna* (Crustacea:Cladocera): I. Temporal Changes in the Clonal Structure of a Natural Population. *The Journal of Animal Ecology* 56: 2: 453.

Cha-Molstad H, Keller DM, Yochum GS, Impey S and Goodman RH. (2004) Cell-type-specific binding of the transcription factor CREB to the cAMP-response element. *Proc.Natl.Acad.Sci.U.S.A.* 101: 37: 13572-13577.

Chattoraj P, Mohapatra SS, Rao JLUM and Biswas I. (2011) Regulation of Transcription by SMU.1349, a TetR Family Regulator, in *Streptococcus* mutans. *J.Bacteriol.* 193: 23: 6605-6613.

Chen S, Chen DF, Yang F, Nagasawa H and Yang WJ. (2011) Characterization and processing of superoxide dismutase-fused vitellogenin in the diapause embryo formation: a special developmental pathway in the brine shrimp, *Artemia parthenogenetica*. *Biol.Reprod.* 85: 1: 31-41.

Choi KY, Ji YJ, Dhakal BK, Yu JR, Cho C, Song WK and Ahnn J. (2003) Vacuolar-type H+-ATPase E subunit is required for embryogenesis and yolk transfer in *Caenorhabditis elegans*. *Gene* 311: 13-23.

Chorley BN, Campbell MR, Wang X, Karaca M, Sambandan D, Bangura F, Xue P, Pi J, Kleeberger SR and Bell DA. (2012) Identification of novel NRF2-regulated genes by ChIP-Seq: influence on retinoid X receptor alpha. *Nucleic Acids Res.* 40: 15: 7416-7429.

Colbourne JK, Hebert PDN and Taylor DJ. (1997) Evolutionary origins of phenotypic diversity in *Daphnia*. In: *Molecular Evolution and Adaptive Radiation.*, edited by Cambridge University Press. Cambridge: Givnish, T.J.; Sytsma, K.J., , p. 163-188.

Colbourne JK, Pfrender ME, Gilbert D, Thomas WK, Tucker A, Oakley TH, Tokishita S, Aerts A, Arnold GJ, Basu MK, Bauer DJ, Cáceres CE, Carmel L, Casola C, Choi J, Detter JC, Dong Q, Dusheyko S, Eads BD, Fröhlich T, Geiler-Samerotte KA, Gerlach D, Hatcher P, Jogdeo S, Krijgsveld J, Kriventseva EV, Kültz D, Laforsch C, Lindquist E, Lopez J, Manak JR, Muller J, Pangilinan J, Patwardhan RP, Pitluck S, Pritham EJ, Rechtsteiner A, Rho M, Rogozin IB, Sakarya O, Salamov A, Schaack S, Shapiro H, Shiga Y, Skalitzky C, Smith Z, Souvorov A, Sung W, Tang Z, Tsuchiya D, Tu H, Vos H, Wang M, Wolf YI, Yamagata H, Yamada T, Ye Y, Shaw JR, Andrews J, Crease TJ, Tang H, Lucas SM, Robertson HM, Bork P, Koonin EV, Zdobnov EM, Grigoriev IV, Lynch M and Boore JL. (2011) The Ecoresponsive Genome of *Daphnia pulex*. *Science* 331: 6017: 555-561.

Colbourne J, Singan V and Gilbert D. (2005) wFleaBase: the *Daphnia* genome database. *BMC Bioinformatics* 6: 1: 45.

Conway EM, Liu L, Nowakowski B, Steiner-Mosonyi M, Ribeiro SP and Michalak M. (1995) Heat shock-sensitive expression of calreticulin. In vitro and in vivo up-regulation. *J.Biol.Chem.* 270: 28: 17011-17016.

Coss RA and Linnemans WA. (1996) The effects of hyperthermia on the cytoskeleton: a review. *Int.J.Hyperthermia* 12: 2: 173-196.

Cousyn C, De Meester L, Colbourne JK, Brendonck L, Verschuren D and Volckaert F. (2001) Rapid, local adaptation of zooplankton behavior to changes in predation pressure in the absence of neutral genetic changes. *Proc.Natl.Acad.Sci.U.S.A.* 98: 11: 6256-6260.

Craig R and Beavis RC. (2004) TANDEM: matching proteins with tandem mass spectra. *Bioinformatics* 20: 9: 1466-1467.

D'Andrea LD and Regan L. (2003) TPR proteins: the versatile helix. *Trends Biochem.Sci.* 28: 12: 655-662.

Das AK, Cohen PW and Barford D. (1998) The structure of the tetratricopeptide repeats of protein phosphatase 5: implications for TPR-mediated protein-protein interactions. *EMBO J.* 17: 5: 1192-1199.

Davies G and Henrissat B. (1995) Structures and mechanisms of glycosyl hydrolases. *Structure* 3: 9: 853-859.

De Meester L. (1996) Local genetic differentiation and adaptation in freshwater zooplankton populations: Patterns and processes. *Ecoscience* 3: 4: 385-399.

De Nadal E, Ammerer G and Posas F. (2011) Controlling gene expression in response to stress. *Nat.Rev.Genet.* 12: 12: 833-845.

Deng W and Roberts SG. (2005) A core promoter element downstream of the TATA box that is recognized by TFIIB. *Genes Dev.* 19: 20: 2418-2423.

Dikstein R. (2011) The unexpected traits associated with core promoter elements. *Transcription* 2: 5: 201-206.

Doi T. (2005) Transcription Factors Responsible for Megakaryocyte-Specific Gene Expression. *ChemInform* 36: 52: .

Ebert D. (2011) A genome for the environment. *Science* 331: 6017: 539-540.

Ebert D. (2005) *Ecology, epidemiology, and evolution of parasitism in Daphnia [Internet]*. http://www.ncbi.nlm.nih.gov/books/NBK2036/: Bethesda (MD): National Center for Biotechnology Information (US), .

Ebert D, Yampolsky L and van Noordwijk AJ. (1993) Genetics of life history in *Daphnia magna*. II. Phenotypic plasticity. *Heredity* 70: 4: 344-352.

Edwards D, Murray JA and Smith AG. (1998) Multiple genes encoding the conserved CCAAT-box transcription factor complex are expressed in *Arabidopsis*. *Plant Physiol.* 117: 3: 1015-1022.

Edwards SR, Braley R and Chaffin WL. (1999) Enolase is present in the cell wall of *Saccharomyces cerevisiae*. *FEMS Microbiol.Lett.* 177: 2: 211-216.

El-Deiry WS, Kern SE, Pietenpol JA, Kinzler KW and Vogelstein B. (1992) Definition of a consensus binding site for p53. *Nat.Genet.* 1: 1: 45-49.

Elendt B and Bias W. (1990) Trace nutrient deficiency in *Daphnia magna* cultured in standard medium for toxicity testing. Effects of the optimization of culture conditions on life history parameters of *Daphnia magna*. *Water Research,* 24: 9: 1157-1167.

Elfakess R and Dikstein R. (2008) A translation initiation element specific to mRNAs with very short 5'UTR that also regulates transcription. *PLoS One* 3: 8: e3094.

Enkhbayar P, Kamiya M, Osaki M, Matsumoto T and Matsushima N. (2004) Structural principles of leucine-rich repeat (LRR) proteins. *Proteins* 54: 3: 394-403.

Entelis N, Brandina I, Kamenski P, Krasheninnikov IA, Martin RP and Tarassov I. (2006) A glycolytic enzyme, enolase, is recruited as a cofactor of tRNA targeting toward mitochondria in *Saccharomyces cerevisiae*. *Genes Dev.* 20: 12: 1609-1620.

Ferguson AA, Springer MG and Fisher AL. (2010) skn-1-Dependent and -Independent Regulation of aip-1 Expression following Metabolic Stress in *Caenorhabditis elegans*. *Mol.Cell.Biol.* 30: 11: 2651-2667.

Fisk DL, Latta LC,4th, Knapp RA and Pfrender ME. (2007) Rapid evolution in response to introduced predators I: rates and patterns of morphological and life-history trait divergence. *BMC Evol.Biol.* 7: 22.

Flössner D. (2000) *Die Haplopoda und Cladocera (ohne Bosminidae) Mitteleuropas.* Backhuys Leiden, .

Forgac M. (2007) Vacuolar ATPases: rotary proton pumps in physiology and pathophysiology. *Nat.Rev.Mol.Cell Biol.* 8: 11: 917-929.

Fossett N, Tevosian SG, Gajewski K, Zhang Q, Orkin SH and Schulz RA. (2001) The Friend of GATA proteins U-shaped, FOG-1, and FOG-2 function as negative regulators of blood, heart, and eye development in *Drosophila*. *Proc.Natl.Acad.Sci.U.S.A.* 98: 13: 7342-7347.

Friling RS, Bergelson S and Daniel V. (1992) Two adjacent AP-1-like binding sites form the electrophile-responsive element of the murine glutathione S-transferase Ya subunit gene. *Proc.Natl.Acad.Sci.U.S.A.* 89: 2: 668-672.

Fröhlich T, Arnold G, Fritsch R, Mayr T and Laforsch C. (2009) LC-MS/MS-based proteome profiling in *Daphnia pulex* and *Daphnia longicephala*: the *Daphnia pulex* genome database as a key for high throughput proteomics in *Daphnia*. *BMC Genomics* 10: 1: 171.

Fulda S, Gorman AM, Hori O and Samali A. (2010) Cellular Stress Responses: Cell Survival and Cell Death. *International Journal of Cell Biology* 2010: 1 - 23.

Gasteiger E, Hoogland C, Gattiker A, Duvaud S, Wilkins MR, Appel RD and Bairoch A. (2005) Protein identification and analysis tools on the ExPASy server. In: *The Proteomics Protocols Handbook*, edited by Walker JMHumana Press, , p. 571-607.

Geer LY, Markey SP, Kowalak JA, Wagner L, Xu M, Maynard DM, Yang X, Shi W and Bryant SH. (2004) Open mass spectrometry search algorithm. *J.Proteome Res.* 3: 5: 958-964.

Gelebart P, Opas M and Michalak M. (2005) Calreticulin, a Ca2+-binding chaperone of the endoplasmic reticulum. *Int.J.Biochem.Cell Biol.* 37: 2: 260-266.

Geller W and Müller H. (1981) The filtration apparatus of Cladocera: Filter mesh-sizes and their implications on food selectivity. *Oecologia* 49: 3: 316-321.

Gerke P, Börding C, Zeis B and Paul RJ. (2011) Adaptive haemoglobin gene control in *Daphnia pulex* at different oxygen and temperature conditions. *Comparative Biochemistry and Physiology - Part A: Molecular & Integrative Physiology* 159: 1: 56-65.

Gophen M and Geller W. (1984) Filter mesh size and food particle uptake by *Daphnia*. *Oecologia* 64: 3: 408-412.

Gorr TA, Cahn JD, Yamagata H and Bunn HF. (2004) Hypoxia-induced synthesis of hemoglobin in the crustacean *Daphnia magna* is hypoxia-inducible factor-dependent. *J.Biol.Chem.* 279: 34: 36038-36047.

Granzin J, Eckhoff A and Weiergraber OH. (2006) Crystal structure of a multi-domain immunophilin from *Arabidopsis thaliana*: a paradigm for regulation of plant ABC transporters. *J.Mol.Biol.* 364: 4: 799-809.

Gresham D, Boer VM, Caudy A, Ziv N, Brandt NJ, Storey JD and Botstein D. (2011) System-Level Analysis of Genes and Functions Affecting Survival During Nutrient Starvation in *Saccharomyces cerevisiae*. *Genetics* 187: 1: 299-317.

Grigoriev IV, Nordberg H, Shabalov I, Aerts A, Cantor M, Goodstein D, Kuo A, Minovitsky S, Nikitin R, Ohm RA, Otillar R, Poliakov A, Ratnere I, Riley R, Smirnova T, Rokhsar D and Dubchak I. (2012) The genome portal of the Department of Energy Joint Genome Institute. *Nucleic Acids Res.* 40: Database issue: 26-32.

GuhaThakurta D, Palomar L, Stormo GD, Tedesco P, Johnson TE, Walker DW, Lithgow G, Kim S and Link CD. (2002) Identification of a novel cis-regulatory element involved in the heat shock response in *Caenorhabditis elegans* using microarray gene expression and computational methods. *Genome Res.* 12: 5: 701-712.

Guisande C, Duncan A and Lampert W. (1991) Trade-offs in *Daphnia* vertical migration strategies. *Oecologia* 87: 3: 357-359.

Gupta RS. (1995) Evolution of the chaperonin families (Hsp60, Hsp10 and Tcp-1) of proteins and the origin of eukaryotic cells. *Mol.Microbiol.* 15: 1: 1-11.

Haag CR and Ebert D. (2004) Parasite-mediated selection in experimental metapopulations of *Daphnia magna*. *Proc.Biol.Sci.* 271: 1553: 2149-2155.

Hairston NG,Jr, Holtmeier CL, Lampert W, Weider LJ, Post DM, Fischer JM, Caceres CE, Fox JA and Gaedke U. (2001) Natural selection for grazer resistance to toxic cyanobacteria: evolution of phenotypic plasticity? *Evolution* 55: 11: 2203-2214.

Hairston NG, Kearns CM, Perry Demma L and Effler SW. (2005) Species-Specific *Daphnia* Phenotypes: A History of Industrial Pollution and Pelagic Ecosystem Response. *Ecology* 86: 7: 1669 -1678.

Haluskova L, Valentovicova K, Huttova J, Mistrik I and Tamas L. (2009) Effect of abiotic stresses on glutathione peroxidase and glutathione S-transferase activity in barley root tips. *Plant Physiol.Biochem.* 47: 11-12: 1069-1074.

Han D, Huang SSY, Wang W, Deng D and Hung SSO. (2012) Starvation reduces the heat shock protein responses in white sturgeon larvae. *Environ.Biol.Fishes* 93: 3: 333-342.

Hanson RD, Grisolano JL and Ley TJ. (1993) Consensus AP-1 and CRE motifs upstream from the human cytotoxic serine protease B (CSP-B/CGL-1) gene synergize to activate transcription. *Blood* 82: 9: 2749-2757.

Harvey WR and Wieczorek H. (1997) Animal plasma membrane energization by chemiosmotic H+ V-ATPases. *J.Exp.Biol.* 200: Pt 2: 203-216.

Hatahet F and Ruddock LW. (2007) Substrate recognition by the protein disulfide isomerases. *FEBS J.* 274: 20: 5223-5234.

Hebert PD and Ward RD. (1972) Inheritance during parthenogenesis in *Daphnia magna*. *Genetics* 71: 4: 639-642.

Hebert PDN and Beaton MJ. (1989) *Methodologies for Allozyme Analysis Using Cellulose Acetate Electrophoresis. A Practical Handbook.* Helena Laboratories, Beaumont, Texas: .

Hershberger PA, LaCount DJ and Friesen PD. (1994) The apoptotic suppressor P35 is required early during baculovirus replication and is targeted to the cytosol of infected cells. *J.Virol.* 68: 6: 3467-3477.

Hess J, Angel P and Schorpp-Kistner M. (2004) AP-1 subunits: quarrel and harmony among siblings. *J.Cell.Sci.* 117: Pt 25: 5965-5973.

Hochachka PW. (2000) Environmental Stressors and Gene Responses; Chapter 1 Cell homeostasis and stress at year 2000—Two solitudes and two research approaches. 1: 1-16.

Hochachka PW and Somero GN. (2002) *Biochemical adaptation: mechanism and process in physiological evolution.* Oxford [u.a.]: Oxford Univ. Press, , p. 466.

Hochstrasser M. (2009) Origin and function of ubiquitin-like proteins. *Nature* 458: 7237: 422-429.

Hollenhorst PC, Chandler KJ, Poulsen RL, Johnson WE, Speck NA and Graves BJ. (2009) DNA specificity determinants associate with distinct transcription factor functions. *PLoS Genet.* 5: 12: e1000778.

Ignoul S and Eggermont J. (2005) CBS domains: structure, function, and pathology in human proteins. *Am.J.Physiol.Cell.Physiol.* 289: 6: C1369-78.

Ingle L, Wood TR and Banta AM. (1937) A study of longevity, growth, reproduction and heart rate in *Daphnia longispina* as influenced by limitations in quantity of food. *J.Exp.Zool.* 76: 2: 325-352.

Isern E, Gustems M, Messerle M, Borst E, Ghazal P and Angulo A. (2010) The Activator Protein 1 Binding Motifs within the Human *Cytomegalovirus Major* Immediate-Early Enhancer Are Functionally Redundant and Act in a Cooperative Manner with the NF- B Sites during Acute Infection. *J.Virol.* 85: 4: 1732-1746.

Itoh H, Komatsuda A, Ohtani H, Wakui H, Imai H, Sawada K, Otaka M, Ogura M, Suzuki A and Hamada F. (2002) Mammalian HSP60 is quickly sorted into the mitochondria under conditions of dehydration. *Eur.J.Biochem.* 269: 23: 5931-5938.

Jarilla BR and Agatsuma T. (2010) Phosphagen kinases of parasites: unexplored chemotherapeutic targets. *Korean J.Parasitol.* 48: 4: 281-284.

Jethmalani SM and Henle KJ. (1998) Calreticulin associates with stress proteins: Implications for chaperone function during heat stress. *J.Cell.Biochem.* 69: 1: 30-43.

Jeyasingh PD, Ragavendran A, Paland S, Lopez JA, Sterner RW and Colbourne JK. (2011) How do consumers deal with stoichiometric constraints? Lessons from functional genomics using *Daphnia pulex*. *Mol.Ecol.* 20: 11: 2341-2352.

Jeyasingh PD, Weider LJ and Sterner RW. (2009) Genetically-based trade-offs in response to stoichiometric food quality influence competition in a keystone aquatic herbivore. *Ecol.Lett.* 12: 11: 1229-1237.

Jolly C and Morimoto RI. (2000) Role of the heat shock response and molecular chaperones in oncogenesis and cell death. *J.Natl.Cancer Inst.* 92: 19: 1564-1572.

Jörnvall H, Persson B, Krook M, Atrian S, Gonzalez-Duarte R, Jeffery J and Ghosh D. (1995) Short-chain dehydrogenases/reductases (SDR). *Biochemistry* 34: 18: 6003-6013.

Juven-Gershon T, Hsu JY and Kadonaga JT. (2006) Perspectives on the RNA polymerase II core promoter. *Biochem.Soc.Trans.* 34: Pt 6: 1047-1050.

Juven-Gershon T, Hsu JY, Theisen JW and Kadonaga JT. (2008) The RNA polymerase II core promoter - the gateway to transcription. *Curr.Opin.Cell Biol.* 20: 3: 253-259.

Juven-Gershon T and Kadonaga JT. (2010) Regulation of gene expression via the core promoter and the basal transcriptional machinery. *Dev.Biol.* 339: 2: 225-229.

Kadonaga JT. (2002) The DPE, a core promoter element for transcription by RNA polymerase II. *Exp.Mol.Med.* 34: 4: 259-264.

Kang CB, Hong Y, Dhe-Paganon S and Yoon HS. (2008) FKBP Family Proteins: Immunophilins with Versatile Biological Functions. *Neurosignals* 16: 4: 318-325.

Kato Y, Tokishita S, Ohta T and Yamagata H. (2004) A vitellogenin chain containing a superoxide dismutase-like domain is the major component of yolk proteins in cladoceran crustacean *Daphnia magna*. *Gene* 334: 157-165.

Kaufman BA, Kolesar JE, Perlman PS and Butow RA. (2003) A function for the mitochondrial chaperonin Hsp60 in the structure and transmission of mitochondrial DNA nucleoids in *Saccharomyces cerevisiae*. *J.Cell Biol.* 163: 3: 457-461.

Kaufmann SHE. (2008) Elie Metchnikoff's and Paul Ehrlich's impact on infection biology. *Microb.Infect.* 10: 14-15: 1417-1419.

Kenyon CJ. (2010) The genetics of ageing. *Nature* 464: 504–512.

Kim H, Kim A and Cunningham KW. (2012) Vacuolar H+-ATPase (V-ATPase) promotes vacuolar membrane permeabilization and nonapoptotic death in stressed yeast. *J.Biol.Chem.* 287: 23: 19029-19039.

Kim JB, Spotts GD, Halvorsen YD, Shih HM, Ellenberger T, Towle HC and Spiegelman BM. (1995) Dual DNA binding specificity of ADD1/SREBP1 controlled by a single amino acid in the basic helix-loop-helix domain. *Mol.Cell.Biol.* 15: 5: 2582-2588.

Ko LJ and Engel JD. (1993) DNA-binding specificities of the GATA transcription factor family. *Mol.Cell.Biol.* 13: 7: 4011-4022.

Kohlstaedt LA, Wang J, Friedman JM, Rice PA and Steitz TA. (1992) Crystal structure at 3.5 A resolution of HIV-1 reverse transcriptase complexed with an inhibitor. *Science* 256: 5065: 1783-1790.

Koll H, Guiard B, Rassow J, Ostermann J, Horwich AL, Neupert W and Hartl F. (1992) Antifolding activity of hsp60 couples protein import into the mitochondrial matrix with export to the intermembrane space. *Cell* 68: 6: 1163-1175.

Kourtis N and Tavernarakis N. (2011) Cellular stress response pathways and ageing: intricate molecular relationships. *EMBO J.* 30: 13: 2520-2531.

Kristensen AR, Schandorff S, Hoyer-Hansen M, Nielsen MO, Jaattela M, Dengjel J and Andersen JS. (2008) Ordered organelle degradation during starvation-induced autophagy. *Mol.Cell.Proteomics* 7: 12: 2419-2428.

Kültz D. (2005) Molecular and evolutionary basis of the cellular stress response. *Annu.Rev.Physiol.* 67: 1: 225-257.

Kültz D. (2003) Evolution of the cellular stress proteome: from monophyletic origin to ubiquitous function. *Journal of Experimental Biology* 206: 18: 3119-3124.

Kuwahara M. (1991) Thermosensitivity of glioma cells with special reference to changes in cytoskeletons. *Neurol.Med.* 31: 13: 853-858.

Lackner DH, Schmidt MW, Wu S, Wolf DA and Bähler J (2012) Regulation of transcriptome, translation, and proteome in response to environmental stress in fission yeast. *Genome Biol* 13.

Laforsch C, Ngwa W, Grill W and Tollrian R. (2004) An acoustic microscopy technique reveals hidden morphological defenses in *Daphnia*. *Proc.Natl.Acad.Sci.U.S.A.* 101: 45: 15911-15914.

Lagrange T, Kapanidis AN, Tang H, Reinberg D and Ebright RH. (1998) New core promoter element in RNA polymerase II-dependent transcription: sequence-specific DNA binding by transcription factor IIB. *Genes Dev.* 12: 1: 34-44.

Lamanda A, Zahn A, Roder D and Langen H. (2004) Improved Ruthenium II tris (bathophenantroline disulfonate) staining and destaining protocol for a better signal-to-background ratio and improved baseline resolution. *Proteomics* 4: 3: 599-608.

Lamkemeyer T, Zeis B and Paul RJ. (2003) Temperature acclimation influences temperature-related behaviour as well as oxygen transport physiology and biochemistry in the water flea *Daphnia magna*. *Can.J.Zool.; Can.J.Zool.* 81: 2: 37–249.

Lampert W, ed. (1985) *Food limitation and the structure of zooplankton communities.* Stuttgart: Schweizerbart, , p. 497.

Lampert W and Rothhaupt KO. (1991) Alternating dynamics of rotifers and *Daphnia magna* in a shallow lake. *Archiv für Hydrobiologie* 120: 4: 447-456.

Lampert W. (1994) Phenotypic plasticity of the filter screens in *Daphnia*: Adaptation to a low-food environment. *Limnol. Oceanogr.* 39: 5: 997-1006.

Lampert W. (1989) The Adaptive Significance of Diel Vertical Migration of Zooplankton. *Funct.Ecol.* 3: 1: 21.

Lampert W. (1978) A field study on the dependence of the fecundity of *Daphnia* spec. on food concentration. *Oecologia* 36: 3: 363-369.

Laneve P, Gioia U, Ragno R, Altieri F, Di Franco C, Santini T, Arceci M, Bozzoni I and Caffarelli E. (2008) The tumor marker human placental protein 11 is an endoribonuclease. *J.Biol.Chem.* 283: 50: 34712-34719.

Lee DH, Gershenzon N, Gupta M, Ioshikhes IP, Reinberg D and Lewis BA. (2005) Functional characterization of core promoter elements: the downstream core element is recognized by TAF1. *Mol.Cell.Biol.* 25: 21: 9674-9686.

Lee MV, Topper SE, Hubler SL, Hose J, Wenger CD, Coon JJ and Gasch AP. (2011) A dynamic model of proteome changes reveals new roles for transcript alteration in yeast. *Mol Syst Biol* 7: 514.

Leicht BG, Biessmann H, Palter KB and Bonner JJ. (1986) Small heat shock proteins of *Drosophila* associate with the cytoskeleton. *Proc.Natl.Acad.Sci.U.S.A.* 83: 1: 90-94.

Li L, Chen Y and Gibson SB. (2013) Starvation-induced autophagy is regulated by mitochondrial reactive oxygen species leading to AMPK activation. *Cell.Signal.* 25: 1: 50-65.

Lim CY, Santoso B, Boulay T, Dong E, Ohler U and Kadonaga JT. (2004) The MTE, a new core promoter element for transcription by RNA polymerase II. *Genes Dev.* 18: 13: 1606-1617.

Lin N, Beyer C, Giessl A, Kireva T, Scholtysek C, Uderhardt S, Munoz LE, Dees C, Distler A, Wirtz S, Kronke G, Spencer B, Distler O, Schett G and Distler JHW. (2013) Autophagy regulates TNF -mediated joint destruction in experimental arthritis. *Ann.Rheum.Dis.* 72: 5: 761-768.

Lindquist S and Craig EA. (1988) The heat-shock proteins. *Annu.Rev.Genet.* 22: 1: 631-677.

Loots GG, Ovcharenko I, Pachter L, Dubchak I and Rubin EM. (2002) rVista for comparative sequence-based discovery of functional transcription factor binding sites. *Genome Res.* 12: 5: 832-839.

Lynch M, Seyfert A, Eads B and Williams E. (2008) Localization of the Genetic Determinants of Meiosis Suppression in Daphnia pulex. *Genetics* 180: 1: 317-327.

Lynch M and Gabriel W. (1987) Environmental Tolerance. *Am.Nat.* 129: 2: 283-303.

Malashkevich VN, Chan DC, Chutkowski CT and Kim PS. (1998) Crystal structure of the simian immunodeficiency virus (SIV) gp41 core: conserved helical interactions underlie the broad inhibitory activity of gp41 peptides. *Proc.Natl.Acad.Sci.U.S.A.* 95: 16: 9134-9139.

Mande SS, Sarfaty S, Allen MD, Perham RN and Hol WG. (1996) Protein-protein interactions in the pyruvate dehydrogenase multienzyme complex: dihydrolipoamide dehydrogenase complexed with the binding domain of dihydrolipoamide acetyltransferase. *Structure* 4: 3: 277-286.

Mantovani R. (1998) A survey of 178 NF-Y binding CCAAT boxes. *Nucleic Acids Res.* 26: 5: 1135-1143.

Martin J, Horwich AL and Hartl FU. (1992) Prevention of protein denaturation under heat stress by the chaperonin Hsp60. *Science* 258: 5084: 995-998.

McLennan AG. (2006) The Nudix hydrolase superfamily. *Cell Mol.Life Sci.* 63: 2: 123-143.

Mikulski A, Grzesiuk M, Kloc M and Pijanowska J. (2009) Heat shock proteins in *Daphnia* detected using commercial antibodies: description and responsiveness to thermal stress. *Chemoecology* .

Mikulski A, Bernatowicz P, Grzesiuk M, Kloc M and Pijanowska J. (2011) Differential levels of stress proteins (HSPs) in male and female *Daphnia magna* in response to thermal stress: a consequence of sex-related behavioral differences? *J.Chem.Ecol.* 37: 7: 670-676.

Miller KP, Chen YH, Hastings VL, Bral CM and Ramos KS. (2000) Profiles of antioxidant/electrophile response element (ARE/EpRE) nuclear protein binding and c-Ha-ras transactivation in vascular smooth muscle cells treated with oxidative metabolites of benzo[a]pyrene. *Biochem.Pharmacol.* 60: 9: 1285-1296.

Miner BE, De Meester L, Pfrender ME, Lampert W and Hairston NG. (2012) Linking genes to communities and ecosystems: *Daphnia* as an ecogenomic model. *Proceedings of the Royal Society B: Biological Sciences* 279: 1735: 1873-1882.

Mistry J and Finn R. (2007) Pfam: a domain-centric method for analyzing proteins and proteomes. *Methods Mol.Biol.* 396: 43-58.

Mitchell ES, Halves J and Lampert W. (2004) Coexistence of similar genotypes of *Daphnia magna* in intermittent populations: response to thermal stress. *Oikos* 106: 3: 469-478.

Miyakawa H, Imai M, Sugimoto N, Ishikawa Y, Ishikawa A, Ishigaki H, Okada Y, Miyazaki S, Koshikawa S, Cornette R and Miura T. (2010) Gene up-regulation in response to predator kairomones in the water flea, *Daphnia pulex*. *BMC Dev.Biol.* 10: 45.

Moenickes S, Richter O and Pirow R. (2010) Approaching the evolutionary advantage of ancillary types of haemoglobin in *Daphnia magna* by simulation of oxygen supply. *J.Exp.Biol.* 213: 3: 408-417.

Moinova HR and Mulcahy RT. (1998) An electrophile responsive element (EpRE) regulates beta-naphthoflavone induction of the human gamma-glutamylcysteine synthetase regulatory subunit gene. Constitutive expression is mediated by an adjacent AP-1 site. *J.Biol.Chem.* 273: 24: 14683-14689.

Morrish F, Giedt C and Hockenbery D. (2003) c-MYC apoptotic function is mediated by NRF-1 target genes. *Genes Dev.* 17: 2: 240-255.

Müller-Navarra DC. (1995) Biochemical versus mineral limitation in *Daphnia*. *Limnol.Oceanogr.* 40: 7: 1209-1214.

Müller-Navarra DC and Lampert W. (1996) Seasonal patterns of food limitation in *Daphnia galeata* : separating food quantity and food quality effects. *J. Plankron Res.* 18: 7: 1137-1157.

Murphy CT. (2006) The search for DAF-16/FOXO transcriptional targets: approaches and discoveries. *Exp.Gerontol.* 41: 10: 910-921.

Negri A, Ceciliani F, Tedeschi G, Simonic T and Ronchi S. (1992) The primary structure of the flavoprotein D-aspartate oxidase from beef kidney. *J.Biol.Chem.* 267: 17: 11865-11871.

Neuwald AF, Aravind L, Spouge JL and Koonin EV. (1999) AAA+: A class of chaperone-like ATPases associated with the assembly, operation, and disassembly of protein complexes. *Genome Research* 9: 1: 27-43.

Nishitoh H. (2011) CHOP is a multifunctional transcription factor in the ER stress response. *J.Biochem.* 151: 3: 217-219.

Nogales E, Downing KH, Amos LA and Lowe J. (1998) Tubulin and FtsZ form a distinct family of GTPases. *Nat.Struct.Biol.* 5: 6: 451-458.

Odrowaz Z and Sharrocks AD. (2012) ELK1 uses different DNA binding modes to regulate functionally distinct classes of target genes. *PLoS Genet.* 8: 5: e1002694.

Pao GM and Saier MH. (1995) Response regulators of bacterial signal transduction systems: Selective domain shuffling during evolution. *J.Mol.Evol.* 40: 2: 136-154.

Pao SS, Paulsen IT and Saier MH,Jr. (1998) Major facilitator superfamily. *Microbiol.Mol.Biol.Rev.* 62: 1: 1-34.

Parry TJ, Theisen JW, Hsu JY, Wang YL, Corcoran DL, Eustice M, Ohler U and Kadonaga JT. (2010) The TCT motif, a key component of an RNA polymerase II transcription system for the translational machinery. *Genes Dev.* 24: 18: 2013-2018.

Paul RJ, Zeis B, Lamkemeyer T, Seidl M and Pirow R. (2004) Control of oxygen transport in the microcrustacean *Daphnia*: regulation of haemoglobin expression as central mechanism of adaptation to different oxygen and temperature conditions. *Acta Physiol.Scand.* 182: 3: 259-275.

Paul RJ, Mertenskötter A, Pinkhaus O, Pirow R, Gigengack U, Buchen I, Koch M, Horn W and Zeis B. (2012) Seasonal and interannual changes in water temperature affect the genetic structure of a *Daphnia* assemblage (*D. longispina* complex) through genotype-specific thermal tolerances. *Limnol.Oceanogr.* 57: 2: 619-633.

Pauwels K, Stoks R and de Meester L. (2005) Coping with predator stress: interclonal differences in induction of heat-shock proteins in the water flea Daphnia magna. *J.Evol.Biol.* 18: 4: 867-872.

Pereira CA, Alonso GD, Ivaldi S, Silber A, Alves MJ, Bouvier LA, Flawia MM and Torres HN. (2002) Arginine metabolism in *Trypanosoma cruzi* is coupled to parasite stage and replication. *FEBS Lett.* 526: 1-3: 111-114.

Perry RP. (2005) The architecture of mammalian ribosomal protein promoters. *BMC Evol.Biol.* 5: 15.

Peters RH and Bernardi R, R. (1987) *Daphnia*. In: *Memorie dell'Istituto Italiano di Idrobiologia*Anonymous . Pallanza: Istituto Italiano di Idrobiologia, .

Peters JM. (1994) Proteasomes: protein degradation machines of the cell. *Trends Biochem.Sci.* 19: 9: 377-382.

Petersen TN, Brunak S, von Heijne G and Nielsen H. (2011) SignalP 4.0: discriminating signal peptides from transmembrane regions. *Nat Meth* 8: 10: 785-786.

Pinkhaus O, Schwerin S, Pirow R, Zeis B, Buchen I, Gigengack U, Koch M, Horn W and Paul RJ. (2007) Temporal environmental change, clonal physiology and the genetic structure of a *Daphnia* assemblage (*D. galeata-hyalina* hybrid species complex). *Freshwat.Biol.* 52: 8: 1537.

Platini F, Perez-Tomas R, Ambrosio S and Tessitore L. (2010) Understanding autophagy in cell death control. *Curr.Pharm.Des.* 16: 1: 101-113.

Podrabsky JE and Somero GN. (2004) Changes in gene expression associated with acclimation to constant temperatures and fluctuating daily temperatures in an annual killifish *Austrofundulus limnaeus*. *J.Exp.Biol.* 207: Pt 13: 2237-2254.

Pörtner HO. (2002a) Climate variations and the physiological basis of temperature dependent biogeography: systemic to molecular hierarchy of thermal tolerance in animals. *Comp.Biochem.Physiol.A.Mol.Integr.Physiol.* 132: 4: 739-761.

Pörtner HO. (2002b) Climate variations and the physiological basis of temperature dependent biogeography: systemic to molecular hierarchy of thermal tolerance in animals. *Comparative Biochemistry and Physiology - Part A: Molecular & Integrative Physiology* 132: 4: 739-761.

Pörtner HO. (2001) Climate change and temperature-dependent biogeography: oxygen limitation of thermal tolerance in animals. *Naturwissenschaften; Naturwissenschaften* 88: 4: 137-146.

Pörtner HO and Farrell AP. (2008) Physiology and climate change. *Science* 322: 5902: 690-692.

Pörtner HO and Knust R. (2007) Climate change affects marine fishes through the oxygen limitation of thermal tolerance. *Science* 315: 5808: 95-97.

Prasad SC, Soldatenkov VA, Kuettel MR, Thraves PJ, Zou X and Dritschilo A. (1999) Protein changes associated with ionizing radiation-induced apoptosis in human prostate epithelial tumor cells. *Electrophoresis* 20: 4-5: 1065-1074.

Punta M, Coggill PC, Eberhardt RY, Mistry J, Tate J, Boursnell C, Pang N, Forslund K, Ceric G, Clements J, Heger A, Holm L, Sonnhammer ELL, Eddy SR, Bateman A and Finn RD. (2012) The Pfam protein families database. *Nucleic Acids Res.* 40: D1: D290-D301.

Puthalakath H, O'Reilly LA, Gunn P, Lee L, Kelly PN, Huntington ND, Hughes PD, Michalak EM, McKimm-Breschkin J, Motoyama N, Gotoh T, Akira S, Bouillet P and Strasser A. (2007) ER stress triggers apoptosis by activating BH3-only protein Bim. *Cell* 129: 7: 1337-1349.

Qin G, Jia M, Liu T, Xuan T, Yan Zhu K, Guo Y, Ma E and Zhang J. (2011) Identification and characterisation of ten glutathione S-transferase genes from oriental migratory locust, *Locusta migratoria manilensis* (Meyen). *Pest Manag.Sci.* 67: 6: 697-704.

Qin G, Jia M, Liu T, Zhang X, Guo Y, Zhu KY, Ma E and Zhang J. (2012) Heterologous expression and characterization of a sigma glutathione S-transferase involved in carbaryl detoxification from oriental migratory locust, *Locusta migratoria manilensis* (Meyen). *J.Insect Physiol.* 58: 2: 220-227.

Ren J, Sainsbury S, Nettleship JE, Saunders NJ and Owens RJ. (2010) The crystal structure of NGO0477 from *Neisseria gonorrhoeae* reveals a novel protein fold incorporating a helix-turn-helix motif. *Proteins* 78: 7: 1798-1802.

Richter K, Haslbeck M and Buchner J. (2010) The heat shock response: life on the verge of death. *Mol.Cell* 40: 2: 253-266.

Roelofs D, Aarts MGM, Schat H and Van Straalen NM. (2008) Functional ecological genomics to demonstrate general and specific responses to abiotic stress. *Funct.Ecol.* 22: 1: 8-18.

Roux MM, Pain A, Klimpel KR and Dhar AK. (2002) The Lipopolysaccharide and -1,3-Glucan Binding Protein Gene Is Upregulated in White Spot Virus-Infected Shrimp (*Penaeus stylirostris*). *J.Virol.* 76: 14: 7140-7149.

Roy D and Tamuli R. (2014[2/19/2014]) NRF1 (nuclear respiratory factor 1) [Online]. http://atlasgeneticsoncology.org/Genes/NRF1ID44233ch7q32.html.

Ryjenkov DA, Tarutina M, Moskvin OV and Gomelsky M. (2005) Cyclic diguanylate is a ubiquitous signaling molecule in bacteria: insights into biochemistry of the GGDEF protein domain. *J.Bacteriol.* 187: 5: 1792-1798.

Sarkar S. (1999) From the Reaktionsnorm to the Adaptive Norm: The Norm of Reaction, 1909–1960. *Biology and Philosophy* 14: 2: 235-252.

Sazuka T, Tomooka Y, Ikawa Y, Noda M and Kumar S. (1992) DRG: a novel developmentally regulated GTP-binding protein. *Biochem.Biophys.Res.Commun.* 189: 1: 363-370.

Scherz-Shouval R, Shvets E, Fass E, Shorer H, Gil L and Elazar Z. (2007) Reactive oxygen species are essential for autophagy and specifically regulate the activity of Atg4. *EMBO J.* 26: 7: 1749-1760.

Schwarzenberger A, Courts C and von Elert E. (2009) Target gene approaches: Gene expression in *Daphnia magna* exposed to predator-borne kairomones or to microcystin-producing and microcystin-free *Microcystis aeruginosa*. *BMC Genomics* 10: 1: 527.

Schwerin S, Bettina Z, Wolfgang H, Heidemarie H and Rüdiger J, Paul. (2010) Hemoglobin concentration in *Daphnia* (*D. galeata–hyalina*) from the epilimnion is related to the state of nutrition and the degree of protein homeostasis. *Limnol. Oceanogr.* 55: 2: 639-652.

Schwerin S, Zeis B, Lamkemeyer T, Paul RJ, Koch M, Madlung J, Fladerer C and Pirow R. (2009) Acclimatory responses of the *Daphnia pulex* proteome to environmental changes. II. Chronic exposure to different temperatures (10 and 20 degrees C) mainly affects protein metabolism. *BMC Physiol.* 9: 8.

Segal JA, Barnett JL and Crawford DL. (1999) Functional analyses of natural variation in Sp1 binding sites of a TATA-less promoter. *J.Mol.Evol.* 49: 6: 736-749.

Seitz V, Butzhammer P, Hirsch B, Hecht J, Ines GÃ¼tgemann, Ehlers A, Lenze D, Oker E, Sommerfeld A, Edda von dW, Christoph KÃ¶nig, Zinser C, Spang R and Hummel M. (2011) Deep Sequencing of MYC DNA-Binding Sites in *Burkitt Lymphoma*. *PLoS ONE* 6: 11: .

Sell AF. (1998) Adaptation to oxygen deficiency: Contrasting patterns of haemoglobin synthesis in two coexisting *Daphnia* species. *Comparative Biochemistry and Physiology Part A* 120: 119–125.

Selye H. (1973) The Evolution of the Stress Concept: The originator of the concept traces its development from the discovery in 1936 of the alarm reaction to modern therapeutic applications of syntoxic and catatoxic hormones. *Am.Sci.* 61: 6: 692-699.

Serafini L, Hann JB, Kultz D and Tomanek L. (2011) The proteomic response of sea squirts (genus *Ciona*) to acute heat stress: a global perspective on the thermal stability of proteins. *Comp.Biochem.Physiol.Part D.Genomics Proteomics* 6: 3: 322-334.

Sheehan D, Meade G, Foley VM and Dowd CA. (2001) Structure, function and evolution of glutathione transferases: implications for classification of non-mammalian members of an ancient enzyme superfamily. *Biochem.J.* 360: Pt 1: 1-16.

Shevchenko A, Tomas H, Havlis J, Olsen JV and Mann M. (2007) In-gel digestion for mass spectrometric characterization of proteins and proteomes. *Nat.Protocols* 1: 6: 2856-2860.

Shirakihara Y, Leslie AG, Abrahams JP, Walker JE, Ueda T, Sekimoto Y, Kambara M, Saika K, Kagawa Y and Yoshida M. (1997) The crystal structure of the nucleotide-free a3ß3 subcomplex of F1-ATPase from the thermophilic Bacillus PS3 is a symmetric trimer. *Structure* 5: 6: 825-836.

Shalgi R, Hurt JA,1 Krykbaeva I, Taipale M, Lindquist S and Burge CB. (2013) Widespread regulation of translation by elongation pausing in heat shock. *Mol Cell* 49: 439–452

Shirane M and Nakayama KI. (2003) Inherent calcineurin inhibitor FKBP38 targets Bcl-2 to mitochondria and inhibits apoptosis. *Nat.Cell Biol.* 5: 1: 28-37.

Skerker JM, Prasol MS, Perchuk BS, Biondi EG and Laub MT. (2005) Two-component signal transduction pathways regulating growth and cell cycle progression in a bacterium: a system-level analysis. *PLoS Biol.* 3: 10: e334.

Snapp E. (2012) Unfolded Protein Responses With or Without Unfolded Proteins? *Cells* 1: 4: 926-960.

Sommer U, Adrian R, De Senerpont Domis L, Elser JJ, Gaedke U, Ibelings B, Jeppesen E, Lürling M, Molinero JC, Mooij WM, van Donk E and Winder M. (2012) Beyond the Plankton Ecology Group (PEG) Model: Mechanisms Driving Plankton Succession. *Annual Review of Ecology, Evolution, and Systematics* 43: 1: 429-448.

Sommer U, Gliwicz ZM, Lampert W and Duncan A. (1986) The PEG-model of seasonal succession of planktonic events in fresh waters. *Archiv für Hydrobiologie* 106: 4: 433.

Specht M, Kuhlgert S, Fufezan C and Hippler M. (2011) Proteomics to go: Proteomatic enables the user-friendly creation of versatile MS/MS data evaluation workflows. *Bioinformatics* 27: 8: 1183-1184.

Spriggs KA, Bushell M and Willis AE. (2010) Translational regulation of gene expression during conditions of cell stress. *Mol Cell* 40: 228–237

Steinberg CEW. (2011) *Stress Ecology: Environmental stress as ecological driving force and key player in evolution.* Springer, .

Steinberg CEW, Stürzenbaum SR and Menzel R. (2008) Genes and environment — Striking the fine balance between sophisticated biomonitoring and true functional environmental genomics. *Sci.Total Environ.* 400: 1-3: 142-161.

Steinmetz CG, Xie P, Weiner H and Hurley TD. (1997) Structure of mitochondrial aldehyde dehydrogenase: the genetic component of ethanol aversion. *Structure* 5: 5: 701-711.

Sterner RW, Hagemeier DD, Smith WL and Smith RF. (1993) Phytoplankton nutrient limitation and food quality for *Daphnia*. *Limnology and Oceanography* 38: 4: 857-871.

Storey KB. (1996) Oxidative stress: animal adaptations in nature. *Braz.J.Med.Biol.Res.* 29: 12: 1715-1733.

Sung MH, Tanizawa K, Tanaka H, Kuramitsu S, Kagamiyama H, Hirotsu K, Okamoto A, Higuchi T and Soda K. (1991) Thermostable aspartate aminotransferase from a thermophilic Bacillus species. Gene cloning, sequence determination, and preliminary x-ray characterization. *J.Biol.Chem.* 266: 4: 2567-2572.

Suzuki O, Mochida K, Yamamoto Y, Noguchi Y, Takano K, Matsuda J and Ogura A. (2002) Comparison of glycoprotein hormone alpha-subunits of laboratory animals. *Mol.Reprod.Dev.* 62: 3: 335-342.

Tarr JM, Young PJ, Morse R, Shaw DJ, Haigh R, Petrov PG, Johnson SJ, Winyard PG and Eggleton P. (2010) A mechanism of release of calreticulin from cells during apoptosis. *J.Mol.Biol.* 401: 5: 799-812.

Thoden JB, Hegeman AD, Wesenberg G, Chapeau MC, Frey PA and Holden HM. (1997) Structural analysis of UDP-sugar binding to UDP-galactose 4-epimerase from Escherichia coli. *Biochemistry* 36: 21: 6294-6304.

Tokishita S, Kato Y, Kobayashi T, Nakamura S, Ohta T and Yamagata H. (2006) Organization and repression by juvenile hormone of a vitellogenin gene cluster in the crustacean, *Daphnia magna*. *Biochem.Biophys.Res.Commun.* 345: 1: 362-370.

Tokishita S, Shiga Y, Kimura S, Ohta T, Kobayashi M, Hanazato T and Yamagata H. (1997) Cloning and analysis of a cDNA encoding a two-domain hemoglobin chain from the water flea *Daphnia magna*. *Gene; Gene* 189: 1: 73-78.

Uda K, Fujimoto N, Akiyama Y, Mizuta K, Tanaka K, Ellington WR and Suzuki T. (2006) Evolution of the arginine kinase gene family. *Comp.Biochem.Physiol.Part D.Genomics Proteomics* 1: 2: 209-218.

Urabe J. (1991) Effect of food concentration on growth, reproduction and survivorship of *Bosmina longirostris* (Cladocera): an experimental study. *Freshwater Biology* 25: 1-8.

Van Straalen NM. (2003) Ecotoxicology becomes stress ecology. *Environ.Sci.Technol.* 37: 17: 324A-330A.

Vargas-Parada L, Solis CF and Laclette JP. (2001) Heat shock and stress response of *Taenia solium* and *T. crassiceps* (Cestoda). *Parasitology* 122: Pt 5: 583-588.

von Elert E, Agrawal MK, Gebauer C, Jaensch H, Bauer U and Zitt A. (2004) Protease activity in gut of *Daphnia magna*: evidence for trypsin and chymotrypsin enzymes. *Comp.Biochem.Physiol.B.Biochem.Mol.Biol.* 137: 3: 287-296.

von Elert E, Zitt A and Schwarzenberger A. (2012) Inducible tolerance to dietary protease inhibitors in *Daphnia magna*. *J.Exp.Biol.* 215: Pt 12: 2051-2059.

von Schwarzenberg K, Wiedmann RM, Oak P, Schulz S, Zischka H, Wanner G, Efferth T, Trauner D and Vollmar AM. (2012) Mode of cell death induction by pharmacological vacuolar H+-ATPase (V-ATPase) inhibition. *J.Biol.Chem.*

Vrijenhoek RC. (1979) Factors Affecting Clonal Diversity and Coexistence. *Integrative and Comparative Biology* 19: 3: 787-797.

Walsh MR and Post DM. (2012) The impact of intraspecific variation in a fish predator on the evolution of phenotypic plasticity and investment in sex in *Daphnia ambigua*. *J.Evol.Biol.* 25: 1: 80-89.

Walter MF, Petersen NS and Biessmann H. (1990) Heat shock causes the collapse of the intermediate filament cytoskeleton in *Drosophila* embryos. *Dev.Genet.* 11: 4: 270-279.

Wang Y, Jiang Y, Meyering-Voss M, Sprinzl M and Sigler PB. (1997) Crystal structure of the EF-Tu.EF-Ts complex from *Thermus thermophilus*. *Nat.Struct.Biol.* 4: 8: 650-656.

Weers PMM and Gulati RD. (1997) Growth and reproduction of *Daphnia galeata* in response to changes in fatty acids, phosphorus, and nitrogen in *Chlamydomonas reinhardtii*. *Limnology and Oceanography* 42: 7: 1584-1589.

Wehrly K and Chesebro B. (1997) P24 Antigen Capture Assay for Quantification of Human Immunodeficiency Virus using Readily Available Inexpensive Reagents. *Methods* 12: 4: 288-293.

Weisiger RA. (2002) Cytosolic fatty acid binding proteins catalyze two distinct steps in intracellular transport of their ligands. *Mol.Cell.Biochem.* 239: 1-2: 35-43.

Welch WJ and Suhan JP. (1985) Morphological study of the mammalian stress response: characterization of changes in cytoplasmic organelles, cytoskeleton, and nucleoli, and appearance of intranuclear actin filaments in rat fibroblasts after heat-shock treatment. *J.Cell Biol.* 101: 4: 1198-1211.

Werck-Reichhart D and Feyereisen R. (2000) Cytochromes P450: a success story. *Genome Biol.* 1: 6: REVIEWS3003.

West AH and Stock AM. (2001) Histidine kinases and response regulator proteins in two-component signaling systems. *Trends Biochem.Sci.* 26: 6: 369-376.

Wieczorek H. (1992) The insect V-ATPase, a plasma membrane proton pump energizing secondary active transport: molecular analysis of electrogenic potassium transport in the tobacco hornworm midgut. *J.Exp.Biol.* 172: 335-343.

Winklmayr M, Schmid C, Laner-Plamberger S, Kaser A, Aberger F, Eichberger T and Frischauf AM. (2010) Non-consensus GLI binding sites in Hedgehog target gene regulation. *BMC Mol.Biol.* 11: 2: 1-9.

Xie X, Lu J, Kulbokas EJ, Golub TR, Mootha V, Lindblad-Toh K, Lander ES and Kellis M. (2005) Systematic discovery of regulatory motifs in human promoters and 3' UTRs by comparison of several mammals. *Nature* 434: 7031: 338-345.

Yang C, Bolotin E, Jiang T, Sladek FM and Martinez E. (2007) Prevalence of the initiator over the TATA box in human and yeast genes and identification of DNA motifs enriched in human TATA-less core promoters. *Gene* 389: 1: 52-65.

Yao J, Liao K, Li Q, Wang C, Wang H, Lai S and Zhong J. (2011) mRNA expression of Glutathione S-Transferase Pi (GSTP1) under heat stress and association of genotypes with heat tolerance ability in *Holstein*. *Journal of Animal and Veterinary Advances* 10: 6: 757-763.

Yarden G, Elfakess R, Gazit K and Dikstein R. (2009) Characterization of sINR, a strict version of the Initiator core promoter element. *Nucleic Acids Res.* 37: 13: 4234-4246.

Zeis B, Maurer J, Pinkhaus O, Bongartz E and Paul RJ. (2004) A swimming activity assay shows that the thermal tolerance of *Daphnia magna* is influenced by temperature acclimation. *Can.J.Zool.* 82: 10: 1605.

Zeis B, Lamkemeyer T, Paul RJ, Nunes F, Schwerin S, Koch M, Schutz W, Madlung J, Fladerer C and Pirow R. (2009) Acclimatory responses of the *Daphnia pulex* proteome to environmental changes. I. Chronic exposure to hypoxia affects the oxygen transport system and carbohydrate metabolism. *BMC Physiol.* 9: 7.

Zeng L, Liu YP, Sha H, Chen H, Qi L and Smith JA. (2010) XBP-1 couples endoplasmic reticulum stress to augmented IFN-beta induction via a cis-acting enhancer in macrophages. *J.Immunol.* 185: 4: 2324-2330.

Zerrad L, Merli A, Schroder GF, Varga A, Graczer E, Pernot P, Round A, Vas M and Bowler MW. (2011) A spring loaded release mechanism regulates domain movement and catalysis in phosphoglycerate kinase. *J.Biol.Chem.*

Zhang E, Brewer JM, Minor W, Carreira LA and Lebioda L. (1997) Mechanism of enolase: the crystal structure of asymmetric dimer enolase-2-phospho-D-glycerate/enolase-phosphoenolpyruvate at 2.0 A resolution. *Biochemistry* 36: 41: 12526-12534.

Zhang J, Bui TN, Xiang J and Lin A. (2006) Cyclic AMP inhibits p38 activation via CREB-induced dynein light chain. *Mol.Cell.Biol.* 26: 4: 1223-1234.

Zhang K and Kaufman RJ. (2006) The unfolded protein response: a stress signaling pathway critical for health and disease. *Neurology* 66: 2 Suppl 1: S102-9.

Zhang X, Odom DT, Koo SH, Conkright MD, Canettieri G, Best J, Chen H, Jenner R, Herbolsheimer E, Jacobsen E, Kadam S, Ecker JR, Emerson B, Hogenesch JB, Unterman T, Young RA and Montminy M. (2005) Genome-wide analysis of cAMP-response element binding protein occupancy, phosphorylation, and target gene activation in human tissues. *Proc.Natl.Acad.Sci.U.S.A.* 102: 12: 4459-4464.

Zhao J, Williams CC and Last RL. (1998) Induction of *Arabidopsis* tryptophan pathway enzymes and camalexin by amino acid starvation, oxidative stress, and an abiotic elicitor. *Plant Cell* 10: 3: 359-370.

Zhao Q, Wang J, Levichkin IV, Stasinopoulos S, Ryan MT and Hoogenraad NJ. (2002) A mitochondrial specific stress response in mammalian cells. *EMBO J.* 21: 17: 4411-4419.